Universidade do Estado do Rio de Janeiro
Centro de Tecnologia e Ciências
Instituto de Física Armando Dias Tavares

Breno Almeida da Silveira Dultra Chrispim

Weyl superconductor with dynamical pseudo-axion field, an interplay between high energy and condensed matter physics

Rio de Janeiro
2022

Breno Almeida da Silveira Dultra Chrispim

Weyl superconductor with dynamical pseudo-axion field, an interplay between high energy and condensed matter physics

Tese apresentada, como requisito parcial para obtenção do título de Doutor, ao Programa de Pós-Graduação em Física, da Universidade do Estado do Rio de Janeiro.

Orientador: Prof. Dr. Marcelo Santos Guimarães

Rio de Janeiro

2022

CATALOGAÇÃO NA FONTE
UERJ/ REDE SIRIUS / BIBLIOTECA CTC/D

C555w Chrispim, Breno Almeida da Silveira Dultra.
Weyl superconductor with dynamical pseudo-axion field, an interplay between high energy and condensed matter physics / Breno Almeida da Silveira Dultra Chrispim. - 2022.
149 f. : il.

Orientador: Marcelo Santos Guimarães.
Tese (doutorado) - Universidade do Estado do Rio de Janeiro, Instituto de Física Armando Dias Tavares.

1. Matéria condensada – Aparelhos e materiais eletrônicos – Teses. 2. Isolantes topológicos – Teses. 3. Supercondutores – Teses. 4. Renormalização (Física) – Teses. 5. Partículas (Física nuclear) – Teses. 6. Teoria quântica de campos – Teses. I. Guimarães, Marcelo Santos. II. Universidade do Estado do Rio de Janeiro. Instituto de Física Armando Dias Tavares. III. Título.

CDU 538.9:621.382

Bibliotecária: Teresa da Silva CRB7/5209

Breno Almeida da Silveira Dultra Chrispim

Weyl superconductor with dynamical pseudo-axion field, an interplay between high energy and condensed matter physics

Tese apresentada, como requisito parcial para obtenção do título de Doutor, ao Programa de Pós-Graduação em Física, da Universidade do Estado do Rio de Janeiro.

Aprovada em 04 de Maio de 2022.

Banca Examinadora:

Prof. Dr. Marcelo Santos Guimarães (Orientador)
Instituto de Física Armando Dias Tavares – UERJ

Prof. Dr. Marcio André Lopes Capri
Instituto de Física Armando Dias Tavares - UERJ

Prof. Dr. Letícia Faria Domingues Palhares
Instituto de Física Armando Dias Tavares - UERJ

Prof. Dr. Luis Esteban Oxman
Universidade Federal Fluminense

Prof. Dr. Carlos Alfonso Martin Ballon Bayona
Universidade Federal do Rio de Janeiro

Rio de Janeiro

2022

ACKNOWLEDGMENTS

This work was carried out with the support of the Coordination of Improvement of Higher Education Personnel - Brazil (CAPES) - Financing Code 001.

ABSTRACT

CHRISPIM, B. A. S. D. *Weyl superconductor with dynamical pseudo-axion field, an interplay between high energy and condensed matter physics*. 2022. 152 f. Tese (Doutorado em Física) – Instituto de Física Armando Dias Tavares, Universidade do Estado do Rio de Janeiro, Rio de Janeiro, 2022.

Similar structures that arise in a different field are recurrent themes in physics, with the classic example being the renormalization group which was developed simultaneously in both the high energy and condensed matter physics communities. In recent years, another instance, the topological materials, have extended the applications of axion physics beyond its initial purpose in high energy physics. The characterization of such materials requires a new concept called topological order, which links different phases of matter that are not distinguishable by symmetry considerations. Such materials, with some noteworthy examples as topological insulators, Weyl/Dirac semimetals, and Axionic insulators, possess their electromagnetic response rooted in the so-called theta term. This term has different forms. In Weyl semimetal, the theta term has a linear space-time dependency, akin to the CFJ action investigated in the context of Lorentz violating field theories while in axionic insulators this term appears similar to the coupling of the axion-like field (fluctuations of the symmetry breaking chiral condensate). To better understand this connection, we will examine the basics of topological materials and their field theory description. Also, we investigate the electromagnetic response of semimetals when a particular quartic fermionic pairing perturbation triggers the formation of charged chiral condensates resulting in an axionic superconductor (massive photons interacting with axion-like particles). The axion fluctuations corrections to the Yukawa-like potential up to one-loop order and compute the modifications of the London penetration length are also analyzed.

Keywords: Quantum Field Theory. Superconductivity. Topological Materials.

RESUMO

CHRISPIM, B. A. S. D. *Supercondutor de Weyl com campo pseudo-axion dinâmico, uma interação entre alta energia e física da matéria condensada.* 2022. 152 f. Tese (Doutorado em Física) – Instituto de Física Armando Dias Tavares, Universidade do Estado do Rio de Janeiro, Rio de Janeiro, 2022.

Conceitos semelhantes surgindo em diferentes campos são um tema recorrente na física. Um exemplo clássico é o grupo de renormalização que foi desenvolvido simultaneamente em física de alta energia e matéria condensada. Nos últimos anos, outra instância, os materiais topológicos, estenderam as aplicações da física axiônica para além de seu propósito inicial em física de altas energias. A descrição dessa fase da matéria necessita de uma nova caracterização, chamado ordem topológica, que liga diferentes fases da matéria que não são distinguíveis através de considerações de simetria. Tais materiais, onde podemos citar alguns exemplos notáveis como isolantes topológicos, semimetais Weyl/Dirac e isolantes axiônicos, possuem uma resposta eletromagnética enraizada no chamado termo theta. Esse termo possui diferentes formas; os semimetais de Weyl apresentam um temo theta com dependência linear no espaço-tempo, semelhante à ação CFJ investigada no contexto de teorias de campo com violação de Lorentz. Em isolantes axiônicos ele aparece de forma similar ao acoplamento do campo tipo-axion (flutuações do condensado que quebra a simetria quiral). Para entender melhor essa conexão, examinaremos os fundamentos dos materiais topológicos e sua descrição dentro da teoria de campos. Além disso, foi investigada a resposta eletromagnética de um semimetal quando uma perturbação particular, dada por um pareamento fermiônico quártico, desencadeia a formação de um condensado quiral carregado, resultando em um supercondutor axiônico (fótons massivos em interação com partículas tipo-axions). Também serão analisadas as correções quânticas a 1-loop, geradas por flutuações do axiônico, para o potencial de Yukawa e as modificações geradas no comprimento de penetração de London.

Palavras-chave: Teoria Quântica de Campos. Supercondutividade. Materiais Topológicos.

LIST OF FIGURES

LIST OF TABLES

LIST OF ABBREVIATIONS AND ACRONYMS

AHE	Anomalous Hall Effect
ALPs	Axion-like particles
BCS	Bardeen–Cooper–Schrieffer
CME	Chiral Magnetic Effect
CPT	Charge, Parity, and Time reversal
CS	Chern-Simons
HS	Hubbard-Stratanovich
Im	Imaginary
IQH	Integer Quantum Hall
LHC	Large Hadron Collider
LIV	Lorentz Invariance Violation
MS	Minimal Subtraction
OS	On-shell
QED	Quantum Electrodynamics
QFT	Quantum Field Theory
QG	Quantum Gravity
Re	Real
TKNN	Thouless, Kohmto, Nightingale, and den Nijs
TME	Topological magneto-electric
TSMs	Topological Semimetals
UV	Ultraviolet
WSM	Weyl semimetal

TABLE OF CONTENTS

INTRODUCTION

Historically, axion physics originates from an intriguing problem of quantum chromodynamics (QCD). One expects that the existence of quark chiral condensate in QCD would lead to a spontaneous break in the U(1) chiral symmetry resulting in the existence of quasi-Goldstone bosons. The problem is that such particles do not occur in observations (WEINBERG, 1975). To explain this contradiction, 't Hooft (HOOFT, 1976; HOOFT et al., 1980; HOOFT, 1986) proposed that the chiral anomaly could lead to an explicit symmetry breaking due to instantons contributions, consequently solving the U(1) issue. This solves one problem but raises another inquiry since, as a consequence, it is predicted that violation of parity $\mathbb{P}$ and time-reversal $\mathbb{T}$ would be detectable. Again, this does not materialize in observations, the symmetry breaking parameter is extremely small, and this fine tuning problem is known as the strong CP problem (since charge conjugation C is preserved). The initial axion formulation, proposed by Peccei and Quinn (PECCEI; QUINN, 1977b; PECCEI; QUINN, 1977a) (see (PECCEI, 2008) for a review), creates a mechanism that aims at solving the unpleasant fine-tuning by promoting the symmetry-breaking parameter to a dynamical field along with a abelian global symmetry called $U(1)_{PQ}$ and with a new pseudoscalar particle called axion (by Weinberg (WEINBERG, 1978a)). This formulation has been examined, with no success, but other formulations based on the same “idea” are still present as a feasible option (KIM, 1979; SHIFMAN; VAINSHTEIN; ZAKHAROV, 1980; DINE; FISCHLER; SREDNICKI, 1981). Beyond the QCD context, axion-like particles are expected to appear in any system that shares the same “mechanism” presented by Peccei and Quinn. That is, axion-like particles will couple to any gauge field for which the anomalous fermions have charge since this is a consequence of the chiral transformations of the integration measure (Fujikawa method (FUJIKAWA; SUZUKI, 2004; FUJIKAWA, 1979)).

In recent years, topological materials (MOORE, 2010; HASAN; KANE, 2010; QI; ZHANG, 2011; HASAN; MOORE, 2011) extended the applications of axion physics beyond its application in high energy physics (HEP). Now, the so-called axion electrodynamics (WILCZEK, 1987) holds numerous applications in the condensed matter phenomenology of such materials. The formation of such phenomena is similar to the one in HEP, the effective emergent chiral symmetries appear in their mathematical modeling, which has been shown to lead to the unavoidable introduction of effective axion-like excitations. The axionic coupling plays an essential role in the effective description of the electromagnetic response. In particular, because of this unique coupling with the gauge fields, it is intertwined with the topological structure of gauge fields which appears in some phenomena like the integer quantum Hall effect (IQHE). Beyond the IQHE, phenomena the topological insulators (QI; HUGHES; ZHANG, 2008), Weyl/Dirac semimetals

(ARMITAGE; MELE; VISHWANATH, 2018; YAN; FELSER, 2017), Axionic insulators (WANG; ZHANG, 2013; MACIEJKO; NANDKISHORE, 2014; YOU; CHO; HUGHES, 2016), etc. have a relation with axion-like physics. In particular, the Weyl semimetal cases present an axion-like field with linear spacetime dependency which is akin to the system investigated in the context of Lorentz violating field theories (CARROLL; FIELD; JACKIW, 1990), another link between the two distinct fields (GRUSHIN, 2012).

Similar structures that arise in different fields are recurrent themes in physics. A noteworthy example is the renormalization group, which was developed simultaneously in both the high energy and condensed matter physics communities (ZEE, 2010), leading to other works, concentrated on the link between different fields of physics e.g. the book Universe in a Helium Droplet by Grigory E. Volovik (VOLOVIK, 2009). This thought is well expressed in "unifying themes, concepts, structures, and ideas are the cornerstone of understanding physical reality" (STANESCU, 2016, p. 95).

This serves as a motivation to explore some concepts in both condensed matter and high energy physics. This will be done in the following way, in chapter 1 I will introduce the basics of spinor (Dirac/Weyl), vector and scalar fields on a need-to-know basis (property of the spinor fields, minimal coupling to the gauge field, and their transformations rules). This part will not be the usual textbook treatment because I will include the constant four-vector b_μ in the form $\overline{\psi}\gamma^\mu b_\mu \psi$ (similar to the minimal coupling with the gauge field). The chapter continues with the computation of the low energy effective description, equations of motion, and the so-called "topological currents" of different microscopic theories. The last part will be the computation of the electrodynamics coupled to an Axion-like space-time dependent term (non-dynamical) obtained from the inclusion of four fermion interaction term that breaks chiral symmetry dynamically. This is a review of (WANG; ZHANG, 2013; MACIEJKO; NANDKISHORE, 2014; YOU; CHO; HUGHES, 2016) that will be important to the computation in chapter 4.

The previous discussion will be the foundation for the chosen topic in condensed matter in chapter 3. There, we will do a brief historical review and explore the connections between the previous calculation and the themes in the condensed matter. The essential point here is the so-called quantum Hall effect. The ordinary (or normal) Hall effect (HALL, 1879) is described as the presence of electrical resistance (Hall resistance) proportional to the applied magnetic field. The quantum version of this phenomenon is proportional to the factor $\frac{h}{e^2\nu}$ where ν can be either an integer (integer quantum Hall) or a fraction (fractional quantum Hall). The anomalous Hall effect has the distinct behavior that it is present at zero external magnetic field due to the spontaneous magnetization of the ferromagnetic material sample. As we will see, those phenomena are liked to the topological currents computed in the last chapter.

The chapter 4 will be dedicated to the computation of the axion-superconductor with a dynamical Axion-like (real pseudo-scalar) field. This "fine-tuned" effective massive theory is obtained by generalizing the coupling discussed in section 2.3 the dynamical axion case to introduce a four-fermion interaction that breaks both charge symmetry as well as chiral symmetry. This is a new result since we arrived at this effective description by making contact with usual superconducting couplings in doped Weyl metals (ZYUZIN; BURKOV, 2012; CHRISPIM; BRUNI; GUIMARAES, 2021).

In chapter 5, the previous model will be investigated in the “Dirac” approximation with the computation of the 1-loop correction to the massive photon due to pseudoscalar fluctuations. This calculation is done by using the non-renormalizable approach and has nuances (ghost states) that are explained in detail. The final part is the investigation of the axion corrections to the Yukawa-like and London penetration length which has not been computed until now.

Lastly, this thesis does not aim to be an extensive reexamination of the topics discussed here. Most topics will be introduced as needed and the relevant citations will be provided as best as possible.

1 NECESSARY ELEMENTS OF DIRAC/WEYL ELECTRODYNAMICS

The beginning of this first chapter will be dedicated to introducing the basics of Dirac/Weyl fields, and their dynamics, on a need-to-know basis. This will consist of a brief revision of their properties and minimal coupling to the gauge field, along with the fixation of the notation that will be used. The following section treats the inclusion of the constant four-vector b_μ, that will be essential to the development of this thesis. Motivation for the inclusion of this term, based on concepts of high energy physics, will be given. The central modifications are examined in the following sections with a focus on the changes to the excitation spectrum in the presence of the b_μ term. All those concepts will be essential to making the connection with the following topics (especially to the condensed matter part).

A necessary warning is in order: This thesis is not an extensive review of none of the topics treated here. The topics will be introduced as needed, and relevant citations will be provided.

1.1 Necessary concepts

Initially, the introduction of Dirac and Weyl fields occurred in the context of high-energy physics. This area of physics treats (in the broad sense) the elementary particles of nature and their symmetries. Dirac proposed his famous equation for the fermion field intending to describe the dynamics of the free electron (DIRAC, 1928) (massive charged spin 1/2 particle) and ended in predicting the positron (electrons antiparticle, same quantum numbers with opposite charge) in the process. The Dirac equation in natural units ($c = \hbar = m_{\text{electron}} = \epsilon_0 = 1$, c is the speed of light in vacuum, $\hbar = \frac{h}{2\pi}$ is the reduced Planck constant and ϵ_0 is the vacuum permittivity) is

$$\Big(i\partial\!\!\!/ - m\Big)\psi = 0, \tag{1}$$

where $\partial\!\!\!/ \equiv \gamma^\nu \partial_\nu$, m is a mass parameter measured in terms of the electron mass, and Greek letters in general labels the space-time components (in $3+1$ it goes from 0 to 3). This is a matrix equation, the Dirac field $\psi(x)$ is a four-components quantity, and the gammas are matrices that obey Clifford algebra (defined in appendix C.1). In this case, there are four gamma matrices plus an "extra" one defined by $\gamma^5 = i\gamma^0\gamma^1\gamma^2\gamma^3$. To describe the antiparticle one uses the conjugate field $\overline{\psi} \equiv \psi^\dagger\gamma_0$ (where $\dagger$ is the Hermitian conjugate operation). It was noted by Weyl (WEYL, 1929) that, for odd spatial dimensions plus time, the four-component Dirac spinor can be written in terms of two Weyl spinors ψ_R

and ψ_L (each one with two degrees of freedom) so that $\psi(x) = \begin{pmatrix} \psi_L \\ \psi_R \end{pmatrix}$ or $\psi_{R/L} = P_{R/L}\psi$ ($P_{R/L}$ are projectors defined as $P_R = \frac{1}{2}(1+\gamma^5)$ and $P_L = \frac{1}{2}(1-\gamma^5)$). Dirac's equation of motion splits into two

$$i(\partial_0 - \boldsymbol{\sigma}\cdot\boldsymbol{\nabla})\psi_R = m\psi_L \ , \quad \text{and} \quad i(\partial_0 + \boldsymbol{\sigma}\cdot\boldsymbol{\nabla})\psi_L = m\psi_R, \tag{2}$$

where was used Weyl's representation of the gamma matrices (see the appendix C.2 for more information) and $\boldsymbol{\sigma}$ are the Pauli matrices, as expected. In the massless case, the left- and right-handed states are eigenstates of the helicity operator $\hat{h} = \frac{\boldsymbol{\sigma}\cdot\mathbf{p}}{|\mathbf{p}|}$ (which projects the spin on the direction of motion) with opposite signs as one can see by the equation of motion (2) in Fourier space with $m = 0$, that is

$$i(E - \boldsymbol{\sigma}\cdot\mathbf{p})\psi_{R/L} = 0 \rightarrow iE\left(1 \pm \hat{h}\right)\psi_{R/L} = 0 \tag{3}$$

since $E = |\mathbf{p}|$ for massless particles. This translates into the central fact that Weyl fermions propagate parallel (or antiparallel) to the spin direction. In the end, Weyl fermions can be represented in terms of three quantum numbers; spin, helicity, and chirality. The presence of a mass term mixes the two Weyl fermions so that helicity is no longer a good quantum number although its total number is still conserved. A more in-depth discussion on this topic can be found in (SCHWARTZ, 2013).

The dynamics of the field are dictated by a quantity called Lagrangian density throughout the least action principle. Functional variations of the Lagrangian over field configurations, together with the appropriate boundary conditions, result in the Euler-Lagrange equations which can be used to obtain the classical equation of motion. Dirac's equation of motion is the result of the least action principle applied to the action

$$S_{\text{Dirac}} = \int \mathrm{d}^4x\, \overline{\psi}(x)\left(i\partial\!\!\!/ - m\right)\psi(x). \tag{4}$$

Although ψ and $\overline{\psi}$ (Dirac adjoint) are related by $\overline{\psi} = \psi^\dagger\gamma^0 = \begin{pmatrix} \psi_R^\dagger & \psi_L^\dagger \end{pmatrix}$, they are treated as independent fields. In quantum mechanics, to obtain the probability of some event must sum over all possible trajectories that contribute to that event's occurrence. Consequently, one must use the path integral formulation (which generalizes the classical concept of a single trajectory) to compute physically observable quantities. The classical behavior emerges as the tree-level approximation (first-order approximation in $\hbar$) of the path integral

$$Z = \int \mathcal{D}\left(\psi^\dagger, \psi\right) e^{iS_{\text{Dirac}}} \ , \tag{5}$$

which encodes the complete quantum theory at zero temperature (in this case of the system described by the action (4)). This also shifts the physical interest from the classical equation of motions to the correlation functions (or n-point functions) $\langle \mathcal{O}(x_1)\mathcal{O}(x_2)\cdots\mathcal{O}(x_n)\rangle$ which are appropriate to describe the quantum nature of the system behavior. The computation of such objects is throughout the perturbation of the Lagrangian such that

$$\mathcal{L} \to \mathcal{L} + J(x)\mathcal{O}(x). \tag{6}$$

Here $J(x)$ are arbitrary functions known as sources, and the $\mathcal{O}(x)$ are local operators. Now doing the functional derivative of the generating functional with respect to these source we obtain the connected n-point functions

$$\left\langle \prod_i \mathcal{O}(x_i) \right\rangle = \prod_i \frac{\delta}{\delta J(x_i)} \log Z[J] \bigg|_{J=0}. \tag{7}$$

These objects includes all physical phenomena of a given known action, that is, if it is possible to compute all of the n-point functions then the theory is solvable. All measurable pieces of information (such as scattering amplitudes, decay rates, etc.) to all orders are, in principle, obtainable in this case. This is (obviously) not achievable in most physical systems with the next best option being the computation to a given order of approximation. Now if one is interested in a system on which these Dirac/Weyl fermions interact with the electromagnetic field one must minimally couple them to the gauge field A_μ, through $\partial_\mu \to D_\mu \equiv \partial_\mu + iqA_\mu$ in the spinor sector, and add the appropriate action for the gauge field, the well-known Maxwell action

$$S_{\text{Maxwell}} = \int d^4x \left(-\frac{1}{4} F^{\mu\nu} F_{\mu\nu} - A_\mu J^\mu \right). \tag{8}$$

where the four-vector $J_\mu = (\rho, \boldsymbol{J})$ describes the electric density ρ and current $\boldsymbol{J}$. Variations with respect to classical configurations of the gauge field $A_\mu = (\phi, \boldsymbol{A})$ ($\boldsymbol{A}$ and ϕ are the vector and scalar potentials which relates to electric and magnetic fields by $\boldsymbol{E} = -\boldsymbol{\nabla}\phi - \frac{\partial \boldsymbol{A}}{\partial t}$ and magnetic $\boldsymbol{B} = \boldsymbol{\nabla} \times \boldsymbol{A}$) gives the Maxwell equation

$$\partial_\mu F^{\mu\nu} = J^\nu \tag{9}$$

The description of a physical system is not complete until the gauge invariance is fixed by imposing a gauge condition e.g. Lorenz gauge condition $\frac{1}{c^2}\frac{\partial \phi}{\partial t} + \boldsymbol{\nabla} \cdot \boldsymbol{A} = 0$ reducing the equations of motion to

$$\Box^2 A_\mu = J_\mu \tag{10}$$

The symbol $\Box^2$ is the Laplacian and represents $\boldsymbol{\nabla}^2 - \frac{\partial^2}{\partial t^2}$. The field strength tensor in terms of the electric and magnetic field is

$$F^{\mu\nu} = \frac{\partial A^{\nu}}{\partial x_{\mu}} - \frac{\partial A^{\mu}}{\partial x_{\nu}} = \begin{bmatrix} 0 & -E_x & -E_y & -E_z \\ E_x & 0 & -B_z & B_y \\ E_y & B_z & 0 & -B_x \\ E_z & -B_y & B_x & 0 \end{bmatrix} , \tag{11}$$

the equations of motions take the form

$$\begin{aligned} \boldsymbol{\nabla} \cdot \boldsymbol{E} = \rho, \qquad \boldsymbol{\nabla} \times \boldsymbol{E} = -\frac{\partial \boldsymbol{B}}{\partial t}, \\ \boldsymbol{\nabla} \cdot \boldsymbol{B} = 0, \quad \boldsymbol{\nabla} \times \boldsymbol{B} = \boldsymbol{J} + \frac{\partial \boldsymbol{E}}{\partial t}, \end{aligned} \tag{12}$$

these are the Maxwell equations without electric sources.

This is the very basics of what will be necessary for the next few sections. For more information on these subjects please consult textbooks on quantum field theory like (ZEE, 2010; SCHWARTZ, 2013; PESKIN; SCHROEDER, 1995). In the next section, I will introduce one more ingredient to our system and explore some of the consequences.

1.2 New ingredient with the “coupling” b_μ

Foreshadowing the discussion in the next sections, it is interesting to include one extra term in the fermionic action. The inclusion of the action

$$S = \int \mathrm{d}^4x \, \overline{\psi}(x) \not{b} \gamma^5 \psi(x), \tag{13}$$

where the b_μ is a constant four-vector. It is easy to see that this term modifies Dirac's equation of motion to

$$\left(i\not{D} - \gamma_5 \not{b} - m\right)\psi = 0 \tag{14}$$

or, in terms of the Weyl spinors

$$\left(i\not{\partial} + \not{b}\gamma^5\right)\psi = 0 \to \begin{cases} \sigma^{\mu}(i\partial_{\mu} + b_{\mu})\psi_R = 0 \\ \sigma^{\mu}(i\partial_{\mu} - b_{\mu})\psi_L = 0 \ . \end{cases} \tag{15}$$

The spatial component of b_μ enters the equation of motion as a Zeeman term $\mathbf{b} \cdot \boldsymbol{\sigma}$ which represents a magnetic interaction. The time-like component b_0 enters the description as an energy shift that depends on the chirality of the Weyl spinor. Beyond that, since b_μ is a constant vector, it allows for different field behaviors depending on the direction thus breaking particle-Lorentz symmetry (this will be explained in the next section).

The motivation, at this point, is that the realm beyond Einstein's General theory of Relativity and the Standard model of particle physics, that is, the unification of those two theories, is still a mystery. This theory is generically called quantum gravity (QG) (see (ROVELLI, 2004; THIEMANN, 2007; ORITI, 2009) for modern reviews) and is expected to be valid for energies close to the Planck scale which is far beyond direct experimentation in today's technology such as the Large Hadron Collider (LHC). This makes the only viable path to make indirect detection of possible effects that originates from QG and survives in the effective low energy theory (DONOGHUE, 1995; LIBERATI; MACCIONE, 2009; KOSTELECKÝ, 2004). Those relics would allow us to reconstruct the fundamental theory without direct experimentation but the downside is that it is necessary to guess the general features of QG. One of those suppositions is that, in the Planck scale, space-time is no longer continuous because of the minimum fundamental length $l_P = 1.6 \times 10^{-35}$m (Planck length). As a consequence, one of the fundamental symmetries of the physics, Lorentz symmetry, would be broken at that energy level. This rationalization is the basis of extensions of the standard model that includes some form of Lorentz Invariance Violation (LIV). In fact proposed theories for QG such as String theory (KOSTELECKÝ; SAMUEL, 1989), loop quantum gravity (ASHTEKAR, 1986; ROVELLI, 1998), Horava-Lifshitz gravity (HOŘAVA, 2009), non-commutative geometry (CONNES; KREIMER, 1998) (see (POTTING, 2013) for a review on some of those theories) predict some kind of manifestation of Lorentz symmetry breaking as an effective low energy phenomena. The physical effects of such theories must be very small due to various experimental constraints (LIBERATI; MACCIONE, 2009). In another words, our universe appears to obey Lorentz invariance to a very high accuracy (KOSTELECKÝ; RUSSELL, 2011).

Lorentz invariance and CPT symmetry are connected. The CPT theorem (STREATER; WIGHTMAN, 1964; SCHWARTZ, 2013) tells us that any local quantum field theory that is Hermitian and Lorentz invariant must obey CPT. Beyond that, any unitary interacting theory that violates CPT must also be LIV. The reciprocal affirmation is not true, it is possible to violate Lorentz invariance but maintain CPT symmetry. This opens for two kinds of LIV, the first one that breaks CPT and Lorentz (CPT-odd interaction) and the second that violates Lorentz but keeps CPT (CPT-even interactions).

In the next section, we will see that the inclusion of the action in eq. (13) breaks CPT and Lorentz so it falls in the CPT-odd classification. Also, we will explore some of the previous statements regarding the symmetries and transformation rules of the action terms exhibited in these last two sections.

1.3 Transformation properties

Going back to the nature of the Lagrangian density, one must notice that all elements used in its construction are Lorentz scalars, i.e. the action is Lorentz invariant. This is a necessary restriction if one wants to obey special relativity, that is, if the original field solves the equations of motion then the transformed fields must also solve them, meaning that the physics is invariant under those transformations. The (pseudo-) scalar, (pseudo-) vector, and spinor fields are elements of the general Poincaré group of which the Lorentz transformation is part. The Poincaré group is composed of translations in space-time, rotations, and boosts while the last two compose the Lorentz group. The Lorentz transformations are those who preserve the Minkowski metric g, in other words, the transformation Λ in this group must obey

$$\Lambda^T g \Lambda = g \qquad \text{or} \qquad \Lambda^{\mu}{}_{\sigma} g^{\sigma\tau} \Lambda_{\tau}{}^{\nu} = g^{\mu\nu} . \tag{16}$$

This quantity is a four-vector that can be written as

$$x_\mu \to (x_\mu)' = \Lambda_\mu{}^\nu x_\nu \ . \tag{17}$$

This is the transformation acting on the coordinates. It is possible to represent them on the fields. That is, if one applies transformation $x \to \Lambda x$ then the field also transforms as

$$\phi(x) \to \phi'(x) = \phi(\Lambda^{-1}x) \ , \tag{18}$$

$$V^\mu(x) \to V^{\mu\prime}(x) = \Lambda_V{}^\mu_\nu V^\nu(\Lambda^{-1}x) \ , \tag{19}$$

$$\psi^\alpha(x) \to \psi^{\alpha\prime}(x) = \Lambda_S{}^\alpha_\sigma \psi^\sigma(\Lambda^{-1}x) \ , \tag{20}$$

with the definitions $\Lambda_V = \exp(i\theta_{\mu\nu}V^{\mu\nu})$ and $\Lambda_S = \exp(i\theta_{\mu\nu}S^{\mu\nu})$ where V (S) are the Lorentz group generators that acts on vector (spinor) fields. The actual form of this transformation is not important but can be found in textbooks such as (PESKIN; SCHROEDER, 1995; SCHWARTZ, 2013). These transformations form a continuous group (called Lie group), but, beyond that, one can inquire about the discrete transformations, which can not be achieved by continuous Lorentz transformation starting from identity $\mathbb{1}$. There are two discrete transformations that are important, called Parity conjugation ($\mathbb{P}$), and time-reversal ($\mathbb{T}$). The first one reverses the handedness of space and the latter interchanges the forward and backward light cones. One can express them as

$$\mathbb{P}: \quad (t, \vec{\mathbf{x}}) \to (t, -\vec{\mathbf{x}}) \ , \tag{21}$$

$$\mathbb{T}: \quad (t, \vec{\mathbf{x}}) \to (-t, \vec{\mathbf{x}}) \ . \tag{22}$$

On the fields, these discrete transformations act as

$$\begin{aligned}
\mathbb{P}: \quad & \phi(t,\vec{\mathbf{x}}) \to \pm\phi(t,-\vec{\mathbf{x}}) \ , \\
& V_\mu(t,\vec{\mathbf{x}}) \to (\pm V_0(t,-\vec{\mathbf{x}}), \mp V_i(t,-\vec{\mathbf{x}})) \ , \\
& \psi(t,\vec{\mathbf{x}}) \to \gamma_0\psi(t,-\vec{\mathbf{x}}) = \begin{pmatrix} \psi_R(t,-\vec{\mathbf{x}}) \\ \psi_L(t,-\vec{\mathbf{x}}) \end{pmatrix} \ ,
\end{aligned} \tag{23}$$

and

$$\begin{aligned}
\mathbb{T}: \quad & \phi(t,\vec{\mathbf{x}}) \to \phi(-t,\vec{\mathbf{x}}), \\
& V_\mu(t,\vec{\mathbf{x}}) \to +(V_0(-t,\vec{\mathbf{x}}), -V_i(-t,\vec{\mathbf{x}})) \ , \\
& \psi(t,\vec{\mathbf{x}}) \to \gamma_1\gamma_3\psi(-t,\vec{\mathbf{x}}) = \begin{pmatrix} -\sigma^1\sigma^3\psi_L(-t,\vec{\mathbf{x}}) \\ -\sigma^1\sigma^3\psi_R(-t,\vec{\mathbf{x}}) \end{pmatrix} \ .
\end{aligned} \tag{24}$$

Some comments are in order. The difference in sign on the parity transformation represents the distinction between “pseudo” and “normal” behavior. If the scalar (vector) field transforms with the plus (minus) sign it is “normal” but if it changes with the minus (plus) sign it is an “pseudo” (it is also common to use axial vector instead of pseudovector). On the spinor representation, parity conjugation acts to reverse the momentum of a particle without flipping its spin, this also can be described as a swap between the left-handed and right-handed components. There is one more discrete symmetry called charge conjugation $\mathbb{C}$. The distinction here is that this transformation is not directly associated with the Poincaré group but with the internal symmetry of the system. Charge conjugation interchanges particles with antiparticles and flips the spin direction, so this does not affect the real scalar field. This last discrete transformations acts as

$$\begin{aligned}
\mathbb{C}: \quad & A_\mu \to -A_\mu \ , \\
& \psi \to -i\gamma_2\psi^* \ .
\end{aligned} \tag{25}$$

It is relevant to notice that another transformation is possible once the Dirac field is coupled minimally to the gauge field. This transformation is a local phase rotation

$$\begin{aligned}
\psi(x) &\to e^{i\alpha(x)}\psi \ , \\
A_\mu &\to A_\mu - \frac{1}{e}\partial_\mu\alpha(x) \ .
\end{aligned} \tag{26}$$

The system is invariant under this transformation since this is not a “physical” transformation; it originates from the redundant description of the vector field A_μ (of the four degrees of freedom, only two have physical significance), known as gauge invariance. The global version (or space-time independent) of this last transformation is

$$\psi(x) \to e^{i\alpha}\psi \ . \tag{27}$$

Another kind of transformation is possible, a global transformation that does not depend on the spacetime position but that is constructed with the γ_5 matrix. This transformation is the chiral transformation, given by

$$\psi(x) \to e^{i\beta\gamma_5}\psi \ . \tag{28}$$

This transformation will be vital in the development done in the following sections. With these transformations rules, it is possible to verify how the previously mentioned field composite terms transform. This is described for the discrete transformations in table 1. As stated before, the fermion mass term mixes the right and left chirality, meaning that

Table 1 - Discrete transformation properties

	ϕ^2	A^2	$\overline{\psi}\psi$	$i\overline{\psi}\gamma^5\psi$	$\overline{\psi}\gamma^\mu\psi$	$\overline{\psi}\gamma^\mu\gamma^5\psi$
$\mathbb{P}$	$+1$	$+1$	$+1$	-1	$+1$ for $\mu = 0$ -1 for $\mu = i$	-1 for $\mu = 0$ $+1$ for $\mu = i$
$\mathbb{T}$	$+1$	$+1$	$+1$	-1	$+1$ for $\mu = 0$ -1 for $\mu = i$	$+1$ for $\mu = 0$ -1 for $\mu = i$
$\mathbb{C}$	$+1$	$+1$	$+1$	$+1$	-1	$+1$
CPT	$+1$	$+1$	$+1$	$+1$	-1	-1

Subtitle: These are the discrete transformation properties of some compounds terms in the fields.

Source: PESKIN; SCHROEDER, 1995, p. 71. Adapted by the author.

it transforms as

$$m\overline{\psi}(x)\psi(x) \to me^{-i2\beta\gamma_5}\overline{\psi}(x)\psi(x) = m\Big(e^{2i\beta}\psi_L^\dagger\psi_R + e^{-2i\beta}\psi_R^\dagger\psi_L\Big) \tag{29}$$

under rule (28). After establishing the discrete transformations one can inquire if the system described with Dirac's and Maxwell's action (respectively equations (4) and (8)) is invariant under any of them. The field terms $\overline{\psi}i\partial\!\!\!/\psi$, $m\overline{\psi}\psi$ and $ie\overline{\psi}A\!\!\!/\psi$ obey $\mathbb{C}$, $\mathbb{P}$, $\mathbb{T}$, and CPT as expected.

The four-vector component, introduced in equation (13), which contains $\overline{\psi}b\!\!\!/\gamma^5\psi$, is a special case since b_μ is not technically a vector in the Poincaré group. This means that it does not transform following the vector rule. Another form is to consider it as a constant vector in a particular direction in space-time. Actually, it is understood that this term transforms in the particle (or passive) Lorentz transformation rule (changes of the coordinate system). These transformations are different from the active Lorentz that actually transforms the fields, e.g. a viewer can observe a particle that experiences only a magnetic field in one frame of reference, but for an observer on another frame, this same particle can be regarded as subjected to both magnetic and electric field influences (GRIFFITHS, 2013). The consequence is that the transformations for terms with the Lorentz index are not valid for b_μ and the presence of these terms breaks $\mathbb{T}$ if $\mathbf{b} \neq 0$, $\mathbb{P}$ if $b_0 \neq 0$ and, consequently, $\mathbb{T}$ and $\mathbb{P}$ if $b_\mu \neq 0$. This is in consensus with the previous affirmation that this interaction term is CPT-odd.

1.4 Excitation spectrum in the presence of b_μ

To describe the behavior of particles in this model, we need to compute the dispersion relations (energy and momentum condition). This can be done by “squaring” Dirac’s equation of motion (1) and using the plane-wave approximation $\psi \sim e^{-i(Et-\mathbf{p}\cdot\mathbf{x})}$ one obtains Klein-Gordon equation $E^2 - \mathbf{p}^2 = m^2$. For completeness, the 1D energy plot, for the massive and massless case, is represented in figure 1 . When the mass term is pre-

Figure 1 - Dispersion relations for massive and massless Dirac equations

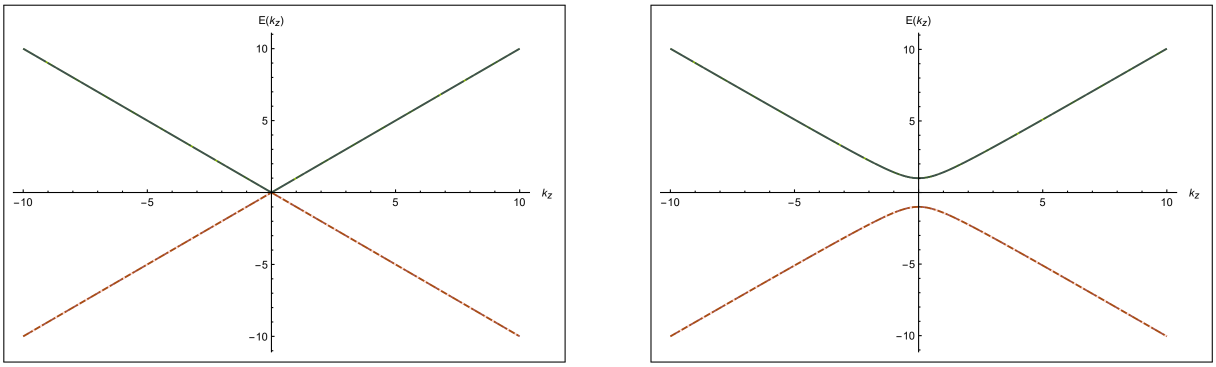

(a) (b)

Subtitle: Figure (a) represents the dispersion relations for massless Dirac equations, the excitation are linear in the momentum. Figure (b) represents the dispersion relations for massive Dirac equations, in this case the excitation present an energy gap given by the mass parameter. This gives a physical interpretation to the notion that the ground state on the gapped system has excitations that are well-separated from the ground state. Both cases respect $\mathbb{T}$ and $\mathbb{P}$ symmetries and presents only one symmetric point which is $k_z = 0$.

Source: The author, 2022.

sent there is minimum energy for the excitation of the system, this is commonly known as the energy gap. The same “squaring” can be done in equation (14) where the b_μ term is included. This leads to the modified dispersion relations

$$\left(E^2 - \mathbf{p}^2 + b^2 - m^2\right)^2 = 4\Big[(E\ b_0 - \mathbf{p}\cdot\mathbf{b})^2 - m^2 b^2\Big]\ . \tag{30}$$

Since this relation is more complex due to the different choices of b_μ one can start by considering (COLLADAY; KOSTELECKÝ, 1997) a pure time-like fix vector $b_\mu = (b_0, \mathbf{0})$, resulting in

$$E_\pm^2 = m^2 + \left(\mathbf{p}^2 \pm b_0\right)^2\ , \tag{31}$$

or a pure space-like fix vector $b_\mu = (0, \mathbf{b})$, leading to

$$E_\pm^2 = m^2 + \mathbf{p}^2 + \mathbf{b}^2 \pm \sqrt{m^2\mathbf{b}^2 + (\mathbf{b}\cdot\mathbf{p})^2}\ . \tag{32}$$

Graphs 3 and 2 describe some particular choices of parameters of those two cases. We can extract physical information from these quantities if we recall that wavelength and linear momentum, or frequency and energy, are interchangeable by using Planck's constant $\hbar$ meaning that we can investigate physical quantities like (classical or Einstein's) causality and stability from the relation dispersion. The first can be reached by verifying if the theory allows superluminal propagation (ADAM; KLINKHAMER, 2001) by computing the group velocity, defined by

$$v_g = \frac{d\omega}{d|\boldsymbol{k}|}\ , \tag{33}$$

which must be less than 1, otherwise, Einstein's causality would be violated. For an pure time-like fix vector we get (ADAM; KLINKHAMER, 2001)

$$v_{g\pm} = \frac{|\mathbf{p}| \pm b_0}{\sqrt{(|\mathbf{p}| \pm b_0)^2 + m^2}} \leq 1\ , \tag{34}$$

and for the case pure space-like vector is

$$v_{g\pm} = \frac{|\mathbf{p}| - \frac{|\mathbf{b}|}{2\sqrt{\mathbf{b}^2 m^2 + \mathbf{b}\cdot\mathbf{p}}}}{\sqrt{\mathbf{b}^2 + m^2 + \mathbf{p}^2 \pm \sqrt{\mathbf{b}^2 m^2 + \mathbf{b}\cdot\mathbf{p}}}} \leq 1\ . \tag{35}$$

Both cases respect classical causality. Next, we can check this theory's stability by verifying if the energy is positive definite in order to guarantee that the vacuum is stable in any frame of reference. If the energy has an imaginary contribution then it is possible to spontaneously decay to a lower energy level. This problem can only occur due to the influence of the zeroth component of b_μ since it is the only form to introduce a negative contribution. The expression eq. (30) is not positive for all values of $b_0 > 0$ thus, in prin-

Figure 2 - Excitation spectrum for fermions with space-like Lorentz breaking coupling

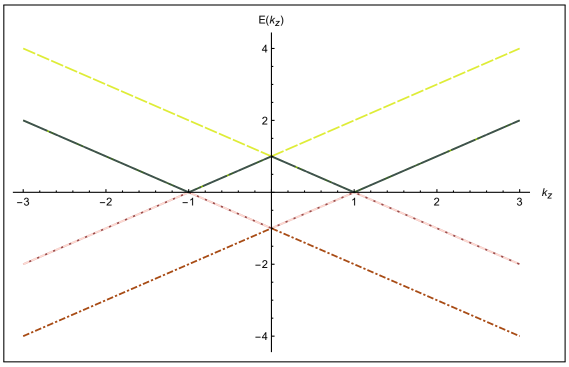

(a)

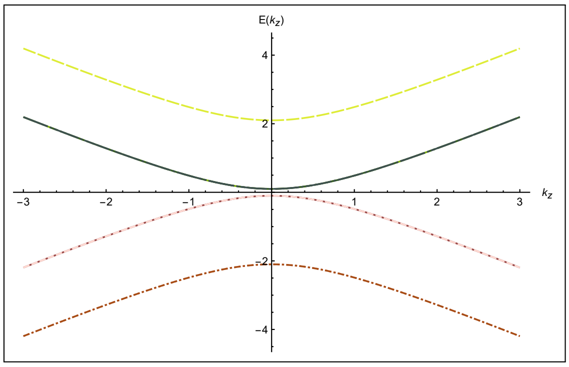

(b)

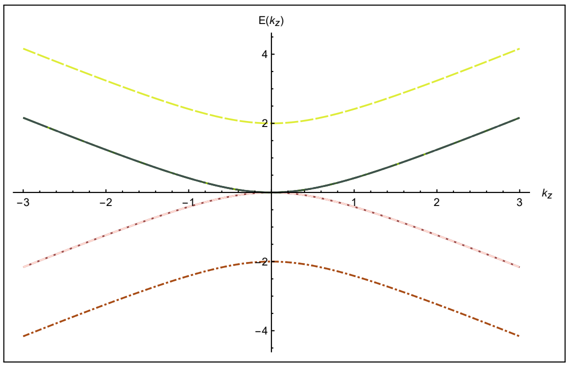

(c)

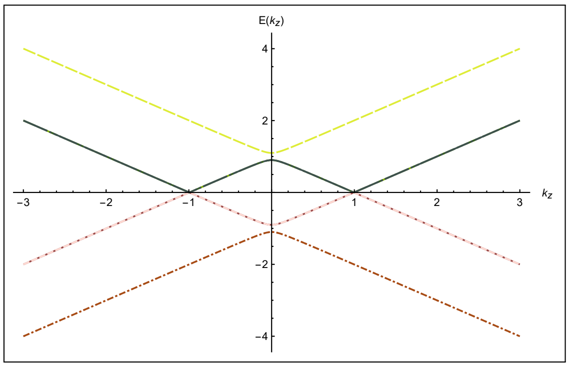

(d)

Subtitle: Each graph represents the energy levels for a system, equation (32), considering $b_\mu = (0, 0, 0, b_z)$ and; $b_z^2 > 0$ with $m = 0$ (a), $b_z^2 < m^2$ (b), $b_z^2 = m^2$ (c), and $b_z^2 > m^2$ (d). The distance between the two points with zero energy, i.e. $E(k_z) = 0$, in (a) and (d) is $2b_z$. In the vicinity of this points the system behaves as the spectra for massless Dirac fermions.

Source: The author, 2022.

Figure 3 - Excitation spectrum for fermions with time-like Lorentz breaking coupling

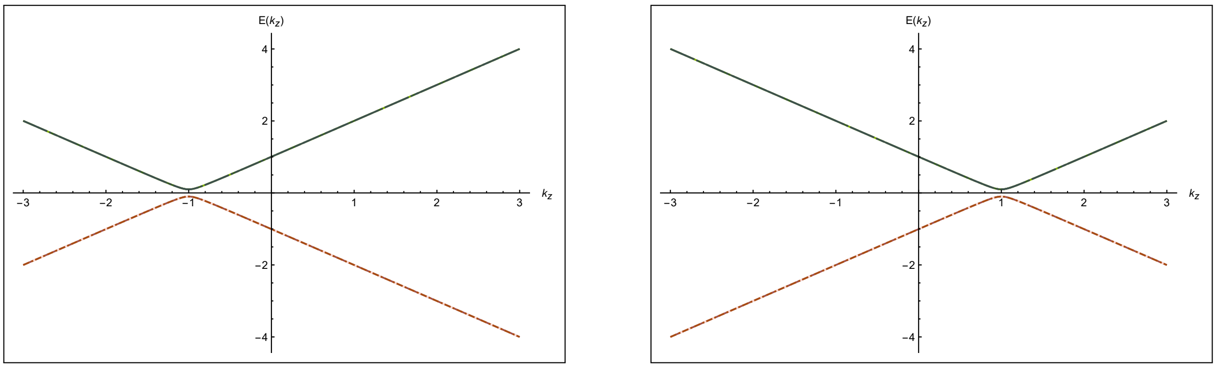

(a)

(b)

Subtitle: Representation of the energy level for the modified dispersion relations (31) with $b_0^2 > m^2$ (fig. (a)) and $b_0^2 < m^2$ (fig. (b)). It is easy to see that the presence of this term breaks the parity in the z-direction as the excitation spectrum is no longer symmetric.

Source: The author, 2022.

ciple, is unstable, although it is arguable if this violation is physical since the momentum necessary to reach this instability is of Planck's mass scale (KOSTELECKÝ; LEHNERT, 2001). We will come back on this topic later.

1.5 Tuning massive to massless

In the current context, $U(1)$ chiral symmetry, unlike parity and time-reversal symmetries, does not survive in quantum theory. This is not a farfetched idea. There is no good reason in the physical world suggesting that every symmetry of classical physics is necessarily a symmetry of its quantum version. In those cases, the symmetry is dubbed anomalous. In the chiral case, the anomaly can be traced to the path integral measure not being invariant under the classical symmetry. This is one of the possible ways to understand it since it is possible to compute the anomaly by other paths as in (FRASER, 1985; AITCHISON; FRASER, 1985). The fact that chiral symmetry is anomalous leads to the expectation that it is only valid in the low energy approximation. In other words, the system described by Weyl fermions (chiral invariant action) is generically uncommon since any "higher" energy contribution would lead to the appearance of a mass term that breaks chiral symmetry. The inclusion of the b_μ term changes this notion because, with the right choice of parameters, it is possible to obtain effective massless dispersion relations. That is, although the Lagrangian has a mass term, the energy and momentum relations have gapless points. Looking at graph 2d (from the last section), it is possible to see that a fine-tune b_μ (in that case $b_z^2 > m^2$) closes the mass gap. More generically this condition translates to imposing $-b_\mu b^\mu = -b_0^2 + b_i^2 < m^2$. The difference between the system described by Weyl action (in graphs 2a) and the one with the special condition on the b_μ term (in graphs 2d) is the high energy spectrum (in the first is gapless, the second is not) but this does not change the low energy description (if we measure the momentum relative to the touching point[1]). Now, for a gap to be opened in the dispersion relations, it is necessary that $b_i^2 < m^2$ (as one can infer from graph 2b and 2c). The presence of the b_0 term does not change this conclusion as its main effect is to shift the touching points as one can see in graph 3. This analysis will be necessary for the discussion in chapter 3. This finishes the chapter, and in the next one, we will do (mostly) the computation of the effective theory that originates from the system studied here.

[1] These points are also called Weyl points of nodes in general

2 EFFECTIVE THEORY CALCULATION

In this chapter, I will compute the low energy description of the Dirac/Weyl actions in the presence of the b_μ term. The result is the electrodynamics coupled to an Axion-like space-time dependent term (non-dynamical). Along with this calculation, we will discuss some concepts (like the definition of effective action), as they will be essential later on. The first one to be explored will be the fermions interacting with the gauge field in the presence of the b_μ term. This is a somehow basic example of how to proceed with the fermionic integration to obtain an effective Lagrangian by the use of the Fujikawa method (nontrivial transformation of the path integral by a chiral rotation). I will also discuss (briefly) its connection with the high energy community concept of Lorentz invariance breaking theory. Next (section 2.2), I particularize the b_μ to be an angle and make the connection with an emergent effect at the boundary of two different systems known as the TME (topological magnetic electric) effect. Finally, section 2.3 is dedicated to the formation of a dynamical axion in the effective theory via the inclusion of a chiral breaking interaction term. This is a review of the works of (WANG; ZHANG, 2013; MACIEJKO; NANDKISHORE, 2014; YOU; CHO; HUGHES, 2016) and serves as a basic calculation for our model that will be discussed in chapter 4.

The same caveat as the last chapter is in order. This work is not an extensive review of none of the topics treated here. The introduction of the topics will be done as needed, and appropriate references will be provided.

2.1 Axion electrodynamics

We start with a theoretical description of a system composed of two Weyl points that are separated in momentum and energy. This situation can be conveniently expressed by a Dirac action where the right and left Weyl modes are arranged, again, in a Dirac spinor $\psi = \begin{pmatrix} \psi_L \\ \psi_R \end{pmatrix}$ with $\overline{\psi} = \psi^\dagger \gamma^0 = \begin{pmatrix} \psi_R^\dagger & \psi_L^\dagger \end{pmatrix}$

$$S_0 = \int \mathrm{d}^4x\, \overline{\psi}(x) \left(i\partial\!\!\!/ - m + b\!\!\!/\gamma^5 + ieA\!\!\!/(x) \right) \psi(x), \tag{36}$$

along with electromagnetic gauge potential A_μ action

$$S_{\text{Maxwell}} = \int \mathrm{d}^4x \left(-\frac{1}{4} F_{\mu\nu} F^{\mu\nu} \right) \tag{37}$$

so that generating function is

$$Z = \int \mathcal{D}\Big(\psi^\dagger, \psi, A\Big) e^{i(S_0 + S_{\text{Maxwell}})} \ . \tag{38}$$

In this notation $\mathcal{D}\Big(\psi^\dagger, \psi, A\Big)$ stands for $\mathcal{D}\psi^\dagger\mathcal{D}\psi\mathcal{D}A$ that is the usual path integral measure. In order to obtain the effective description in term of the gauge field alone we must integrate the fermions degree of freedom in the path integral. This is a well-known computation but, since we must include the contribution of the chiral anomaly, I will follow it in some detail. This procedure can be found textbooks like (PESKIN; SCHROEDER, 1995; SCHWARTZ, 2013; ZEE, 2010; PESKIN; SCHROEDER, 1995) but I will follow the more direct steps of (ZYUZIN; BURKOV, 2012) to some extent (some other details can be found in Appendix A). The method of derivation of the anomaly contribution is based on Fujikawa's work (FUJIKAWA, 1979; FUJIKAWA; SUZUKI, 2004) and is cored on the realization that the path integral measure is sensible to chiral gauge transformations.

The first step is to eliminate b_μ from the Lagrangian in eq. (36). This can be done by performing a (local) chiral transformation

$$\psi(x) \to \psi'(x) = e^{i\frac{1}{2}\beta(x)\gamma^5}\psi(x) \ , \tag{39}$$

leading to

$$\begin{aligned} S_0 \to S_0' &= \int \mathrm{d}^4x \, \overline{\psi}(x) \left(i\partial\!\!\!/ - \partial\!\!\!/\beta(x)\gamma^5 + b\!\!\!/\gamma^5 + ieA\!\!\!/(x) \right) \psi(x) \ , \\ &= \int \mathrm{d}^4x \, \overline{\psi}(x) \left(i\partial\!\!\!/ - b\!\!\!/\gamma^5 + b\!\!\!/\gamma^5 + ieA\!\!\!/(x) \right) \psi(x) \ , \\ &= \int \mathrm{d}^4x \, \overline{\psi}(x) \left(i\partial\!\!\!/ + ieA\!\!\!/(x) \right) \psi(x) \ , \\ &= \int \mathrm{d}^4x \, \overline{\psi}(x) \left(iD\!\!\!\!/ \right) \psi(x) \ , \end{aligned} \tag{40}$$

where it was used $\beta(x) = 2b_\mu x^\mu$. This is, of course, not a symmetry of the action, but just a change in the fermionic variables. The principal point in Fujikawa's work that in the quantum path integral formulation, this transformation gives rise to a non-trivial contribution from the Jacobian of the fermionic integration measure

$$\mathcal{D}\Big(\psi^\dagger, \psi, A\Big) \to \mathcal{D}\Big(\psi'^\dagger, \psi', A\Big) = \mathcal{J}^{-2} \cdot \mathcal{D}\Big(\psi^\dagger, \psi, A\Big) \ , \tag{41}$$

where $\mathcal{J}$ is the determinant of the chiral transformation. The explicit computation must be carefully done since it involves the regularization of the eigenstate sum in a gauge-invariant (a brief review can be found in appendix A, or one can use any of the previously mentioned references like (PESKIN; SCHROEDER, 1995; SCHWARTZ, 2013; ZYUZIN;

BURKOV, 2012)). The result is

$$\mathcal{J} = \exp\left[-\frac{ie^2}{32\pi^2}\int \mathrm{d}^4x\,\beta(x)\epsilon_{\mu\nu\alpha\kappa}F^{\mu\nu}F^{\alpha\kappa}\right] . \tag{42}$$

Now we can add the anomaly contribution (equation (41) and (42)) to the functional (38) resulting in

$$Z = \int \mathcal{D}\Big(\psi^\dagger,\psi,A\Big)e^{i\left(S_0'+S_{\text{Anomaly}}+S_{\text{Maxwell}}\right)} , \tag{43}$$

with

$$S_{\text{Anomaly}} = \frac{e^2}{32\pi^2}\int \mathrm{d}^4x\,\beta(x)F\tilde{F} , \tag{44}$$

where $F\tilde{F} = F^{\mu\nu}\tilde{F}_{\mu\nu} = \frac{1}{2}\epsilon_{\mu\nu\alpha\beta}F^{\mu\nu}F^{\alpha\beta}$. The resulting theory consists of fermions and photons, and the effect of the b_μ is encoded in the anomaly term. The fermions in this context are part of the free asymptotic states allowed. If one is interested on the contribution on which the fermion degree of freedom are not excited then one must integrate out the fermions degree of freedom. Mathematically, the functional generating of the full microscopic system is

$$Z(j,\eta) = \int \mathcal{D}\Big(\psi^\dagger,\psi,A\Big)e^{i\left(S_0+S_{\text{Maxwell}}+\int \mathrm{d}^4x\left(\overline{\eta}\psi+\overline{\psi}\eta+j_\mu A^\mu\right)\right)} , \tag{45}$$

where j_μ and η are the external sources for the photon and electron fields, they are the external perturbation which generates the n-point function (discussed briefly in section 1.1). The effective action, that lacks the "integrated out" fermionic fields, is (usually) non renormalizable, and is valid in a certain range of energies. I will follow the notation of (SCHWARTZ, 2013) and refer to the effective action as Γ with $\Gamma = \int \mathrm{d}^4x\,\mathcal{L}_{\text{eff}}(x)$ so that $\mathcal{L}_{\text{eff}}(x)$ is the effective Lagrangian. The functional integration of the fermionic field is

$$Z(j) \equiv Z(j,\eta)\Big|_{\eta=\overline{\eta}=0} = \int \mathcal{D}(A)e^{i\left(\Gamma+S_{\text{Anomaly}}+S_{\text{Maxwell}}+\int \mathrm{d}^4x j_\mu A^\mu\right)}. \tag{46}$$

The computation of Γ in

$$e^{i\Gamma} = \int \mathcal{D}\Big(\psi^\dagger,\psi\Big)e^{iS_0} = e^{i\int \mathrm{d}^4x\mathcal{L}_{\text{eff}}(x)} , \tag{47}$$

the effective Lagrangian, is not straightforward as we will see. The first step is to write the fermionic integration as

$$\int \mathcal{D}\Big(\psi^\dagger,\psi\Big)e^{iS_0} = \mathcal{N}\det\Big(i\not{D}\Big) , \tag{48}$$

and, mathematically, this expression is

$$
\begin{aligned}
\det\Big(i\not{D}\Big) &= \det\Big(i\not{\partial} - e\not{A}\Big) \;, \\
&= \det\Big(i\not{\partial}\Big)\det\bigg(1 - \frac{1}{i\not{\partial}}\Big(-ie\not{A}\Big)\bigg) \;, \\
&= \exp\bigg[\mathrm{Tr}\Big(\ln\Big(i\not{\partial}\Big)\Big)\,\mathrm{Tr}\bigg(\ln\bigg(1 - \frac{1}{i\not{\partial}}\Big(-ie\not{A}\Big)\bigg)\bigg)\bigg] \;, \\
&= e^{\mathrm{Tr}\left(\ln\left(i\not{\partial}\right)\right)}\exp\bigg[\mathrm{Tr}\bigg(\ln\bigg(1 - \frac{1}{i\not{\partial}}\Big(-ie\not{A}\Big)\bigg)\bigg)\bigg] \;.
\end{aligned}
\tag{49}
$$

The first term is an infinite constant and is fixed by setting $Z|_{\psi=0} = 1$, this sets $\mathcal{N}$ and we can suppress this from now on. Expanding the remaining part results in

$$
\det\Big(i\not{D}\Big) = \exp\bigg[-\sum_{n=1}\frac{1}{n}\,\mathrm{Tr}\bigg[\bigg(\frac{-ie\not{A}}{i\not{\partial}}\bigg)^n\bigg]\bigg] \;. \tag{50}
$$

Going back to the effective action one can write

$$
Z(j) = \int \mathcal{D}(A)e^{i\left(S_{\mathrm{eff}} + S_{\mathrm{Anomaly}} + S_{\mathrm{Maxwell}} + \int \mathrm{d}^4x j_\mu A^\mu\right)} \;, \tag{51}
$$

with

$$
\mathcal{S}_{\mathrm{eff}} = \sum_{n=1}\frac{i}{n}\,\mathrm{Tr}\bigg[\bigg(\frac{-ie\not{A}}{i\not{\partial}}\bigg)^n\bigg] \;. \tag{52}
$$

In terms of Feynman's diagrams, this expression is the fermion bubble with n insertion of gauge lines (see (PESKIN; SCHROEDER, 1995) for more details on this computation), which translates to

$$
\sum_{n=1}\frac{i}{n}\,\mathrm{Tr}\bigg[\bigg(\frac{-ie\not{A}}{i\not{\partial}}\bigg)^n\bigg] \rightarrow
$$

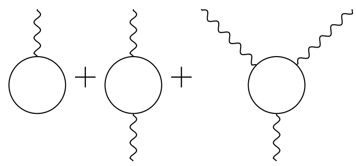

$$
+\cdots \;. \tag{53}
$$

The problem is that this expression is ill-defined since the fermion bubble has an IR-divergence. We can see this by opening one of the graphs

$$
\begin{aligned}
\propto \mathrm{Tr}\bigg[\bigg(\frac{-ie\not{A}}{i\not{\partial}}\bigg)^2\bigg] &= -e^2\,\mathrm{Tr}\bigg[\frac{1}{\not{p}}\not{A}\frac{1}{\not{p}}\not{A}\bigg] \\
&= -e^2\int\frac{\mathrm{d}^4p}{(2\pi)^4}\frac{1}{(p^2)^2}\,\mathrm{Tr}\Big[\not{p}\not{A}\not{p}\not{A}\Big] \\
&= -e^2A^2\frac{1}{2}\int\frac{\mathrm{d}^4p}{(2\pi)^4}\frac{1}{p^2}
\end{aligned}
\tag{54}
$$

where the last integral is divergent. If we had included a mass term for the fermions, i.e.

$m\overline{\psi}\psi$, in the initial action, this problem is bypassed but the computation involving the chiral rotation becomes trickier. As we saw in equation (29) of section 1.3, the mass term breaks chirality, meaning that it is not invariant under the chiral transformation (defined in eq. (39) as $\psi(x) \to e^{i\beta\gamma_5}\psi$).

I will skip the recalculation and naively introduce the mass term in the effective action since this particular system was extensively studied in the context of an extension of the standard model to include violations of the Lorentz symmetry in $U(1)$ gauge sector since the 90's (CARROLL; FIELD; JACKIW, 1990; COLLADAY; KOSTELECKÝ, 1998; JACKIW; KOSTELECKÝ, 1999). Beyond mathematical details, the main difference that the inclusion of the mass term generates is the ambiguity in the exact relation between the term microscopic parameter b_μ and the generated correction k_μ (JACKIW, 2000). In the previous case, the term $\overline{\psi}\not{b}\gamma^5\psi(x)$ generated (with $\beta(x) = 2b_\mu x^\mu$)

$$S_{\text{Anomaly}} = \frac{e^2}{32\pi^2}\int \mathrm{d}^4x\, \beta(x) F\tilde{F} = \int \mathrm{d}^4x\, \epsilon_{\mu\nu\alpha\kappa} k^\mu A^\nu F^{\alpha\kappa} \tag{55}$$

where $k^\mu = -\frac{ie^2}{16\pi^2}b^\mu$. The question of the proper value of the correction triggered a series of theoretical investigations, e.g. using Fujikawa's method (PÉREZ-VICTORIA, 1999), non-perturbative analysis in b_μ (CHEN, 2001), symmetry, and causality restraints (COLEMAN; GLASHOW, 1999; CIMA et al., 2010; ADAM; KLINKHAMER, 2001). Some results are (for a more detailed list/description on the results and possible origins on the ambiguity consult (CHEN, 2001))

- $k_\mu = 0$ (ADAM; KLINKHAMER, 2001; COLEMAN; GLASHOW, 1999; CARROLL; FIELD, 1997);
- $k_\mu = \frac{3e^2}{16\pi^2}b_\mu$ (CARROLL; FIELD; JACKIW, 1990; COLLADAY; KOSTELECKÝ, 1998; JACKIW; KOSTELECKÝ, 1999);
- $k_\mu = Cb_\mu$, C is an arbitrary constant, (CHUNG, 1999; FREEDMAN; JOHNSON; LATORRE, 1992);
- $k_\mu = \frac{e^2}{8\pi^2}b_\mu$ (CHAN, 1986; GAILLARD, 1986).

Past those inquiries, it is usual to investigate the general consistency factors (namely stability, causality, and unitarity) of Lorentz violating theories. The microscopic (fermionic) theory with the mentioned LIV term is well behaved if one ignores the stability issue, but the effective theory does have more deep problems. The space-like constant vector does not introduce problems on those factors, the same is not true for the time-like b_μ which introduces problems in both stability and causality (ADAM; KLINKHAMER, 2001; KOSTELECKÝ; LEHNERT, 2001). It is important to remember that, even if those effects are present in nature, experimental bounds dictates that any LIV parameter is extremely small (KOSTELECKÝ; RUSSELL, 2011).

Beyond those points, the resulting contributions must be gauge invariant. We can see this (and avoid doing the very extensive calculation) in a simple way. Before the fermionic integration, the system is gauge invariant, as expected by

$$Z[\psi, A_\mu] \to Z\Big[\psi e^{i\alpha(x)}, A_\mu + \frac{1}{e}\partial_\mu \alpha(x)\Big] = Z[\psi, A_\mu] \ , \tag{56}$$

where the $[\cdots]$ indicates the field content. After the integration of the spinor degree of freedom, this must still be true, gauge symmetry is not anomalous here. That means that

$$Z[A_\mu] \to Z\Big[A_\mu + \frac{1}{e}\partial_\mu \alpha(x)\Big] = Z[A_\mu] \ . \tag{57}$$

The same transformation can be done in the effective Lagrangian

$$\int \mathcal{D}A e^{iS_{\text{eff}}(A_\mu)} = \int \mathcal{D}A e^{iS_{\text{eff}}(A_\mu + \frac{1}{e}\partial_\mu \alpha(x))} \ , \tag{58}$$

so it must be true that

$$\mathcal{L}_{\text{eff}}(A) = \mathcal{L}_{\text{eff}}(F) \ . \tag{59}$$

This is one of the ways to verify the gauge invariance of the effective action. All terms that originate from the trace expansion are powers of F^2 (akin to Euler–Heisenberg Lagrangian). In the end, the low energy effective theory does not contain external fermions and can be schematically written as

$$\mathcal{S} = \int \mathrm{d}^4x \left[-\frac{1}{4}F^2 + \frac{e^2}{32\pi^2}\beta(x)F\tilde{F} + j_\mu A^\mu + (\text{powers of } F^2) \right] . \tag{60}$$

So, in essence, this system naturally displays a non-dynamical axion-like term $\beta(x)$ (this nomenclature is due to the resemblance between the result and the hypothetical Axion particle coupling originally introduced by Wilczek (WILCZEK, 1987)) that encodes the energy-momentum separation of the Weyl nodes and any power of the tensor field strength. Historically, in high energy physics, the axion was proposed to solve the CP problem in quantum chromodynamics (QCD) (PECCEI; QUINN, 1977b; WEINBERG, 1978b; WILCZEK, 1978). This problem consists of the non-observation of $\mathbb{P}$ and $\mathbb{T}$ symmetry[2] violations in QCD experiments or, similarly, that the violating parameter theta is extremely small. A solution to this to this unpleasant fine-tuning was proposed by Peccei and Quinn (PECCEI; QUINN, 1977b; PECCEI; QUINN, 1977a) (see (PECCEI, 2008) for a review) that promoted the theta parameter to a dynamical field associated with a new

[2] In HEP it is usual to use CP instead of $\mathbb{T}$ since the only difference between the two transformations is that CP is unitary and $\mathbb{T}$ is anti-unitary.

pseudoscalar particle called axion (by Wilczek (WILCZEK, 1978)). This formulation has been investigated with no success and was ultimately discarded but this generated other constructions with different fields such as the "invisible Axion" models that are still alive as viable options (KIM, 1979; SHIFMAN; VAINSHTEIN; ZAKHAROV, 1980; DINE; FISCHLER; SREDNICKI, 1981). Beyond this trail, Axion physics has been revisited repeatedly over the years upon the expectation that it can serve as a good description of a variety of phenomena. As we will see in chapter 3, the previous action can be linked to the phenomenology of topological materials.

On linear order (ignoring the higher-order terms in the field strength tensor), this action is responsible for the phenomenology described by the following equations of motion

$$\begin{aligned} \nabla\cdot\boldsymbol{E} &= \rho + \frac{e^2}{8\pi^2}\nabla\beta\cdot\boldsymbol{B} \ , \\ \nabla\times\boldsymbol{E} &= -\frac{\partial\boldsymbol{B}}{\partial t} \ , \\ \nabla\cdot\boldsymbol{B} &= 0 \ , \\ \nabla\times\boldsymbol{B} &= \frac{\partial\boldsymbol{E}}{\partial t} + \boldsymbol{j} + \frac{e^2}{8\pi^2}\left(\frac{\partial\beta}{\partial t}\boldsymbol{B} + \nabla\beta\times\boldsymbol{E}\right) \ . \end{aligned} \tag{61}$$

We can extract some insight from these equations of motion as to what happens in the region that β varies. The first equation indicates that, in this region, a magnetic field act as a source for the electric field, and the last equation tells us that the combination $\frac{\partial\beta}{\partial t}\boldsymbol{B} + \nabla\beta\times\boldsymbol{E}$ acts as a current if there is a temporal variation of beta and the magnetic field or space variation and perpendicular electric field.

Computing the derivative of the effective Lagrangian (to linear order) in terms of the electric field (using eq. (11)) gives the electric polarization $\mathbf{D}$

$$\mathbf{D} = \frac{\partial\mathcal{L}_{\text{eff}}}{\partial\mathbf{E}} = \mathbf{E} - \frac{e^2}{8\pi^2}\beta\mathbf{B} \ , \tag{62}$$

and in terms of the magnetic field the magnetic polarization $\mathbf{H}$

$$\mathbf{H} = -\frac{\partial\mathcal{L}_{\text{eff}}}{\partial\mathbf{B}} = \mathbf{B} + \frac{e^2}{8\pi^2}\beta\mathbf{E} \ . \tag{63}$$

The presence of the β term changes the constituent relations that are necessary to understand how the electric and magnetic fields polarizes the system. The cross-field polarization (an electric field induce an magnetization and vice-versa) is known as TME (topological magneto-electric) effect (QI et al., 2009b; KANE; MELE, 2005; MOORE, 2010) and we will revisit this in chapter 3.

Beyond this, we can compute the change in the action in terms of the gauge field

A_μ. This results in what is called "topological currents" represented by

$$j_\alpha = \frac{e^2}{4\pi^2} b_j \epsilon_{j\nu\alpha\beta} \partial_\nu A_\beta \qquad \text{or} \qquad \boldsymbol{j} = \frac{e^2}{4\pi^2} \boldsymbol{E} \times \boldsymbol{b} \ , \tag{64}$$

that describes the anomalous Hall effect (AHE). This phenomenon is characterized by the appearance of the Hall resistance even in the absence of an external magnetic field (here the driven factor is the presence of an external magnetic field and an orthogonal background space-like vector $\boldsymbol{b}$. The other relevant phenomena are given by

$$j_\alpha = -\frac{e^2}{4\pi^2} b_0 \epsilon_{0\nu\alpha\beta} \partial_\nu A_\beta \qquad \text{or} \qquad \boldsymbol{j} = \frac{e^2}{4\pi^2} b_0 \boldsymbol{B} \ , \tag{65}$$

which is the chiral magnetic effect (CME). This effect is peculiar since it indicates that a static magnetic field generates an electric current. More on these two in chapter 3.

2.2 $\theta = 0$ or π electrodynamics

The discussion done in the last section about the chiral phase in the mass term can be made "trivial" by removing the space-time dependency and choosing $\beta(x) = \theta$ with θ being 0 or π so that

$$m\bar{\psi}\psi \to \begin{cases} +m\bar{\psi}\psi, & \text{for } \theta = 0 \\ -m\bar{\psi}\psi, & \text{for } \theta = \pi \ . \end{cases} \tag{66}$$

This removes completely b_μ from the action since the choice of $\beta = 2b_\mu x^\mu$ is no longer possible because it must now be space-time independent. The anomaly computation can follow the same path if the mass term obey[3]

$$\begin{cases} m > 0, & \text{for } \theta = 0 \\ m < 0, & \text{for } \theta = \pi \ , \end{cases} \tag{67}$$

and the resulting anomaly term is

$$S_{\text{Anomaly}} = \frac{e^2\theta}{32\pi^2} \int \mathrm{d}^4x \, F\tilde{F} \tag{68}$$

[3] One could think that the mass parameter variates in one direction as $m(z)$ equals $+m$ for $z > 0$ and $-m < 0$ ($z = 0$ is a smooth transition as we expect from the discussion in the next part of this section). In this way, we only do the chiral rotation for the region $z < 0$ and introduce the nontrivial theta term.

where $F\tilde{F} = F^{\mu\nu}\tilde{F}_{\mu\nu} = \frac{1}{2}\epsilon_{\mu\nu\alpha\beta}F^{\mu\nu}F^{\alpha\beta}$ as always. The affirmation that θ equals 0 or π is not fully correct. The theta term, to be compatible with the topology of the $U(1)$ gauge theory, is periodic mod 2π (or $\theta \in [0, 2\pi)$). There are various derivations of this condition based on different assumptions (see (VAZIFEH; FRANZ, 2010; WITTEN, 2016) for two examples[4]) but the principal point is that, after imposing suitable boundary conditions, the action obeys

$$S_{\text{Anomaly}} = \theta N \qquad \text{with } N \in \mathbb{Z} \tag{69}$$

Following this, the generating functional becomes

$$\exp\left(iS_{\text{Anomaly}}\right) = e^{iN\theta} \tag{70}$$

which deduces that the values of theta are periodic mod 2π. This open an interesting case, the θ contribution, together with the Maxwell term is

$$\mathcal{L}_{\text{eff}} = \frac{1}{2}(\mathbf{E}^2 - \mathbf{B}^2) + \frac{e^2}{8\pi^2}\theta\mathbf{B}\cdot\mathbf{E} \tag{71}$$

Under parity $\mathbb{P}$ (rules in eq. (23)) and time-reversal $\mathbb{T}$ (rules in eq. (24)) this term transform as

$$\mathbb{P}: \quad \mathbf{B}\cdot\mathbf{E}(t,\vec{\mathbf{x}}) \to \mathbf{B}\cdot(-\mathbf{E})(t,-\vec{\mathbf{x}}), \tag{72}$$

$$\mathbb{T}: \quad \mathbf{B}\cdot\mathbf{E}(t,\vec{\mathbf{x}}) \to (-\mathbf{B})\cdot\mathbf{E}(-t,\vec{\mathbf{x}}), \tag{73}$$

meaning that

$$\mathbb{P} \text{ or } \mathbb{T}: \quad \theta \to -\theta. \tag{74}$$

This translates to the affirmation that a generic θ breaks both parity and time-reversal but, there is a clear exception which is the value of $\theta = 0$. The interesting is that another value is possible once we consider the definition of θ up mod 2π; the value of $\theta = \pi$ is also valid in this case. Both values correspond to equivalent systems, which are $\mathbb{P}$ and $\mathbb{T}$ invariant. If we include the fact that the origin of this quantization lies on the topology of the U(1) gauge theory we can expect that the value of $\theta = \pi$ has non-trivial topology. This is what happens in the so-called topological insulators (QI; HUGHES; ZHANG, 2008) which have two distinct phases (or has a $\mathbb{Z}_2$ classification). The first one is the normal (or trivial) insulator phase with $\theta = 0$ (mod 2π), the second is the topological time-reversal invariant insulator with $\theta = \pi$ (mod 2π). We will leave most of the discussion involving

[4] Another good material is David Tong's lectures on Gauge Theory (TONG, 2018).

topological insulators and their relevance in condensed matter to chapter 3. Here we will concentrate on more generic features linked to the field theory characterization.

Let us examine a few characteristics of this model. The effect of the theta term is non-trivial as well since a partial derivative on the effective action indicates that theta term does not contribute to the system dynamics since it is a total derivative, e.g.

$$S_{\text{Anomaly}} = \frac{e^2\theta}{32\pi^2}\int \mathrm{d}^4x\,\partial_\mu(\epsilon^{\mu\nu\rho\sigma}A_\nu\partial_\rho A_\sigma)\ , \tag{75}$$

this suggests that the non-trivial contribution occurs due to the boundary effects. One easy way to see this is to compute the modification of the constituent relations introduced by the θ. Varying the Lagrangian in terms of the electric field (similar to the computation in the final part of sec. 2.1) gives the electric polarization $\mathbf{D}$

$$\mathbf{D} = \frac{\partial\mathcal{L}}{\partial\mathbf{E}} = \mathbf{E} - \frac{e^2}{8\pi^2}\theta\mathbf{B}\ , \tag{76}$$

and in terms of the magnetic field the magnetic polarization $\mathbf{H}$

$$\mathbf{H} = -\frac{\partial\mathcal{L}}{\partial\mathbf{B}} = \mathbf{B} + \frac{e^2}{8\pi^2}\theta\mathbf{E}\ . \tag{77}$$

Those modified constitutive relations indicate that it is possible to generate a mixed polarization when θ changes from one constant value to the other one. This is exactly what one expects to happen in the boundary between a usual and topological insulator. The smooth change between $\theta = 0$ and $\theta = \pi$ produces a magnetic polarization in the electric field and vice-versa. Another similar form to reaching those conclusions is to do a partial derivation on the anomaly contribution, and consider the variation of θ in the μ "direction" at the boundary as $\partial_\mu\theta$, reaching

$$S_{\text{Anomaly}} = -\frac{e^2}{32\pi^2}\int \mathrm{d}^4x\,\epsilon^{\mu\nu\rho\sigma}(\partial_\mu\theta)A_\nu\partial_\rho A_\sigma\ . \tag{78}$$

Now, varying the action in terms of gauge field results in what is called "topological currents" represented by

$$j_\alpha = \frac{e^2}{4\pi^2}\partial_j\theta\epsilon_{j\nu\alpha\beta}\partial_\nu A_\beta \qquad \text{or} \qquad \boldsymbol{j} = \frac{e^2}{4\pi^2}\boldsymbol{E}\times\boldsymbol{\partial}\theta \tag{79}$$

$$j_\alpha = -\frac{e^2}{4\pi^2}\partial_0\theta\epsilon_{0\nu\alpha\beta}\partial_\nu A_\beta \qquad \text{or} \qquad \boldsymbol{j} = \frac{e^2}{4\pi^2}\partial_t\theta\boldsymbol{B}\ , \tag{80}$$

that describes the anomalous Hall effect (AHE), and the chiral magnetic effect (CME) but only on the boundary where the value of θ changes from $\theta = 0$ to $\theta = \pi$. This is commonly known as topological magneto-electric (TME) effect (QI et al., 2009b; KANE; MELE, 2005; MOORE, 2010) and is responsible for some interesting phenomena on its boundary[5]. An interesting effect occurs when an electric charge is placed near a topological insulator induces, the induced mirror charge inside the material has magnetic charge and it is possible to realize the Witten effect (QI et al., 2009a) that assign a fractional electric charge to a magnetic monopole (thus appearing to be a dyon) (WITTEN, 1979). We will revisit those topics in section 3.

2.3 Dynamical axion electrodynamics

As pointed out in (WANG; ZHANG, 2013; MACIEJKO; NANDKISHORE, 2014; YOU; CHO; HUGHES, 2016), if one is interested in dynamic Axion-like field then it is a fruitful endeavor to include an interaction. This allows for the chiral symmetry to be dynamically broken due to the formation of a chiral condensation induced by the four fermions pairing, as we will see. The starting point is the same as the section 2.1 but, with the inclusion of the interaction the system is

$$Z = \int \mathcal{D}\Big(\psi^\dagger, \psi, A\Big) e^{i\left(S_0 + S_{\text{Maxwell}} + \int \mathrm{d}^4x \mathcal{L}_{\text{int}}\right)} \ , \tag{81}$$

with S_0 being given by eq. (36) and S_{Maxwell} by (37). The pairing in this case is

$$\mathcal{L}_{\text{int}} = -\lambda^2 \left(\overline{\psi}(x) P_L \psi(x)\right) \left(\overline{\psi}(x) P_R \psi(x)\right) \ , \tag{82}$$

where $P_L = \frac{1}{2}(1 - \gamma^5)$ and $P_R = \frac{1}{2}(1 + \gamma^5)$ are chiral projectors and the coupling λ has mass dimension -1 as expected to give the action term the correct mass dimension. Note that this pairing connects left and right handed fields as one can see in

$$\begin{aligned} \overline{\psi}(x) P_L \psi(x) &= \psi_R^\dagger(x) \psi_L(x) \\ \overline{\psi}(x) P_R \psi(x) &= \psi_L^\dagger(x) \psi_R(x) \end{aligned} \tag{83}$$

so that $\mathcal{L}_{\text{int.}} = -\lambda^2 \Big(\psi_R^\dagger \psi_L\Big) \Big(\psi_L^\dagger \psi_R\Big)$ (for more details on this interaction see appendix D). To "decouple" the interaction term, one can use a auxiliary complex field $\phi(x)$. In this case, we can choose

$$\begin{aligned} \phi(x) &= \lambda \overline{\psi}(x) P_L \psi(x) \ , \\ \phi^*(x) &= \lambda \overline{\psi}(x) P_R \psi(x) \ . \end{aligned} \tag{84}$$

[5] Other intriguing topics could be discussed, like the connection between the Atiyah-Singer index theorem and Fermi zero modes, which links to integer quantities with two distinct origins. One is an integer because of quantum mechanics and the other because of the topology. See lectures on Gauge Theory (TONG, 2018).

The auxiliary field ϕ respects $\mathbb{C}, \mathbb{T}$, and $U(1)$, but it transforms under chiral rotation and Parity $\mathbb{P}$ (see, respectively, appendix D.4, D.3, D.5, D.6 and D.2 for more information). Specifically, if the spinor field transforms under chirality as $\psi \to e^{i\beta\gamma_5}\psi$ then the field transforms as $\phi(x) \to e^{-2i\beta}\phi(x)$. Using this auxiliary fields the interaction term can be "decoupled" through the Hubbard-Stratanovich transformation (see (ALTLAND; SIMONS, 2010) for more details)

$$e^{-\lambda^2\left(\psi_R^\dagger\psi_L\right)\left(\psi_L^\dagger\psi_R\right)} = \int \mathcal{D}(\phi,\phi^*)e^{\int \mathrm{d}^4x\left(|\phi|^2-\lambda(\phi^*\overline{\psi}P_L\psi+\phi\overline{\psi}P_R\psi)\right)} \ . \tag{85}$$

This transformation introduces dynamics (it is integrated in the field functional) for the complex scalar field $\phi(x)$ so that

$$Z[\psi, A] \to Z[\psi, A, \phi] = \int \mathcal{D}\left(\psi^\dagger, \psi, A, \phi, \phi^*\right)e^{i\left(S_0+S_{\text{Maxwell}}+\int \mathrm{d}^4x\mathcal{L}_{\text{H-S}}\right)} \ , \tag{86}$$

where, again, the $(\cdots)$ indicates the field content of the generating functional, with HS action

$$\mathcal{L}_{\text{H-S}} = -\lambda\overline{\psi}(x)(\phi^*P_L + \phi P_R)\psi(x) + |\phi|^2 \ . \tag{87}$$

Now the process is similar to section 2.1, we can eliminate the b_μ term with the transformation $\psi(x) \to \psi' = e^{i\frac{1}{2}\beta(x)\gamma^5}\psi(x)$ with $\beta(x) = 2b_\mu x^\mu$. As expected, this also contribute with a non-trivial factor to the Jacobian integration measure, the chiral anomaly. Following similar steps as to the ones done in section 2.1, the system becomes

$$Z = \int \mathcal{D}\left(\psi^\dagger, \psi, A, \phi, \phi^*\right)e^{i\left(S_0'+S_{\text{Maxwell}}+S_{\text{Anomaly}}+\int \mathrm{d}^4x\mathcal{L}'_{\text{H-S}}\right)} \ , \tag{88}$$

with $\mathcal{L}_0' = \overline{\psi}(x)\left(i\not{D}\right)\psi(x)$ and $\mathcal{L}_{\text{Anomaly}} = \frac{e^2}{32\pi^2}\beta(x)F\tilde{F}$ and, as noted before, the Hubbard-Stratanovich auxiliary complex field $\phi(x)$ also transforms and their Lagrangian becomes

$$\mathcal{L}_{\text{H-S}} \to \mathcal{L}'_{\text{H-S}} = -\lambda\overline{\psi}(x)e^{i\beta\gamma_5}(\phi^*P_L + \phi P_R)\psi(x) + |\phi|^2 \ . \tag{89}$$

It is argued in (WANG; ZHANG, 2013; MACIEJKO; NANDKISHORE, 2014) that the strong coupling dynamics of the theory favor the formation of a condensate $\langle\phi\rangle \neq 0$, resulting in the dynamical break of the chiral symmetry resulting in the appearance of a new pseudoscalar particle akin to the axion in the Peccei-Quinn mechanism. Supposing that small fluctuations around the condensate $\langle\psi_R^\dagger(x)\psi_L(x)\rangle = v^3$ can be approximated by

$$\phi(x) = \lambda v^3 e^{i\frac{\theta(x)}{f}} \tag{90}$$

where f is a mass scale and v^3 is a constant of mass dimension 3. This also changes the integral measure from $\mathcal{D}(\phi, \phi^*)$ to $\mathcal{D}\theta$, i.e. the only degree of freedom relevant is the "phase" $\theta(x)$[6]. This allows for the interaction part to be written as

$$\begin{aligned} \phi^* P_L + \phi P_R &= \frac{\lambda v^3}{2}\left(e^{-i\frac{\theta(x)}{f}}(1-\gamma_5) + e^{i\frac{\theta(x)}{f}}(1+\gamma_5)\right) \\ &= \lambda v^3\left(\cos\left(\frac{\theta(x)}{f}\right) + \gamma_5 \sin\left(\frac{\theta(x)}{f}\right)\right) \\ &= \lambda v^3 e^{i\frac{\theta(x)}{f}\gamma_5} \end{aligned} \tag{91}$$

also $|\phi|^2 = \lambda^2 v^6$. The Hubbard-Stratanovich Lagrangian becomes

$$\mathcal{L}'_{\text{H-S}} = -\lambda^2 v^3 \overline{\psi}(x) e^{i\left(\beta + \frac{\theta(x)}{f}\right)\gamma_5}\psi(x) + \lambda^2 v^6 \ . \tag{92}$$

Now we can do a field redefinition $\frac{\theta'(x)}{f'} = \beta(x) + \frac{\theta(x)}{f}$, to simplify the phase of the last equation, the scalar field leading to

$$\mathcal{L}'_{\text{H-S}} \to \mathcal{L}''_{\text{H-S}} = -\lambda^2 v^3 \overline{\psi}(x) e^{i\frac{\theta'(x)}{f'}\gamma_5}\psi(x) + \lambda^2 v^6 \ . \tag{93}$$

This field redefinition does not change the scalar field integral measure (only "relabels" $\mathcal{D}\theta$ to $\mathcal{D}\theta'$) but allow for the cancelation with the chiral rotation

$$\psi \to \psi' = e^{-\frac{i}{2}\frac{\theta'(x)}{f'}\gamma_5}\psi \tag{94}$$

so that

$$\mathcal{L}_{\text{H-S}} = -\lambda^2 v^3 \overline{\psi}(x)\psi(x) + \lambda^2 v^6 \ , \tag{95}$$

where the $''$ were dropped. We can not forget that this chiral rotation results in a new Jacobian for the anomaly with the $\frac{\theta'(x)}{f'}$ angle leading to

$$S_{\text{Anomaly}} = \int \mathrm{d}^4x \left(\beta(x) - \frac{\theta'(x)}{f'}\right)\frac{e^2}{32\pi^2}F\tilde{F} \tag{96}$$

where $F\tilde{F} = F^{\mu\nu}\tilde{F}_{\mu\nu} = \frac{1}{2}\epsilon_{\mu\nu\alpha\beta}F^{\mu\nu}F^{\alpha\beta}$ as always. One major difference from the computation done 2.1 is the contribution from the quadratic fermionic part leading to the appearance of a fermionic mass $-m\overline{\psi}(x)\psi(x)$ with $m = \lambda^2 v^3$, leading to the following

[6] This is equivalent to parametrizing the condensate with $\phi(x) = \lambda v^2 \eta(x) e^{i\frac{\theta(x)}{f}}$ and making the field $\eta(x)$ static.

fermionic Lagrangian

$$\mathcal{L}_{\text{fermion}} = \overline{\psi}(x)\left(i\not{D} - m - \frac{1}{2f'}\gamma_5\not{\partial}\theta'(x)\right)\psi(x)\ . \tag{97}$$

where the last term originates from the local chiral transformation 94. The final system of this computation is

$$Z = \int \mathcal{D}\left(\psi^\dagger, \psi, A, \theta'\right) e^{i\left(S_{\text{fermion}} + S_{\text{Maxwell}} + S_{\text{Anomaly}} + \lambda^2 v^6\right)}\ , \tag{98}$$

with S_{Maxwell} given by equation (37), S_{Anomaly} is equation (96) and S_{fermion} is equation (97). This finalizes the necessary steps on the microscopic fermionic system, and we can compute the effective action by integrating out the fermions degree of freedoms. I will drop the $'$ from the scalar field, and its factors, from now on. Following the same steps as 2.1 we obtain

$$Z(j) = \int \mathcal{D}(A, \theta) e^{i\left(S_{\text{eff}} + S_{\text{Anomaly}} + S_{\text{Maxwell}} + \int d^4x\left(\lambda^2 v^6 + j_\mu A^\mu + J\theta\right)\right)}\ , \tag{99}$$

with

$$S_{\text{eff}} = \sum_{n=1} \frac{i}{n} \operatorname{Tr}\left[\left(\frac{-ie\not{A} - \frac{1}{2}\gamma_5\not{\partial}\frac{\theta(x)}{f}}{i\not{\partial} - m}\right)^n\right]\ . \tag{100}$$

Again we can understand this expression in terms of Feynman's diagrams. This trace will generate various graphs, some are

$$\sum_{n=1} \frac{i}{n} \operatorname{Tr}\left[\left(\frac{-ie\not{A} - \frac{1}{2}\gamma_5\not{\partial}\frac{\theta(x)}{f}}{i\not{\partial} - m}\right)^n\right] \rightarrow$$

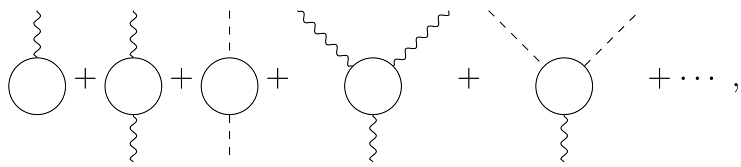

where the lines represent the scalar field (dashed), the photon (wave), and the fermion (solid) field. We can see that new interaction terms can be created from this computation and some general points can be explored here. The term proportional to the gauge field A alone contribute with the same terms that were described in 2.1, the fermion bubble with insertion of n insertion of gauge lines. Other terms are allowed to be included but, since gauge invariance is still valid, the resulting effective action must obey $\mathcal{L}_{\text{eff}}(F^2)$.

Another point is that there only can be generated graphs with an even number of scalar lines since θ carries a γ_5 matrix, the trace of an odd number of these is always zero (SCHWARTZ, 2013). The first contribution (third term of right hand side of last equation in momentum space), therefore, is

$$
\begin{aligned}
\propto \operatorname{Tr}\left[\left(\frac{\gamma_5 \not{\partial}\frac{\theta(x)}{f}}{i\not{\partial}-m}\right)^2\right] &= \operatorname{Tr}\left[\frac{1}{\not{p}-m}\gamma_5\not{\partial}\frac{\theta(x)}{f}\frac{1}{\not{p}-m}\gamma_5\not{\partial}\frac{\theta(x)}{f}\right] \\
&= \frac{1}{f^2}\int\frac{\mathrm{d}^4p}{(2\pi)^4}\frac{1}{(p^2-m^2)^2}\operatorname{Tr}\Big[(\not{p}+m)\gamma_5\not{\partial}\theta(x)(\not{p}+m)\gamma_5\not{\partial}\theta(x)\Big] \\
&= \frac{1}{f^2}\int\frac{\mathrm{d}^4p}{(2\pi)^4}\frac{1}{(p^2-m^2)^2}\Big(p_\mu\partial_\nu\theta p_\alpha\partial_\tau\theta\operatorname{Tr}[\gamma^\mu\gamma^\nu\gamma^\alpha\gamma^\tau]-m^2\partial_\mu\theta\partial_\nu\theta\operatorname{Tr}[\gamma^\mu\gamma^\nu]\Big) \\
&= -\left(\frac{\partial\theta}{f}\right)^2\int\frac{\mathrm{d}^4p}{(2\pi)^4}\frac{1}{(p^2-m^2)^2}\left(\frac{p^2}{2}+4m^2\right)
\end{aligned}
\tag{101}
$$

where a series of properties of Dirac's algebra were used (SCHWARTZ, 2013). For our purpose, we only need the leading term which is

$$
\overset{\text{leading}}{\propto} -\frac{m^2}{f^2}(\partial\theta)^2\int\frac{\mathrm{d}^4p}{(2\pi)^4}\frac{1}{f^2(p^2-m^2)^2} \propto \frac{m^2}{f^2}(\partial\theta)^2\ln\frac{m^2}{\Lambda^2_{\text{cutoff}}}
\tag{102}
$$

where it was used the derivative method to regularize the momentum integral, Λ_{cutoff} is a generic cutoff (see (SCHWARTZ, 2013)). The point is that the term proportional to $\not{\partial}\theta$ originates the dynamical part of the axion-like field $\theta(x)$ with the form $\propto \frac{m^2}{f^2}(\partial\theta)^2$. We will set it to the canonical form later on.

We still need to address the origin of the mass term for the scalar field. The previous calculation shows the impossibility of generating the mass term from the diagrammatic expansion of the trace. This is an expected result since this term appears in a nonperturbative way. Only a handful of special theories can be done non perturbatively. One such example is the Gross-Neveu (GROSS; NEVEU, 1974; SAZDJIAN, 2015). This theory describes N massless Dirac fermions with a four fermi interaction. The central point is that in this case it is possible to compute the effective potential of the composite field. That is, the computation of

$$
e^{i\Gamma} = \int\mathcal{D}\Big(\psi^\dagger,\psi\Big)e^{iS_0} = e^{i\int\mathrm{d}^4x\mathcal{L}_{\text{eff}}(x)}
\tag{103}
$$

can be done exactly, the relation between $\mathcal{V}(\overline{\psi}\psi)$ (the potential before the fermionic integration) and the $V(\theta)$ (potential after the integration) is computable. This includes the extraction of the minimum of the potential. In order to avoid this computation, we started with the supposition of the potential minimum in equation (90). With that being said, we can illustrate the appearance of the mass term for the θ field by doing perturbation $\phi \to \lambda \left\langle \psi_R^\dagger(x)\psi_L(x)\right\rangle + \phi = \lambda v^3 + \phi$ with $\phi(x) = \lambda v^3 e^{i\left(\frac{\theta(x)}{f} - \beta(x)\right)}$[7] in the HS Lagrangian term $\mathcal{L}_{\text{H-S}} = \cdots + |\phi|^2$. This results in

$$
\begin{aligned}
|\phi|^2 &\to |\phi|^2 + \lambda^2 v^6 + \lambda v^3(\phi^* + \phi) \\
&= \lambda^2 v^6 \left(2 + e^{i\left(\frac{\theta(x)}{f} - \beta(x)\right)} + e^{-i\left(\frac{\theta(x)}{f} - \beta(x)\right)}\right) \\
&= 2\lambda^2 v^6 \left(1 + \cos\left(\frac{\theta(x)}{f} - \beta(x)\right)\right) .
\end{aligned} \tag{104}
$$

Here we can see that, for small values of the pseudo-scalar field, the mass term is proportional to $\propto \frac{\lambda^2 v^6}{f^2}\theta^2$ since $|\phi|^2 \sim \frac{\lambda^2 v^6}{f^2}\theta^2 + \cdots$. The mass term for the pseudo-Axion field is generated by the same principle that generated the mass for the spinor in equation (97) (which originated from the condensate). This is analogous to the charge density waves proposed in the description of a topological magnetic insulator in (LI et al., 2010) as one can see by computing the expected value of the charge density $j_0 = \psi^\dagger\psi$

$$
\langle j_0 \rangle = \left\langle \psi^\dagger\psi \right\rangle = \left\langle \psi^\dagger (P_L + P_R)\psi \right\rangle = \frac{1}{\lambda}(\phi^* + \phi) = 2v^3 \cos\left(\frac{\theta(x)}{f} - \beta(x)\right) \tag{105}
$$

so that the relation is $|\phi|^2 \sim \lambda^2 |\langle j_0 \rangle|^2$. All those ingredients results in the effective Lagrangian

$$
\mathcal{L}_{\text{eff.}} \propto \lambda^2 v^6 + \lambda^2 v^6 \cos\left(\frac{\theta}{f} - \beta\right) + \frac{m^2}{f^2}(\partial\theta)^2 + \text{combinations of } \left((\partial\theta)^2, F^2\right) \tag{106}
$$

which can be expanded for small values of $\theta(x)$ and $\beta(x)$ resulting in

$$
\mathcal{L}_{\text{eff.}} \propto \lambda^2 v^6 + \frac{\lambda^2 v^6}{f^2}\theta^2 + \frac{m^2}{f^2}(\partial\theta)^2 + \lambda^2 v^6 \beta^2 + \frac{\lambda^2 v^6}{f}\beta\theta + \cdots \tag{107}
$$

where the $\cdots$ indicates combinations of θ, β (and combinations of both), $(\partial\theta)^2$ and F^2. Choosing f as to the pseudo-scalar field to be in the canonical form results in $f \propto m \propto \lambda^2 v^3$. This makes the massive term to be $\frac{\lambda^2 v^6}{f^2} \propto \frac{\lambda^2 v^6}{\lambda^4 v^6} \propto \frac{1}{\lambda^2}$ which motivates the definition of a scalar mass $m_\theta \propto \frac{1}{\lambda}$. Writing the full action (expanded for small θ) in its canonical form results in

$$
\mathcal{L} = -\frac{1}{4}F^2 + \frac{e^2 g}{32\pi^2}\left(\frac{\beta(x)}{g} - \theta\right)F\tilde{F} + \frac{1}{2}m_\theta^2\theta^2 + \frac{1}{2}(\partial\theta)^2 + \frac{m_\theta}{g}\beta\theta + \frac{m_\theta^2}{g^2}\beta^2 + \cdots , \tag{108}
$$

where the $\cdots$ stands for the various powers of $\left(\theta, \beta, \theta\beta, \cdots, (\partial\theta)^2, F^2\right)$ and their combina-

[7] To obtain this parametrization it is necessary to use eq. (90) along with redefinition $\frac{\theta'(x)}{f'} = \beta(x) + \frac{\theta(x)}{f}$ (remember that the $'$'s were dropped in the final computation).

tions plus $\lambda^2 v^6$. In last equation it was defined $g \sim 1/f \sim 1/(\lambda^2 v^3)$. The resulting system is similar to the one proposed as a description of a topological magnetic insulator in (LI et al., 2010) which can be called (generically) an "axion insulator" (WANG; ZHANG, 2013). This hints at a possible transition from Weyl semimetals to topological magnetic insulators induced by the vacuum instability resulting from the four fermions interaction.

Some comments are in order. Different from the resulting effective system obtained in section 2.1, here we have the contribution from the anomaly (composed of the term used to cancel the b_μ and the condensate's phase) to the linear "theta" term (in this notation the β) and the presence of the θ which is a massive dynamical field. In addition, there is a coupling between the two which originates from $\cos\left(\frac{\theta(x)}{f} - \beta(x)\right)$. This term generates a space-time anisotropy linked to the beta term since $\frac{m_\theta}{g}\beta\theta = \frac{m_\theta}{g}(\partial_\mu b^\mu)\theta \to -\frac{m_\theta}{g} b_\mu(\partial^\mu \theta)$. If we eliminate the β from the Lagrangian we recover the invariance under $\theta \to -\theta$ and the resulting system is exactly the effective description of the topological magnetic insulator (SEKINE; NOMURA, 2021).

Another point, it is possible to trace some analogies between the axion-like excitation and the pion particle from high energy physics. In this context, the parameter f is the "axion decay constant" and the effective action is similar to the two-photon decay of neutral pion (WANG; ZHANG, 2013). The relation between the microscopic parameter and the axion-photon coupling, namely $g \sim 1/g \sim 1/(\lambda^2 v^3)$, indicates that when the chiral condensate gets weaker the axion-photon coupling becomes stronger. The simplification introduced by the small theta approximation excludes from the system effects like axion string (WANG; ZHANG, 2013; YOU; CHO; HUGHES, 2016) and other non-perturbative effects. These singular states, such as vortices, can be described by multivalued fields (BRAGA; GUIMARAES; PAGANELLY, 2020). These non-perturbative effects are indispensable if one is interested in a comprehensive characterization of the system. The vortices of θ are called chiral vortices in (QI; WITTEN; ZHANG, 2013). They don't carry magnetic flux but are responsible for a nonconservation of the naive supercurrent of the superconductor (BRAGA et al., 2016), see also (STONE; LOPES, 2016). The non-perturbative regime allows for the exploration of the dilution and condensation of such configurations (BRAGA et al., 2016) but, if the goal is the perturbative analysis of the resulting effective theory, such non-perturbative effects are not relevant. Finally, the discussion of section 2.1 indicates that the relation between the fermionic factor b_μ and the effective description is ambiguous. I will postpone this discussion to the next section as we enter with new information from a condensed matter perspective.

Now we can look at the equation of motions of this system. Suppressing the field operators of higher dimension we can compute the equation of motions (sources less) for the gauge and pseudo-scalar fields in this system, they are

$$\begin{aligned} \nabla\cdot\boldsymbol{E} &= \frac{e^2 g}{8\pi^2}\nabla\left(\frac{\beta(x)}{g}-\theta\right)\cdot\boldsymbol{B}\ , \\ \nabla\times\boldsymbol{E} &= -\frac{\partial\boldsymbol{B}}{\partial t}\ , \\ \nabla\cdot\boldsymbol{B} &= 0\ , \\ \nabla\times\boldsymbol{B} &= \frac{\partial\boldsymbol{E}}{\partial t}+\frac{e^2 g}{8\pi^2}\left(\frac{\partial}{\partial t}\left(\frac{\beta(x)}{g}-\theta\right)\boldsymbol{B}+\nabla\left(\frac{\beta(x)}{g}-\theta\right)\times\boldsymbol{E}\right)\ , \\ (\Box - m_\theta^2)\theta &= \frac{e^2 g}{8\pi^2}\boldsymbol{E}\cdot\boldsymbol{B}-\frac{m_\theta}{g}\beta\ . \end{aligned} \tag{109}$$

The electromagnetic response is also modified to

$$\mathbf{D}=\frac{\partial\mathcal{L}_{\text{eff}}}{\partial\mathbf{E}}=\mathbf{E}-\frac{e^2 g}{8\pi^2}\left(\frac{\beta(x)}{g}-\theta\right)\mathbf{B}\ , \tag{110}$$

and

$$\mathbf{H}=-\frac{\partial\mathcal{L}_{\text{eff}}}{\partial\mathbf{B}}=\mathbf{B}+\frac{e^2 g}{8\pi^2}\left(\frac{\beta(x)}{g}-\theta\right)\mathbf{E}\ . \tag{111}$$

We have encountered similar equations in the previous section. The difference here is that the effects explored in the boundary in section 2.2 were exclusive of the boundary, in the present case this is not true since the theta filed has its dynamics (WANG; ZHANG, 2013).

Here we also see the presence of the so-called topological currents but with the inclusion of the axion-like term. They are obtainable by variating the action in terms of the gauge field and are represented by

$$j_\alpha=\frac{e^2 g}{4\pi^2}\left(\frac{b_j}{g}-\partial_j\theta\right)\epsilon_{j\nu\alpha\beta}\partial_\nu A_\beta \qquad \text{or} \qquad \boldsymbol{j}=\frac{e^2 g}{4\pi^2}\left(\frac{\boldsymbol{b}}{g}-\nabla\theta\right)\times\boldsymbol{E}\ , \tag{112}$$

which describes the anomalous Hall effect (AHE), and

$$j_\alpha=-\frac{e^2 g}{4\pi^2}\left(\frac{b_0}{g}-\partial_0\theta\right)\epsilon_{0\nu\alpha\beta}\partial_\nu A_\beta \qquad \text{or} \qquad \boldsymbol{j}=\frac{e^2 g}{4\pi^2}\left(\frac{b_0}{g}-\frac{\mathrm{d}\theta}{\mathrm{d}t}\right)\boldsymbol{B}\ , \tag{113}$$

which is the chiral magnetic effect (CME). More on these two in chapter 3.

3 BRIEF CONCEPTS IN CONDENSED MATTER PHYSICS

The previous discussion, chapters 1 and 2, serves as the foundation as we proceed to more specific topics in condensed matter. This chapter develops as follows. I start with the very basics of Bloch' and Wilson's band theory and Landau's symmetry breaking theory, two essential points in understanding the basics of condensed matter physics. Then I proceed to discuss the integer quantum Hall (IQH) phase which acts as a gateway to the concept of topological order in the following section. This new kind of invariant can be characterized using topological field theory (which Chern-Simons is part of) or thru the Bloch-state wave function of the system. Topological field theory will be used to link the introductory chapters and the appearance of Axion physics in condensed matter physics. The first example is the topological insulator characterized by a topological term called theta term, which compares the axion interaction. Despite the resemblance between these terms, the axion-like term lacks dynamics. This is addressed as we talk about the Weyl/Dirac semimetals. In this particular case, the presence of band-touching points (know as Weyl points) introduces a space-time dependency encoded in the electromagnetic response. The case on which a specific interaction is included is also approached. This will be important to the construction of our model in the next chapter.

This work is not an extensive review of none of the topics treated here as it is not the focus of the thesis. The topics will be introduced as needed and the relevant citations will be provided.

3.1 Introduction

Up until the 1980s (EL-BATANOUNY, 2020), the base of description for the electronic phases were the elctronic band theory proposed by Bloch and Wilson (BLOCH, 1929; WILSON, 1931a; WILSON, 1931b) along with the symmetry-based description of Landau (GINZBURG; LANDAU, 1950; LANDAU, 1937).

The later, Landau's symmetry breaking theory (GINZBURG; LANDAU, 1950; LANDAU, 1937), explains the various phases of matter (such as solid, liquid, gas, ferromagnetic, etc.) elegantly. Although all matter is formed by the same basic constituents (electrons, protons, and neutrons) they can be organized in ways that effectively behave differently. These patterns of organization are essential to the description of the emergent behavior and are called "order". The most basic example is the order that differentiates the particles in the liquid from the crystal state. In the first, the particles maintain continuous translation symmetry order (i.e. can freely move), but when they lose this (in a phase transition) they become bound to a particular set of positions in the crystal structure. The new order now is the discrete translation symmetry thus the change between the two states is described by a spontaneous symmetry breaking (spontaneous meaning that the system reorganizes itself to reach a stable configuration).

Now, Bloch' and Wilson's band theory (BLOCH, 1929; WILSON, 1931a; WILSON, 1931b), understands that the electron states within a periodic potential created by the material (or crystalline structure) are no longer described by a plane wave. Instead, they are described by Bloch wave state $|u_{nk}\rangle$ where k is the crystal momentum and n the band index, all those quantities are defined for a specific unit cell. This way, an electron wavefunction is represented by

$$\psi_{nk}(\mathbf{r}) = u_{nk}(\mathbf{r})e^{i\mathbf{k}\cdot\mathbf{r}} \tag{114}$$

with $u_{nk}(\mathbf{r})$ being a periodic function that respects the appropriate boundary conditions of the lattice. If a is the lattice constant then $u_{nk}(\mathbf{r}) = u_{nk}(\mathbf{r}+\mathbf{a})$. This allows for the definition of a Bloch Hamiltonian $H(\mathbf{k})$ whose eigenstate is the Bloch wave and eigenvalue is the energy $E_n(\mathbf{k})$. For each Brillouin zone, $E_n(\mathbf{k})$ describes the energy bands that are used to classify the solid into the usual phases (insulator, metalic, semimetalic, conductor and semicondutcor).

In the next section, we examine a phenomenon that, once fully understood, expands the paradigm created by Landau's symmetry-breaking theory.

3.2 **Integer quantum Hall and topology, changing the paradigm**

This paradigm changes after the observation of the different quantum Hall effects (QHE) (KLITZING; DORDA; PEPPER, 1980; TSUI; STORMER; GOSSARD, 1982). The point is that distinct quantum Hall states can not be characterized by the usual prescription with local parameters like symmetries, it is necessary to include the topological properties. For a more complete (and pedagogical) discussion on the connection between topological nontrivial quantum phases and quantum entanglement see (STANESCU, 2016), also discussed in articles like (CHEN; GU; WEN, 2010). In our discussion, I will illustrate these topological features by examining the integer quantum Hall (IQH) phase that was characterized by von Klitzing et al (KLITZING; DORDA; PEPPER, 1980) (for a recent general review on the subject see (KLITZING et al., 2020)).

Figure 4a represents the basics of the quantum Hall setup. The applied voltage in the y-direction V_y generates a current in this same direction I_y in addition to a current in the x-direction I_x. This last is known as Hall current and is the fruit of the Lorentz force. More generically, we can write

$$\boldsymbol{V} = \rho \boldsymbol{I} \rightarrow \begin{pmatrix} V_x \\ V_y \end{pmatrix} = \begin{pmatrix} \rho_{xx} & \rho_{xy} \\ -\rho_{xy} & \rho_{xx} \end{pmatrix} \begin{pmatrix} I_x \\ I_y \end{pmatrix} \tag{115}$$

where ρ defines the resistance (the "usual" resistance is the ρ_{xx}). In the "normal" behaviour there is the presence of the electrical resistance (main diagonal) plus the Hall resistance $\rho_{xy} = \frac{B}{\rho_e}$ (here ρ_e is the electron gas density) which indicates that the resistance is proportional to the applied magnetic field. When the gas of electrons is at low temperatures,

Figure 4 - Inter quantum Hall schematics and Landau levels

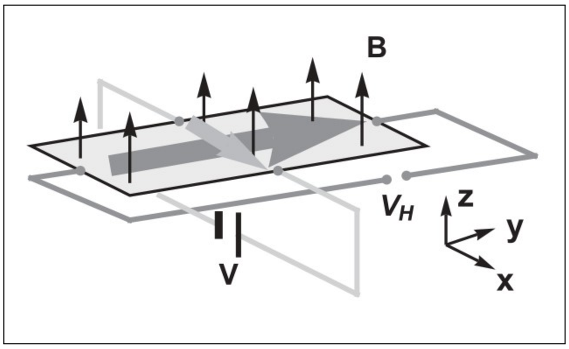

(a)

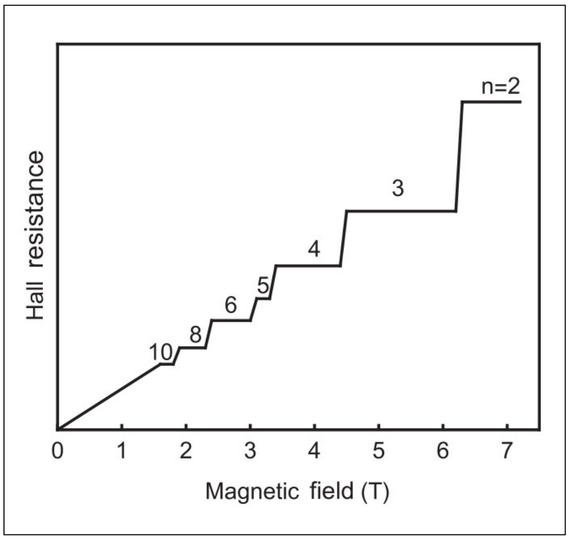

(b)

Subtitle: Figure (a) illustrates the experimental setup for measuring the voltage in a two-dimensional gas of electrons under the influence of a magnetic field. Figure (b) represents the Hall resistance, the plateau is represents the IQHE, and the "slope" is the usual Hall resistance.
Source: EL-BATANOUNY, 2020, p. 220

and under a strong magnetic field, a new phenomena occurs. Under those circumstances, the energy spectrum exhibits flat energy bands known as Landau levels. On this plateau, the system is in an insulating phase ($\rho_{xx} = 0$) but the Hall resistance is quantized ($\rho_{xy} = \nu^{-1} h/e^2$ with $\nu \in \mathbb{N}$). This is evident from the graph of the Hall resistance, each flat line is associated with an integer value, and between then we have the expected Hall resistance proportional behavior (figure 4b). Beyond the clue of the proportionality factor being similar to the fine-structure constant of QED, the phenomenon is independent of the detailed description of its constituents. Information like the geometry and impurities are irrelevant (given that the gap between Landal levels is large enough). More information on those topics can be found in textbooks like (EL-BATANOUNY, 2020; ALTLAND; SIMONS, 2010). The relevant point in this discovery is the observation that this new phase can not be distinguished by any observable symmetry break, it is quantized and robust against smooth changes in the system.

Since the two-dimensional system is in the insulating phase, the only form to be a current is if the propagation occurs through the perimeter. These states, which are confined to the edge of the system, are called edge states. Another feature is their robustness against the effect of impurities (they can not negates the flow of current) which leads to the idea that the current is being carried by chiral edge states. In this context, chiral is referring to the unidirectional electron motion without any possibility to move in the opposite direction as it occurs in the case of Weyl fermions. It is possible to visualize these edge modes by considering the movement of particles, in a close 2d system, in a magnetic field. They will make circular paths in a fixed direction that depends on the orientation of the magnetic field and the electric charge (as is expected by Lorentz force). Near the edge of the system, the orbital motion will be interrupted by the boundary which will result in a skipping orbit running parallel to the 1-dimensional edge (see (EL-BATANOUNY, 2020; STANESCU, 2016) for more pedagogical view). This motivates the chiral edge states and their unidimensional movement[8]. In reality, the existence of such states is enforced by topological considerations in the so-called bulk-boundary correspondence (EL-BATANOUNY, 2020; STANESCU, 2016). This is a general observation, valid for any system where there is an interface between a "trivial" state and a "topologically nontrivial" state, where there will always be a gapless state at the boundary.

Here we can diverge from the historical reasoning and talk about how this effect can be described, without knowing the internal electronic structure, in terms of gauge fields (WITTEN, 2016)[9]. The basic assumptions are two; the system is in the insulator phase (meaning that there is an energy gap between the ground state and the first excited state) and, there are no extra relevant degrees of freedom besides the electromagnets ones, namely the $U(1)$ gauge field A_μ. As previously mentioned, the IQH effect occurs in a two-dimensional scenario (or $2+1$ dimensions). In this dimensionality, the unique term that can be constructed that respect the previous assumptions (and is also gauge invariant) is the Chern-Simons term

$$S_{\mathrm{CS}} = \frac{k}{4\pi}\int \mathrm{d}^3x\, \epsilon^{\mu\nu\rho} A_\mu \partial_\nu A_\rho \ . \tag{116}$$

The epsilon symbol $\epsilon^{\mu\nu\rho}$ has tree indexes varying from 0 to 2 (as expected from $2+1$

---

[8] This has other interesting consequences. The chiral anomaly (in QFT) dictates that one can not construct a system with only chiral particles in one dimension and a similar outcome is expected in many-bode systems (Nielsen-Ninomiya theorem). The loophole, in the previous explanation, is the detail that the 1d system is the boundary of a 2d system. For more pieces of information see (WITTEN, 2016).

[9] Another good resource is David Tong's lectures on quantum hall effect (TONG, 2016).

dimensions) and is totally antisymmetrical. The catch in this term is that the density itself is not gauge-invariant but the integral is up to a total derivative. This is straightforward, doing a gauge transformation $A_\mu \to A_\mu + \partial_\mu \omega$ results in

$$S_{\text{CS}} \to S_{\text{CS}} + \frac{k}{4\pi} \int \mathrm{d}^3x \, \partial_\mu (\omega \epsilon^{\mu\nu\rho} \partial_\nu A_\rho) \ , \tag{117}$$

the second term is a total derivative as previously mentioned. Another quality of the Chern-Simons term is that it breaks both parity and time-reversal (as one can see by applying the rules 23 and 24 from the section 1.3). Now to connect this term with the IQH effect we can compute the induced current in a material that is characterized by the Chern-Simons action. The electromagnetic response is

$$J_i = \frac{\delta S_{\text{CS}}}{\delta A_i} = -\frac{k}{2\pi} \epsilon_{ij} E_j \ , \tag{118}$$

where the proportional coefficient is the Hall conductivity. It is easy to see that this is indeed the Hall current if we assume a material in the $z = 0$ planes, the current in the x-direction is

$$J_x = -\frac{k}{2\pi} E_y, \qquad \sigma_{xy} = \frac{k}{2\pi} \ , \tag{119}$$

meaning that it is proportional to the electric field in the y-direction, as expected from the Hall current. The Chern-Simons term captures the basics of the IQH but only if $k = \frac{e^2 \nu}{\hbar}$ is an integer value identified with the energy levels ν. As a fact, this is an imposition that originates from the consistency between the gauge fields and quantum mechanics[10] (similar to the discussion in sec. 2.2) that tells us that the CS term is gauge-invariant mod $2\pi\mathbb{Z}$.

The IQHE servers as an example of how the electromagnetic response of material with non-trivial topology is expressed in the Chern-Simons term. The “reasoning” to construct the electromagnetic description is greatly simplified in 2+1 dimensions, in general, this kind of logic can not be applied to other cases. A more concrete approach would be to compute the fermionic integration of the microscopic theory to obtain the effective action. Luckily, we have already encountered the generalization of the CS term in the previous chapter. In the next part, we will make the connection between the effective action computed in ch. 2 and the systems in condensed matter physics.

Now we can go back to the historical view. In 1982, the connection with topology was made by Thouless, Kohmto, Nightingale, and den Nijs (TKNN) (THOULESS et

---

[10] The basic idea is the same employed by Dirac in the theory of magnetic monopoles that argued that the action is only gauge-invariant mod $2\pi\mathbb{Z}$. See (WITTEN, 2016) or (TONG, 2018).

al., 1982) by showing that the IQH is associated with the topological invariant known as the first Chern number. It become clear in 1984 that these concepts were linked to Berry's geometric phase framework (BERRY, 1984) which is sensitive to the topology of the momentum space spawned by Bloch wavefunction. We will leave this subject to be discussed in the next section where we will examine the Weyl semimetal.

Topology, in an oversimplified way, is a field of mathematics focused on particular characteristics, dubbed topological properties, that are invariant under continuous deformations. These properties can be attributed to different objects. In one example, geometric forms are labeled by an integer number called genus g and, mathematically, the relation between this integer and the geometric properties of the space is given by

$$\int_{\mathcal{A}} \mathcal{K} d\mathcal{A} = 2\pi(2-2g) \ . \tag{120}$$

This is known as the Gauss-Bonnet theorem (NAKAHARA, 1990), the local dependence is embedded in $\mathcal{A}$ (boundary) and $\mathcal{K}$ (Gaussian curvature). Any object in the same topological class has the same genus, to change it is necessary to make a non-smooth transformation (like punching a hole or patching two parts). A usual example is a connection between a mug and a torus. It is possible to transform one into the other since they belong to the same topological order, i.e. they have the same genus number. This is not the case between a torus and a sphere. The fields of topology treat many objects, including one without geometrical correspondent (STANESCU, 2016).

In physics, the topological order identifies any system that can be smoothly transformed, or adiabatically, into another of the same class. Within Band theory's perspective, the crystal momentum is a good quantum number, allowing us to view the Block wavefunction as a mapping between the Brillouin zone and the Hilbert space. This opens the possibility that the topology structure of the Hilbert space is relevant for the effective description. The principal lacking point of Landau's theory is that even without any symmetry breaking it is possible to change the phase of the system by changing its topological order (CHEN; GU; WEN, 2010) [11], this is a groundbreaking concept [12].

This is a fascinating notion. The quantization number in the Hall conductivity can be analyzed in the macroscopic description (using the Chern-Simons theory, the "topological" effective field theory[13], (QI; HUGHES; ZHANG, 2008)) or using the microscopic description (topological invariant thru the Bloch-state wave function of the system, the TKNN invariant (THOULESS et al., 1982)), both result in a quantization condition.

[11] This article presents a good discussion about topological order and long-range quantum entanglement. If the reader wish to learn more about topological order consult (ZENG et al., 2015).

[12] Acknowledged in the 2016 Nobel prize https://www.nobelprize.org/prizes/physics/2016/prize-announcement/

[13] To avoid any confusion. Here I am referring to general field theories that show topological properties.

In the following section, we will explore more of this matter since we will discuss some realizations of axion physics in condensed matter.

3.3 Material realizations of axion physics

3.3.1 Topological insulators

Table 2 - Discrete symmetry and value of θ term

Time-reversal	Inversion	Value of θ (mod 2π)
Yes	Yes	0 or π
Yes	No	0 or π
No	Yes	0 or π
No	No	Arbitrary

Subtitle: These are the constraints imposed by the discrete symmetries on the value of the θ term. The case without time-reversal and inversion will be important for the theta term with space-time dependence.

Source: SEKINE; NOMURA, 2021, p. 4. Adapted by the author.

Historically, this new phase of matter was observed in 2005 (KANE; MELE, 2005; HASAN; KANE, 2010), and it is very similar to the IQHE, as it is a bulk insulator (gapped energy spectrum) with gapless boundary states akin to the edge states previously discussed. In the topological field theory description of the integer Hall effect, the 2+1 dimensions Chern-Simons theory, both parity $\mathbb{P}$ and time-reversal $\mathbb{T}$ symmetries are broken. The previous affirmation does not hold in 3+1 dimensions because it is possible to break either one of the symmetries (see table 2). It is possible to construct a topological insulator with, at least, one of the symmetries of time-reversal and inversion. Specifically, topological/normal insulators have discrete values of the theta term because, in the presence of time-reversal and/or parity symmetry, theta is quantized with $\theta = 0$ for the trivial insulator (mod 2π) and $\theta = \pi$ (mod 2π) for the topological insulator. It can be expected that the interface between these two topological phases must be a smooth transition between the two values of θ, that can occur with a spacetime varying Axion field interpolating between 0 and π. We already encounter a similar system in section 2.2 so it is convenient to revise it briefly.

There we started with the microscopic action composed of the massive Dirac field plus the electromagnetic interaction and action. The presence of a fermion mass in the microscopic description indicates that the system is in the insulator state. We supposed that the mass term would flip from $+m$ to $-m$ when the theta term passes from 0 to π.

This is consistent with the change that occurs in the boundary between two topological distinct materials, the chiral rotation (that introduces the anomaly) is only relevant in the topological insulator region, resulting in the contribution described in eq. (68), or

$$S_{\text{Anomaly}} = \frac{e^2\theta}{32\pi^2}\int \mathrm{d}^4x\, F\tilde{F}\ , \tag{121}$$

where $F\tilde{F} = F^{\mu\nu}\tilde{F}_{\mu\nu} = \frac{1}{2}\epsilon_{\mu\nu\alpha\beta}F^{\mu\nu}F^{\alpha\beta}$. The computation is similar to section 2.1 but with the simplification introduced by the theta being an angle. There are other forms to calculate this contribution (SEKINE; NOMURA, 2021). The topological term in the case of 3D insulators is known as theta term, and its theoretical description, involving axion-like interaction term, was developed in (QI; HUGHES; ZHANG, 2008). The boundary effects of this term are explored in section 2.2, the principal is the topological magneto-electric (TME) effect (QI et al., 2009b; KANE; MELE, 2005; MOORE, 2010), which can be described as the generation of a cross-field polarization (an electric polarization is generated by an external magnetic field and vice-versa). Some consequences are the appearance of the anomalous (half-quantized) Hall effect, observed experimentally (CHANG et al., 2013; CHECKELSKY et al., 2014), see (SEKINE; NOMURA, 2021) for more information) and the chiral magnetic effect, and Faraday and Kerr rotations (QI; HUGHES; ZHANG, 2008; MACIEJKO et al., 2010; TSE; MACDONALD, 2010), this last is an effect first known in particle physics (ABBOTT; SIKIVIE, 1983; WILCZEK, 1987). Another interesting phenomenon occurs when an electric charge is placed near a topological insulator, the exotic material induces a mirror magnetic charge inside it, and is possible to realize the Witten effect (QI et al., 2009a) that assign a fractional electric charge to a magnetic monopole (WITTEN, 1979).

If we relax this constraint, i.e. consider a system with broken time-reversal and parity symmetry (e.g. in a magnetically order phase breaks reversal symmetry), the theta term can assume arbitrary values (ESSIN; MOORE; VANDERBILT, 2009) as one can see in table 2. Beyond not being bound to the values of 0 or π, this term can also be space-time dependent as $\theta(\mathbf{x}, t)$ but, this does not relax the mod 2π restraint since the origins of this are the topology of the U(1) gauge and quantum mechanics (we already noted this in ch. 2). One system where this can be realized is the Weyl semimetal which will be discussed in the next subsection.

3.3.2 Weyl/Dirac semimetals

The systems described above are insulators (which have an energy gap in their electronic band), now we will address the theta term in semimetals. Semimetals refer to a solid-state system whose electronic bandstructure (conduction and valence bands) touches at one point near the Fermi energy leading to a gapless phase. In 2011 it was proposed a material called Weyl semimetal (WSM) (WAN et al., 2011) which extends the area to Topological semimetals (TSMs). We will concentrate on the topological field aspect of this particular system and the similar one known as Dirac Semimetals.

The definition of a topological invariant in a gapless system is not trivial since the requirement of a global gap is a prerequisite for its basic definition. This can be bypassed if one defines a surface around the touching points and excludes the gapless points similarly to the construction of singular charger points in classical electrodynamics. This interpretation can be further explored since the mathematical structure of the flux in those singular points in momentum space resembles the dual magnetic field.

The quantity that is sensible to the topology is the Berry phase that the Bloch wavefunction acquires in a close loop ξ around the sink/sources of Berry flux, namely

$$\gamma_n = \oint_\xi \mathrm{d}\mathbf{k} \cdot \mathcal{A}_n(\mathbf{k}) \tag{122}$$

where $\mathcal{A}_n(\mathbf{k}) = \langle u_{nk}| \, i\boldsymbol{\nabla}_k \, |u_{nk}\rangle$ is the Berry connection. A non-zero Berry curvature is similar to a non-zero "electromagnetic" curvature, that is, by Maxwell equations, the curl of the magnetic field is non-zero only if there is a source of magnetic flux. The curl of the Berry vector potential (or Berry connection) $\mathcal{B}_n(\mathbf{k}) = \boldsymbol{\nabla}_k \times \mathcal{A}_n(\mathbf{k})$ indicates the presence of the singular point. That is, this term is similar to the magnetic field but in the momentum space. Now it is possible to compute the total flux of Berry curvature through the previously defined surface around the touching points. This results in the topological invariant Chern number

$$\mathcal{C} = \frac{1}{2\pi} \int_S \mathrm{d}\mathbf{S} \cdot \mathcal{B} = n \in \mathbb{Z} \tag{123}$$

where S is the space containing the path ξ and the result is an integer as expected. The Chern number is the chirality (the plus represents a source and the minus a sink of Berry curvature in momentum space) of the Weyl/Dirac point, or topologic charge, which describes the topology of the Weyl/Dirac semimetal. In a Weyl semimetal, the Weyl points (band touching points) carry a topological charge (or chirality)[14] ± 1 and the presence of these points are said to be topologically protected. One can view this in two related ways.

The first one is to notice that for these band-touching points to occur one of the discrete symmetries of parity conjugation ($\mathbb{P}$) or time-reversal ($\mathbb{T}$) has to be broken. The breaking of one (or both) of these symmetries shifts the energy bands in momentum

[14] This is also a consequence of the Nielsen-Ninomyia theorem (NIELSEN; NINOMIYA, 1981; FRIEDAN, 1982), which explains why Weyl fermions always appear in pairs of opposite chirality

space of either inversion symmetry or the Weyl points are protected by the accidental degeneracy that originates by breaking one of two symmetries. The second is to consider that each subspace of the Brillouin zone has only one Weyl point, and to "merge" these two subspaces a non-adiabatic transformation is required so these points are said to be topologically protected.

The previous mechanism do not work in the Dirac semimetal since the source/sink points are in the same subspace and thus can annihilate. Each Dirac point can be considered as the combination (at the same momentum) of two Weyl points with opposite chirality. As stated before, Weyl points are protected in Weyl semimetals but the same does not occur with Dirac points in Dirac semimetals. There are (at least) two different "paths" to the construction of a Dirac semimetal, one is the unstable Dirac points, and the other the stable and happens in quantum critical points between a 3D topological insulator and a normal insulator. The origins of this instability are related to the discussion in sections 1.4 and 1.5, where we discussed chiral symmetry violation by quantum corrections. The other is to stabilize the Dirac points by imposing additional crystalline symmetry. Depending on this last factor, the effective description can be constructed with two Weyl points with chirality ± 1 (linear band structure) or two Weyl points with chirality ± 2 (quadratic band structure) (YANG; NAGAOSA, 2014). The exposition done in the previous paragraphs is brief and only serves to be introductory. It lacks some interesting themes like the Fermi arc surface states and discussion about the Hamiltonian description of the energy bands in the microscopic theory. About those topics, more comprehensive explanations can be found at (for example) (SEKINE; NOMURA, 2021; ARMITAGE; MELE; VISHWANATH, 2018; EL-BATANOUNY, 2020).

If we restrict ourselves to the simplest possibility of Dirac semimetal (given by the usual Dirac action) the difference in the topological description of Weyl and Dirac semimetals is the presence of the b_μ term in the microscopic fermionic Lagrangian. In section 1.4 and 1.5 we explored the conditions around the b_μ term leading to the appearance of two touching points in the energy spectrum.

In sections 1.4 and 1.5, we explored conditions $-b_\mu b^\mu = -b_0^2 + b_i^2 < m^2$ (where m is the fermion mass), which led to the appearance of two touching points in the energy spectrum. Withing this condition, we can approximate the low energy description by Weyl action if we measure the momentum relative to the touching point (the discrepancy only occurs in the high-energy spectrum). This results in the microscopic action considered at the beginning of section 2.1, namely action

$$Z = \int \mathcal{D}\Big(\psi^\dagger, \psi, A\Big) e^{i(S_0 + S_{\text{Maxwell}})} \tag{124}$$

composed of the Dirac action

$$S_0 = \int d^4x\, \overline{\psi}(x) \left(i\partial\!\!\!/ + b\!\!\!/\gamma^5 + ieA\!\!\!/(x) \right) \psi(x), \tag{125}$$

(with the inclusion of the b_μ term) expressed with Dirac spinors $\psi = \begin{pmatrix} \psi_L \\ \psi_R \end{pmatrix}$ with $\overline{\psi} = \psi^\dagger\gamma^0 = \begin{pmatrix} \psi_R^\dagger & \psi_L^\dagger \end{pmatrix}$, and the Maxwell action for the gauge potential A_μ. This system was investigated, and we obtained the effective description (up to linear electrodynamics) in equation (60) which is

$$\mathcal{S}_{\text{eff}} = \int d^4x \left[-\frac{1}{4}F^2 + \frac{e^2}{32\pi^2}\beta(x)F\tilde{F} + (\text{powers of } F^2) \right] \tag{126}$$

with $\beta(x) = 2b_\mu x^\mu$.

Although the theta term is similar to the topological insulator case the effect is distinct. In the previous section, we explored the concept that the variation of the θ occurs at the boundary between distinct topological insulators, this is the reason for the smooth variation in theta. In the current case, the theta term has space-time dependency, meaning that the effect is not limited to the boundary between topological distinct materials. The effective electromagnetic response of this system (at linear order in F^2) is encoded in current

$$\mathbf{j} = \frac{e^2}{\pi^2}(\mathbf{b} \times \mathbf{E} - b_0\mathbf{B}) \tag{127}$$

The electric response is called the anomalous Hall (AHE) effect and the magnetic one chiral magnetic effect (CME) (ZYUZIN; BURKOV, 2012; GRUSHIN, 2012; WANG; ZHANG, 2013; GOSWAMI; TEWARI, 2013; FUKUSHIMA; KHARZEEV; WARRINGA, 2008). The AHE is characterized by the appearance of the Hall resistance even when the magnetic field is absent. In this case, the driven factor is the presence of the **b** perpendicular to the electric field, and it is usually said to be an intrinsic effect since it originates from the topology factors (contrary to the extrinsic that is relater disorder of charges). There is an interesting discussion regarding the CME. It appears that the CME allows for the presence of a direct current along a static magnetic field even in the lack of electric fields. This motivates the notation $b_\mu = (\mu_5, \mathbf{b})$ (SEKINE; NOMURA, 2021), where $\mu_5 = b_0$ is the chemical potential between the two Weyl nodes. But, the presence of such equilibrium current is prohibited by material considerations in crystalline solids (ARMITAGE; MELE; VISHWANATH, 2018; BURKOV, 2018; VAZIFEH; FRANZ, 2013). That is, static magnetic fields do not induce equilibrium currents. In other words, the system needs to be driven out of equilibrium by applying magnetic and electric fields which generates the chiral flow which has been experimentally observed as the negative magnetoresistance in Weyl semimetals (SEKINE; NOMURA, 2021). The means for the generation of the chemical potential (or a charge pump between the nodes) is the chiral anomaly which is the nonconservation of the number of electrons in a given Weyl cone under the effect of parallel electric and magnetic fields. More details on this can be found in (SEKINE; NOMURA, 2021; ARMITAGE; MELE; VISHWANATH, 2018) and, a discussion more focused on particle physics (BURKOV, 2018).

Two points are still missing in our discussion. In ch. 1 (specifically in sections 1.2 and 1.4) the link between b_μ and Lorentz invariance violation theories were made. One of the concerns in this field is the consistency of both microscopic (Dirac action with the inclusion of the LIV term) and the effective (induced LIV term in the electromagnetic sector). As discussed there (based on (KOSTELECKÝ; LEHNERT, 2001)), the microscopic part is unstable, but to reach this physical violation, it is necessary to reach a momentum scale in the order of Planck's energy. In the material realization, this energy scale is not reachable.

In section 2.1, it was explored some of the discussion around the ambiguity in the calculation of the exact relation between the microscopic parameter b_μ and the generated correction k_μ. It is argued in (GRUSHIN, 2012) that the ambiguity would manifest in the Hall conductivity and the existence of a microscopic action (which considers the whole Brillouin zone) fixed the problem. One last comment can be made here regarding the connection between LIV and its realization in a material. Usually, the time-like component of b_μ introduces causality and stability problems in the context of LIV theories. Stability is not an issue in the material realization since the presence of such a term indicates an evanescent effect (ZHANG et al., 2015). The violation of causality (or Einstein's causality) is considered when the group and front velocity are greater than the vacuum light velocity (ADAM; KLINKHAMER, 2001). This criterion for the material interpretation is controversial since it can be argued that the anomalous dispersion regime of some material media, or a homogeneously broadened absorbing media, the relevant aspect should be the propagation of information instead (BRILLOUIN, 1960; MILLONNI, 2004; DIENER, 1996; DIENER, 1997). That is, the careful analysis leads to the conclusion that no propagation of information occurs regardless of the group velocity being greater than c (BRUNI; GUIMARAES; CHRISPIM, 2021).

3.3.3 Topological magnetic insulator

The next system is very similar to the Weyl/Dirac semimetal explored in the last subsection but with the difference that, beyond the effect of the b_μ term, we have the influence of a dynamical axion-like field. This is possible if one includes a specific interaction term that allows for the chiral symmetry to be broken dynamically (due to the chiral condensation) and results in a new pseudo-scalar particle, akin to the Peccei-Quin mechanism, as pointed out in (WANG; ZHANG, 2013; MACIEJKO; NANDKISHORE, 2014; YOU; CHO; HUGHES, 2016). The microscopic action explored in section 2.3 is similar to the one studied in sec. 2.1 (and review in the last subsection) but, with the inclusion of the interaction. The system is

$$Z = \int \mathcal{D}\Big(\psi^\dagger, \psi, A\Big) e^{i\left(S_0 + S_{\text{Maxwell}} + \int \mathrm{d}^4 x \mathcal{L}_{\text{int}}\right)} , \tag{128}$$

where S_0 is the Dirac action with the inclusion of the b_μ term and S_{Maxwell} is the usual Maxwell action. The new ingredient here is the pairing which is

$$\mathcal{L}_{\text{int}} = -\lambda^2 \left(\overline{\psi}(x) P_L \psi(x)\right) \left(\overline{\psi}(x) P_R \psi(x)\right) , \tag{129}$$

where $P_L = \frac{1}{2}(1-\gamma^5)$ and $P_R = \frac{1}{2}(1+\gamma^5)$ is chiral projectors. Furthermore, the coupling λ has mass dimension -1 as discussed in sec. 2.3 and it connects left and right-handed fields. This interaction term is detailed in appendix D. As a result, the effective description (after the condensation, i.e. $\langle \psi_R^\dagger(x) \psi_L(x) \rangle = v^3$, which is parametrized in eq. (90) as $\phi(x) = \lambda v^3 e^{i\frac{\theta(x)}{f}}$ with f being a mass scale and v^3 of mass dimension 3) of the system (at linear order) is

$$S = \int \mathrm{d}^4 x \left[-\frac{1}{4} F^2 + \frac{e^2 g}{32\pi^2} \left(\frac{\beta(x)}{g} - \theta \right) F\tilde{F} + \frac{1}{2} m_\theta^2 \theta^2 + \frac{1}{2} (\partial\theta)^2 + \cdots \right] \tag{130}$$

where $g \sim 1/(\lambda^2 v^3)$ and the $\cdots$ are proportional to various powers of $\left(\theta, \beta, \theta\beta, \cdots, (\partial\theta)^2, F^2\right)$ and their combinations plus $\lambda^2 v^6$. Here, beyond the usual term which originates from the separation of the Weyl nodes in energy and momentum, there is the presence of a pseudo-scalar (or axion-like) field θ. The interaction term has the effect that, once the condensation occurs, generates a mass for the fermionic field. The mass, in terms of the microscopic variables, is $m = \lambda^2 v^3$ (v has mass dimension 1 and was introduced in the parametrization of the condensate). This is the reason for this system to have an effective mass gap meaning that it is similar to a topological magnetic insulator (LI et al., 2010) or an axion insulator (WANG; ZHANG, 2013) (indicating a possible transition between a Weyl semimetal and topological magnetic insulators induced by the vacuum instability resulting from the four fermions interaction). The difference here is the full coupling term between the theta and beta which is $\cos\left(\frac{\theta(x)}{f} - \beta(x)\right)$ (obtained in sec. 2.3). This introduces a space-time anisotropy because $\frac{m_\theta}{g}\beta\theta = \frac{m_\theta}{g}(\partial_\mu b^\mu)\theta \to -\frac{m_\theta}{g} b_\mu (\partial^\mu \theta)$. Eliminating the β from the Lagrangian restores the symmetry $\theta \to -\theta$. The resulting system is exactly the effective description of the topological magnetic insulator (SEKINE; NOMURA, 2021). In this approximation non-perturbative effects are excluded as discussed previously. In the same way that the mass for the spinor appears, the mass term for the θ ($m_\theta \sim \lambda^{-1}$) is generated by the condensate after the integration of the fermion degree of freedom.

Both masses have their origins in the so-called charge density waves (LI et al., 2010). The electromagnetic response of the system is

$$j_\alpha = \frac{e^2 g}{4\pi^2}\left(\frac{b_j}{g} - \partial_j\theta\right)\epsilon_{j\nu\alpha\beta}\partial_\nu A_\beta \qquad \text{or} \qquad \boldsymbol{j} = \frac{e^2 g}{4\pi^2}\left(\frac{\boldsymbol{b}}{g} - \nabla\theta\right)\times\boldsymbol{E}\ , \tag{131}$$

which describes the anomalous Hall effect (AHE), and

$$j_\alpha = -\frac{e^2 g}{4\pi^2}\left(\frac{b_0}{g} - \partial_0\theta\right)\epsilon_{0\nu\alpha\beta}\partial_\nu A_\beta \qquad \text{or} \qquad \boldsymbol{j} = \frac{e^2 g}{4\pi^2}\left(\frac{b_0}{g} - \frac{\mathrm{d}\theta}{\mathrm{d}t}\right)\boldsymbol{B}\ , \tag{132}$$

which is the chiral magnetic effect (CME) (WANG; ZHANG, 2013; MACIEJKO; NANDKISHORE, 2014; YOU; CHO; HUGHES, 2016). As expected the appearance of the axion-like term in the anomaly contribution changes the topological current[15]. Most of the discussion was done in section 2.3 but further pieces of information can be found in (WANG; ZHANG, 2013; SEKINE; NOMURA, 2021; YOU; CHO; HUGHES, 2016; LI et al., 2010).

This finishes the relevant topics of condensed matter physics. Again most concepts are only touched briefly and the references contain more profound discussions. In the next chapter, our microscopic model will be constructed based on the topological field theory using the model with dynamics axion-like excitations (obtainable by the inclusion of an interaction term for the fermions) as a basis.

[15] The presence of the axion-like term in the anomaly, together with the idea that the axion-like is linked to charge density waves, appears to indicate that this is an extrinsic effect.

4 WEYL-SUPERCONDUCTOR WITH DYNAMICAL PSEUDO-AXION FIELD

In this section, I will construct the microscopic description of our model. The model is the Weyl-superconductor with a dynamical pseudo-Axion field. The understanding of chapter 2 will come in handy in this lengthy calculation in two ways. First, the computation has similarities, and second, the basic is the generalization of the interaction studied there. The main point of section 2.3 is the formation of a dynamical axion in the effective theory via the inclusion of a chiral breaking interaction term. Our generalization consists of the inclusion of an interaction term that, once condensed, breaks charge symmetry as well as chiral symmetry. This is obtained by the introduction of a four-fermion interaction in the microscopic model. The principal difference between this calculation and the one done in section 2.3 is the necessity of the introduction of an "enlarged" spinor to be able to "decouple" the interaction using an auxiliary field (Hubbard-Stratanovich transformation). This, along with the consequences, is treated in section 4.1. The following section, namely 4.2, clarifies how gauge invariance is encoded in this system. The last section is where we calculate the fermionic determinant resulting in the effective description of our model in its canonical form.

This model was proposed in (CHRISPIM; BRUNI; GUIMARAES, 2021) and some calculations will be explored in more details in this chapter.

4.1 Action transformations

With the knowledge of the second chapter (specially sections 2.1 and 2.3) we are well-equipped to construct an microscopic theory that, once condensate, will originate an effective massive electrodynamics with the presence of a dynamics pseudoscalar field (Axion-like). To that end, we can inquire about the consequence of other possible pairings in the effective axion-electromagnetic theory. An interesting proposal is to consider the formation of condensates that breaks charge symmetry as well as chiral symmetry. This would lead to an axionic superconductor. In this case one expects the system to be characterized by four active degrees of freedom (two charges and two chiralities). A simple choice is to encode those degrees of freedom in two complex fields that represent two possible condensates, as we will see. We start this with the following system (same as the section 2.3)

$$Z = \int \mathcal{D}\Big(\psi^\dagger, \psi, A\Big) e^{i\left(S_{\text{Weyl}} + S_{\text{Maxwell}} + \int \mathrm{d}^4x \mathcal{L}_{\text{int}}\right)} \tag{133}$$

but now the four fermion interaction is

$$\mathcal{L}_{\text{int}} = -\lambda_R^2 \psi_R \psi_R \psi_R^\dagger \psi_R^\dagger - \lambda_L^2 \psi_L \psi_L \psi_L^\dagger \psi_L^\dagger \ , \tag{134}$$

where the coupling $\lambda_{R/L}$ has mass dimension -1. This pairing separates left and right-handed fields into two separate quartic terms (see the appendix D and E for more details).

This interaction term introduces new complications in the mathematical procedure because in order to "decoupled" the interaction using an auxiliary fields thru the Hubbard-Stratanovich we must first "enlarge" the matrix structure[16] But first we will write this interaction using a charge conjugate spinor as

$$\mathcal{L}_{\text{int}}(x) = -\lambda_R^2 (\overline{\psi}_c P_R \psi)(\overline{\psi} P_L \psi_c) - \lambda_L^2 (\overline{\psi}_c P_L \psi)(\overline{\psi} P_R \psi_c) \ , \tag{135}$$

where $\psi_c = \begin{pmatrix} \sigma_2 \psi_R^\dagger \\ -\sigma_2 \psi_L^\dagger \end{pmatrix}$ is the charge conjugate spinor field. (see E.1.3 for more information) and $P_{R/L}$ are the usual projector. Introducing the extended spinor

$$\Psi = \begin{pmatrix} \psi \\ \psi_c \end{pmatrix} , \qquad \overline{\Psi} = \begin{pmatrix} \overline{\psi} & \overline{\psi}_c \end{pmatrix} , \tag{136}$$

that adds another layer of matrix structure, the Pauli matrices ρ, acting on "charge space". The total matrix structure schematically is

$$\Gamma = \sigma \otimes \tau \otimes \rho \tag{137}$$

with σ, τ, and ρ are the Pauli matrices acting on the spin, handiness, and charge, respectively[17]. The massless Weyl action thus is (see appendix E.1.2 for more details)

$$S_{\text{Weyl}} = \int \mathrm{d}^4 x \, \frac{1}{2} \overline{\Psi} \Big[\big(i \not{\partial} + \not{b} \gamma_5 \big) \rho_0 + i e \not{A} \rho_3 \Big] \Psi \ . \tag{138}$$

The Maxwell action does not need any modification but the interaction in eq. (134) needs to be written in terms of this new spinors. The process is explained in E.1.3 and results in

$$\mathcal{L}_{\text{int}}(x) = -\lambda_R^2 \Big(\overline{\Psi} P_R P_- \Psi \Big) \Big(\overline{\Psi} P_L P_+ \Psi \Big) - \lambda_L^2 \Big(\overline{\Psi} P_L P_- \Psi \Big) \Big(\overline{\Psi} P_R P_+ \Psi \Big), \tag{139}$$

---

[16] This idea is similar to the Nambu spinor, which comprises the creation and annihilator operator in a single object (see (ALTLAND; SIMONS, 2010) for more information), but with the distinction that here the spinor, and its charge conjugate, fields.

[17] The usual gamma notation can be extended too (see (CHRISPIM; BRUNI; GUIMARAES, 2021) and the relevant matrices are given by $\gamma^0 \to \sigma_0 \otimes \tau_1 \otimes \rho_0$, $\gamma^i \to i\sigma_i \otimes \tau_2 \otimes \rho_0$ and $\gamma^5 \to -\sigma_0 \otimes \tau_3 \otimes \rho_0$ but in this thesis I will leave this Kronecker notation implicit.

where it was defined the operators $P_\pm = \frac{1}{2}(\rho_1 \pm i\rho_2)$. Now we can proceed to the introduction of the two sets of Hubbard-Stratanovich $\phi_{R/L}$ defined as

$$\begin{aligned} \phi_R &= \lambda_R \psi_R \psi_R = \lambda_R \overline{\psi}_c P_R \psi = \lambda_R \overline{\Psi} P_R P_- \Psi \ , \\ \phi_R^* &= \lambda_R \psi_R^\dagger \psi_R^\dagger = \lambda_R \overline{\psi} P_L \psi_c = \lambda_R \overline{\Psi} P_L P_+ \Psi \ , \end{aligned} \tag{140}$$

and

$$\begin{aligned} \phi_L &= \lambda_L \psi_L \psi_L = \lambda_L \overline{\psi}_c P_L \psi = \lambda_L \overline{\Psi} P_L P_- \Psi \ , \\ \phi_L^* &= \lambda_L \psi_L^\dagger \psi_L^\dagger = \lambda_L \overline{\psi} P_R \psi_c = \lambda_L \overline{\Psi} P_R P_+ \Psi \ . \end{aligned} \tag{141}$$

Both auxiliary fields $\phi_R(x)$ and $\phi_L(x)$ carry the same charges ($2e$ if e is the fermion charge) but have opposite chirality. The full set of discrete transformations of the auxiliary field can be found in appendix E.1.4. Using these auxiliary fields the interaction term can be “decoupled” (similar to the computation in (85) in chapter 2). This results in

$$e^{S_{\text{int.}}} = \int \mathcal{D}(\phi_R, \phi_L) e^{S_{\text{H-S}}} \ , \tag{142}$$

where $\mathcal{D}(\phi_R, \phi_L)$ stands for $\mathcal{D}\phi_R^* \mathcal{D}\phi_R \mathcal{D}\phi_L^* \mathcal{D}\phi_L$, and

$$S_{\text{H-S}} = \int \mathrm{d}^4x \left[\left(|\phi_R|^2 + |\phi_L|^2 \right) - \overline{\Psi}(\lambda_R \phi_R P_L + \lambda_L \phi_L P_R) P_+ \Psi + \text{h.c.} \right] \tag{143}$$

where h.c. stand for the hermitian conjugate of the prior term. The full system thus is

$$Z = \int \mathcal{D}\left(\Psi^\dagger, \Psi, A, \phi_R, \phi_L\right) e^{i\left(S_{\text{Weyl}} + S_{\text{Maxwell}} + S_{\text{H-S}}\right)}. \tag{144}$$

It is a dynamical question whether these couplings can give rise to the condensates in the same sense exposed in section 2.3 and, at this point, we can only suppose that the condensation occurs. If this happens, the system will develop a superconducting phase once $\phi_R(x)$ and $\phi_L(x)$ are charged. Upon condensation we have

$$\begin{aligned} \langle \phi_R(x) \rangle &= \lambda_R v_R^3 e^{i\delta_R} \ , \\ \langle \phi_L(x) \rangle &= \lambda_L v_L^3 e^{i\delta_L} \ . \end{aligned} \tag{145}$$

Any choice of parameters breaks $\mathbb{T}$ once the system undergoes condensation. If $\lambda_R v_R^3 = \lambda_L v_L^3$ then we have the following choices:

- $\delta_R = \delta_L$, $\mathbb{P}$ is preserved and $\mathbb{C}$ is broken;
- $\delta_R = -\delta_L$, $\mathbb{C}$ is preserved and $\mathbb{P}$ is broken;
- $\delta_R = \delta_L = 0$ then $\mathbb{C}$ and $\mathbb{P}$ are preserved.

The effective action can be constructed by considering fluctuations of the phases around the vacuum values δ_R and δ_L

$$\begin{aligned}\phi_R(x) &= \lambda_R v_R^3 e^{i\frac{R(x)}{f_R}}\\ \phi_L(x) &= \lambda_L v_L^3 e^{i\frac{L(x)}{f_L}}\end{aligned} \tag{146}$$

where $R(x)$ and $L(x)$ are the fluctuations that parameterize δ_R and δ_L. This effectively locks two degrees of freedom, and the H-S Lagrangian becomes

$$\mathcal{L}_{\text{H-S}} = \left(\left(\lambda_R v_R^3\right)^2 + \left(\lambda_L v_L^3\right)^2\right) - \overline{\Psi}\left(\lambda_R^2 v_R^3 e^{i\frac{R(x)}{f_R}} P_L + \lambda_L^2 v_L^3 e^{i\frac{L(x)}{f_L}} P_R\right) P_+ \Psi + \text{h.c.} \tag{147}$$

and, lastly, the functional now is $\mathcal{D}\left(\Psi^\dagger, \Psi, A, R, L\right)$. Making, for simplicity, $\lambda_R = \lambda_L = \lambda$ and $v_R = v_L = v$, simplifies the expression to

$$\mathcal{L}_{\text{H-S}} = 2\left(\lambda v^3\right)^2 - \lambda^2 v^3 \overline{\Psi}\left(e^{i\frac{R(x)}{f_R}} P_L + e^{i\frac{L(x)}{f_L}} P_R\right) P_+ \Psi + \text{h.c.}\ . \tag{148}$$

Performing the redefinition

$$\Psi(x) \to \Psi(x)' = e^{i\frac{1}{4}\left(\frac{R(x)}{f_R} - \frac{L(x)}{f_L}\right)\gamma^5} \Psi(x) \tag{149}$$

results in a new term in the Weyl action

$$S_{\text{Weyl}} = \int \mathrm{d}^4 x\, \frac{1}{2} \overline{\Psi}\left[\left(i\partial\!\!\!/ + b\!\!\!/\gamma_5 + \frac{1}{4}\gamma_5 \partial\!\!\!/\left(\frac{R(x)}{f_R} - \frac{L(x)}{f_L}\right)\right)\rho_0 + ieA\!\!\!/\rho_3\right]\Psi, \tag{150}$$

a non-trivial Jacobian of the fermionic measure

$$S_{\text{Anomaly}} = \int \mathrm{d}^4 x\, 2\left(\frac{R(x)}{f_R} - \frac{L(x)}{f_L}\right) \frac{e^2}{32\pi^2} F F^\star\ , \tag{151}$$

and a phase for the Hubbard-Stratanovich Lagrangian

$$\begin{aligned}\mathcal{L}_{\text{H-S}} &= 2\left(\lambda v^3\right)^2 - \lambda^2 v^3 \overline{\Psi} e^{\frac{i}{2}\left(\frac{R(x)}{f_R} - \frac{L(x)}{f_L}\right)\gamma^5}\left(e^{i\frac{R(x)}{f_R}} P_L + e^{i\frac{L(x)}{f_L}} P_R\right) P_+ \Psi + \text{h.c.}\ ,\\ &= 2\left(\lambda v^3\right)^2 - \lambda^2 v^3 e^{\frac{i}{2}\left(\frac{R(x)}{f_R} + \frac{L(x)}{f_L}\right)} \overline{\Psi} P_+ \Psi + \text{h.c.}\end{aligned} \tag{152}$$

where it was used the properties described in the appendix C.1 (equation 420). Performing now yet another field redefinition but using the new extended charge space

$$\Psi(x) \to \Psi'(x) = e^{i\frac{1}{4}\left(\frac{R(x)}{f_R} + \frac{L(x)}{f_L}\right)\rho_3} \Psi(x)\ . \tag{153}$$

This gauge transformation does not introduces an anomaly because it is a local transformation, contributes with a new term for the Weyl action

$$
\begin{aligned}
S_{\text{Weyl}} = \int \mathrm{d}^4x\, \frac{1}{2}\overline{\Psi}\Bigg[&\bigg(i\partial\!\!\!/ + b\!\!\!/\gamma_5 + \frac{1}{4}\gamma_5\partial\!\!\!/\Big(\frac{R(x)}{f_R} - \frac{L(x)}{f_L}\Big)\bigg)\rho_0 \\
&+\bigg(ieA\!\!\!/ - \frac{1}{4}\partial\!\!\!/\Big(\frac{R(x)}{f_R} + \frac{L(x)}{f_L}\Big)\bigg)\rho_3\Bigg]\Psi,
\end{aligned} \tag{154}
$$

and, again, a phase for the Hubbard-Stratanovich Lagrangian but that simplify it

$$
\begin{aligned}
\mathcal{L}_{\text{H-S}} &= 2\Big(\lambda v^3\Big)^2 - \lambda^2 v^3 e^{\frac{i}{2}\left(\frac{R(x)}{f_R}+\frac{L(x)}{f_L}\right)}\overline{\Psi}e^{-i\frac{1}{2}\left(\frac{R(x)}{f_R}+\frac{L(x)}{f_L}\right)\rho_3}P_+\Psi + \text{h.c.}\ , \\
&= 2\Big(\lambda v^3\Big)^2 - \lambda^2 v^3 e^{\frac{i}{2}\left(\frac{R(x)}{f_R}+\frac{L(x)}{f_L}\right)}e^{-\frac{i}{2}\left(\frac{R(x)}{f_R}+\frac{L(x)}{f_L}\right)}\overline{\Psi}P_+\Psi + \text{h.c.}\ , \\
&= 2\Big(\lambda v^3\Big)^2 - \lambda^2 v^3\overline{\Psi}(P_+ + P_-)\Psi\ , \\
&= 2\Big(\lambda v^3\Big)^2 - \lambda^2 v^3\overline{\Psi}\rho_1\Psi\ ,
\end{aligned} \tag{155}
$$

where it was used propriety eq. (508) from the appendix. Now the system can be written in a nicer form if we introduce the following fields

$$
\frac{\theta(x)}{f} + \theta_0(x) = \frac{1}{4}\left(\frac{R(x)}{f_R} - \frac{L(x)}{f_L}\right)\ , \tag{156}
$$

$$
\frac{\theta'(x)}{f'} = \frac{1}{4}\left(\frac{R(x)}{f_R} + \frac{L(x)}{f_L}\right)\ , \tag{157}
$$

with $\theta_0(x) = 2b_\mu x^\mu$, that cancels the b_μ contribution in the same way as the done in section 2.3. The initial field fluctuations parametrization of the complex fields, $\phi_R(x) = \lambda v^3 e^{i\frac{R(x)}{f}}$ and $\phi_L(x) = \lambda v^3 e^{i\frac{L(x)}{f}}$ also changes

$$
\phi_R(x) = \lambda v^3 e^{2i\left(\frac{\theta(x)}{f}+\theta_0(x)+\frac{\theta'(x)}{f'}\right)}\ ,\quad \phi_L(x) = \lambda v^3 e^{2i\left(-\frac{\theta(x)}{f}-\theta_0(x)+\frac{\theta'(x)}{f'}\right)}\ , \tag{158}
$$

and our system thus becomes

$$
Z = \int \mathcal{D}\Big(\Psi^\dagger, \Psi, A, \theta, \theta'\Big)e^{i\left(S_{\text{fermion}}+S_{\text{Maxwell}}+S_{\text{Anomaly}}+\int \mathrm{d}^4x 2\lambda^2 v^6\right)}\ , \tag{159}
$$

$$
S_{\text{fermion}} = \int \mathrm{d}^4x\, \frac{1}{2}\overline{\Psi}\left[\left(i\partial\!\!\!/ + \gamma_5\partial\!\!\!/\frac{\theta(x)}{f}\right)\rho_0 + \left(ieA\!\!\!/ - \partial\!\!\!/\frac{\theta'(x)}{f'}\right)\rho_3 - \lambda^2 v^3\rho_1\right]\Psi, \tag{160}
$$

$$
S_{\text{Anomaly}} = \int \mathrm{d}^4x\, \frac{1}{2}\left(\frac{\theta(x)}{f} + \theta_0(x)\right)\frac{e^2}{32\pi^2}FF^\star\ . \tag{161}
$$

The computation is not complete yet. Apart from the fermionic integration (and the calculation of the leading trace contributions that fixates the parameter relation), we must understand the mechanics of the mass generation of the vector field and for the pseudo-scalar field.

4.2 Gauge invariance considerations

Before advancing in our effective action calculation it is convenient to describe how gauge invariance acts on the system described by (159). The extended spinor, defined in equation (136), transforms as (appendix E.1.1)

$$\Psi(x) \to e^{-i\alpha(x)\rho_3}\Psi(x) \tag{162}$$

under a gauge transformation

$$A_\mu \to A_\mu - \frac{i}{e}\partial_\mu \alpha(x) \tag{163}$$

We have already done this transformation in equation (153). Applying the gauge transformation of the extended spinor (162) on the action functional $Z[\Psi, A, \theta, \theta']$ does not affect the anomaly, but the fermionic action (160) changes to

$$S_{\text{fermion}} \to S'_{\text{fermion}} = S_{\text{fermion}} + \int \mathrm{d}^4x\, \frac{1}{2}\overline{\Psi}\Big[-\not{\partial}\rho_3 - \lambda^2 v^3 e^{-2i\alpha(x)\rho_3}\rho_1\Big]\Psi\ . \tag{164}$$

We can see that the gauge transformation (163) cancels the first factor but not the second. The added term $e^{-2i\alpha\rho_3}$ does not vanish. The main problem is that we are not taking into account the field redefinition (153) which means that the extended spinor in our calculation is

$$\Psi(x) \to \Psi'(x) = e^{i\frac{\theta'}{f'}\rho_3}\Psi(x), \tag{165}$$

where we already considered the definition in equation (158). Let us redo the gauge transformation, using (162) on this spinor field amounts to

$$\Psi(x) \to e^{i\left(\alpha(x)+\frac{\theta'}{f'}\right)\rho_3}\Psi(x)\ . \tag{166}$$

The presence of θ' allows for the cancellation of the previous problematic extra contribution. If we transform the θ' field as

$$\frac{\theta'(x)}{f'} \to \frac{\theta'(x)}{f'} - \alpha \tag{167}$$

the $e^{-2i\alpha\rho_3}$ contribution vanishes. This eliminates the exponential factor but changes the $\not{\partial}\frac{\theta'}{f'}$ to $\not{\partial}\Big(\frac{\theta'(x)}{f'} - \alpha(x)\Big)$. The total transformation (also taking into account the gauge field transformation) is

$$ieA_\mu - \partial_\mu\frac{\theta'(x)}{f'} \to ie\Big(A_\mu + \frac{i}{e}\partial_\mu\alpha\Big) - \partial_\mu\bigg(\frac{\theta'(x)}{f'} - \alpha\bigg) = ieA_\mu - \partial_\mu\frac{\theta'(x)}{f'}\ . \tag{168}$$

This motivates the definition of

$$A^\mu(x) + \frac{i}{e}\partial^\mu \frac{\theta'(x)}{f'} \equiv C^\mu(x) \tag{169}$$

so that the this a gauge invariant field that enters the fermion action as

$$S_{\text{fermion}} = \int \mathrm{d}^4x\, \frac{1}{2}\overline{\Psi}\left[\left(i\partial\!\!\!/ + \gamma_5 \partial\!\!\!/ \frac{\theta(x)}{f}\right)\rho_0 + ie C\!\!\!/ \rho_3\right]\Psi\ . \tag{170}$$

The Maxwell term F^2 follows $F^2(A) = F^2(C)$ due to its anti-symmetric properties. This allows us to change $A_\mu \to C_\mu$ without any problems. The consequence is that now that $\theta'(x)$ is the would-be Goldstone boson that is combined with the gauge field in the Higgs mechanism to furnish the gauge-invariant field $C^\mu(x) = A^\mu(x) + \frac{i}{e}\partial^\mu \frac{\theta'(x)}{f'}$ where $\frac{i}{e}\partial^\mu \frac{\theta'(x)}{f'}$ represents the longitudinal term for the vector field, thus leading to a consistent mass term for the photon, characterizing the Meissner effect. This will lead to the appearance of a mass term in our effective action.

4.3 **Effective action computation**

At this point, we already encounter the fermionic integration computation in sections 2.1 and 2.3. Using the same method on the system defined by

$$Z(j, J, \eta) = \int \mathcal{D}\Big(\Psi^\dagger, \Psi, C, \theta\Big) e^{i\left(S_{\text{fermion}} + S_{\text{Maxwell}} + \int \mathrm{d}^4x \left(2\lambda^2 v^6 + j_\mu C^\mu + J\theta + \overline{\eta}\Psi + \eta\overline{\Psi}\right)\right)}\ , \tag{171}$$

$$S_{\text{fermion}} = \int \mathrm{d}^4x\, \frac{1}{2}\overline{\Psi}\left[\left(i\partial\!\!\!/ + \gamma_5 \partial\!\!\!/ \frac{\theta(x)}{f}\right)\rho_0 + ie C\!\!\!/ \rho_3 - m\rho_1\right]\Psi\ , \tag{172}$$

$$S_{\text{Anomaly}} = \int \mathrm{d}^4x\, \frac{1}{2}\left(\frac{\theta(x)}{f} + \theta_0(x)\right)\frac{e^2}{32\pi^2} F F^\star \tag{173}$$

where $F_{\mu\nu} = \partial_\mu C_\nu - \partial_\nu C_\mu$, and $m = \lambda^2 v^3$, results in

$$Z(j, J) = \int \mathcal{D}(C, \theta) e^{i\left(S_{\text{eff}} + S_{\text{Anomaly}} + S_{\text{Maxwell}} + \int \mathrm{d}^4x \left(\lambda^2 v^6 + j_\mu A^\mu + J\theta\right)\right)}\ , \tag{174}$$

with

$$S_{\text{eff}} = \sum_{n=1} \frac{i}{n}\, \mathrm{Tr}\left[\left(\frac{-ie C\!\!\!/ - \frac{1}{2}\gamma_5 \partial\!\!\!/ \frac{\theta(x)}{f}}{i\partial\!\!\!/ - m\rho_1}\right)^n\right]\ , \tag{175}$$

where the extended fermionic field has been integrated out. As in the previous instances, we can use Feynman's diagrams to understand this expression, but with additional considerations. Some terms in this expansion are represented in

$$\sum_{n=1} \frac{i}{n} \operatorname{Tr}\left[\left(\frac{-ie\not{C} - \frac{1}{2}\gamma_5 \not{\partial}\frac{\theta(x)}{f}}{i\not{\partial} - m\rho_1}\right)^n\right] \rightarrow$$

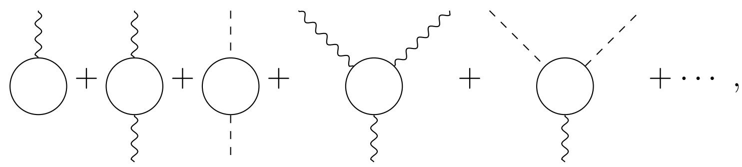

where the lines are the scalar field (dashed), the massive vector (wave), and the extended fermion (solid) field. As in the case of section 2.3 we have that new interaction terms can be created from the fermion bubble with insertion of n external fields. Let's focus on the gauge sector first, then compute the leading terms of the pseudo-scalar sector.

4.3.1 Gauge sector

Mathematically, the term proportional to the gauge-invariant field C_μ in the trace contributes to the same kind of factors that one expects in sections 2.3 and 2.1 but with the major difference that no limitation on terms proportional to C^2 are present. To make things clear, although both terms are very similar (the only apparent difference is the letter) field C_μ is gauge invariant. This allows for the construction of terms proportional to C^2 while preserving gauge invariance [18]. We can explore the leading one in the same form that was done in equation (102), the principal steps are

$$\begin{aligned}
\propto \operatorname{Tr}\left[\left(\frac{-ie\not{C}}{i\not{\partial} - m\rho_1}\right)^2\right] &= -e^2 \operatorname{Tr}\left[\frac{1}{\not{p} - m\rho_1}\not{C}\frac{1}{\not{p} - m\rho_1}\not{C}\right] \\
&= -e^2 \int \frac{\mathrm{d}^4 p}{(2\pi)^4}\frac{1}{(p^2 - m^2)^2} \operatorname{Tr}\Big[(\not{p} + m\rho_1)\not{C}(\not{p} + m\rho_1)\not{C}\Big] \\
&= -e^2 \int \frac{\mathrm{d}^4 p}{(2\pi)^4}\frac{1}{(p^2 - m^2)^2}\Big(p_\mu C_\nu p_\alpha C_\tau \operatorname{Tr}[\gamma^\mu\gamma^\nu\gamma^\alpha\gamma^\tau] - m^2 C_\mu C_\nu \operatorname{Tr}[\gamma^\mu\gamma^\nu]\Big) \\
&= -e^2 C^2 \int \frac{\mathrm{d}^4 p}{(2\pi)^4}\frac{1}{(p^2 - m^2)^2}\left(\frac{p^2}{2} + 4m^2\right) \\
&\overset{\text{leading}}{\propto} -e^2 m^2 C^2 \int \frac{\mathrm{d}^4 p}{(2\pi)^4}\frac{1}{(p^2 - m^2)^2} \\
&\overset{\text{leading}}{\propto} e^2 m^2 C^2 \ln\frac{m^2}{\Lambda^2_{\text{cutoff}}}
\end{aligned} \tag{176}$$

[18] One could inquire how this process differs in the actual calculation. The reason is subtle and can be traced to the lack of the Ward-Takahashi identities. It is possible to evaluate the graphs in a gauge-invariant violating way and use the identities to write the final result in the appropriate gauge invariant form.

where a series of properties of Dirac's algebra were used (SCHWARTZ, 2013) and some properties described in appendix E. Ignoring the cutoff, the gauge sector (now massive) is

$$S_{\text{eff.}}\Big|_{\text{gauge sector}} \propto e^2 m^2 C^2 + F^2(C) + \text{powers of } \left(C^2, F^2\right) \text{ and their combinations .} \tag{177}$$

Next, I will explore the pseudoscalar sector to compute the relevant factors.

4.3.2 Pseudo-Scalar sector

The origin of the mass term for the pseudo-scalar field is the condensate as expected from the computation done in section 2.3 which is analogous to the charge density waves proposed in the description of a topological magnetic insulator in (LI et al., 2010). As happens there, it is impossible to generate the mass term from the diagrammatic expansion of the trace since it is a nonperturbative phenomenon. The leading contribution is the kinetic term for the pseudo scalar field

$$\overset{\text{leading}}{\propto} \frac{m^2}{f^2}(\partial\theta)^2 \ln \frac{m^2}{\Lambda^2_{\text{cutoff}}} \ . \tag{178}$$

We need to look at the condensate to extract the mass term. The parametrization, after some redefinitions, took the form of equation (158) and can be used to that end. We can follow the same steps done in sec. 2.3 to obtain the general parameter dependency of the pseudo-scalar mass. The difference is that the perturbation must be done in both ϕ_R and ϕ_L leading to

$$\phi_R \to \lambda \left\langle \overline{\Psi} P_R P_- \Psi \right\rangle + \phi_R = \lambda v^3 + \lambda v^3 e^{2i\left(\frac{\theta(x)}{f} + \theta_0 + \frac{\theta'(x)}{f'}\right)} \tag{179}$$

and

$$\phi_L \to \lambda_L \left\langle \overline{\Psi} P_L P_- \Psi \right\rangle + \phi_L = \lambda v^3 + \lambda v^3 e^{-2i\left(\frac{-\theta(x)}{f} - \theta_0 + \frac{\theta'(x)}{f'}\right)} \ . \tag{180}$$

The variation on ϕ_R results in

$$|\phi_R|^2 \to |\phi_R|^2 + \lambda^2 v^6 + \lambda v^3(\phi_R + \phi_R^*) = 2\lambda^2 v^6 \left(1 + \cos\left(2\left(\frac{\theta(x)}{f} + \theta_0 + \frac{\theta'(x)}{f'}\right)\right)\right) \tag{181}$$

and ϕ_L gives a similar result which is

$$|\phi_L|^2 \to 2\lambda^2 v^6 \left(1 + \cos\left(2\left(-\frac{\theta(x)}{f} - \theta_0 + \frac{\theta'(x)}{f'}\right)\right)\right) \tag{182}$$

so the final result is

$$|\phi_R|^2 + |\phi_L|^2 = 4\lambda^2 v^6 \left(1 + \cos\left(2\frac{\theta'}{f'}\right)\cos\left(2\left(\frac{\theta}{f} + \theta_0\right)\right)\right) \tag{183}$$

where the trigonometric identity $2\cos\theta_1\cos\theta_2 = \cos(\theta_1 - \theta_2) + \cos(\theta_1 + \theta_2)$ was used. Using the cos expansion for small values of both θ and θ_0 leads to

$$|\phi_R|^2 + |\phi_L|^2 \sim 8\lambda^2 v^6 - 8\lambda^2 v^6 \left(\frac{\theta}{f} + \theta_0\right)^2 + \cdots \tag{184}$$

this indicates that the scalar field was a mass term proportional to $\propto \frac{\lambda^2 v^6}{f^2}\theta^2$. We can make two remarks at this point. The first one is that we expect combination $\frac{\theta}{f} + \theta_0$ to appear since they share the same roots. Both are linked to the chiral breaking sector of our condensate. One way to see this is to recall that the combination that originates (156) transforms under chiral rotations (see appendixes E.1.4.4 and E.1.4.5 along with the definition in equation (156)). The second point is the issue of the presence of the $\theta'(x)$ in our last calculation. Although we expanded the trigonometric for small values of $\theta'(x)$ (which is not a problem since it is a dynamical field), the problem is the presence of this term. This contribution transforms under gauge rotation, and we expect that no observable should include such contributions, the physical observable should be gauge invariant as always. To understand this we can go back to section 4.2. We can demonstrate that this problem is misleading by doing a gauge shift and "holding" the ϕ' transformation. This amounts to

$$\left\langle \overline{\Psi}\rho_1\Psi \right\rangle \to \left\langle \overline{\Psi}e^{-2i\alpha\rho_3}\rho_1\Psi \right\rangle \tag{185}$$

where we can use the more complex identity

$$e^{-2i\alpha\rho_3}\rho_1 = ((P_+ + P_-)\cos(2\alpha) - i(P_+ - P_-)\sin(2\alpha))(P_R + P_L) \tag{186}$$

where it was used the properties described in C.2. Computing the charged density current again results in

$$\left\langle \overline{\Psi}e^{-2i\alpha\rho_3}\rho_1\Psi \right\rangle = 4v^3 \cos\left(2\left(\frac{\theta'}{f'} + \alpha\right)\right)\cos\left[2\left(\frac{\theta}{f} + \theta_0\right)\right] \tag{187}$$

which clearly is invariant if $\frac{\theta'(x)}{f'} \to \frac{\theta'(x)}{f'} - \alpha$ as expected.

Lastly, the presence of the mass term for the pseudo-scalar field can be traced to the density wave[19] (similar to the charge density wave discussed in sec. 2.3). Using the extended spinor definition, the current density associated with ρ_1 is $J_0 = \Psi^\dagger \rho_1 \Psi$

$$\begin{aligned}\langle J_0 \rangle &= \left\langle \overline{\Psi}\rho_1\Psi \right\rangle \\ &= \left\langle \overline{\Psi}(P_+ + P_-)(P_R + P_L)\Psi \right\rangle = \frac{1}{\lambda}(\phi_R + \phi_R^* + \phi_L + \phi_L^*) \\ &= 4v^3 \cos\left(\frac{2\theta'}{f'}\right) \cos\left[2\left(\frac{\theta}{f} + \theta_0\right)\right]\end{aligned} \tag{188}$$

where it was used the relations $\rho_1 = P_+ + P_-$ and $1 = P_R + P_L$. Expanding results in

$$\begin{aligned}\langle J_0 \rangle &\sim 4v^3 - 4v^3\left(\frac{\theta}{f} + \theta_0\right)^2 + \cdots \\ &\sim 8v^3 - 8\frac{v^3}{f^2}\theta^2 + \cdots\end{aligned} \tag{189}$$

where again is valid $|\phi_R|^2 + |\phi_L|^2 \sim \lambda^2 |\langle J_0 \rangle|^2$.

Now we can express the effective Lagrangian for the pseudo-scalar field sector as

$$\mathcal{L}_{\text{eff.}}\Big|_{\text{pseudo scalar sector}} \propto \lambda^2 v^6 + \lambda^2 v^6 \left(\frac{\theta}{f} + \theta_0\right)^2 + \frac{m^2}{f^2}(\partial\theta)^2 + \cdots \ . \tag{190}$$

In the next section, I will combine the leading terms for the vector and pseudoscalar fields and chose the parameters to make the Lagrangian be in the canonical form.

4.3.3 Canonical effective action and comments

In the end, the effective response of the system is

$$\mathcal{L}_{\text{eff.}} \propto e^2 m^2 C^2 + F^2(C) + \lambda^2 v^6 \left(\frac{\theta}{f} + \theta_0\right)^2 + \frac{m_\theta^2}{f^2}(\partial\theta)^2 + \cdots \ , \tag{191}$$

where the $\cdots$ stands for the various powers of $\left(\theta, \theta_0, \theta\theta_0, \cdots, (\partial\theta)^2, C^2\right)$ and their combinations plus $\lambda^2 v^6$. Now it is possible to see that the Proca mass is $M \propto em \propto e\lambda^2 v^6$. Now it is simple to choose f as to be in the canonical form (which also fixates the f in the anomaly contribution). This results in the kinetic term results in $f \propto m \propto \lambda^2 v^3$ and the massive term to be $\frac{\lambda^2 v^6}{f^2} \propto \frac{\lambda^2 v^6}{\lambda^4 v^6} \propto \frac{1}{\lambda^2}$ which motivates the definition of a scalar mass to be $m_\theta \propto \frac{1}{\lambda}$. That is, the relation between the microscopic parameters and the effective

[19] It is not clear what kind of wave is present here since the extended spinor formalism blurs the usual definitions.

ones are

$$
\begin{aligned}
g &= \frac{e^2}{16\pi^2 f} \sim \frac{e^2}{\lambda^2 v^3} \ , \\
M &\sim e\lambda^2 v^3 \ , \\
m_\theta &\sim \frac{\lambda v^3}{f} \sim \frac{1}{\lambda} \ ,
\end{aligned}
\tag{192}
$$

This set the scaling behavior of the parameters of the effective theory as a function of the ones of the microscopic theory, and we can see that, although there are various parameters, they all originate from the same parameters in the microscopic Lagrangian. Again, the relationship between parameters in the macroscopic and microscopic description indicates that when the chiral condensate gets weaker the axion-photon coupling and the axion mass becomes stronger but the photon mass decreases.

The full system in it's canonical form (and ignoring the higher order terms) is

$$
Z(j,J) = \int \mathcal{D}(C,\theta) e^{i\int \mathrm{d}^4x \left(\mathcal{L}(C,\theta)+\lambda^2 v^6 + j_\mu C^\mu + J\theta\right)} \ , \tag{193}
$$

with

$$
\begin{aligned}
\mathcal{L}(C,\theta) = &-\frac{1}{4}F_{\mu\nu}F^{\mu\nu} + \frac{1}{2}M^2 C_\mu C^\mu + \frac{1}{2}(\partial\theta)^2 - \frac{1}{2}m_\theta^2\theta^2 \\
&+ \frac{m_\theta}{g}\theta\theta_0 + \frac{m_\theta^2}{g^2}\theta_0^2 + \frac{1}{4}g\left(\theta + \frac{\theta_0}{g}\right)\tilde{F}_{\mu\nu}F^{\mu\nu}
\end{aligned}
\tag{194}
$$

where $F_{\mu\nu} = \partial_\mu C_\nu - \partial_\nu C_\mu$. Before finishing this chapter we can make some comments.

The effective action (193) describes the electromagnetic response of a microscopic system characterized by chiral and charge condensates, whose fluctuations give rise to the dynamic of the axion field and to the photon mass, through the Higgs mechanism. Using our analysis in section 2.3 we can see that this system can be called a topological magnetic "superconductor" (or the superconductor version of (LI et al., 2010) but with the inclusion of the term θ_0) or, more generically, axion "superconductor" (akin to the terminology in (WANG; ZHANG, 2013)). It is important to comment that this is not the only form to obtain this system. The same effective theory can be obtained by dimension reduction from a 5D theory (QI; WITTEN; ZHANG, 2013) and also from general reasoning about condensation of charges and defects guided by symmetry considerations (BRAGA et al., 2016). But it is important to point out that we arrived at this action considering an interaction that makes contact with usual superconducting couplings in doped Weyl metals (ZYUZIN; BURKOV, 2012).

The inclusion, or not, of the term θ_0 is relevant (as noted in sec. 2.3) since it breaks invariance under $\theta \to -\theta$ and its coupling $\cos\left(\frac{\theta(x)}{f} - \beta(x)\right)$ generates a space-time anisotropy linked to the b_μ term since $\frac{m_\theta}{g}\beta\theta = \frac{m_\theta}{g}(\partial_\mu b^\mu)\theta \to -\frac{m_\theta}{g}b_\mu(\partial^\mu\theta)$. This is the major motivation for simplification $\theta_0 = 0$ in the next chapter, this will greatly simplify the 1-loop calculation of the correction to the massive photon propagator.

Before making some more considerations we need to recall the pairing used in section 2.3. That interaction term establishes an inter-node connection that breaks chiral symmetry resulting in an electromagnetic theory with axionic fluctuations. In our case, axion superconductor, we used a pairing that breaks charge symmetry and chiral symmetry. The question about the leading mechanism for the superconducting instability and the different pairings that can lead to it in a Weyl semimetal system has been a subject of intense investigation during the last few years, see (BEDNIK; ZYUZIN; BURKOV, 2015; CHO et al., 2012; WEI; CHAO; AJI, 2014; LI; HALDANE, 2018; SCALAPINO, 2012) for some examples. The consideration behind our choice of pairing is based on the notion that the effective theory is essentially fixed by the general requirements of chiral symmetry breaking and charge symmetry breaking. The specific pairing (134), which can be classified as intra-node s-wave (CHRISPIM; BRUNI; GUIMARAES, 2021), results in an effective theory of a superconductor with dynamical axion interaction as our calculation indicates. The general phenomenological features of this model, such as the penetration length to be discussed in the final part of ch. 5, are shared with any model that displays the same symmetries and symmetry-breaking patterns.

The non-perturbative effects in our model are encoded in

$$|\phi_R|^2 + |\phi_L|^2 = 4\lambda^2 v^6 \left(1 + \cos\left(2\frac{\theta'}{f'}\right)\cos\left(2\left(\frac{\theta}{f} + \theta_0\right)\right)\right) . \tag{195}$$

The small θ and θ_0 approximation remove from the system the information about the compactness (which is essential to the description of multivalued fields (BRAGA; GUIMARAES; PAGANELLY, 2020)) in those terms and exclude effects like axion string (WANG; ZHANG, 2013; YOU; CHO; HUGHES, 2016) among other possible non-perturbative effects. The vortices of θ are called chiral vortices in (QI; WITTEN; ZHANG, 2013) and the vortices of θ' are the usual ones from a superconductor and carry quantized magnetic flux. Chiral vortices don't carry magnetic flux but are responsible for a nonconservation of the naive supercurrent of the superconductor (BRAGA et al., 2016), see also (STONE; LOPES, 2016). Both kinds of vortices must be taken into account if one is interested in the topological features of the superconducting state and one can construct the corresponding effective topological field theories by reasoning about the dilution and condensation of such configurations. That is, these non-perturbative effects are indispensable if one is interested in a comprehensive description and classification of the system (GU; QI, 2015; QI; WITTEN; ZHANG, 2013).

Now, one could ask what are modifications, to the resulting effective theories, that distinct pairing creates. This is a complicated inquisition since the main point in the effective description is the identification of the relevant low energy degrees of freedom (including possible defects) so the answer depends on the system in consideration. But, in general, it seems to involve topological BF theories, as discussed in (HANSSON; OGANESYAN; SONDHI, 2004) for the usual superconductor, in (HANSSON et al., 2015) for a p-type superconductor, and in (BRAGA et al., 2016) for the axionic superconductor. Again, in our case, the general characteristics of the electromagnetic response are fixed, as discussed above.

4.3.4 Equation of motion and electromagnetic response

As previously commented, this system is very similar to the one we encountered in section 2.3. Here I will comment on some differences but the major part of new effects is discussed there. This Lagrangian results in the following equations of motion

$$\begin{aligned}
&\nabla \cdot \boldsymbol{E} = -M^2\phi + g\boldsymbol{\nabla}\left(\theta + \frac{\theta_0}{g}\right) \cdot \boldsymbol{B} \ , \\
&\nabla \times \boldsymbol{E} = -\frac{\partial \boldsymbol{B}}{\partial t}, \\
&\nabla \cdot \boldsymbol{B} = 0 \ , \\
&\nabla \times \boldsymbol{B} = \frac{\partial \boldsymbol{E}}{\partial t} - M^2\boldsymbol{A} + g\left(\frac{\partial\left(\theta + \frac{\theta_0}{g}\right)}{\partial t}\boldsymbol{B} + \boldsymbol{\nabla}\left(\theta + \frac{\theta_0}{g}\right) \times \boldsymbol{E}\right), \\
(\Box - m_\theta^2)\theta &= \frac{e^2 g}{8\pi^2}\boldsymbol{E} \cdot \boldsymbol{B} - \frac{m_\theta}{g}\beta \ .
\end{aligned} \tag{196}$$

We can see that the result is similar to the one obtained in section 2.3 but with the modifications introduced by the Proca mass term. This also changes the current in the system (obtainable by varying the action in terms of the massive vector field) to

$$j^\alpha = g\left(\frac{b_\mu}{g} - \partial_\mu\theta\right)\epsilon^{\mu\nu\alpha\beta}\partial_\nu A_\beta + M^2 A^\alpha \tag{197}$$

where we have the presence of the topological currents (anomalous Hall effect and chiral magnetic effect) plus the massive vector contribution.

5 1-LOOP CORRECTION TO THE PHOTON SELF-ENERGY

Before starting with the topic of this chapter we need to revise the story so far. The main focus of the previous chapters (namely chapters 1 to 3) weres the understanding of the microscopic model with an emphasis on the description of Weyl/Dirac semimetals and its resemblance with the Lorentz violating theories studied in high energy physics. In chapter 4, those concepts were used to construct a theoretical microscopic model that results in the effective theory dubbed Weyl-superconductor interacting with the dynamical pseudo-Axion field. For the sake of this computation, M, m, and g as treated as independent quantities. Another simplification will be the setting of θ_0 to zero, which will simplify, considerably, the computations. This changes the microscopic theory that no longer has separated (in momentum space) Weyl points meaning that we will be analyzing the physics of a Dirac semimetal (defined by $b_\mu = 0$). To compute the 1-loop correction to the photon propagator it is necessary to revise some concepts of quantum field theory (QFT). In special we need to make some consideration about the renormalizability of the effective theory along with the necessary steps to guarantee a physical result thru the renormalization process and eliminate some unphysical degrees of freedom (that are linked to ghost states). The higher-order terms in the fields, that were ignored in the trace calculation in last chapter, will play an important role in the renormalization process of this effective theory. In special, it will be necessary to include some of them to cancel the divergences in the modifications on the Yukawa potential induced by axionic fluctuations. This will be done in sections 5.1 and 5.2. After that, we will be able to proceed with the main point which is the computation of the photon self-energy that arises due to quantum fluctuations introduced by the axion field. Most of the computation is done in section 5.3 with some of the details being reserved for appendix B. Completing this computation, we will obtain the potential correction in section 5.5. In the last section (sec. 5.6), the asymptotics of the quantum corrected potential will be explored to give a physical interpretation. The bulk of this process was published in (CHRISPIM; BRUNI; GUIMARAES, 2021).

5.1 Non-renormalization treatment

The starting point is the action obtained in chapter 4 (equation (194)) written in terms of "bare" fields, which will be essential to the renormalization process as we will see. The field strength tensor is $f_{\mu\nu} = \partial_\mu \bar{a}_\nu - \partial_\nu \bar{a}_\mu$, with the dual tensor $\tilde{f}_{\mu\nu} = \frac{1}{2}\epsilon_{\mu\nu\sigma\rho} f^{\sigma\rho}$.

The action reads (in natural units and $\mathrm{diag}(g_{\mu\nu}) = (1, -1, -1, -1)$)

$$\tilde{S}_{\overline{g}} = \int d^4x \left(-\frac{1}{4} f_{\mu\nu} f^{\mu\nu} + \frac{1}{2} \overline{M}^2 \overline{a}_\mu \overline{a}^\mu + \frac{1}{2} \partial_\mu \overline{\theta} \partial^\mu \overline{\theta} - \frac{1}{2} \overline{m}^2 \overline{\theta}^2 + \frac{1}{4} \overline{g} \overline{\theta} \tilde{f}_{\mu\nu} f^{\mu\nu} \right) \ . \tag{198}$$

The elements are the same as before, the effective action describes the dynamics of a massive vector field (Proca) $\overline{a}_\mu(x)$, a massive pseudo-scalar field $\overline{\theta}(x)$, and displaying an axion-like interaction through the coupling constant $\overline{g}$. This parameter has a mass dimension -1 as one can see by counting the mass dimension of this Lagrangian term (here with Lorentz index suppressed) in

$$[g][\theta][F][\tilde{F}] = [g][\theta][\partial][A][\partial][A] = [g] + 5 \ . \tag{199}$$

Together with the fact that $[\mathrm{d}^4x] = -4$ means that for the action to be mass adimensional, e.g. $[S] = 0$, requires that $[g] = -1$ as previous mentioned.

The usual classification relies on what is called power counting which links the mass dimension of the coupling constant to the classification of the theory as non-renormalizable. Another classification that uses the mass dimension to classify the coupling is marginal (zero mass dimension), relevant (positive mass dimension), or irrelevant (negative mass dimension). This is the terminology of the Wilsonian renormalization group on which the axion interaction would be called irrelevant.

The nomenclature used (that is, calling theories with negative mass dimension coupling non-renormalizable theories) is unfortunate since such theories can be renormalizable if they are considered an effective description valid up to a cutoff threshold. As stated in the textbook (ZEE, 2010) this understanding is especially due to the work of Kenneth G. Wilson which used the effective field theory approach to describe critical phenomena in connection with phase transitions. This was recognized in 1982 by awarding him with a Noble prize[20].

Renormalizable theories have their infinities but, with only a finite number of counter-terms (free parameter capable of absorbing it), it is possible to eliminate those singularities and compute any physical observable given that only a handful of parameters are known. The usual example of a renormalizable theory (which will be important in the next sections) is quantum electrodynamics (QED). With just five parameters (the electron mass m, its charge e, the vacuum energy density ρ, and the renormalization of the electron ψ and photon fields A), all possible infinities can be countered. See textbooks on QFT as (SCHWARTZ, 2013) for more details.

The negative in non-renormalizable appear to indicate that this is not the case and one would be inclined to conclude that this theory generates no finite result or does

[20] https://www.nobelprize.org/prizes/physics/1982/summary/

not have any prediction power (unique results based on know quantities). In fact, these kinds of theories develop new divergences in the computation of physical observables as one explores higher energy phenomena. But, this is not a problem since, based on Wilson's work, non-renormalizable theories can be used to make predictions at a certain precision level if the appropriate higher dimension counter-terms are included. That is, non-renormalizable still has some forecasting power but the consequence is that this Lagrangian must be comprehended as describing the physics at energies much lower than the cut-off $\Lambda_{UV} \sim 1/g$. Furthermore, some physical quantities will be dependent on the specific cut-off which indicates that the physics beyond this scale is still relevant.

This is not a problem and this view on nonrenormalizable theories is widely used. Some examples of this process can be found in, quantum gravity (HOOFT; VELTMAN, 1974; STELLE, 1977; GOROFF; SAGNOTTI, 1985; GOROFF; SAGNOTTI, 1986; DONOGHUE, 1994a; DONOGHUE, 1994b) , chiral perturbation theory (WEINBERG, 1979; GASSER; LEUTWYLER, 1984; GASSER; LEUTWYLER, 1985; ECKER, 1996), nonlinear QED (HALTER, 1993; KONG; RAVNDAL, 1998; DICUS; KAO; REPKO, 1998), and axion-electrodynamics (VILLALBA-CHÁVEZ; GOLUB; MüLLER, 2018; CHRISPIM; BRUNI; GUIMARAES, 2021).

This method is based on the observation that, for a given order of precision, it is sufficient, for the cancellation of divergences, the inclusion of the counter-terms of the next order in that specific coupling.

The full theory (UV-completion) is not necessary in this approach (although we know it from ch. 4), but all the counter-terms that originate from the next-to-leading order in the coupling should be considered (in a renormalizable theory this process would be not necessary (SCHWARTZ, 2013)).

This is an expected consequence as one can see by remembering the computation done in chapter 4. Specifically, we skipped the computation of higher-order terms in our effective theory but, in principle, they are present and it is only natural that those terms do play a role here. But, leaving this computation to be done later (after we decided which process we want to compute) has its advantages because we can reduce the list of terms that needs to be considered. Not all terms in the Lagrangian will be relevant to the specific quantum process, known as vacuum polarization of the photon (or Proca) propagator, at 1 -loop. Also, those next-to-leading terms, in the appropriate coupling, must obey the symmetries of the initial action.

5.1.1 Next-to-leading identification process

The next-of-leading in the axion coupling takes an g^2 factor or, in terms of its mass dimension, -2. This means that we need to construct field operators with mass dimension 6 to maintain the Lagrangian density mass adimensional. The number of such operators that can be constructed is large, but it is possible to reduce it by considering the previously mentioned features of this specific calculation.

If we consider only pseudo-scalar fields we can construct 12 (reducible) dimension 6 field operators though not all terms will be relevant. We can reduce the number of terms by imposing that they obey the same symmetries of the original system (i.e. this symmetry is not anomalous) and that it produces a relevant contribution to the photon vacuum polarization at 1-loop. An example of this process is in order. The term ϕ^6 gives a six ϕ interaction and for it to be included in the quantum correction for the photon propagator we would need to “close” four lines and then insert it in our vacuum polarization graph which would result in a 3-loop contribution which is outside the desired precision (see figure 5). The same reasoning applies to $\partial^2\phi^4$ since we will not include 2-loop contributions. This means that we do not need to consider any combination that includes more than two scalar fields. Terms like $m^5\phi$ can be also ignored since they just change the vacuum energy by the inclusion of tadpoles and they are not important for our calculation either. In other words, we are interested in terms that will give a modification to the pseudo-scalar propagator at the tree level. Of the possible terms, we still need to consider the different ways we can write it following Lorentz invariance, but they all can be transformed one into the other by partial integration meaning that we only need to consider one and adjust the parameter.

Figure 5 - ϕ^6 interaction term inclusion in the photon propagator quantum correction

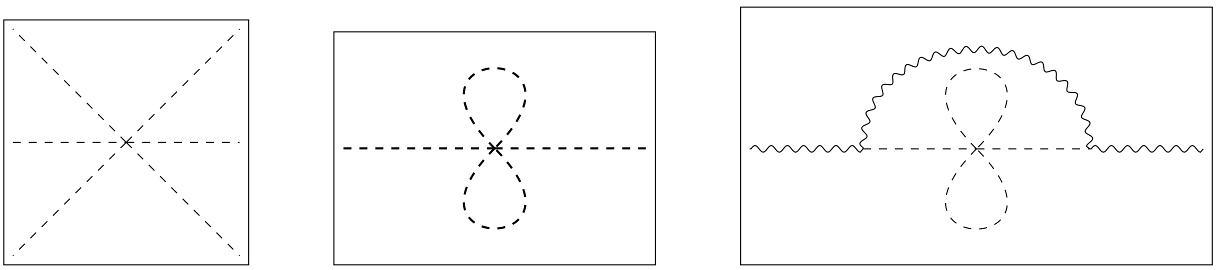

(a) (b) (c)

Subtitle: Process of inclusion of a ϕ^6 vertex in the photon propagator. The dashed lines represents the pseud-scalar and the wave the massive vector field. Figure (a) represents the Feynman graph of an six scalar field vertex, in order to include this term in the internal line of the photon propagator loop is necessary to “close” four scalar lines, as is described in figure (b). The inclusion of this term would generate the Feynman diagram depicted in (c), this would lead to a 3-loop contribution which is outside the desired precision of 1-loop.

Source: The author, 2022.

Now focusing on the massive gauge sector. The lack of gauge invariance, for example, allows for terms like $M_1^2(\overline{a}^2)^2$ to be included at order $\overline{g}^2$, but an odd number of $\overline{a}_\mu$ will not contribute since this would break the discrete symmetry (parity) $\overline{a}_\mu(x) \to -\overline{a}_\mu(x)$.

The same does not apply to the case for the scalar field because the coupling does have an odd number of $\overline{\theta}$'s. One contemplate possibility is $(\overline{a}^2)^3$ but, following the same idea of the six field scalar case, such a term will give a six photon vertex that is only relevant to the propagator if taken at 2-loops (which is outside the current calculation precision). Considering the various ways to combine the Lorentz indexes, the number of different field operators that we can construct in the vector field is greater. One algorithm that describes a similar process, for Proca-electrodynamics, can be found in (CADAVID; RODRIGUEZ, 2019). Lastly, the most general contribution must include terms composed with the dual field strength $\tilde{f}_{\mu\nu}$ but, since we are only interested in the contribution to the massive photon two-point function, they will be zero after we impose momentum conservation at the vertex [21]

In the end, all relevant terms of order $\overline{g}^2$ can be organized into three new Lagrangian pieces

$$\begin{aligned}
\overline{\mathcal{L}}_{\theta g^2} &= -\frac{1}{2}\overline{\theta}^2 m_1^2 + \frac{1}{2}\overline{C}_\theta(\partial\overline{\theta})^2 + \frac{1}{2\overline{m}_s^2}(\partial_\mu\overline{\theta})\Box(\partial^\mu\overline{\theta}) \ , \\
\overline{\mathcal{L}}_{ag^2} &= \frac{1}{2}\overline{M}_1^2\overline{a}^2 - \frac{1}{4}\overline{C}_f f^2 + \frac{1}{2\overline{m}_{gh}^2}(\partial f)^2 + \frac{1}{4!}\frac{1}{2}\overline{a}^4\overline{C}_4 - \frac{1}{4!}\frac{1}{4}\frac{\overline{a}^2}{\overline{M}_2^2}f^2 \ , \\
\overline{\mathcal{L}}_{a\theta g^2} &= -\frac{1}{2}\overline{C}_{a\theta}\overline{\theta}^2\overline{a}^2 + \frac{1}{4}\frac{\overline{\theta}^2}{\overline{m}_{\theta f}^2}f^2 \ ,
\end{aligned} \tag{200}$$

of which $(\partial f)^2 \equiv (\partial_\mu f^{\mu\rho})(\partial_\nu f^\nu_\rho)$. These are the next-of-leading field operators that obey the previously cited symmetry and precision constraints. It is important to notice that the all $\overline{C}_{f,4,a\theta,\theta}$, $\overline{M}_{1,2}$ and $\overline{m}_{1,s,gh}$ are of order $\mathcal{O}(g^2)$ since they are defined in terms of Wilsons's parameter b (which has mass dimension zero) as in

$$\begin{aligned}
&g^2 b^2_{m^4\phi} m^4 = m_1^2 \ , && g^2 b^2_{m^2\phi} m^2 = C_\phi \ , && g^2 b^2_\phi = m_s^{-2} \ , \\
&g^2 b^2_{M^4 a^2} M^4 = M_1^2 \ , && g^2 b^2_{M^2 a^2} M^2 = C_f \ , && g^2 b^2_{a^2} = m_{gh}^{-2} \ , \\
&g^2 b^2_{M^2 a^4} M^2 = C_4 \ , && g^2 b^2_{a^4} = M_2^{-2} \ , && g^2 b^2_{\mu^2 a^2 \phi^2}\mu^2 = C_{a\phi} \ , \\
&g^2 b^2_{\phi f} = m_{\phi f}^{-2} \ .
\end{aligned} \tag{201}$$

In some sense, the Wilson parameters here are reminiscent of fact that we truncate the expansion of the fermionic determinant. It is possible to determine their value by computing the full expression in the UV-complete theory (exposed in chapter 4) and matching it with the previous expression. We will consider them arbitrary, this is the price to pay for skipping that calculation.

[21] The point is that these terms will always contribute with a tensor structure of $\sim (g^{\mu\nu}p_1p_2 + p_1^\mu p_2^\nu)\epsilon_{\mu\nu\alpha\beta}$ and, once we impose momentum conservation in the vertex, the result will be zero by the symmetry of dummy indices. The Axion interaction does not suffer from this fate because of the loop structure.

Further considerations can be done to decrease the number of terms. The first one is to absorb some terms in parameter redefinitions in the normalization using the fact that the diversion is of order g^2 (subsection 5.1.2). As we will see, this will further simplify the new terms but will not affect the terms which involve higher derivatives (i.e. $(\partial^2 f)$ and $(\partial_\mu\overline{\theta})\Box(\partial^\mu\overline{\theta})$). The problem is that these higher derivative contributes to the quadratic portion, modifying the free propagator of the field. This will result in the apparition of a ghost pole (a mass pole with a "wrong" sign) for the free propagator of the pseudoscalar field and massive vector field. This term can not be absorbed in a parameter redefinition because they carry a $\Box^2$ (or in momentum space p^4) dependency, but, luckily this also can be treated in our current theory with a field redefinition. This will be the topic of the section 5.2 and most of the next discussion is based on (VILLALBA-CHÁVEZ; GOLUB; MüLLER, 2018) and (GRINSTEIN; O'CONNELL; WISE, 2008; ACCIOLY; DIAS, 2005).

5.1.2 Renormalization

In the renormalization process, we must replace the "bare" field and parameters with the renormalized ones along with the appropriate renormalization factors Z's. As we will see, this allows making further considerations to decrease the number of terms in our Lagrangian by absorbing some terms in parameter redefinitions. This is only possible because the difference between the two terms is of order g^2 as will be clear in the calculation.

Replacing the following quantities in equations (198) and (200)

$$\begin{aligned}
&\overline{a}_\mu \to A_\mu\ , && f_{\mu\nu} \to F_{\mu\nu}\ , && \overline{\theta} \to \theta\ , \\
&\overline{M} \to M\ , && \overline{m} \to m\ , && \overline{g} \to g\ , \\
&\overline{m}_1 \to m_1\ , && \overline{C}_\theta \to C_\theta\ , && \overline{m}_s \to m_s\ , \\
&\overline{M}_2 \to M_2\ , && \overline{C}_f \to C_f\ , && \overline{m}_{gh} \to m_{gh}\ , \\
&\overline{C}_4 \to C_4\ , && \overline{M}_2 \to M_2\ , && \overline{C}_{a\theta} \to C_{a\theta}\ , && \overline{m}^2_{\theta f} \to m^2_{\theta f}\ .
\end{aligned} \tag{202}$$

The renormalized action becomes

$$S_R = \int d^4x \left(\mathcal{L}_{\text{Proca}} + \mathcal{L}_{\text{axion}} + \mathcal{L}_{\text{interaction}} + \mathcal{L}_{\theta g^2} + \mathcal{L}_{a g^2} + \mathcal{L}_{a\theta g^2}\right)\ , \tag{203}$$

with the Proca and axion Lagrangians being

$$\mathcal{L}_{\text{Proca}} = -\frac{1}{4}Z_3 F_{\mu\nu}F^{\mu\nu} + \frac{1}{2}Z_M M^2 A_\mu A^\mu\ , \tag{204}$$

$$\mathcal{L}_{\text{axion}} = \frac{1}{2}Z_\theta \partial_\mu\theta\partial^\mu\theta - \frac{1}{2}Z_m m^2\theta^2\ , \tag{205}$$

the interaction term $\mathcal{O}(g^1)$

$$\mathcal{L}_{\text{interaction}} = \frac{1}{4} Z_g g \theta \tilde{F}_{\mu\nu} F^{\mu\nu} \ , \tag{206}$$

and the next-to-leading $\mathcal{O}(g^2)$

$$\mathcal{L}_{\theta g^2} = -\frac{1}{2} Z_{m2} \theta^2 m_1^2 + \frac{1}{2} Z_{\theta 2} C_\theta (\partial\theta)^2 + \frac{Z_s}{2m_s^2} (\partial_\mu \theta) \Box (\partial^\mu \theta) \ , \tag{207}$$

$$\mathcal{L}_{Ag^2} = \frac{1}{2} Z_{M2} M_1^2 A^2 - \frac{1}{4} Z_f C_f F^2 + \frac{Z_{gh}}{2m_{gh}^2} (\partial F)^2 + \frac{1}{4!} Z_4 C_4 A^4 - \frac{1}{4!} Z_5 \frac{A^2}{M_2^2} F^2 \ , \tag{208}$$

$$\mathcal{L}_{A\theta g^2} = -\frac{1}{4} Z_{a\theta} C_{a\theta} \theta^2 A^2 + \frac{1}{4} Z_{\theta f} \frac{\theta^2}{m_{\theta f}^2} F^2 \ . \tag{209}$$

The inclusion of one renormalization factor Z for each term (including the next-to-leading ones) is a necessity in the perturbative renormalization of our effective theory. Each Z factor carries the tree-level value (namely 1) plus counterterms that are of order $\mathcal{O}(g^2)$ (δ's). Generically one can write

$$Z_i = 1 + \delta_i \ . \tag{210}$$

One major point is that we still can do any parameter redefinition that amounts to changes that are outside the precision of order $\mathcal{O}(g^2)$. This can be used to our advantage since, as the following process will show, not all terms are necessary if we work at a certain accuracy. In this way, some next-to-leading terms can be assimilated into the quadratic section of the fields. As an example, the factor $Z_{M2}M_1^2$ (in eq. (208)) can be absorbed in the Proca mass term $Z_M M^2$ (in eq. (204))

$$\begin{aligned} Z_M M^2 + Z_{M2} M_1^2 &= Z_M M^2 + (1 + \delta_{M2}) M_1^2 \ , \\ &= Z_M M^2 + M_1^2 + \mathcal{O}\left(g^4\right) \ , \\ &= Z_M M^2 + \mathcal{O}\left(g^4\right) \ , \end{aligned} \tag{211}$$

where it was used the redefinition $M^2 Z_M \to (M^2 - M_1^2) Z_M$ and kept terms of order $\mathcal{O}(g^4)$. This same process can be done for other factors with the following redefinitions (and subsequent approximations to the correct order)

$$\begin{aligned} &Z_3 \to (1 - C_f) Z_3, \qquad M^2 Z_M \to (M^2 - M_1^2) Z_M \ , \\ &Z_\theta \to (1 - C_\theta) Z_\theta, \qquad m^2 Z_m \to (m^2 - m_1^2) Z_m \ . \end{aligned} \tag{212}$$

This changes the next-to-leading sector to

$$\mathcal{L}_{\theta g^2} = \frac{Z_s}{2m_s^2}(\partial_\mu\theta)\Box(\partial^\mu\theta) \ , \tag{213}$$

$$\mathcal{L}_{Ag^2} = \frac{Z_{gh}}{2m_{gh}^2}(\partial F)^2 + \frac{1}{4!}Z_4C_4A^4 - \frac{1}{4!}Z_5\frac{A^2}{M_2^2}F^2 \ , \tag{214}$$

$$\mathcal{L}_{A\theta g^2} = -\frac{1}{4}Z_{a\theta}C_{a\theta}\theta^2A^2 + \frac{1}{4}Z_{\theta f}\frac{\theta^2}{m_{\theta f}^2}F^2 \ . \tag{215}$$

The connection between the "bare" parameters and the renormalized ones is easily obtained by applying the kinetic prescription, $A^\mu = Z_3^{-1/2}a^\mu$ and $\theta = Z_\theta^{-1/2}\overline{\theta}$. The results are

$$\begin{array}{ccc} \overline{M} = M\left(\frac{Z_M}{Z_3}\right)^{1/2}, & \overline{m} = m\left(\frac{Z_m}{Z_\theta}\right)^{1/2}, & \overline{m}_{gh} = m_{gh}\left(\frac{Z_3}{Z_{gh}}\right)^{1/2}, \\ \overline{m}_s = m_s\left(\frac{Z_\theta}{Z_s}\right)^{1/2}, & \overline{C}_4 = C_4\frac{Z_3}{Z_{a^4}^{1/2}}, & \overline{M}_2 = M_2\frac{Z_3}{Z_5^{1/2}}, \\ \overline{m}_{\theta f} = m_{\theta f}\left(\frac{Z_3Z_\theta}{Z_{\theta f}}\right)^{1/2}, & \overline{C}_{a\theta} = C_{a\theta}\left(\frac{Z_{a\theta}}{Z_3Z_\theta}\right)^{1/2}, & \overline{g} = g\frac{Z_g}{Z_3^{1/2}Z_\theta^{1/2}}. \end{array} \tag{216}$$

The next-to-leading Lagrangian (equations (213), (214) and (215)), along with the free sector and their renormalization factors, contain all the necessary counterterms to cancel any divergence in our calculation. A trained viewer can see that the process is not done since the Lagrangians still possess higher derivative contributions to the quadratic sector. This fact will be made clear in the topic of the section 5.2 but with some extra considerations since it involves derivatives. The process of elimination is similar to the elimination of the parameters M_1, m_2, C_f, and C_θ. Most of the next discussion is based on (VILLALBA-CHÁVEZ; GOLUB; MüLLER, 2018) (and references within), and (GRINSTEIN; O'CONNELL; WISE, 2008; ACCIOLY; DIAS, 2005).

5.2 Ghost states and elimination process

The process done in the last section, the elimination of parameters in the renormalization of the counterterms up to a chance in next-to-next-leading-order, can not affect the terms which involve higher derivatives (i.e. $(\partial^2 f)$ and $(\partial_\mu\overline{\theta})\Box(\partial^\mu\overline{\theta})$ present in equations (213) and (214)). These terms can not be ignored since they contribute to the quadratic portion, modifying the free propagator of the field and generating nonphysical states. We will enlighten these affirmations by remembering how the computation for the propagator is done in the scalar field case. Afterward, it will demonstrate how this is not an issue once the perturbation nature of our calculation is considered. A similar discussion can be found in (ACCIOLY; DIAS, 2005; GRINSTEIN; O'CONNELL; WISE, 2008; VILLALBA-CHÁVEZ; GOLUB; MüLLER, 2018). The generating function of the pseudo-scalar field is

$$Z(J) = \int \mathcal{D}(\theta) e^{i\left(S_{axion}+S_{\theta g^2}\right)+i\int \mathrm{d}^4x\phi J} \;, \tag{217}$$

where S_{axion} is free massive pseudo scalar action of the axion field, $S_{\theta g^2}$ is the next-to-leading order in the coupling conteining only the pseudo-scalar field and J is a source (as discussed in chapter 1). The Lagrangian can be written as (without the Z's for simplicity)

$$S_{axion} + S_{\theta g^2} = \int \mathrm{d}^4x \left(\frac{1}{2}(\partial\theta)^2 - \frac{1}{2}m^2\theta^2 - \frac{1}{2m_s^2}\theta\Box\theta\right) = \int \mathrm{d}^4x \,\frac{1}{2}\theta\Big(-\Box - m^2 - \frac{p^4}{m_s^2}\Big)\theta \;. \tag{218}$$

Following the usual steps (see (SCHWARTZ, 2013)) (doing the integral using the Gaussian integral since the integrand is quadratic in the fields) leads to Green function

$$\left(\frac{\Box^2}{2m_s^2} + \Box + m^2\right)\Delta_0(x-x') = -\delta(x-x') \;, \tag{219}$$

that is solved by the Feynman propagator

$$\Delta_0(x-x') = \int \frac{\mathrm{d}^4x}{(2\pi)^2}\frac{e^{ip(x-x')}}{p^2 - m^2 - \frac{\Box^2}{m_s^2} + i\epsilon} \;, \tag{220}$$

or in momentum space

$$\Delta_0(p^2) = \frac{i}{p^2 - m^2 - \frac{p^4}{m_s^2} + i\epsilon} = \frac{1}{p^2-m^2} - \frac{1}{p^2 - m_s^2} + \mathcal{O}\Big(g^2\Big) \;, \tag{221}$$

where it was used that m_s^{-2} is of order $\mathcal{O}(g^2)$ (see relations in eq. (201)). The factor $i\epsilon$, as usual, is included to make the propagator mathematically well defined and consistent with physical causality due to the time ordering of events. This prescription dictated that at the physical mass pole $p^2 = m^2$, the residue of the Green function has[22] to be

$$\mathrm{Res}\Big\{\Delta_0(p^2)\Big\}\Big|_{p^2=m^2} = 1 \;, \tag{222}$$

but the modified propagator for the pseudo-scalar field has another mass pole at m_s with residue

$$\mathrm{Res}\Big\{\Delta_0(p^2)\Big\}\Big|_{p^2=m_s^2} = -1 \tag{223}$$

[22] This is a justification since this is only true for the on-shell renormalization scheme, if one uses the $\overline{MS}$ then the affirmation must be done using the physical mass. The significant point here is the sign of the pole, which is the same as the Pauli-Villars ghost.

characterizing a ghost state. These are the non-physical states mentioned before. This spoils the quantum system since the Hilbert space no longer has a positive definite norm when associated with this state, unitarity is thus violated (GRINSTEIN; O'CONNELL; WISE, 2008). These terms can not be absorbed in a parameter shift (as was done in the renormalization section) because they carry a $\Box^2$ (or in momentum space, p^4) dependency.

The same problem occurs in the massive vector sector in the presence of the high derivative order term, but this fact is not straightforward to see from the propagator, as in the scalar case, because the gauge field has unphysical states from the beginning (see (SCHWARTZ, 2013)). The propagator in the massive gauge case

$$G^{\mu\nu}(x-x') = \int \frac{\mathrm{d}^4 p}{(2\pi)^4} e^{ip\cdot(x-x')} \frac{1}{p^2 - M^2 - \frac{p^4}{m_{gh}^2}} + (p^\mu p^\nu - \text{terms}) \tag{224}$$

or, again writing in momentum space and expanding

$$G^{\mu\nu}(p^2) = \frac{1}{p^2 - M^2 - \frac{p^4}{m_{gh}^2}} = \frac{1}{p^2 - M^2} - \frac{1}{p^2 - m_{gh}^2} + \mathcal{O}\Big(g^2\Big) \ , \tag{225}$$

where, as in the scalar case, there is a new problematic mass pole $p^2 = m_{gh}^2$. The longitudinal contribution, which is expressed in the $(p_\mu p_\nu)$ terms, is irrelevant since it does not appear in the S-matrix. The problem is the presence of the metric tensor responsible for unphysical states that need to be removed in the quantization process. One easy workaround is to consider the saturated Green function

$$\mathcal{G}(p^2) = j_\mu G^{\mu\nu}(p^2) j_\nu \ . \tag{226}$$

This process is explored in ((ACCIOLY; DIAS, 2005; NIEUWENHUIZEN, 1973; SEZGIN; NIEUWENHUIZEN, 1980; VILLALBA-CHÁVEZ; GOLUB; MüLLER, 2018) and simplify the process. The residue $\mathrm{Res}\{\mathcal{G}(p^2)\}|_{p^2=M^2}$ is positive while $\mathrm{Res}\{\mathcal{G}(p^2)\}|_{p^2=m_{gh}^2}$ is negative. Now, in order to remove those problems, we need to treat those terms with a perturbative approach. These parameters, as stated before, are of order $\mathcal{O}(g^2)$ meaning that they are suppressed at a low energy spectrum. If this was not the case, a violation of unitarity would be present, spoiling the quantum correction calculation. It is possible to eliminate this kind of non-physical contribution by performing field redefinitions so that the free propagator will remain well-behaved and unitary (up to the desired precision) without changing any observable parameter (ARZT, 1995; KNETTER, 1994). The transformation is

$$\theta \to \theta - \frac{\Box}{2m_s^2}\theta \ , \qquad A_\mu \to A_\mu - \frac{\Box}{2m_{gh}^2} A_\mu \ . \tag{227}$$

This strategy is straightforward to see the pseud-scalar sector. Starting with the Lagrangian with the inclusion of other renormalization factors and the high derivative contribution the dynamics are

$$\mathcal{L}_{axion+\theta g^2} = \frac{1}{2}\theta\left(Z_3 p^2 - Z_m m^2 - \frac{Z_s}{m_s^2}p^4\right)\theta \ . \tag{228}$$

Now doing the redefinition (in momentum space) $\theta \rightarrow \left(1 + \frac{p^2}{2m_s^2}\right)\theta$

$$\begin{aligned}
\mathcal{L} \rightarrow \mathcal{L}' &= \frac{1}{2}\theta\left(1 + \frac{p^2}{2m_s^2}\right)\left(Z_3 p^2 - Z_m m^2 - \frac{Z_s}{m_s^2}p^4\right)\left(1 + \frac{p^2}{2m_s^2}\right)\theta \ , \\
&= \frac{1}{2}\theta\left(\left(Z_3 - Z_m\frac{m^2}{m_s^2}\right)p^2 - Z_m m^2 + (Z_3 - Z_s)\frac{p^4}{m_s^2}\right)\theta + \mathcal{O}\left(m_s^{-4}\right) \ , \\
&= \frac{1}{2}\theta\left(Z_3 p^2 - Z_m m^2 + \delta_s\frac{p^4}{m_s^2}\right)\theta + \mathcal{O}\left(m_s^{-4}\right) \ ,
\end{aligned} \tag{229}$$

where it was used the fact that the Z's are $1 + \mathcal{O}(g^2)$, m_s^{-2} is $\mathcal{O}(g^2)$ along with the redefinition of the δ. The same process can be applied to the vector field with similar redefinitions and more details can be found in (VILLALBA-CHÁVEZ; GOLUB; MüLLER, 2018; CHRISPIM; BRUNI; GUIMARAES, 2021). The final product is the original Lagrangian minus the problematic ghosts terms but with the inclusion of their counter-term. These new characters are crucial to the renormalization process in subsection 5.3.2. The resulting action is

$$\mathcal{L}_R = \mathcal{L}_{\text{Proca}} + \mathcal{L}_{\text{axion}} + \mathcal{L}_{\text{interaction}} + \frac{\delta_s}{2m_s^2}(\partial_\mu\theta)\Box(\partial^\mu\theta) + \frac{\delta_{gh}}{2m_{gh}^2}(\partial F)^2 + \mathcal{L}_{4\gamma} + \mathcal{L}_{2\gamma,2\theta} \ , \tag{230}$$

with

$$\mathcal{L}_{4\gamma} = \frac{1}{4!}Z_4 C_4 A^4 - \frac{1}{4!}Z_5\frac{A^2}{M_2^2}F^2 \ , \tag{231}$$

$$\mathcal{L}_{2\gamma,2\theta} = -\frac{1}{4}Z_{a\theta}C_{a\theta}\theta^2 A^2 + \frac{1}{4}Z_{\theta f}\frac{\theta^2}{m_{\theta f}^2}F^2 \ , \tag{232}$$

along with equations (204), (205) and (206). All these interactions will furnish 1-loop contributions to the massive vector self-energy that now can be fully renormalized thanks to the new counterterms. As stated in (VILLALBA-CHÁVEZ; GOLUB; MüLLER, 2018), the final contribution of the inclusion of the next-to-leading order terms is the insertion of ghosts states (Pauli-Villars) that is unabsorbable in the physics (up to the considered precision) but with the major contribution of new counter-terms which will be necessary to remove all infinities from the theory (again up to a regarded precision in the coupling).

5.3 **Photon self-energy**

We want to compute quantum corrections to the massive vector self-energy introduced by axion fluctuations. These fluctuations are the reason for the contrast between the free and interacting theory as it includes the effect of particles metamorphosing into another. As an example, in the usual QED, the possibility of a photon decaying into an electron and a positron (its antiparticle) generates measurable changes (the Lamb shift effect). In our model, the dressed massive vector propagator will include 1-loop contributions that originates from the axion coupling ($\mathcal{O}(g)$) and from $\mathcal{L}_{4\gamma}$ and $\mathcal{L}_{2\gamma,2\theta}$ ($\mathcal{O}(g^2)$). The exact Green function for the photon $G^{\mu\nu}(p)$ is given by the geometric sum of 1PI graphs

$iG^{\mu\nu}(p) =$ 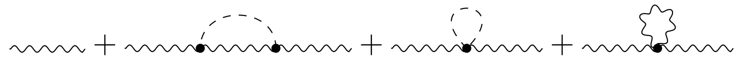 $+ \cdots \,, \qquad (233)$

$$= iG_0{}^{\mu\nu}(p) + iG_0{}^{\mu\sigma}(p)\,(i\Pi_{\sigma\rho}(p))\,iG_0{}^{\rho\nu}(p) + \mathcal{O}\Big(g^4\Big) \,, \tag{234}$$

where $G_0^{\mu\nu}(p)$ is the free massive vector propagator, defined as $G_0^{\mu\nu}(p) = -iP^{\mu\nu}(p)/(p^2 - M^2)$ with $P_{\mu\nu}(p) = g_{\mu\nu} - p_\mu p_\nu/M^2$, and $i\Pi_{\sigma\rho}(p)$ is the 1-loop contributions (consult figure 6 for exact Feynman's diagram anatomy) with the additional factors given by counterterms. It is important to remember that here we have two kinds of counterterms, the ones that originate from the free sector (the relevant are Z_3 and Z_M), and those that originate from the next-to-leading terms (in this case the δ_{gh}). The respective graphs are described in appendices B.1 and B.3.

$$\begin{aligned} i\Pi_{\sigma\rho}(p) = \sum_{i=1}^{3} K^{(i)}_{\sigma\rho}(p^2) - i(Z_3 - 1)(p^2 g_{\sigma\rho} - p_\sigma p_\rho) + i(Z_M - 1)(Z_3 - 1)M^2 g_{\sigma\rho} \\ + i\frac{\delta_{gh}}{m_{gh}^2} p^2(p^2 g_{\sigma\rho} - p_\sigma p_\rho) \,. \end{aligned} \tag{235}$$

The terms in $\sum_i^3 K^{(i)}_{\sigma\rho}(p^2)$ represents each graph that contribute to our correction to the massive vector propagator. In the next section I will compute (in some details) each one.

5.3.1 Loop integrals

In this section I will compute the three factors, $K^{(1)}_{\sigma\rho}(p^2)$ (axion loop fig. 6a), $K^{(2)}_{\sigma\rho}(p^2)$ (photon-axion loop fig 6b) and $K^{(3)}_{\sigma\rho}(p^2)$ (photon-photon loop fig. 6c). The Feynman rules are described in the appendix B.

Figure 6 - Sum of Feynman's graphs that contribute to the photon self energy in axion-Proca electrodynamics.

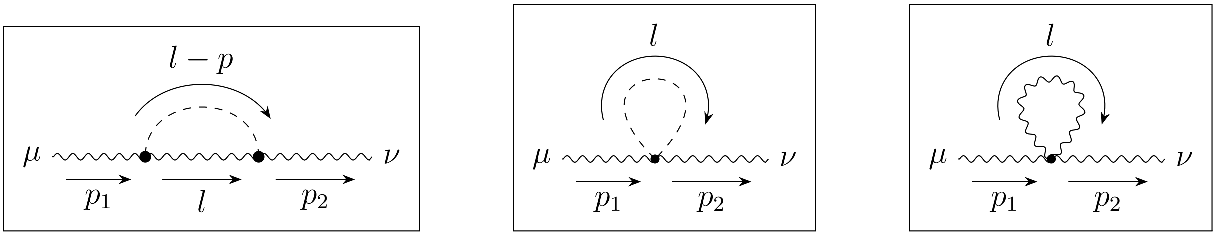

(a) (b) (c)

Subtitle: Diagram of *photon-axion loop* $K^{(1)}_{\mu\nu}$ (a), *axion loop* $K^{(2)}_{\mu\nu}$ (b) and *photon loop* $K^{(3)}_{\mu\nu}$ (c)
Source: CHRISPIM; BRUNI; GUIMARAES, 2021, p. 14.

5.3.1.1 Axion-photon loop

The axion coupling introduces a momentum dependent vertex that can be written schematically as $V_{\mu\nu}(p_1, p_2) = (-igZ_g)\epsilon_{\mu\nu\alpha\beta}p_1^\alpha p_2^\beta$ where the vector line carries outgoing momentum p_2 and p_1 (the definition can be found in the appendix B.2). In the Feynman's diagrams, represented in figure 6a, is shown the chosen momentum directions along with the correct momentum labels. The vertex construction results in

$$K^{(1)}_{\mu\nu} = \int \frac{\mathrm{d}^4 l}{(2\pi)^4} V_{\mu\sigma}(-p_1, l) D_0^{\sigma\rho}(l)\Delta_0(l-p)V_{\rho\nu}(l, -p_2) \ , \tag{236}$$

where $\Delta_0(p) = i/(p^2 - m^2)$ is the free massive pseudo scalar propagator in momentum space (see appendix B.1). Now we must do a series of computations and simplifications. The expression with all its Lorentz indexes is

$$K^{(1)}_{\mu\nu} = (i\ gZ_g)^2 \epsilon_{\mu\sigma ab}\epsilon_{\nu\rho cd}{p_1}^a {p_2}^c \int \frac{d^4 l}{(2\pi)^4} \frac{l^b l^d}{l^2 - M^2} \frac{P^{\sigma\rho}(l)}{(l-p)^2 - m^2} \ , \tag{237}$$

with $P_{\mu\nu}(l) = g_{\mu\nu} - l_\mu l_\nu / M^2$. This complicated expression is due to the combination of two Levi-Citiva tensors. The following relation is useful for this calculation

$$\epsilon_{\mu\gamma\alpha\nu}\epsilon^{\nu\sigma\rho\beta} = \delta^\sigma_\mu\left(\delta^\rho_\gamma\delta^\beta_\alpha - \delta^\beta_\gamma\delta^\rho_\alpha\right) - \delta^\rho_\mu\left(\delta^\sigma_\gamma\delta^\beta_\alpha - \delta^\beta_\gamma\delta^\sigma_\alpha\right) + \delta^\beta_\mu\left(\delta^\sigma_\gamma\delta^\rho_\alpha - \delta^\rho_\gamma\delta^\sigma_\alpha\right) \ , \tag{238}$$

to do the simplification contractions resulting in

$$K^{(1)}_{\mu\nu}(p^2) = -g^2 \int \frac{\mathrm{d}^4 l}{(2\pi)^4} \frac{Y_{\mu\nu}(p, l)}{l^2 - M^2} \frac{1}{(l-p)^2 - m^2} \ , \tag{239}$$

with $Y^{\mu\nu}(p, l) = g^{\mu\nu}\left(l^2 p^2 - (l \cdot p)^2\right) + l^\mu\left(p^\nu(l \cdot p) - p^2 l^\nu\right) + p^\mu\left(l^\nu(l \cdot p) - l^2 p^\nu\right)$ and $Z_g = 1 + O[g^2]$ (so that $(igZ_g)^2 \sim -g^2$). It was also used the momentum conservation condition to impose $p_1 = p_2 = p$. Next we introduce a Feynman's parametrization so that

$$\int \frac{d^4l}{(2\pi)^4} \frac{Y^{\mu\nu}(p,l)}{l^2 - M^2} \frac{1}{(l-p)^2 - m^2} = \int \frac{d^4l}{(2\pi)^4} \int_0^1 ds \frac{Y^{\mu\nu}(p,l)}{(q^2 - \Delta(s,p^2))^2} \ , \tag{240}$$

with $q_\nu = l_\nu - s\ p_\nu$ and $\Delta(s,p^2) = m^2 s - M^2(s-1) - p^2 s(1-s)$. Now doing a change of variables $l \to q + ps$ gives

$$\int \frac{d^4q}{(2\pi)^4} \int_0^1 ds \frac{Y^{\mu\nu}(p, q+ps)}{(q^2 - \Delta(s,p^2))^2} \ . \tag{241}$$

This result in

$$Y^{\mu\nu}(p,q+ps) = g^{\mu\nu}\left(p^2q^2 - (p\cdot q)^2\right) + p^\mu\left(q^\nu(p\cdot q) - q^2p^\nu\right) + q^\mu\left(p^\nu(p\cdot q) - p^2q^\nu\right) \ . \tag{242}$$

Using that $q^\mu q^\nu \to \frac{1}{D}q^2 g^{\mu\nu}$ (which is valid only inside the integral (SCHWARTZ, 2013)) we get (for $D = 4$)

$$Y^{\mu\nu}(p,q+ps) = q^2(g^{\mu\nu}p^2 - p^\mu p^\nu)\left(1 - \frac{2}{D}\right) = \frac{q^2}{2}(g^{\mu\nu}p^2 - p^\mu p^\nu) \ . \tag{243}$$

This result in

$$K^{(1)}_{\mu\nu}(p^2) = -\frac{g^2}{2}(g^{\mu\nu}p^2 - p^\mu p^\nu)\int \frac{d^4q}{(2\pi)^4}\int_0^1 ds \frac{q^2}{(q^2 - \Delta(s,p^2))^2} \ , \tag{244}$$

with $\Delta(s,p^2) = m^2 s - M^2(s-1) - p^2 s(1-s)$. As we can see, even though gauge invariance is explicitly broken by the mass term, the longitudinal component is effectively decoupled and the result can still be written using the usual transverse operator

$$K^{(1)}_{\mu\nu}(p^2) = (g_{\mu\nu}p^2 - p_\mu p_\nu)k^{(1)}(p^2) \ , \tag{245}$$

with

$$k^{(1)}(p^2) = -\frac{g^2}{2}\int \frac{d^4q}{(2\pi)^4}\int_0^1 ds \frac{q^2}{(q^2 - \Delta(s,p^2))^2} \ . \tag{246}$$

This can be formally established by a Ward identity (HEES, 2003) showing that only the transverse part will contribute to the final result. Now we must extend $k^{(1)}(p^2)$ to $D-$dimensions and redefine the dimensional coupling as $g \to g\mu^{\frac{4-D}{2}}$ (μ is an arbitrary parameter of mass dimension 1 so that the coupling g is now dimensionless). Also, this rescaling must be followed by a redefinition of the Wilson parameters $b_i \to b_i\mu^{\frac{D-4}{2}}$ so that

b_i is also dimensionless. This leads to

$$k^{(1)}(p^2) = -\frac{g^2\mu^{4-D}}{2}\int\frac{d^Dq}{(2\pi)^D}\int_0^1 ds\frac{q^2}{(q^2-\Delta(s,p^2))^2} \ . \tag{247}$$

Changing the integrating order, doing a Wick rotation, and using the usual formula (SCHWARTZ, 2013)

$$\int\frac{d^Dk}{(2\pi)^D}\frac{k^{2D}}{(k^2-\Delta)^b} = i(-1)^{a-b}\frac{1}{(4\pi)^{\frac{D}{2}}}\frac{1}{\Delta^{b-a-\frac{D}{2}}}\frac{\Gamma\left(a+\frac{D}{2}\right)\Gamma\left(b-a-\frac{D}{2}\right)}{\Gamma\left(b\right)\Gamma\left(\frac{D}{2}\right)} \tag{248}$$

gives

$$k^{(1)}(p^2) = \frac{ig^2\mu^{4-D}D}{4(4\pi)^{D/2}}\Gamma\left(1-\frac{D}{2}\right)\int_0^1 ds\Delta^{\frac{D}{2}-1} \ . \tag{249}$$

Expanding for $D = 4-\epsilon$ with $\epsilon\to 0$ we obtain

$$k^{(1)}(p^2) = 1-\frac{ig^2}{8\pi^2\epsilon}\int_0^1 ds\Delta + \frac{ig^2}{16\pi^2}\int_0^1 ds\Delta\left(-\frac{1}{2}+\log\frac{\Delta}{\tilde{\mu}^2}\right) \tag{250}$$

$$= 1-\frac{ig^2}{16\pi^2}\left(\frac{2}{\epsilon}+\frac{1}{2}\right)\left(\frac{m^2}{2}+\frac{M^2}{2}-\frac{p^2}{6}\right)+\frac{ig^2}{16\pi^2}\int_0^1 ds\Delta\log\frac{\Delta}{\tilde{\mu}^2} \ , \tag{251}$$

with the usual definition $\tilde{\mu}^2 = e^{-\gamma}4\pi\mu^2$ (γ is the Euler-Mascheroni constant). In this computation, any part that is not divergent or that don't have any kind of discontinuity can be ignored since they will simply be absorbed by a finite redefinition of the original action. This gives

$$k^{(1)}(p^2) = -\frac{ig^2}{16\pi^2}\left[\frac{2}{\epsilon}\left(\frac{m^2}{2}+\frac{M^2}{2}-\frac{p^2}{6}\right)-\int_0^1 \mathrm{d}s\,\Delta\log\frac{\Delta}{\tilde{\mu}^2}\right] . \tag{252}$$

5.3.1.2 Axion loop

To construct the axion loop graph (represented in figure 6b) one must use the interaction term which generates the two-photon-two-axion vertex (described in appendix B.5) and "close" the pseudo-vector lines then include an appropriate axion propagator. This results in

$$K^{(2)}_{\mu\nu} = \left[Z_{a\phi}C_{a\theta}g_{\mu\nu}+\frac{Z_{\phi f}}{m^2_{\phi f}}(g_{\mu\nu}(p_1\cdot p_2)-p_{1\mu}p_{2\nu})\right]\int\frac{d^4l}{(2\pi)^4}\frac{1}{l^2-m^2} \ , \tag{253}$$

where the symmetry factor $\frac{1}{2}$ was included (and cancels the 2 from the interaction term). Imposing momentum conservation (so that $p_1 = p_2 = p$) along with the same considerations of precision, e.g. $Z_{a\theta} = 1 + \mathcal{O}(g^2)$ leading to $Z_{a\theta}C_{a\theta} \sim C_{a\theta} + \mathcal{O}(g^4)$, leads to

$$K^{(2)}_{\mu\nu}(p^2) = g_{\mu\nu}k^{(2)}(p^2) + (p_\mu p_\nu - \text{terms}) \tag{254}$$

with

$$k^{(2)}(p^2) = \left(C_{a\theta} + \frac{p^2}{m^2_{\phi f}}\right)\int \frac{d^4 l}{(2\pi)^4}\frac{1}{l^2 - m^2} \ , \tag{255}$$

where we already extracted the longitudinal part. The next steps in the computation of $k^{(2)}(p^2)$ are similar to the ones done in the last part. We extend its dimension to D, redefine the dimensional couplings (in this case only on the Wilson parameters inside the definitions of $C_{a\phi}$ and $m_{\phi f}$). This results in

$$k^{(2)}(p^2) = \left(C_{a\theta} + \frac{p^2}{m^2_{\phi f}}\right)\mu^{4-D}\int \frac{d^D l}{(2\pi)^D}\frac{1}{l^2 - m^2} \ . \tag{256}$$

Now we can use the general formula (248) to compute the momentum integral (after a Wick rotation) which results in

$$k^{(2)}(p^2) = \frac{im^2}{16\pi^2}\left(C_{a\theta} + \frac{p^2}{m^2_{\phi f}}\right)\left(\frac{2}{\epsilon} - \log\left(\frac{m^2}{\tilde{\mu}^2}\right)\right) \tag{257}$$

and, as usual, the definition $\tilde{\mu}^2 = e^{-\gamma}4\pi\mu^2$. Again, any factor that does not contribute to some kind of divergence or discontinuity is ignored.

5.3.1.3 Photon loop

The Feynman graph figure 6c is obtained from the 4γ interaction term (the Feynman rules are described in appendix B.4). The "construction" is simply and consists on "closing" two photon lines and the inclusion of the appropriate internal photon propagator. This results in the contribution

$$K^{(3)}_{\mu\nu} = \frac{i}{6}\int \frac{d^4 l}{(2\pi)^4}\left(Z_4 C_4 T^{(1)}_{\mu\nu\rho\sigma} + \frac{Z_5}{M_2^2}T^{(2)}_{\mu\nu\rho\sigma}(p_1, p_2, -l, l)\right) D_0{}^{\mu\nu}(l) \ , \tag{258}$$

where $D_0^{\sigma\rho}(l) = -iP_{\sigma\rho}(l)/(l^2 - M^2)$ (with $P_{\mu\nu}(l) = g_{\mu\nu} - l_\mu l_\nu/M^2$) is the massive photon propagator. The explicit form of the T's are described in the appendix B.4. Opening this require a little of work so we will first define

$$K^{(3)}_{\mu\nu} = \frac{1}{6}\int \frac{d^4 l}{(2\pi)^4}\left(Z_4 C_4 T^{(1)}_{\mu\nu} + \frac{Z_5}{M_2^2}T^{(2)}_{\mu\nu}(p_1, p_2, -l, l)\right)\frac{1}{l^2 - M^2} \tag{259}$$

so we can workout each expression more easily. These new terms are

$$
\begin{aligned}
T^{(1)}_{\mu\nu} &= T^{(1)}_{\mu\nu\rho\sigma} P^{\sigma\rho}(l) \ , && (260)\\
T^{(2)}_{\mu\nu}(p_1, p_2, -l, l) &= T^{(2)}_{\mu\nu\rho\sigma}(p_1, p_2, -l, l) P^{\sigma\rho}(l) \ . && (261)
\end{aligned}
$$

The next step is to simplify the expression using $l^\mu l^\nu \to \frac{1}{D} l^2 g^{\mu\nu}$ and the fact that an odd potency in the integral variable will give a null result. Another point is that can impose momentum conservation (with $p_1 = -p_2 = p$), use the same precision considerations (as in $Z_4 C_4 \sim C_4 + \mathcal{O}(g^4)$), and $D = 4$ for simplicity. This results in the first term being

$$
T^{(1)}_{\mu\nu} = 6 g_{\mu\nu} \left(1 - 4\frac{l^2}{M^2}\right) \ . \tag{262}
$$

The second term is a little more complicated and gives

$$
\begin{aligned}
T^{(2)}_{\mu\nu}(p, p, -l, l) &= -\left(4 - \frac{l^2}{M^2}\right)(g^{\mu\nu} p^2 - p^\mu p^\nu) - 3 l^2 g^{\mu\nu} \ , \\
&= g_{\mu\nu}\left[p^2\left(-4 + \frac{l^2}{M^2}\right) - 3l^2\right] + (p_\mu p_\nu - \text{terms}) \ .
\end{aligned} \tag{263}
$$

Now we can write the transverse part as

$$
K^{(3)}_{\mu\nu}(p^2) = k^{(3)}(p^2) g_{\mu\nu} + (p_\mu p_\nu - \text{terms}) \tag{264}
$$

with

$$
k^{(3)}(p^2) = \frac{1}{6}\int \frac{d^4 l}{(2\pi)^4}\left\{6C_4\left(1 - 4\frac{l^2}{M^2}\right) + \frac{1}{M_2^2}\left[p^2\left(-4 + \frac{l^2}{M^2}\right) - 3l^2\right]\right\}\frac{1}{l^2 - M^2} \ . \tag{265}
$$

The final part is to do the dimensional regularization by doing the appropriate dimensional coupling redefinitions (as is done in subsection 5.3.1.1), along with the redefinition of the Wilson parameters inside the C_4 and M_2^2. The momentum integral becomes

$$
\begin{aligned}
k^{(3)}(p^2) = \frac{1}{6}\mu^{4-D}\int \frac{\mathrm{d}^D l}{(2\pi)^D}&\left\{6C_4\left(1 - 4\frac{l^2}{M^2}\right)\right. \\
&\left. + \frac{1}{M_2^2}\left[p^2\left(-4 + \frac{l^2}{M^2}\right) - 3l^2\right]\right\}\frac{1}{l^2 - M^2} \ ,
\end{aligned}
$$

and can be done using eq. (248). The result is (after the elimination of the irrelevant numerical contributions)

$$
k^{(3)}(p^2) = -\frac{iM^2}{16\pi^2}\left(3C_4 + \frac{p^2 + M^2}{2M_2^2}\right)\left[\frac{2}{\epsilon} - \log\left(\frac{M^2}{\tilde{\mu}^2}\right)\right] \ . \tag{266}
$$

5.3.1.4 Result

Putting together all elements, computed in the last subsections, we can rewrite equation (235) as

$$i\Pi_{\sigma\rho}(p) = \left(\sum_{i=1}^{3} k^{(i)}(p^2) - i\delta_3 p^2 + i(\delta_M + \delta_3)M^2 + i\frac{\delta_{gh}}{m_{gh}^2}p^4\right)g_{\sigma\rho} + (p_\mu p_\nu - \text{terms}) \tag{267}$$

with

$$\begin{aligned}\sum_{i=1}^{3} k^{(i)}(p^2) = \frac{i}{16\pi^2}\Bigg[&-g^2p^2\left[\frac{2}{\epsilon}\left(\frac{m^2}{2} + \frac{M^2}{2} - \frac{p^2}{6}\right) - \int_0^1 \mathrm{d}s\,\Delta\log\frac{\Delta}{\tilde{\mu}^2}\right] \\ &+m^2\left(\frac{2}{\epsilon} - \log\left(\frac{m^2}{\tilde{\mu}^2}\right)\right)\left(C_{a\theta} + \frac{p^2}{m_{\theta f}^2}\right) \\ &-M^2\left(\frac{2}{\epsilon} - \log\left(\frac{M^2}{\tilde{\mu}^2}\right)\right)\left(3C_4 + \frac{p^2+M^2}{2M_2^2}\right)\Bigg] \ .\end{aligned} \tag{268}$$

In the next section we will organize this result and use the re-normalization conditions to cancel any infinity.

5.3.2 Renormalization

Using equations (267) and (268) results in

$$i\Pi_{\mu\nu}(p) = i\Pi(p^2)g_{\mu\nu} + (p_\mu p_\nu - \text{terms}) \tag{269}$$

$$\Pi(p^2) = \frac{1}{16\pi^2}\left[\Pi^{(0)} + p^2\Pi^{(2)}(p^2) + p^4\Pi^{(4)} - p^2\delta_3 + (\delta_M + \delta_3)M^2 + p^4\frac{\delta_{gh}}{m_{gh}^2}\right] \ . \tag{270}$$

The exact propagator can be found by the successive inclusion of 1PI graphs as in

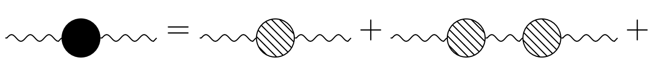

$$, \tag{271}$$

where the *blob* is the sum of the previous computed diagrams

$$i\Pi_{\sigma\rho}(p) =$$

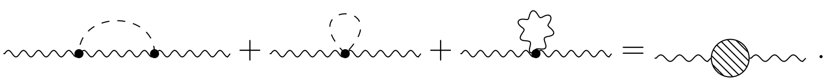

$$. \tag{272}$$

Now, the exact Green's function at one loop, in this context, is given by

$$iG_{\mu\nu}(p^2) = iG_0{}^{\mu\nu} + iG_0{}^{\mu\sigma}\left(i\Pi_{\sigma\rho}\right)iG_0{}^{\rho\nu} + iG_0{}^{\mu\sigma}\left(i\Pi_{\sigma\rho}\right)iG_0{}^{\rho\alpha}\left(i\Pi_{\alpha\beta}\right)iG_0{}^{\beta\nu} + \cdots \ , \tag{273}$$

$$= -i\frac{g_{\mu\nu}}{p^2(1+\Pi^{(2)}) - (M^2 - \Pi^{(0)}) + p^4\Pi^{(4)}(p^2)} + (p_\mu p_\nu - \text{terms}) \ , \tag{274}$$

with

$$\Pi^{(0)} = \left(\frac{2}{\epsilon} - \log\left(\frac{m^2}{\tilde{\mu}^2}\right)\right) m^2 C_{a\theta} - M^2\left(\frac{2}{\epsilon} - \log\left(\frac{M^2}{\tilde{\mu}^2}\right)\right)\left(3C_4 + \frac{M^2}{2M_2^2}\right) + M^2\delta_M \ , \tag{275}$$

$$\Pi^{(2)} = \left(\frac{2}{\epsilon} - \log\left(\frac{m^2}{\tilde{\mu}^2}\right)\right)\frac{m^2}{m_{\theta f}^2} - \left(\frac{2}{\epsilon} - \log\left(\frac{M^2}{\tilde{\mu}^2}\right)\right)\frac{M^2}{2M_2^2}$$
$$+ g^2\left(\frac{2}{\epsilon}\left(\frac{m^2}{2} + \frac{M}{2}\right) + \int_0^1 \mathrm{d}s\, \Delta \log\frac{\Delta}{\tilde{\mu}^2}\right) + \frac{\delta_3}{p^2}\left(M^2 - p^2\right) \ , \tag{276}$$

$$\Pi^{(4)} = g^2\frac{2}{\epsilon}\frac{1}{6} + \frac{\delta_{gh}}{m_{gh}^2} \ , \tag{277}$$

which is organized in powers of p^2 as usual. This expression is correct up to $\mathcal{O}(g^4)$ (with the exception of $\frac{\delta_{gh}}{m_{gh}^2}$) and any finite term[23].

Before proceeding to the renormalization process it should be clear that this expression results in the one found in (VILLALBA-CHÁVEZ; GOLUB; MüLLER, 2018) once we set $M^2 = 0$. Since gauge invariance acts as a custodial symmetry (SCHWARTZ, 2013) to the photon mass it is expected that when the Proca term is set to zero there are no quantum corrections that would generate a mass term. That is when $M^2 = 0$ there should be no term $\sim \Pi^{(0)}$ in our result. This indeed is the case because the term $\sim C_{a^2\theta^2}$ can not be included in $\overline{\mathcal{L}}_{a\theta g^2}$ in equation (200) if we have gauge invariance. In this case, if we make $M^2 = 0$ we will regain gouge invariance and can not include any term with a^2 anywhere in $\mathcal{L}_{g^2}$. This is a case of custodial symmetry and indicated that the photon mass is protected from large mass corrections.

In the next subsections, I will abord the choice of renormalization scheme. This is the part where the connection with the physical quantities is done because, so far, there is no mention of the actual measurable parameters. This connection is not trivial as the modern understanding is due to Ken Wilson at the beginning of 1970 (SCHWARTZ, 2013). The previous calculation was done using the so-called dimensional regularization. This process is based on the shift from four dimensions to d-dimensions to avoid problems of convergence in the momentum integral. The relic is the one divided by epsilon (who is formally zero). But, as is known today, the result should always be in terms of physical quantities. The next part is about this connection and how this process is different in the massless and massive photon cases.

[23] All δ were redefined to include the $16\pi^2$ factor

5.3.2.1 MS-bar scheme (massless case)

In the massless photon case, Axion fluctuations are responsible for a correction of the Coulomb electrostatic potential, felt by a test charge e. The Coulomb potential (in momentum space) can be "read" directly from $G_0(p^2)$ as in

$$iG_{\mu\nu\,M=0}(p^2) = -i\frac{g_{\mu\nu}}{p^2(1+\Pi^{(2)}) + p^4\Pi^{(4)}(p^2)} + (p_\mu p_\nu - \text{terms})\ , \tag{278}$$

$$\to \tilde{V}_{M=0}(p^2) = \frac{e^2}{p^2}\frac{1}{1+\Pi^{(2)} + p^2\Pi^{(4)}(p^2)}\ . \tag{279}$$

This will be made clear in the potential computation. The point is that the parameter is not (yet) the electric charge. To make this connection, one must impose

$$\tilde{V}_{M=0}(p_0^2) \equiv \frac{e^2}{p_0^2} \tag{280}$$

to define e as the actual electric charge measured in the experiment[24]. The three-momentum p_0 is the scale at which the measurement occurs. This means that we can rewrite the potential as

$$\tilde{V}_{M=0}(p^2) = \frac{e^2}{p^2}\left[1 + \frac{1}{p^2}\left(\Pi^{(2)}(p_0^2) - \Pi^{(2)}(p^2) + (p_0^2 - p^2)\Pi^{(4)}\right)\right] + O[e^2g^4] \tag{281}$$

in momentum space evaluated at p concerning it's value at the scale p_0. This potential still is problematic. There are divergencies in the Π's (the ϵ) and the presence of the arbitrary point introduced by the dimensional regularization (the $\tilde{\mu}$). The first problem can be solved by imposing $\overline{MS}$ conditions which cancel only the divergent part. That is, the counter-terms must not contain any finite term. In special, $\Pi^{(4)}$ is constant at this order and can be set to zero by imposing the $\overline{MS}$ scheme. Now, it is physically sensible to make contact with the measured electric charge by defining the potential to have the Coulomb form at spatial infinity, or equivalently at $p_0 = 0$, where the axion effect should be negligible. That is, to fix p_0 is sufficient to impose that the potential is of the usual Coulomb type at $p_0 = 0$ resulting in e being the observable electric charge. This works as a renormalization condition fixing the ambiguity in $\Pi^{(2)}$ since it is possible to compute $\tilde{\mu}$ from the condition $\Pi(0) = 0$ (as is done in (VILLALBA-CHÁVEZ; GOLUB; MüLLER, 2018)). Two modifications to this computation occur when the Proca mass term is included. First, a renormalization additional condition will be necessary for the

[24] Usually, the notation is e for the parameters in the Lagrangian and e_R (or e_{ph}) for the electric charge measured in experiments. I choose to not introduce a new subscript, the context will make clear the distinction.

Proca mass. Second, the computation that allows us to fix the $\overline{MS}$ free parameter $\tilde{\mu}$ using the low energy subtraction point conditions is not clear in the context of massive photons. To illustrate this problem we can write the subtracted potential in moment space, that is the Fourier transform of the potential in two distinct scales (here p and p_0)

$$\tilde{V}(p^2) = \frac{e^2}{p^2 - M^2} \times \\ \times \left(1 + \frac{1}{p^2 - M^2}\left(\frac{p_0^2\Pi^{(2)}(p_0^2) + p_0^4\Pi^{(4)}}{p_0^2 - M^2} - \frac{p^2\Pi^{(2)}(p^2) + p^4\Pi^{(4)}}{p^2 - M^2}\right)\right) + O[e^2 g^4] \ . \tag{282}$$

Note that here the scale p_0 is defined as the scale where the potential is of the Yukawa type, as in

$$\tilde{V}(p_0^2) \equiv \frac{e^2}{p_0^2 - M^2} \ , \tag{283}$$

but now one can not use the asymptotic charge to define a physically motivated renormalization condition as done above in the massless case. The potential of a massive photon is null asymptotically as a result of the screening due to the superconductivity. Physically, due to the massive nature of the photon, test charges will feel no force at spatial infinity. This is a setback for the use of the $\overline{MS}$ scheme because there is no simple way to fix the remaining ambiguity. This problem can be avoided if we impose the so-called on-shell (OS) conditions.

5.3.2.2 OS scheme

It is clear from equation (274) that it will be necessary three conditions to fix the singular ϵ^{-1} contributions that are proportional to p^0, p^2 and p^4. They will be

$$\Pi(M^2) = 0 \ , \tag{284}$$

$$\left.\frac{\partial \Pi(p^2)}{\partial p^2}\right|_{p^2 = M^2} = 0 \ , \tag{285}$$

$$\left.\frac{\partial^2 \Pi(p^2)}{(\partial p^2)^2}\right|_{p^2 = M^2} = 0 \ , \tag{286}$$

but before we apply these conditions we must make a $\mathcal{O}(g^4)$ modification

$$p^4 \frac{\delta_{gh}}{m_{gh}^2} \to \frac{1}{2}(p^2 - M^2)^2 \frac{\delta_{gh}}{m_{gh}^2} \ . \tag{287}$$

The first two conditions fix the mass pole location and the residue (so that the physical photon mass is M^2 with residue i). The third cancel any contribution from $\Pi^{(2)}$ by fixing the ghost counter-term. Now we can impose these restrictions, resulting in a physically consistent potential clear from any infinities and free parameters. The counter terms obtained are

$$\begin{aligned}
\delta_M = -g^2 \int_0^1 \mathrm{d}s \left(m^2 s + M^2(s-1)^2\right) \log\left(\frac{m^2 s + M^2(s-1)^2}{\mu^2}\right) - \\
\log\left(\frac{\mu^2}{m^2}\right)\left(C_{a\theta}\frac{m^2}{M^2} + \frac{m^2}{m_{\theta f}^2}\right) \\
+ \frac{1}{\epsilon}\left(-\frac{2m^2 C_{a\theta}}{M^2} + 6C_4 - \frac{1}{3}g^2\left(3m^2 + 4M^2\right) - \frac{2m^2}{m_{\theta f}^2} + \frac{2M^2}{M_2^2}\right) \\
+ \log\left(\frac{\mu^2}{M^2}\right)\left(3C_4 + \frac{M^2}{M_2^2}\right)
\end{aligned} \tag{288}$$

$$\begin{aligned}
\delta_3 = -g^2 \int_0^1 \mathrm{d}s \left(m^2 s + M^2(s-1)(2s-1)\right) \log\left(\frac{m^2 s + M^2(s-1)^2}{\mu^2}\right) \\
+ \frac{1}{\epsilon}\left(-\frac{1}{3}g^2\left(3m^2 + 5M^2\right) - \frac{2m^2}{m_{\theta f}^2} + \frac{M^2}{M_2^2}\right) \\
- \frac{m^2}{m_{\theta f}^2}\log\left(\frac{\mu^2}{m^2}\right) + \frac{1}{6}\left(g^2 M^2 + \frac{3M^2}{M_2^2}\log\left(\frac{\mu^2}{M^2}\right)\right)
\end{aligned} \tag{289}$$

$$\begin{aligned}
\delta_{gh} = -\frac{2}{3}\frac{g^2 m_{gh}^2}{\epsilon} + \frac{1}{3}g^2 m_{gh}^2 - g^2 m_{gh}^2 \int_0^1 \mathrm{d}s \left(\frac{M^2(s-1)^2 s^2 s}{M^2(s-1)^2 + m^2 s}\right. \\
\left. + 2s(s-1)\log\left(\frac{M^2(s-1)^2 + m^2 s}{\mu^2}\right)\right)
\end{aligned} \tag{290}$$

so that the result is

$$\begin{aligned}
\Pi(p^2) = -\frac{1}{32\pi^2}g^2\left(M^2 - p^2\right)\int_0^1 \mathrm{d}s\,(s-1)s \times \\
\times \frac{-2m^2 p^2 s + M^4(s-1)s + M^2 p^2\left(-3s^2 + 5s - 2\right)}{m^2 s + M^2(s-1)^2} \\
+ \frac{1}{16\pi^2}g^2 p^2 \int_0^1 \mathrm{d}s\,\Delta(s,p^2)\log\left(\frac{\Delta(s,p^2)}{m^2 s + M^2(s-1)^2}\right)
\end{aligned} \tag{291}$$

with the previous definition $\Delta(s, p^2) = m^2 s - M^2(s-1) - p^2 s(1-s)$. This is our result for the quantum correction using the OS re-normalization scheme.

5.4 Imaginary part of the exact propagator

The last section finishes the renormalization process. The result is the exact propagator free of divergences. The On-Schell conditions dictate that the photon mass parameter corresponds to the physical (theoretical) mass of the particle. $p^2 = M^2$ is defined as a pole, but there are additional poles (branch cut) are present. This is expected by the quantum correction as a consequence of unitarity (optical theorem (SCHWARTZ, 2013)). They are encoded in the imaginary part of $\Pi(p^2)$. In this part, I will explain the basic steps to extract this imaginary part.

To extract the imaginary piece it is necessary to reintroduction in $\Pi(p^2)$ (eq. (291) the $i\epsilon$ prescriptions[25] by $M^2 \to M^2 - i\epsilon$. This will result in an expression that has a branch related to the log which allows us to apply the formula $\log(-X \pm i\epsilon) = \log|X| \pm i\pi$ (with $X > 0$) (all other places the $i\epsilon$ appears the resulting expression is well behaved if $\epsilon \to 0$ or is momentum independent). The relevant part is

$$\Pi(p^2)\Big|_{M^2 - i\epsilon} = (\cdots) + \frac{1}{16\pi^2} g^2 p^2 \int_0^1 \mathrm{d}s\, \Delta(s, p^2) \log\left(\frac{\Delta(s,p^2)}{m^2 s + M^2(s-1)^2} - i\epsilon\right) . \tag{292}$$

The cut in the log argument happens when its argument, namely $\frac{m^2 s + (s-1)\left(p^2 s - M^2\right)}{m^2 s + M^2 (s-1)^2}$, becomes negative in the domain of the integration. The denominator is always positive, but the numerator can be negative for the values of s given by

$$s_{\pm} = \frac{1}{2} + \frac{M^2 - m^2}{2p^2} \pm \frac{1}{2p^2}\sqrt{(p^2 - (m+M)^2)(p^2 - (m-M)^2)} . \tag{293}$$

The branch cut starts when this equation has a real solution for $s \in [0, 1]$. This occurs for $p^2 = (m + M)^2$, which is the threshold for the creation of a two-particle system. Indeed this is the momentum in the center-of-mass frame for two particles of mass M and m and total energy $\sqrt{p^2}$. For a fixed value of $p^2 > (M + m)^2$, there will be a branch cut in the log within the integrands value s_- to s_+. Using this fact together with $\mathrm{Im}\{\log(-X \pm i\epsilon)\} = \pm\pi$ leads to

$$\mathrm{Im}\Big\{\Pi(p^2)\Big\} = -\frac{1}{16\pi} g^2 p^2 \int_{s_-}^{s_+} ds \Big(m^2 s + (s-1)\Big(p^2 s - M^2\Big)\Big) \tag{294}$$

$$= \frac{1}{96\pi} \frac{g^2}{p^2} \Big[\Big(p^2 - (m-M)^2\Big)\Big(p^2 - (m+M)^2\Big)\Big]^{3/2} \tag{295}$$

with the condition that $p^2 > (m+M)^2$. This is the threshold for multiparticle production, with the corresponding spectral function proportional to $\mathrm{Im}\{\Pi(p^2)\}$. In special, there is no imaginary part if $\Pi(p^2)$ is on-shell or if the photon limit ($M^2 \to 0$) is taken. The same applies to zero axion mass.

---

[25] Another possibility is to use the prescription $p^2 \to p^2 + i\epsilon$ since the same sign in $i\epsilon$ would appear.

5.5 Potential correction at first order

At the beginning of this calculation (namely in section 5.3), our motivation was to compute the modifications that the interaction terms would introduce to the propagation of a massive vector particle (or massive photon). This information is encoded in the exact propagator in equation (274). Up to 1-loop, we can write

$$G^{\mu\nu}(p) = -i\frac{g^{\mu\nu}}{p^2 - M^2}\left(1 - \frac{\Pi(p^2)}{p^2 - M^2}\right) + \mathcal{O}\Big(g^4\Big) + (p_\mu p_\nu - \text{terms}) \ , \tag{296}$$

where $G^{\mu\nu}(p)$ is the exact propagator, i.e., the propagator for the massive vector field with all its quantum corrections (and finite) computed in eq. (291). These corrections generate a dressed four potential $\mathcal{A}_\mu(x)$[26] given by

$$\mathcal{A}_\mu(x) = -i\int \frac{\mathrm{d}^4p}{(2\pi)^4} e^{-iq\cdot x} G_{\mu\nu}(p)\tilde{j}^\nu(p) \ . \tag{297}$$

Using equation (296) results in

$$\mathcal{A}_\mu(x) = -\int \frac{\mathrm{d}^4p}{(2\pi)^4} e^{-ip\cdot x} \frac{\tilde{j}_\mu(p)}{p^2 - M^2}\left(1 - \frac{\Pi(p^2)}{p^2 - M^2}\right) \ . \tag{298}$$

Now to compute the Yukawa's corrected law we need to use a stationary current $j_\mu(x)$

$$j_\mu(x) = e\delta^3(\vec{\mathbf{x}})\delta_{\mu 0} \to \tilde{j}_\mu(p) = 2\pi e\delta(p_0)\delta_{\mu 0} \ , \tag{299}$$

where e is the electric charge, so that[27]

$$\mathcal{A}_0(\vec{\mathbf{x}}) = e\int \frac{\mathrm{d}^3p}{(2\pi)^3} e^{i\vec{\mathbf{p}}\cdot\vec{\mathbf{x}}} \frac{1}{|\vec{\mathbf{p}}|^2 + M^2}\left(1 + \frac{\Pi(-|\vec{\mathbf{p}}|^2)}{|\vec{\mathbf{p}}|^2 + M^2}\right) \ . \tag{300}$$

This gives the Fourier transform of the corrected Yukawa potential (SCHWARTZ, 2013) felt by a negative charge $-e$

$$\tilde{V}(\vec{\mathbf{p}}) = -e\tilde{\mathcal{A}}_0(\vec{\mathbf{p}}) = \frac{-e^2}{|\vec{\mathbf{p}}|^2 + M^2}\left(1 + \frac{\Pi(-|\vec{\mathbf{p}}|^2)}{|\vec{\mathbf{p}}|^2 + M^2}\right) \tag{301}$$

---

[26] This is the same relation used in (VILLALBA-CHÁVEZ; GOLUB; MüLLER, 2018). The factor $-i$ follows from the definition of the free propagator (that influences the i's in the exact propagator). Another convention is presented in (GREINER; REINHARDT, 1992).

[27] Remember that $p\cdot x = p^0x^0 - \vec{\mathbf{p}}\cdot\vec{\mathbf{x}}$

so that the potential between two identical charges of opposite signs reads

$$V(\vec{\mathbf{x}}) = -e^2 \int \frac{\mathrm{d}^3 p}{(2\pi)^3} e^{i\vec{\mathbf{p}}\cdot\vec{\mathbf{x}}} \frac{1}{|\vec{\mathbf{p}}|^2 + M^2} \left(1 + \frac{\Pi(-|\vec{\mathbf{p}}|^2)}{|\vec{\mathbf{p}}|^2 + M^2} \right) . \tag{302}$$

With this in mind, we can separate this into two contributions

$$V_Y(\vec{\mathbf{x}}) = -e^2 \int \frac{\mathrm{d}^3 p}{(2\pi)^3} e^{i\vec{\mathbf{p}}\cdot\vec{\mathbf{x}}} \frac{1}{|\vec{\mathbf{p}}|^2 + M^2} , \tag{303}$$

$$\delta V_Y(\vec{\mathbf{x}}) = -e^2 \int \frac{\mathrm{d}^3 p}{(2\pi)^3} e^{i\vec{\mathbf{p}}\cdot\vec{\mathbf{x}}} \frac{\Pi(-|\vec{\mathbf{p}}|^2)}{(|\vec{\mathbf{p}}|^2 + M^2)^2} . \tag{304}$$

5.5.1 Yukawa potential calculation

Although the computation of the Yuwaka potential is well known it is convenient to revise it briefly. The momentum integral (303) can be solved via residue theorem, but first one must do a coordinate transformation to spherical (with $r \equiv |\vec{\mathbf{x}}|$ and $p \equiv |\vec{\mathbf{p}}|$) resulting in

$$V_Y(r) = -\frac{e^2}{4\pi r i} \int_{-\infty}^{\infty} \mathrm{d}p \, e^{ipr} \frac{p}{p^2 + M^2} , \tag{305}$$

see (SCHWARTZ, 2013) for more details. The idea is to "compute" a similar integral but in a complex plane. We start with integral

$$-\frac{e^2}{4\pi^2 r i} \int_C \mathrm{d}p \, \frac{p}{p^2 + M^2} e^{ipr} = -\frac{e^2}{4\pi^2 r i} \left(\int_{\gamma_1} \mathrm{d}p \, \frac{p}{p^2 + M^2} e^{ipr} + \int_{\gamma_2} \mathrm{d}p \, \frac{p}{p^2 + M^2} e^{ipr} \right) . \tag{306}$$

Notice that I choose not to introduce a new variable but it is a common practice to do so. The integral has two poles (singularities) that are located in $p = \pm iM$ (figure 7a). The contour C is expressed in figure 7b, the path is separated into two parts, γ_1 and γ_2. In the limit, γ_1 is the same integral that we wish to compute from the beginning, namely

$$V_Y(r) = -\frac{e^2}{4\pi^2 r i} \lim_{\gamma_1 \to \infty} \int_{\gamma_1} \mathrm{d}p \, \frac{p}{p^2 + M^2} e^{ipr} . \tag{307}$$

The upper contour integral γ_2 is zero since it obeys Jordan lemme. The close integral in the complex plane can e solved via the residue theorem and results in

$$-\frac{e^2}{4\pi^2 r i} \int_C \mathrm{d}p \, \frac{p}{p^2 + M^2} e^{ipr} = -\frac{e^2}{4\pi} \frac{e^{-Mr}}{r} . \tag{308}$$

Figure 7 - Complex plane with $\text{Re}\{q\} \times \text{Im}\{q\}$ - Yukawa

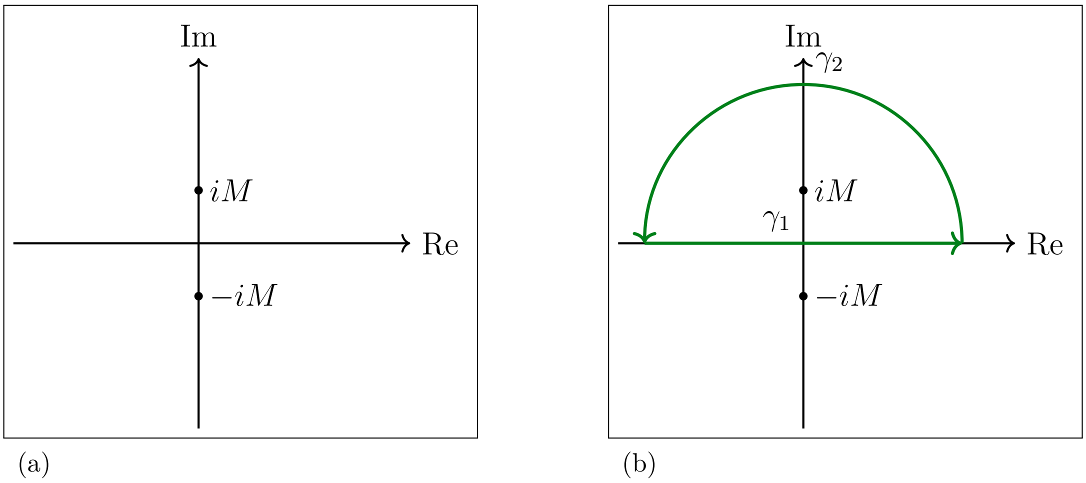

Subtitle: Complex plot of the poles $q = \pm M$ on fig. (a). The contour in the complex plane is represented in (b).
Source: The author, 2022.

Now we can write that our initial integral (306) as

$$V_Y(r) = -\frac{e^2}{4\pi}\frac{e^{-Mr}}{r} \tag{309}$$

with $r \equiv |\vec{\mathbf{x}}|$. This is the Yuwaka potential (or Proca) and results in the Coulomb potential in the massless limit ($M = 0$).

5.5.2 Yukawa potential correction calculation

The computation of the correction to the Yukawa potential in eq. (304), namely

$$\delta V_Y(\vec{\mathbf{x}}) = -e^2 \int \frac{\mathrm{d}^3 p}{(2\pi)^3} e^{i\vec{\mathbf{p}}\cdot\vec{\mathbf{x}}} \frac{\Pi(-|\vec{\mathbf{p}}|^2)}{(|\vec{\mathbf{p}}|^2 + M^2)^2} \ , \tag{310}$$

is considerably more tricky. The reason for that is the extra discontinuity introduced by the multiparticle cut introduced by Π (explored in section 5.4) but this problem can be contoured with a different choice of path in the complex plane as we will see[28]. Consider the analytic continuation $|\vec{\mathbf{p}}| \to iq \in \mathbb{Z}$, which structure is displayed in fig.8a (the

[28] Notice that there is another possibility to compute the potential. The approach is to do a partial integration on Π, eliminate the log, and switch the order of integration from $\mathrm{d}q\,\mathrm{d}s$ to $\mathrm{d}s\,\mathrm{d}q$. The effect separates the discontinuity leading to the pole position depending on the s parameter and the complex contour to be the same as the Yukawa potential.

integrand has a pole at $q = \pm M$ and a cut that starts at $q = (M + m)$). This cut in the complex plane leads to the impossibility of using a simple counter as was done in the Yukawa potential calculation. To elucidate, the potential after the change of variables is

$$\delta V_Y(r) = \frac{e^2}{4\pi^2 ri}\int_{-\infty}^{\infty} \mathrm{d}q\, e^{-rq}\frac{q\Pi(q^2)}{(q^2 - M^2)^2} \ . \tag{311}$$

One possibility consists in choosing the complex path, represented in fig.8, which is a

Figure 8 - Complex plane with Re$\{q\}$ × Im$\{q\}$

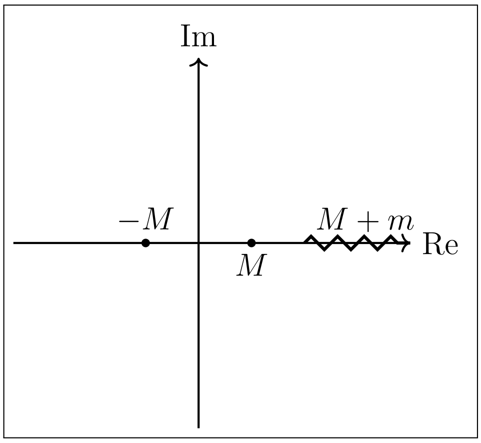

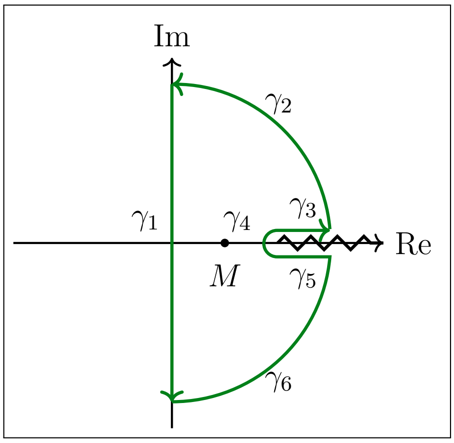

Subtitle: Complex plot of the poles $q = \pm M$ and the cut $q > m + M$ in figure (a). The closed contour in the complex plane is represent in (b) know as ‘half-disk” (or “Pacman”).

Source: CHRISPIM; BRUNI; GUIMARAES, 2021, p. 19.

“half-disk” (or “Pacman”) that avoids the branch cut by using six different parts as in

$$\int_\Gamma \mathrm{d}q\ \ (\cdots) = \sum_{i=1}^{5}\int_{\gamma_i} \mathrm{d}q\,(\cdots)\ . \tag{312}$$

In the same way as the calculation of Yukawa’s potential, the contributions of γ_2 and γ_5 are canceled by Jordan’s lemme. The γ_1 path is just the original integral in the real line so we will replace it with $\delta V_Y(r)$. The paths γ_3, γ_4, and γ_5 can be understood by noticing that the real part is the same in the two half (just remember that it is a function of p^2 and we are considering one part in the first quadrant and the second in the fourth quadrant). The imaginary part has a jump given by the branch cut and is given by equation

$$\Pi(q^2 + i\epsilon) - \Pi(q^2 - i\epsilon) = \Pi(q^2 + i\epsilon) - \Pi(q^2 + i\epsilon)^* = 2i\,\mathrm{Im}\Big\{\Pi(q^2 + i\epsilon)\Big\}\ . \tag{313}$$

The sign in $\pm i\epsilon$ is related to the contour direction and since we are using counter-clockwise we must use the plus sign (ZEE, 2010). The last part is to replace the contour integral with Cauchy's residue theorem leading to

$$\delta V_Y(r) = (Res\ \delta V_Y)(iM) - \frac{e^2}{2\pi^2 r}\int_{-\infty}^{\infty} \mathrm{d}q\, \frac{q\,\mathrm{Im}[\Pi(q^2+i\epsilon)]}{(q^2-M^2)^2} e^{-qr}\ . \tag{314}$$

The residue computed over the path $\Gamma = \sum \gamma$ is zero, but this calculation is lengthy. Basically, one needs to do a partial integration on Π so that it is possible to compute the residue. After that, the integral over dummy parameter s must be done, resulting in a null outcome. The imaginary part is expressed in eq. (295), the expression of the correction to the potential takes the form of

$$\delta V_Y(r) = -\frac{e^2 g^2}{192\pi^3 r}\int_{m+M}^{\infty} \mathrm{d}q\, \frac{e^{-qr}}{q(q^2-M^2)^2}\Big[\Big((m-M)^2-q^2\Big)\Big((m+M)^2-q^2\Big)\Big]^{3/2}\ . \tag{315}$$

Notice that there was a change in the lower bound of the integral. The reason for that is that the imaginary part of Π only exists for values of momentum above the threshold of multiparticle creation (see section 5.4). Finally, the corrected potential is ($q = t(M+m)$)

$$V(r) = -\frac{e^2}{4\pi}\left(\frac{e^{-Mr}}{r} + \frac{g^2(m+M)^2}{3\times 2^4\pi^2}\frac{1}{r}\int_1^{\infty} \mathrm{d}t\, F(m/M,t)\Big(t^2-1\Big)^{3/2}\frac{e^{-(m+M)rt}}{t}\right) \tag{316}$$

with

$$F(m/M,t) = \left(t^2 - \left(\frac{M-m}{M+m}\right)^2\right)^{3/2}\left(t^2 - \left(\frac{M}{M+m}\right)^2\right)^{-2}\ . \tag{317}$$

It is not clear how to compute the t integral in full analytic form, but some doable simplifications can extract analytical information in some limiting cases.

5.6 **Analysis of the results**

In order to analyze how the effective theory changes as the parameters are modified is convenient to introduce a set of dimensionless combinations. The dimensional parameters (m, M, g, r) can be arranged in in three dimensionless terms: Mr (distance scale), $\frac{m}{M}$ (mass ratio scale), and gM (coupling scale). Notice that in this parametrization a larger (smaller) axion mass, than Proca mass, translates to $m/M > 1$ $(0 < m/M < 1)$.

This results in equation (316) and (317) taking the form

$$V(r) = -\frac{e^2}{4\pi}\frac{e^{-Mr}}{r}\delta P(Mr, gM, m/M) \tag{318}$$

$$\begin{aligned}\delta P(Mr, gM, m/M) = 1 + \frac{(gM)^2\left(1+\frac{m}{M}\right)^2}{48\pi^2}\int_1^\infty \mathrm{d}t\, F(m/M, t)\times \\ \times\left(t^2-1\right)^{3/2}\frac{e^{-Mr[t(1+m/M)-1]}}{t}\end{aligned} \tag{319}$$

where $\delta P(Mr, gM, m/M)$ corresponds to deviations from the Yukawa potential introduced by quantum fluctuations of the axion field. We remark that all the computations so far do not rely on any specific relationship between these three parameters but, since this is an emergent description of the system, these are effective parameters that are related to each other and fixed by the microscopic physics as previously discussed in chapter 4. Yet, for the sake of simplicity, we will continue to treat these parameters as independent for now. In order to make appropriate approximations is necessary to respect the impositions of the perturbation theory. To make appropriate approximations is necessary to respect the impositions of the perturbation theory. The quantity

$$\begin{aligned}f(Mr, gM, m/M) := \frac{(gM)^2\left(1+\frac{m}{M}\right)^2}{48\pi^2}\int_1^\infty \mathrm{d}t\, F(m/M, t)\left(t^2-1\right)^{3/2}\times \\ \times\frac{e^{-Mr[t(1+m/M)-1]}}{t}\end{aligned} \tag{320}$$

which was extracted from the polarization (equation 319) with $\delta P(Mr, gM, m/M) = 1 + f(Mr, gM, m/M)$, must be

$$f(Mr, gM, m/M) < 1\ . \tag{321}$$

Any specification of $(Mr, gM, m/M)$ must be consistent with the perturbation theory and physical experimental ranges. This inequality can be studied graphically using numerical inputs of phenomenological characteristic scales.

The outline of the analysis is; It is possible to define a $f(M_0 r_0, (gM)_{crit}, m_0/M_0)$ with some Mg_{crit}. In order to keep the perturbative analysis consistent in a given range $Mr \in [(Mr)_{min}, (Mr)_{max}]$ and $m/M \in [0, (m/M)_{max}]$, it is sufficient to choose a value $Mg < (Mg)_{\mathrm{crit}}$ that can be determined either numerically or graphically using the values of $(Mr, m/M) = ((Mr)_{min}, 0)$.

Considering a separation in the order of nanometers and take the London length usually found in superconductors (that ranges from $\lambda_L \sim 50\,nm$ to $\sim 500\,nm$ (KITTEL, 2004)) as a representative scale for the photon's mass. Theoretically, this setup is experimental feasible since it consists of a thin film of superconductor. Now consider length scales running from $r \sim 1\,nm$ to $r \sim 50\,nm$. This choice of $M \sim 1/50\ nm^{-1}$ lead to

$Mr \in [0.02, 1]$. In order to get a consistent value of Mg for *any* Mr greater than the lower bound it is sufficient to solve (320) for $(Mr, m/M) = (0.02, 0)$. Graphically it can be read from figure 9a that this is true for $Mg|_{crit} \approx 0.43$. This sets the typical length scale above which the perturbative analysis breaks and our model is not reliable anymore.

Figure 9 - Numerical analysis of the inequality in eq. (321)

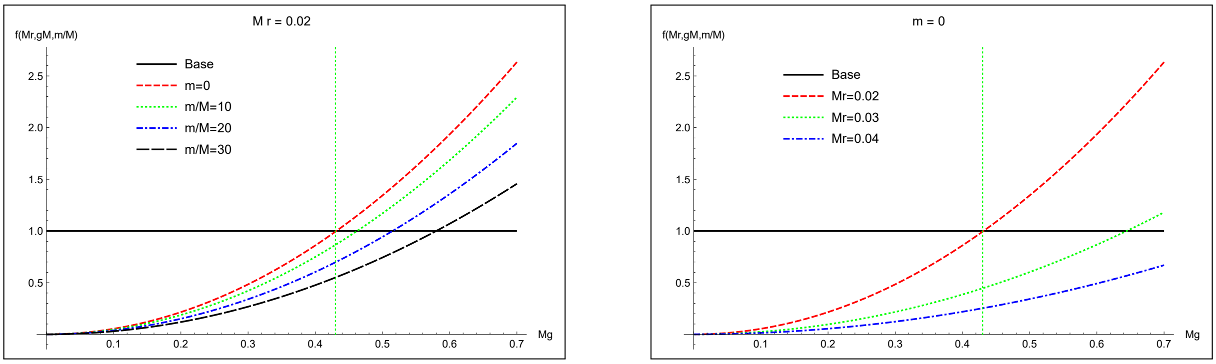

(a) (b)

Subtitle: In figure (a) shows the numerical plot of left and right hand sides of (321), for $Mr = 0.02$. Note that, the critical values of gM that keeps the perturbative analysis valid increases with $\frac{m}{M}$. The other figure (b) represents the numerical plot of left and right hand sides of (321), for $m = 0$. Note that the critical values of gM also increases considerably as one makes slightly modifications on Mr. In both figures the black line represents the upper bound $(f(Mr, gM, m/M) = 1)$ and the vertical dashed line is the critical value $Mg = 0.43$.

Source: CHRISPIM; BRUNI; GUIMARAES, 2021, p. 31.

Within these restraints in the parameters, one can explore the general behavior of the quantum deviation (namely $\delta P - 1$). The graph, pictured in figure 10, represents the different behaviors in terms of different mass ratio values. As the mass ratio increases, the value of the deviation decreases more abruptly. Other approximations of the potential deviation can be done. In special, to develop a physical picture, it is useful to analyze the result (319) imposing large mass hierarchies (large axion mass $m \gg M$ and large Proca mass $M \gg m$). Each approximation will provide an estimated result that, for additional verification, will be compared against the numerical integration.

5.6.1 Small Axion mass

Applying a small axion mass approximation $(M \gg m)$ at zero-order in the mass ratio $\frac{m}{M}$, the expression equation (319) simplifies to

$$\delta P(Mr, gM) = 1 + \frac{g^2 M^2}{48\pi^2} \int_1^\infty \mathrm{d}t \left(t^2 - 1\right) \frac{e^{-Mr(t-1)}}{t} + \mathcal{O}\left(\frac{m}{M}\right) \tag{322}$$

Figure 10 - Quantum deviation as function of the mass ratio

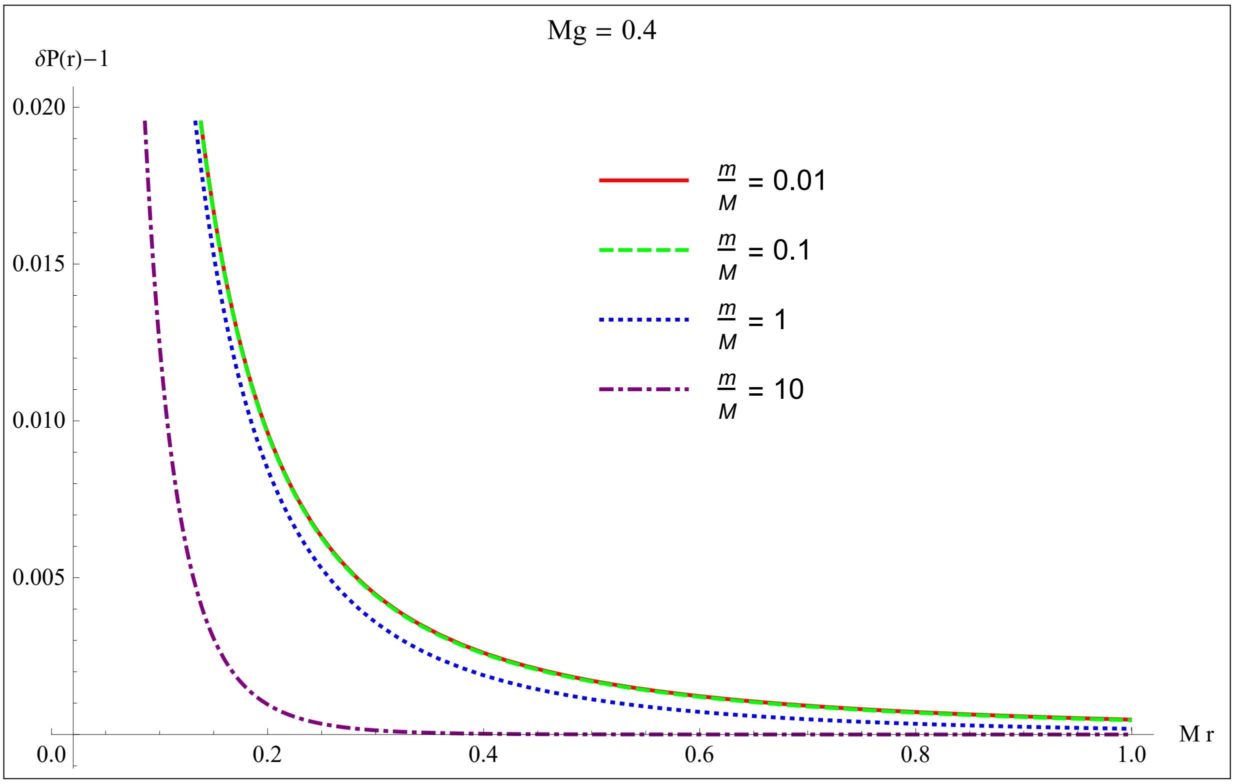

Subtitle: Graph of the exact expression of $\delta P - 1$ (equation 319) for varying values of m/M. The used values are $gM = 0.4$ and $Mr \in (0.02, 1)$.

Source: CHRISPIM; BRUNI; GUIMARAES, 2021, p. 21.

Evaluating the integral we obtain

$$\delta P(Mr, gM) \approx 1 + \frac{g^2 M^2}{48\pi^2}\Big(\Big(\frac{1}{M^2 r^2} + \frac{1}{Mr}\Big) - e^{Mr}\Gamma(0, Mr)\Big) \tag{323}$$

where $\Gamma(0, Mr)$ is the upper incomplete gamma function[29]. The asymptotic approximation results in

$$\delta P(Mr, gM) \approx \begin{cases} 1 + \frac{g^2M^2}{24\pi^2}\frac{1}{(Mr)^2}; \quad \text{for} \quad Mr \gg 1 \\ 1 + \frac{g^2M^2}{48\pi^2}\Big(\frac{1}{(Mr)^2} + \frac{1}{Mr} + \log(e^\gamma Mr)\Big); \quad \text{for} \quad Mr \ll 1 \end{cases} \tag{324}$$

Figure 11a and 11b compare the results with the numerical integration without approximations.

5.6.2 Small Proca mass

In the case of a small Proca mass, in comparison with the axion mass ($M \ll m$), eq. (319) gives

$$\begin{aligned} \delta P(Mr, gM, m/M) = 1 + \frac{g^2 m^2}{48\pi^2}\int_1^\infty \mathrm{d}t \Bigg(&\frac{(t^2-1)^3}{t^5} + 2\frac{M}{m}\frac{(t^2-1)^2(t^2+2)}{t^5} \\ &+ \frac{M^2}{m^2}\frac{(t^2-1)\{2+3t^2+t^6\}}{t^7}\Bigg) e^{-mrt - Mr(t-1)} + \mathcal{O}\Big(\frac{M}{m}\Big)^3 \end{aligned} \tag{325}$$

This integral, that can be computed analytically, but does not bring any valuable insight, is

$$\delta P(r) = 1 + \frac{g^2}{\pi^2}\Big[e^{-mr}Fun1 + e^{Mr}Fun2\Big] + \mathcal{O}\Big(\frac{M}{m}\Big) \tag{326}$$

with

$$\begin{aligned} Fun1 = &\frac{r^3(m+M)^3\,(15m^2 - 60mM + 17M^2)}{17280} - \frac{r^2(m+M)^2\,(5m^2 - 20mM + 7M^2)}{5760} \\ &- \frac{r(m+M)\,(85m^2 - 160mM + 81M^2)}{2880} + \frac{1}{576}\Big(15m^2 - 24mM + 11M^2\Big) \\ &+ \frac{M^2 r^5 (m+M)^5}{17280} - \frac{M^2 r^4 (m+M)^4}{17280} + \frac{m+M}{48r} + \frac{1}{48r^2} \end{aligned} \tag{327}$$

[29] Defined as $\Gamma(a, x) \equiv \int_x^\infty t^{a-1}e^{-t}\,\mathrm{d}t$. The asymptotic expression of $\Gamma(0, Mr)$ for $Mr \gg 1$ is $\propto \frac{e^{-Mr}}{Mr}$, this cancels the possible problem of the positive exponent e^{Mr} in equation (323).

Figure 11 - Quantum deviation as function of the photon mass times the distance

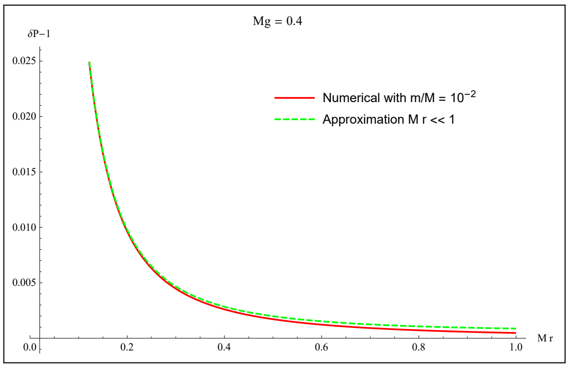

(a)

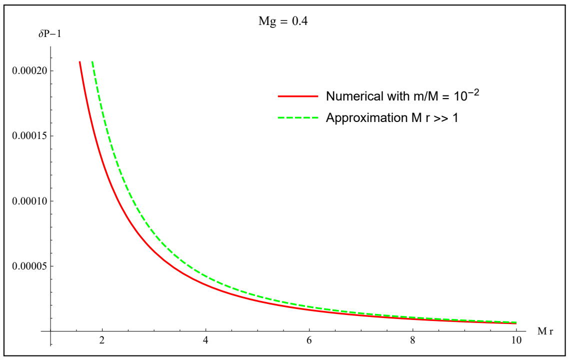

(b)

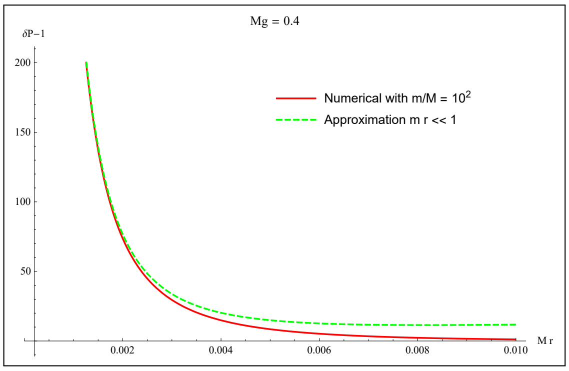

(c)

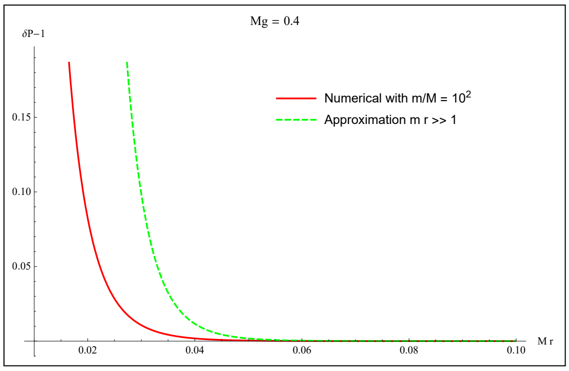

(d)

Subtitle: Plot of $\delta P(r) - 1$ (the deviation from the standard value) as a function of Mr with $gM = 0.4$. The red line is the numerical integration plot of (319). Respectively; 11a and 11b represent the approximated function (324) with $Mr \ll 1$ and with $Mr \gg 1$ (with $\frac{m}{M} = 10^{-2}$). Moreover, 11c and 11d represent (329) with $mr \ll 1$ and with $mr \gg 1$ (with $\frac{m}{M} = 10^{2}$). The estimate of the region of validity of the approximations is read directly from the graph.

Source: CHRISPIM; BRUNI; GUIMARAES, 2021, p. 23.

$$Fun2 = \frac{r^4(m+M)^4\,(m^2-4mM+M^2)\,\mathrm{Ei}(-(m+M)r)}{1152} - \frac{1}{32}r^2\left(m^2-M^2\right)^2\mathrm{Ei}(-(m+M)r)$$
$$+\frac{1}{48}\left(3m^2+M^2\right)\mathrm{Ei}(-(m+M)r) + \frac{M^2r^6(m+M)^6\mathrm{Ei}(-(m+M)r)}{17280} \tag{328}$$

Employing the asymptotic expansion in these expressions results in[30]

$$\delta P(Mr,gM,m/M) \approx \begin{cases} 1+\frac{g^2m^2}{\pi^2}\left(\frac{1}{(m+M)^4r^2}+\frac{M}{m}\frac{1}{(m+M)^3r}+\frac{M^2}{m^2}\frac{1}{4(m+M)^2}\right)\frac{e^{-mr}}{r^2};\ \text{ for } \ mr\gg 1 \\ 1+\frac{g^2m^2}{48\pi^2}\left(\frac{1}{(mr)^2}+\frac{3}{4}+\frac{M}{m}\left(\frac{1}{mr}-3\right)+3\log\left(e^{\gamma}(m+M)r\right)\right. \\ \qquad \left.+\frac{M^2}{m^2}\left(\frac{11}{12}+\log\left(e^{\gamma}(m+M)r\right)\right)\right);\ \text{ for } \ mr\ll 1 \end{cases} \tag{329}$$

The graphs 11c and 11d represents the comparison between the full numerical integration and the approximations. Note that this result is consistent with the massless photon limit that was examined in (VILLALBA-CHÁVEZ; GOLUB; MüLLER, 2018).

5.6.3 Mass relations and London penetration length

Considering the results depicted in figure 12 (the variation of the quantum correction as the mass ratio changes) we see that as m becomes larger than M quantum corrections becomes less and less important. One can also note that for large distances the corrections are very feeble for any values of the masses. This means that we expect noticeable deviations from the usual London results, due to axion effects, at small penetration distances and large photon mass ($M/m > 1$).

In fact, we can explore in more details the variation in the London screening generated by quantum fluctuations of the axion background. To do so, it is useful to redefine eq. (318) with an effective mass by

$$V(r) = -\frac{e^2}{4\pi}\frac{e^{-rM^{\mathrm{eff}}(Mr,Mg,m/M)}}{r} \tag{330}$$

so that

$$M^{\mathrm{eff}}(Mr,Mg,m/M) = M - \frac{\log\delta P}{r} = M - \frac{\delta P-1}{r} + \mathcal{O}\left(g^4\right) \tag{331}$$

where $\delta P = \delta P(Mr,Mg,m/M)$ is given by 319 and the expansion $\log(1+ax) \approx ax$

[30] Note that every term in this expression can be expressed in terms of $(Mr,gM,m/M)$.

Figure 12 - Quantum deviation as function of the mass ration

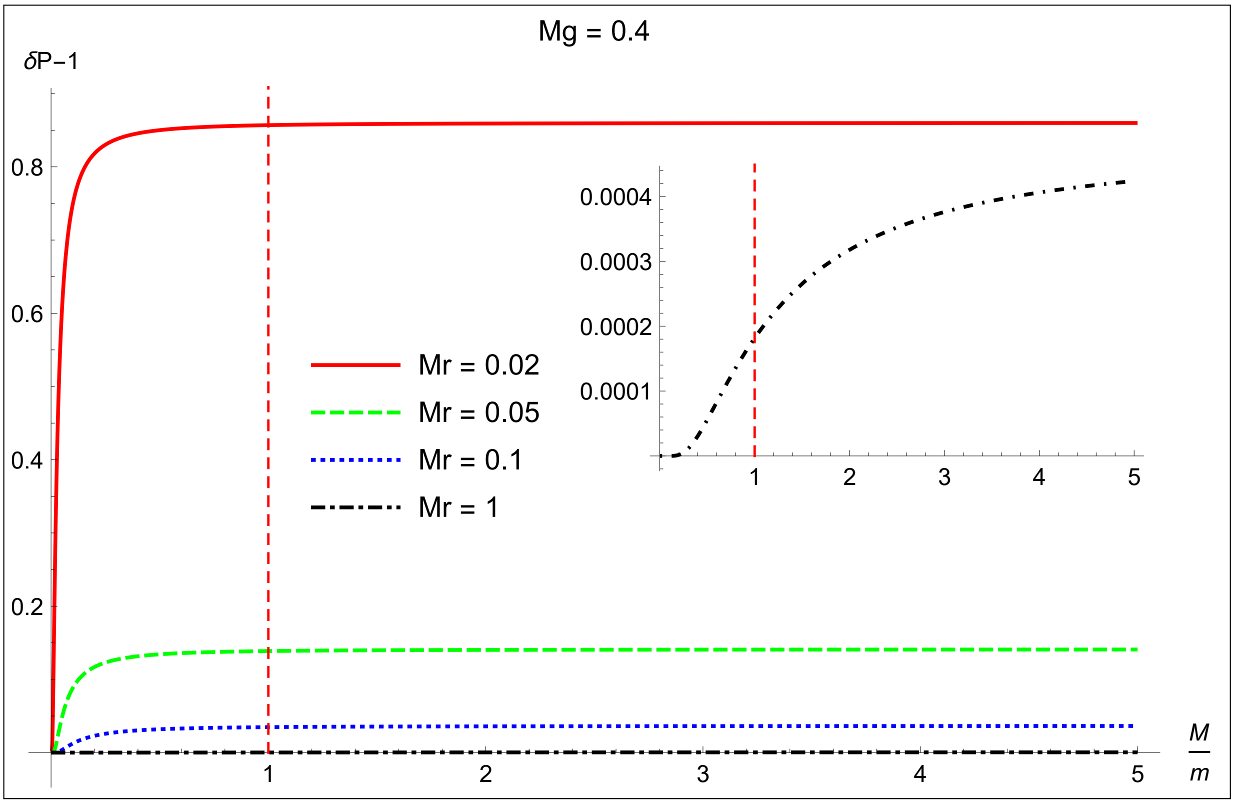

Subtitle: Graph of the exact expression of $\delta P - 1$ (319) as a function of M/m for varying values of the distance scale with fixed $Mg = 0.4$. The inserted graph is the zoom of the curve $Mr = 1$. The red vertical red line $M/m = 1$ separates the region with $M/m < 1$ and $M/m > 1$.

Source: CHRISPIM; BRUNI; GUIMARAES, 2021, p. 24.

was used. The Yukawa tree level interaction, *i.e* $V_Y(r) = -\frac{e^2}{4\pi}\dfrac{e^{-Mr}}{r}$, defines the London length λ_L as the damping coefficient of the exponential via $e^{-M\lambda_L} = e^{-1}$, or equivalently, $\lambda_L = \dfrac{1}{M}$. We can expect that this term receives quantum corrections that can be written in the form

$$r^{eff}M^{eff}(r^{eff}) = 1 + \mathcal{O}\Big(g^2\Big) \tag{332}$$

that is a transcendental equation, but it is possible to solve by considering that

$$r^{eff} = \lambda_L + \delta r + \mathcal{O}\Big(g^4\Big) \tag{333}$$

where $\delta r \in \mathcal{O}(g^2)$ and $M\lambda_L = 1$ resulting in[31]

$$M\delta r = \frac{(gM)^2\Big(1+\frac{m}{M}\Big)^2}{48\pi^2} e^1 \int_1^\infty \mathrm{d}t\, F(m/M,t)\Big(t^2-1\Big)^{3/2}\frac{e^{-t\left(1+\frac{m}{M}\right)}}{t} + \mathcal{O}\Big(g^4\Big)\ . \tag{334}$$

This is the term $\mathcal{O}(g^2)$ (leading contribution) expected in eq. (332) and is independent of the scale Mr. We can see in graph 13 the shift δr (in units of M) in the London penetration length as a function of the mass ratio $\frac{M}{m}$. As stated before, the axionic effects are more relevant for large photon mass.

[31] This expression was obtained by expanding $e^{-Mr^{eff}[t(1+m/M)-1]}$ (with the use of equation (333)) and keeping terms of $\mathcal{O}\big(g^0\big)$ since the whole integral is of $\mathcal{O}\big(g^2\big)$. Note that this follows the same spirit of the renormalization of the charge in QED.

Figure 13 - Quantum deviation of London's mass as function of the mass ration

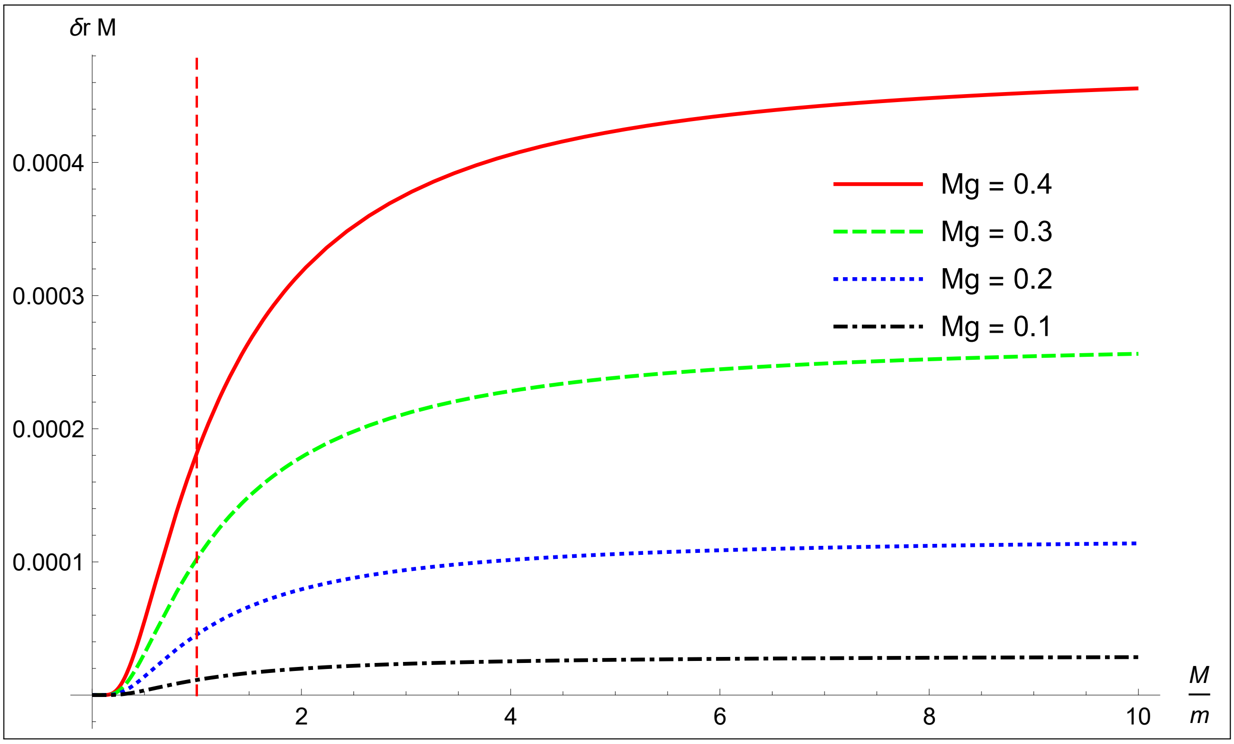

Subtitle: Plot of the expression $M\delta r$ in eq. (319) as a function of M/m with different values of Mg. The red vertical red line $M/m = 1$ separates the region with $M/m < 1$ and $M/m > 1$.

Source: CHRISPIM; BRUNI; GUIMARAES, 2021, p. 25.

CONCLUSION

In this thesis, we examined (shortly) some aspects of the realization of axion physics in particle and condensed matter physics. This topic attracts many researchers in both fields so there is plenty of material available. One of the objectives here is to give a general idea of the motivation behind this fact along with a starting point on this extensive topic.

The starting point in the first chapter is the very basics of the Dirac, Weyl, and gauge fields (properties of the spinor fields, minimal coupling to the gauge field, equation of motion). The Dirac field ψ describes spin 1/2 particles (electron and its antiparticle, for example) and is reducible into two Weyl spinors in odd spatial dimensions. The Weyl fields, ψ_R and ψ_L (each one with two degrees of freedom) so that $\psi(x) = \begin{pmatrix} \psi_L \\ \psi_R \end{pmatrix}$ or $\psi_{R/L} = P_{R/L}\psi$ ($P_{R/L}$ are projectors defined as $P_R = \frac{1}{2}(1+\gamma^5)$ and $P_L = \frac{1}{2}(1-\gamma^5)$), play a vital role in our narrative, although no fundamental particle is associated with it. One extra ingredient (that plays a part in both mentioned research fields) is considered already at the beginning. This factor is the constant four-vector b_μ which appears as $\overline{\psi}(x)\not{b}\gamma^5\psi(x)$ in the fermionic Lagrangian description. The initial motivation here is the extension to the standard model of particles which includes a CPT-odd Lorentz invariance violation term. This is shortly explained in section 1.2. The following section addresses the transformations, symmetries, and excitation spectrum with a focus on the modifications included by the b_μ term. Distinct energy-momentum relations emerge depending on the relation between b_μ and the fermion mass m (including the possibility of closing the mass gap). At this point, some considerations about the physical consequences of the stated term in LSV are made. In particular this term introduces problems of stability in the fermionic action but with the peculiar conclusion that these are (possibly) non-observable since the energy necessary to reach it is of Planck scale. In the final section of the first chapter, we construct an argument (based on the energy spectrum graphs of section 1.4) on how a massive fermionic theory, with the inclusion of the coupling b_μ, can be "approximated" to a massless one with a special condition between the coupling term and the fermionic mass given by $-b_\mu b^\mu = -b_0^2 + b_i^2 < m^2$. This approximation is only valid for the low-energy regime, which is not a problem since this is the region of interest in chapter 2.

The focus of Chapter 2 is the main points (since it is a lengthy calculation) of the computation of the low energy (or effective) description of the systems studied in the previous chapter. The low energy theory is obtainable by the integration of the fermionic degrees of freedom of the microscopic system.

In the first section, the fermionic integration is done, with the inclusion of the previously mentioned coupling and the gauge sector, namely

$$Z = \int \mathcal{D}\Big(\psi^\dagger, \psi, A\Big) e^{i(S_0 + S_{\text{Maxwell}})} \tag{335}$$

$$S_0 = \int \mathrm{d}^4x\, \overline{\psi}(x) \left(i\partial\!\!\!/ - m + b\!\!\!/\gamma^5 + ieA\!\!\!/(x)\right) \psi(x) \;, \tag{336}$$

$$S_{\text{Maxwell}} = \int \mathrm{d}^4x \left(-\frac{1}{4} F_{\mu\nu}F^{\mu\nu}\right) \,. \tag{337}$$

The resulting theory

$$Z = \int \mathcal{D}(A) e^{iS} \tag{338}$$

$$\mathcal{S} = \int \mathrm{d}^4x \left[-\frac{1}{4}F^2 + \frac{e^2}{32\pi^2}\beta(x) F\tilde{F} + j_\mu A^\mu + (\text{powers of } F^2)\right] \tag{339}$$

which presents a connection between the gauge field and the microscopic term b_μ, similar to axionic coupling. This encodes the b_μ profile in the electromagnetic description of the system as one can see by the modifications to the Maxwell equations, constitutive relations, and topological currents. Anticipating the discussion we can connect these modifications to the appearance of the topological magnetic electric which is a cross-field polarization (electric field induces magnetization and vice-versa), the anomalous Hall effect (Hall effect in the absence of magnetic field), and the chiral magnetic effect (electric current induced by a static magnetic field).

Next, we simplify the calculation by considering a case in which the contribution of the coupling reduces to an angle bound to 0 (mod 2π) or $\theta = \pi$ (mod 2π). This transforms the effective theory to

$$Z = \int \mathcal{D}(A) e^{iS} \tag{340}$$

$$\mathcal{S} = \int \mathrm{d}^4x \left(-\frac{1}{4}F^2 + \frac{e^2\theta}{32\pi^2}\theta F\tilde{F} + j_\mu A^\mu\right) \,, \tag{341}$$

which eliminates any modification to the equation of motion (since the anomaly contribution can be written as a total derivative by a partial integration as in $S_{\text{Anomaly}} = \frac{e^2\theta}{32\pi^2}\int \mathrm{d}^4x\, \partial_\mu(\epsilon^{\mu\nu\rho\sigma}A_\nu\partial_\rho A_\sigma)$), but it is still relevant in the boundary between two systems characterized by distinct angles. Again, foreseeing the discussion in the material realization, this effect is observable in the vicinity between a normal and Topological insulator (a consequence of the TME effect in the boundary). Other effects can be realized as well, e.g. the mirror magnetic charge inside the material, and the possible realization of the Witten effect (WITTEN, 1979; QI et al., 2009a).

The commitment of the last part of the second chapter is to a more complex calculation that results in the dynamical axion electrodynamics. The presence of a dynamical component in the axion field is possible because the chiral symmetry is broken dynamically due to the formation of a chiral condensation induced by the four fermions pairing $\lambda^2\left(\overline{\psi}(x)P_L\psi(x)\right)\left(\overline{\psi}(x)P_R\psi(x)\right)$. After the integration of the fermions, the resulting theory is similar to a topological magnetic insulator or (similar) an axion insulator since the pairing generates a fermionic mass which (ultimately) results in the axion-like field mass (in what is called chiral density wave). That is, the system is composed of

$$Z = \int \mathcal{D}(A,\theta)e^{iS} \tag{342}$$

$$S = \int \mathrm{d}^4x \left[-\frac{1}{4}F^2 + \frac{e^2 g}{32\pi^2}\left(\frac{\beta(x)}{g} - \theta\right)F\tilde{F} + \frac{1}{2}m_\theta^2\theta^2 + \frac{1}{2}(\partial\theta)^2\right] \tag{343}$$

where the θ term is a dynamical field that represents the fluctuations of the condensate phase. The β is the contribution from the Weyl point separation. Although this is a review of (WANG; ZHANG, 2013; MACIEJKO; NANDKISHORE, 2014; YOU; CHO; HUGHES, 2016) we also discussed the problem of computing the non-perturbative effects (in which the condensate mass is part) and how the approximations change the "accessible" information on the theory (the details about possible defects are lost). Since the axion-like field couples to the electromagnetic sector in the same way as the b_μ term, the previously discussed effects are still relevant but now gifted with their own equation of motion.

The core of the third chapter was the concepts that were relevant to comprehension of chapter 2 models in the context of their material realization. To this end, the first section explores some historical background and basic concepts (Landau's symmetry breaking theory and Bloch's and Wilson's band theory). In the second section, we follow the path to expanding those ideas consisting of examining the integer quantum Hall effect, which is relevant as an example of the appearance of topological order in the description of a material's phase. This new kind of order can not be distinguished by any observable symmetry break, it is quantized and robust against smooth changes in the system. We showed that the topological electromagnetic response can be characterized by the Chern-Simons action $S_{\text{CS}} = \frac{k}{4\pi}\int \mathrm{d}^3x\,\epsilon^{\mu\nu\rho}A_\mu\partial_\nu A_\rho$, which is quantized by the imposition of consistency between the gauge fields and quantum mechanics. Alternatively, the IQH is also associated with the topological invariant known as the first Chern number by considering the topology of the Brillouin zone and the Hilbert space (a result credited to the work of Thouless, Kohmto, Nightingale, and den Nijs (TKNN) in 1982).

In the next section, we started our exploration of some realization of axion physics in materials. The first example is the topological insulator which is the material realization (observed in 2005) of the system discussed in section 2.2. The IQHE and TI are similar, the previous has a bulk insulator (gapped energy spectrum) with gapless boundary states akin to the edge states previously in the IQHE. Another difference is the role that symmetry play, it is possible to achieve the TI condition by considering either (or both) time-reversal and inversion symmetries on the material. The electromagnetic response is described by action $\frac{e^2\theta}{32\pi^2}\int \mathrm{d}^4x\, F\tilde{F}$ and is quantized to values of 0 (mod 2π) (normal insulator) or $\theta = \pi$ (mod 2π) (topological insulator). The consequences are the TME effect that allows the anomalous Hall and chiral magnetic effects (along with the Faraday and Kerr rotation, mirror magnetic charge, and Witten effect). Those effects are bounded to the boundary between topological distinct materials where the change between the values of the theta term is smooth, the next subsection generalizes this to consider a material where the theta term can be space-time dependent in the bulk.

The formation of Weyl and Dirac semimetals is discussed in some detail since the definition of a topological invariant is nontrivial in a gapless system. The particular information will not be repeated here, the interesting part is the association of the sink/source of Berry curvature with the Chern number which represents the chirality (or topologic charge) of the Weyl points. The difference between the Wely and Dirac semimetals can be linked to the momentum space separation in the first (which protects the system from perturbations). This also links with the previous discussion of condition $-b_\mu b^\mu = -b_0^2 + b_i^2 < m^2$ which allows for approximation to a gapless dispersion even though the action has mass term. In the Dirac semimetal case, the singular points are at the same point in momentum space, meaning that they can be combined which destroys the topological phase (as the discussion about the instability of chiral symmetry in sections 1.4 and 1.5). The path to creating a Dirac semimetal involves either a very fine-tuned system (unstable) or the imposition of additional crystalline symmetry. In the simplest case, the difference between the Dirac's and Weyl's is the presence of the b_μ term. The system studied in section 2.1, namely

$$Z = \int \mathcal{D}\Big(\psi^\dagger, \psi, A\Big) e^{i(S_0 + S_{\text{Maxwell}})} \tag{344}$$

$$S_0 = \int \mathrm{d}^4x\, \overline{\psi}(x) \left(i\partial\!\!\!/ + b\!\!\!/\gamma^5 + ieA\!\!\!/(x) \right) \psi(x) \tag{345}$$

$$S_{\text{Maxwell}} = \int \mathrm{d}^4x \left(-\frac{1}{4} F_{\mu\nu} F^{\mu\nu} \right), \tag{346}$$

results in the effective description of a Weyl semimetal

$$Z = \int \mathcal{D}(A) e^{i(S_{\text{eff}} + S_{\text{Maxwell}})} \tag{347}$$

$$\mathcal{S}_{\text{eff}} = \int \mathrm{d}^4x \left[-\frac{1}{4} F^2 + \frac{e^2}{32\pi^2} \beta(x) F\tilde{F} + (\text{powers of } F^2) \right] \tag{348}$$

with $\beta(x) = 2b_\mu x^\mu$. Although the theta term is similar to the TI the effect is different since it is not restricted to the boundary of topological distinct materials. The presence of the time-like component of the b_μ is peculiar since the resulting CME allows for the presence of a direct current along a static magnetic field (prohibited by material considerations). The workaround is the realization that such an effect occurs outside equilibrium, the "chemical potential" b_0 is generated by the chiral anomaly by the effect of external sources. Beyond this, the problems that appear in the particle realization of this system appear to be avoidable in the material realization. The instability in the microscopic action is not a problem since the material has a natural energy cutoff. The ambiguity also vanishes since the microscopic band theory can be used to fix it. The causality and stability of the effective theory are also bypassable, Einstein's causality, in terms of information transport, is free of problems, and stability is not a problem since evanescent effects can occur in materials.

The last system in this section is the topological magnetic insulator which microscopic and effective theories were explored in sec. 2.3. The microscopic description is similar to the Weyl semimetal but with the inclusion of a four-fermion interaction term that allows for the chiral symmetry to be broken dynamically (due to the chiral condensation) and results in a new pseudo-scalar particle, similar to the Peccei-Quin mechanism. The difference between the usual topological magnetic insulator description and our effective calculation is the presence of terms like $\left(\theta, \beta, \theta\beta, \cdots, (\partial\theta)^2, F^2\right)$ (which originates from the non-perturbative contribution $\cos\left(\frac{\theta(x)}{f} - \beta(x)\right)$). The elimination of beta gives the usual axion insulator and restores the symmetry $\theta \to -\theta$ and space-time isotropy. Most of the effects in the effective description were described in the Weyl semimetal case, most of the distinction comes from the fact that now the theta term has its own dynamics.

In the fourth chapter, we compute the electromagnetic response of a Weyl semimetal with an unusual quartic pairing instability using the mathematical understanding of the second chapter. This is a contemporary development since we reached this description by theoretical considerations based on the usual superconduction coupling in doped Weyl metals (ZYUZIN; BURKOV, 2012; CHRISPIM; BRUNI; GUIMARAES, 2021). The special pairing $-\lambda_R^2(\overline{\psi}_c P_R \psi)(\overline{\psi} P_L \psi_c) - \lambda_L^2(\overline{\psi}_c P_L \psi)(\overline{\psi} P_R \psi_c)$ breaks both charge and chiral symmetries and, as expected, the pairing effectively induces the dynamical formation of a charged chiral condensate whose phases fluctuations give rise to an effective axionic excitation along with a longitudinal mode for the photon excitations through the Higgs mechanism resulting fully gapped system describes an axionic superconductor. The computation is complex, and the introduction of an "enlarged" spinor is necessary to "decouple" the interaction term. The condensate is parametrized by two factors ($R(x)$ and $L(x)$) and their combination is responsible for the longitudinal mode for the gauge field and the mass for the axion-like excitation. Explicitly, $\frac{\theta(x)}{f} + \theta_0(x) = \frac{1}{4}\left(\frac{R(x)}{f_R} - \frac{L(x)}{f_L}\right)$ is gauge-invariant, and $\frac{\theta'(x)}{f'} = \frac{1}{4}\left(\frac{R(x)}{f_R} + \frac{L(x)}{f_L}\right)$ is chiral-invariant. Field $\theta'(x)$ is combined with the gauge field to compose a gauge-invariant field. This is the basics of the Higgs mechanism and the gauge invariance in our system is studied, in some detail, to make sure that no problems arise. The axion-like field is given by the excitations of the $\theta(x)$, the mass term follows the Peccei-Quin mechanism of the axionic insulator, and it is connected to a current density wave of the fermionic condensate. The effective description thus is

$$Z(j,J)=\int\mathcal{D}(C,\theta)e^{i\int\mathrm{d}^4x\left(\mathcal{L}(C,\theta)+\lambda^2v^6+j_\mu C^\mu+J\theta\right)}\ , \tag{349}$$

with

$$\begin{aligned}\mathcal{L}(C,\theta)=\int\mathrm{d}^4x\,\Big(&-\frac{1}{4}F_{\mu\nu}F^{\mu\nu}+\frac{1}{2}M^2A_\mu A^\mu\\&+\frac{1}{2}(\partial\theta)^2-\frac{1}{2}m_\theta^2\theta^2+\frac{m_\theta}{g}\theta\theta_0+\frac{m_\theta^2}{g^2}\theta_0^2+\frac{1}{4}g\left(\theta+\frac{\theta_0}{g}\right)\tilde{F}_{\mu\nu}F^{\mu\nu}+\cdots\Big)\ ,\end{aligned} \tag{350}$$

where $F_{\mu\nu}=\partial_\mu C_\nu-\partial_\nu C_\mu$ and the $\cdots$ stands for the various powers of $\left(\theta,\theta_0,\theta\theta_0,\cdots,(\partial\theta)^2,C^2\right)$ and their combinations plus field independent term. Much of the discussion in the axion insulator case is similar here. The non-perturbative effects materialize from factor

$$4\lambda^2v^6\left(1+\cos\left(2\frac{\theta'}{f'}\right)\cos\left(2\left(\frac{\theta}{f}+\theta_0\right)\right)\right) \tag{351}$$

but with the distinction that here there are two different kinds of vortices (one associated with the chiral and the other with the superconductor flux). Again, approximations exclude this from the excitation spectrum (and restores symmetry $\theta\to-\theta$, and space-time isotropy), similar to the previous discussion.

The final chapter considers a simplification of the previous model, which is

$$Z(j,J)=\int\mathcal{D}(A,\theta)e^{i\int\mathrm{d}^4x(\mathcal{L}+j_\mu A^\mu+J\theta)} \tag{352}$$

$$\mathcal{L}(A,\theta)=\int\mathrm{d}^4x\left(-\frac{1}{4}F_{\mu\nu}F^{\mu\nu}+\frac{1}{2}M^2A_\mu A^\mu+\frac{1}{2}(\partial\theta)^2-\frac{1}{2}m_\theta^2\theta^2+\frac{1}{4}g\theta\tilde{F}_{\mu\nu}F^{\mu\nu}\right) \tag{353}$$

where $F_{\mu\nu}=\partial_\mu A_\nu-\partial_\nu A_\mu$, to compute the two-point function of the massive photon excitation considering one-loop axionic corrections. This calculation is a new result in the literature. The computation includes some not-so-usual steps, such as the inclusion of higher-order field terms, which are necessary to the renormalization process. This is based on the understanding of Wilson's renormalization group, a similar form (accessible to us since we know the microscopic theory) would be the complete calculation of the fermionic determinant in the effective theory computation. Although possible in theory, the easy way is to include only the next-to-leading terms. The method to include those, the renormalization treatment is done in sec. 5.1. Those terms generate unphysical (ghosts) states which can be eliminated (sec. 5.2) by considering the desired precision (1-loop) in the computation. From this point forward, the computation done in section 5.3, is very similar to the textbook approach. The only unusual part is the renormalization scheme choice. Since the potential involves massive particles the choice of subtraction point in the MS-bar scheme is not simple, this favors the choice of the OS scheme as was done in section 5.3.2. Before the computation of the Yuwaka potential, we extract the imaginary part of the exact propagator in sec. 5.4, this will facilitate the potential computation in the next section since allows for a simples choice of contour in the complex plane. The correct Yuwaka potential is

$$V(r) = -\frac{e^2}{4\pi}\frac{e^{-Mr}}{r}\delta P \tag{354}$$

$$\delta P = 1 + \frac{(gM)^2\left(1+\frac{m}{M}\right)^2}{48\pi^2}\int_1^{\infty} \mathrm{d}t\, F(m/M,t)\left(t^2-1\right)^{3/2}\frac{e^{-Mr[t(1+m/M)-1]}}{t} \tag{355}$$

$$F(m/M,t) = \left(t^2 - \left(\frac{M-m}{M+m}\right)^2\right)^{3/2}\left(t^2 - \left(\frac{M}{M+m}\right)^2\right)^{-2}. \tag{356}$$

This system is written in terms of the adimensional parameters Mr (distance scale), $\frac{m}{M}$ (mass ratio scale), and gM (coupling scale). The order of magnitude of distance adopted here applies to thin-films physics.

These corrections naturally induce a modification of typical electromagnetic interaction at short distances. Alternatively, in the asymptotic distance limit, the effective theory is Yukawa-type (Proca) representing a usual superconductor. Other asymptotic limits can be explored. In special, in sections 5.6.1 and 5.6.2, the small axion mass and the small Proca mass limit were studied. The correction also influences the London penetration length (sec. 5.6.3). These effects are computed in the range applicable to thin-films physics meaning that the superconducting Dirac materials could be sensible to those effects. This opens a possible (based on these early findings) form to explore the quantum effects due to axionic coupling. The practical applicability, or even feasibility, to real condensed matter systems is a topic for further investigation.

Some general considerations can be done. The maximum possible value for the correction occurs when the axion-like mass is lesser or equal to the photon mass. (or Axionic effects are more prominent when $M > m$). Oppositely, as the Axion mass becomes larger, i.e. the field becomes harder to excite, the quantum fluctuations become closer to the non-perturbed value ($M^{eff} \sim M$). This reasoning is based, partially, on the fact that axion emission, by a decay process of $\gamma \to \gamma\theta$, is not possible.

One important point in this chapter is the fact that in our calculations we assumed the effective parameter m, M, and g (that compose the adimensional parameters) are independent. However, the computation in ch. 4 shows that the microscopic parameters λ and v and the effective m, M, and g ones are related by $g \sim \frac{1}{\lambda^2 v^3}$, $M \sim \lambda^2 v^3$ and $m \sim \frac{1}{\lambda}$, which can be reduced to $g \sim \frac{1}{M}$ and $m \sim \sqrt{\frac{v^3}{M}}$. These relations are compatible with the range of values considered in our analysis (in sec. 5.6) since the perturbative computations are valid for $gM < 1$.

This concludes this thesis. I hope that goal of exploring the route of the interplay between two distinct areas of physics, with a focus on axion physics, is achieved. Thank you for the time to read my work.

REFERENCES

ABBOTT, L.F.; SIKIVIE, P. A cosmological bound on the invisible axion. *Phys. Lett. B*, [S.l.], v. 120, n. 1, p. 133–136, 1983. ISSN 0370-2693. Disponível em: https://www.sciencedirect.com/science/article/pii/037026938390638X. Acesso em: 04 abr. 2022.

ACCIOLY, A.; DIAS, M. Algorithm for probing the unitarity of topologically massive models. *Int. J. Theor. Phys.*, [S.l.], v. 44, p. 1123–1139, 2005.

ADAM, C.; KLINKHAMER, F.R. Causality and radiatively induced cpt violation. *Phys. Lett. B*, [S.l.], v. 513, n. 1, p. 245–250, 2001. ISSN 0370-2693. Disponível em: https://www.sciencedirect.com/science/article/pii/S0370269301006785. Acesso em: 04 abr. 2022.

AITCHISON, I. J. R.; FRASER, C. M. Derivative expansions of fermion determinants: Anomaly-induced vertices, Goldstone-Wilczek currents, and Skyrme terms. *Phys. Rev. D*, [S.l.], v. 31, n. 10, p. 2605–2615, may 1985. ISSN 0556-2821. Disponível em: https://link.aps.org/doi/10.1103/PhysRevD.31.2605. Acesso em: 04 abr. 2022.

ALTLAND, A.; SIMONS, B. D. *Condensed matter field theory*. Cambridge: Cambridge University Press, 2010.

ARMITAGE, N.P.; MELE, E.J.; VISHWANATH, A. Weyl and dirac semimetals in three-dimensional solids. *Rev. Mod. Phys.*, [S.l.], v. 90, n. 1, p. 015001, jan. 2018.

ARZT, C. Reduced effective lagrangians. *Phys. Lett. B*, Elsevier BV, [S.l.], v. 342, n. 1–4, p. 189–195, Jan 1995. ISSN 0370-2693. Disponível em: http://dx.doi.org/10.1016/0370-2693(94)01419-D. Acesso em: 04 abr. 2022.

ASHTEKAR, A. New variables for classical and quantum gravity. *Phys. Rev. Lett.*, American Physical Society, [S.l.], v. 57, p. 2244–2247, Nov 1986. Disponível em: https://link.aps.org/doi/10.1103/PhysRevLett.57.2244. Acesso em: 04 abr. 2022.

BEDNIK, G.; ZYUZIN, A. A.; BURKOV, A. A. Superconductivity in weyl metals. *Phys. Rev. B*, American Physical Society, [S.l.], v. 92, p. 035153, Jul 2015. Disponível em: https://link.aps.org/doi/10.1103/PhysRevB.92.035153. Acesso em: 04 abr. 2022.

BERRY, M. V. Quantal phase factors accompanying adiabatic changes. *Proceedings of the Royal Society of London. A. Mathematical and Physical Sciences*, [S.l.], v. 392, p. 45 – 57, 1984.

BLOCH, F. Über die quantenmechanik der elektronen in kristallgittern. *Zeitschrift fur Physik*, [S.l.], v. 52, n. 7-8, p. 555–600, jul. 1929.

BRAGA, P.R. et al. Effective field theories for superconducting systems with multiple fermi surfaces. *Annals of Physics*, [S.l.], v. 374, p. 1–15, 2016. ISSN 0003-4916. Disponível em: https://www.sciencedirect.com/science/article/pii/S000349161630152X. Acesso em: 04 abr. 2022.

BRAGA, P.R.; GUIMARAES, M.S.; PAGANELLY, M.M.A. Multivalued fields and monopole operators in topological superconductors. *Annals of Physics*, [S.l.], v. 419, p. 168245, 2020. ISSN 0003-4916. Disponível em: https://www.sciencedirect.com/science/article/pii/S0003491620301792. Acesso em: 04 abr. 2022.

BRILLOUIN, L. *Wave propagation and group velocity.* [S.l.]: Academic Press, 1960. v. 8. ISBN 978-1-4832-3068-9.

BRUNI, R. C. L.; GUIMARAES, M. S.; CHRISPIM, B. A. S. D. Consequences of lorentz violation in the magnetic response of weyl supercondcutors. Unpublished. 2021.

BURKOV, A.A. Weyl metals. *Annual Review of Condensed Matter Physics*, Annual Reviews, [S.l.], v. 9, n. 1, p. 359–378, Mar 2018. ISSN 1947-5462. Disponível em: http://dx.doi.org/10.1146/annurev-conmatphys-033117-054129. Acesso em: 04 abr. 2022.

CADAVID, A. G.; RODRIGUEZ, Y. A systematic procedure to build the beyond generalized proca field theory. *Phys. Lett. B*, [S.l.], v. 798, p. 134958, 2019.

CARROLL, S. M.; FIELD, G. B. Is there evidence for cosmic anisotropy in the polarization of distant radio sources? *Phys. Rev. Lett.*, American Physical Society, [S.l.], v. 79, p. 2394–2397, Sep 1997. Disponível em: https://link.aps.org/doi/10.1103/PhysRevLett.79.2394. Acesso em: 04 abr. 2022.

CARROLL, S. M.; FIELD, G. B.; JACKIW, R. Limits on a Lorentz and Parity Violating Modification of Electrodynamics. *Phys. Rev. D*, [S.l.], v. 41, p. 1231, 1990.

CHAN, L.-H. Derivative expansion for the one-loop effective actions with internal symmetry. *Phys. Rev. Lett.*, American Physical Society, [S.l.], v. 57, p. 1199–1202, Sep 1986. Disponível em: https://link.aps.org/doi/10.1103/PhysRevLett.57.1199. Acesso em: 04 abr. 2022.

CHANG, C.-Z. et al. Experimental observation of the quantum anomalous hall effect in a magnetic topological insulator. *Science*, [S.l.], v. 340, n. 6129, p. 167–170, 2013. Disponível em: https://www.science.org/doi/abs/10.1126/science.1234414. Acesso em: 04 abr. 2022.

CHECKELSKY, J. G. et al. Trajectory of the anomalous hall effect towards the quantized state in a ferromagnetic topological insulator. *Nature Physics*, Springer Science and Business Media LLC, [S.l.], v. 10, n. 10, p. 731–736, Aug 2014. ISSN 1745-2481. Disponível em: http://dx.doi.org/10.1038/nphys3053. Acesso em: 04 abr. 2022.

CHEN, W. F. Issues on radiatively induced lorentz and cpt violation in quantum electrodynamics. *AIP Conference Proceedings*, [S.l.], v. 601, n. 1, p. 242–252, 2001. Disponível em: https://aip.scitation.org/doi/abs/10.1063/1.1435492. Acesso em: 04 abr. 2022.

CHEN, X.; GU, Z.-C.; WEN, X.-G. Local unitary transformation, long-range quantum entanglement, wave function renormalization, and topological order. *Phys. Rev. B*, American Physical Society, [S.l.], v. 82, n. 15, p. 155138, Oct 2010. ISSN 1550-235X. Disponível em: https://link.aps.org/doi/10.1103/PhysRevB.82.155138. Acesso em: 04 abr. 2022.

CHO, G. Y. et al. Superconductivity of doped weyl semimetals: Finite-momentum pairing and electronic analog of the ^{3}he-a phase. *Phys. Rev. B*, American Physical Society, [S.l.], v. 86, p. 214514, Dec 2012. Disponível em: https://link.aps.org/doi/10.1103/PhysRevB.86.214514. Acesso em: 04 abr. 2022.

CHRISPIM, B. A. S. D.; BRUNI, R. C. L.; GUIMARAES, M. S. Massive photon propagator in the presence of axionic fluctuations. *Phys. Rev. B*, American Physical Society, [S.l.], v. 103, n. 16, Apr 2021. ISSN 2469-9969. Disponível em: http://dx.doi.org/10.1103/PhysRevB.103.165120. Acesso em: 04 abr. 2022.

CHUNG, J.-M. Lorentz- and cpt-violating chern-simons term in the functional integral formalism. *Phys. Rev. D*, American Physical Society, [S.l.], v. 60, p. 127901, Oct 1999. Disponível em: https://link.aps.org/doi/10.1103/PhysRevD.60.127901. Acesso em: 04 abr. 2022.

CIMA, O. M. D. et al. Lorentz and cpt violation in qed revisited: A missing analysis. *Phys. Lett. B*, [S.l.], v. 688, n. 2, p. 258–262, 2010. ISSN 0370-2693. Disponível em: https://www.sciencedirect.com/science/article/pii/S0370269310004235. Acesso em: 04 abr. 2022.

COLEMAN, S.; GLASHOW, S. L. High-energy tests of lorentz invariance. *Phys. Rev. D*, American Physical Society, [S.l.], v. 59, p. 116008, Apr 1999. Disponível em: https://link.aps.org/doi/10.1103/PhysRevD.59.116008. Acesso em: 04 abr. 2022.

COLLADAY, D.; KOSTELECKÝ, V. A. Cptviolation and the standard model. *Phys. Rev. D*, American Physical Society, [S.l.], v. 55, n. 11, p. 6760–6774, Jun 1997. ISSN 1089-4918. Disponível em: http://dx.doi.org/10.1103/PhysRevD.55.6760. Acesso em: 04 abr. 2022.

______. Lorentz-violating extension of the standard model. *Phys. Rev. D*, American Physical Society, [S.l.], v. 58, p. 116002, Oct 1998. Disponível em: https://link.aps.org/doi/10.1103/PhysRevD.58.116002. Acesso em: 04 abr. 2022.

CONNES, A.; KREIMER, D. Hopf algebras, renormalization and noncommutative geometry. *Communications in Mathematical Physics*, Springer Science and Business Media LLC, [S.l.], v. 199, n. 1, p. 203–242, Dec 1998. ISSN 1432-0916. Disponível em: http://dx.doi.org/10.1007/s002200050499. Acesso em: 04 abr. 2022.

DICUS, D. A.; KAO, C.; REPKO, W. W. Effective lagrangians and low energy photon-photon scattering. *Phys. Rev. D*, American Physical Society, [S.l.], v. 57, n. 4, p. 2443–2447, Feb 1998. ISSN 1089-4918. Disponível em: http://dx.doi.org/10.1103/PhysRevD.57.2443. Acesso em: 04 abr. 2022.

DIENER, G. Superluminal group velocities and information transfer. *Phys. Lett. A*, [S.l.], v. 223, n. 5, p. 327–331, 1996. ISSN 0375-9601. Disponível em: https://www.sciencedirect.com/science/article/pii/S0375960196007670. Acesso em: 04 abr. 2022.

______. Energy transport in dispersive media and superluminal group velocities. *Phys. Lett. A*, [S.l.], v. 235, n. 2, p. 118–124, 1997. ISSN 0375-9601. Disponível em: https://www.sciencedirect.com/science/article/pii/S0375960197006002.

DINE, M.; FISCHLER, W.; SREDNICKI, M. A Simple Solution to the Strong CP Problem with a Harmless Axion. *Phys. Lett. B*, [S.l.], v. 104, p. 199–202, 1981.

DIRAC, P. A. M. The quantum theory of the electron. *Proceedings of the Royal Society of London Series A*, [S.l.], v. 117, n. 778, p. 610–624, fev. 1928.

DONOGHUE, J. F. General relativity as an effective field theory: The leading quantum corrections. *Phys. Rev. D*, American Physical Society, [S.l.], v. 50, n. 6, p. 3874–3888, Sep 1994. ISSN 0556-2821. Disponível em: http://dx.doi.org/10.1103/PhysRevD.50.3874. Acesso em: 04 abr. 2022.

______. Leading quantum correction to the newtonian potential. *Phys. Rev. Lett.*, American Physical Society, [S.l.], v. 72, n. 19, p. 2996–2999, May 1994. ISSN 0031-9007. Disponível em: http://dx.doi.org/10.1103/PhysRevLett.72.2996. Acesso em: 04 abr. 2022.

______. Introduction to the effective field theory description of gravity. *arXiv e-prints*, [S.l.], 6 1995. Disponível em: https://arxiv.org/abs/gr-qc/9512024. Acesso em: 04 abr. 2022.

ECKER, G. Low-energy QCD. *Prog. Part. Nucl. Phys.*, [S.l.], v. 36, p. 71–84, 1996.

EL-BATANOUNY, M. *Advanced Quantum Condensed Matter Physics: One-Body, Many-Body, and Topological Perspectives.* Cambridge: Cambridge University Press, 2020.

ESSIN, A. M.; MOORE, J. E.; VANDERBILT, D. Magnetoelectric polarizability and axion electrodynamics in crystalline insulators. *Phys. Rev. Lett.*, American Physical Society, [S.l.], v. 102, p. 146805, Apr 2009. Disponível em: https://link.aps.org/doi/10.1103/PhysRevLett.102.146805. Acesso em: 04 abr. 2022.

FRASER, C. M. Calculation of higher derivative terms in the one-loop effective lagrangian. *Zeitschrift für Physik C Particles and Fields*, Springer Science and Business Media LLC, [S.l.], v. 28, n. 1, p. 101–106, mar 1985. ISSN 01709739.

FREEDMAN, D. Z.; JOHNSON, K.; LATORRE, J. Differential regularization and renormalization: a new method of calculation in quantum field theory. *Nuclear Physics B*, [S.l.], v. 371, n. 1, p. 353–414, 1992. ISSN 0550-3213. Disponível em: https://www.sciencedirect.com/science/article/pii/055032139290240C. Acesso em: 04 abr. 2022.

FRIEDAN, D. A proof of the nielsen-ninomiya theorem. *Commun. Math. Phys.*, [S.l.], v. 85, p. 481–490, 1982.

FUJIKAWA, K. Path-integral measure for gauge-invariant fermion theories. *Phys. Rev. Lett.*, American Physical Society, [S.l.], v. 42, p. 1195–1198, Apr 1979. Disponível em: https://link.aps.org/doi/10.1103/PhysRevLett.42.1195.

FUJIKAWA, K.; SUZUKI, H. *Path Integrals and Quantum Anomalies.* [S.l.]: Oxford University Press, 2004. ISBN 9780198529132.

FUKUSHIMA, K.; KHARZEEV, D. E.; WARRINGA, H. J. Chiral magnetic effect. *Phys. Rev. D*, American Physical Society, [S.l.], v. 78, n. 7, Oct 2008. ISSN 1550-2368. Disponível em: http://dx.doi.org/10.1103/PhysRevD.78.074033. Acesso em: 04 abr. 2022.

GAILLARD, M. K. The effective one-loop scalar lagrangian with derivative couplings. *Nuclear Physics B*, [S.l.], v. 268, n. 3, p. 669–692, 1986. ISSN 0550-3213. Disponível em: https://www.sciencedirect.com/science/article/pii/0550321386902646. Acesso em: 04 abr. 2022.

GASSER, J.; LEUTWYLER, H. Chiral Perturbation Theory to One Loop. *Annals of Physics*, [S.l.], v. 158, p. 142, 1984.

_____. Chiral perturbation theory: Expansions in the mass of the strange quark. *Nuclear Physics B*, [S.l.], v. 250, p. 465–516, 12 1985.

GINZBURG, V. L.; LANDAU, L. D. On the theory of superconductivity. *Zh. Eksp. Teor. Fiz.*, [S.l.], v. 20, p. 1064–1082, 1950.

GÓMEZ, A.; URRUTIA, L. The axial anomaly in lorentz violating theories: Towards the electromagnetic response of weakly tilted weyl semimetals. *Symmetry*, [S.l.], v. 13, n. 7, p. 1181, 2021.

GOROFF, M. H.; SAGNOTTI, A. Quantum gravity at two loops. *Phys. Lett. B*, [S.l.], v. 160, n. 1, p. 81–86, 1985. ISSN 0370-2693. Disponível em: https://www.sciencedirect.com/science/article/pii/0370269385914704. Acesso em: 04 abr. 2022.

_____. The Ultraviolet Behavior of Einstein Gravity. *Nuclear Physics B*, [S.l.], v. 266, p. 709–736, 1986.

GOSWAMI, P.; TEWARI, S. Axionic field theory of $(3+1)$-dimensional weyl semimetals. *Phys. Rev. B*, American Physical Society, [S.l.], v. 88, p. 245107, Dec 2013. Disponível em: https://link.aps.org/doi/10.1103/PhysRevB.88.245107. Acesso em: 04 abr. 2022.

GREINER, W.; REINHARDT, J. *Quantum electrodynamics*. Berlin: Springer, 1992. 447 p. ISBN 978-3-540-87560-4.

GRIFFITHS, D. J. *Introduction to electrodynamics*. 4. ed. Boston: Pearson, 2013.

GRINSTEIN, B.; O'CONNELL, D.; WISE, M. B. The Lee-Wick standard model. *Phys. Rev. D*, [S.l.], v. 77, p. 025012, 2008.

GROSS, D. J.; NEVEU, A. Dynamical symmetry breaking in asymptotically free field theories. *Phys. Rev. D*, American Physical Society, [S.l.], v. 10, p. 3235–3253, Nov 1974. Disponível em: https://link.aps.org/doi/10.1103/PhysRevD.10.3235. Acesso em: 04 abr. 2022.

GRUSHIN, A. G. Consequences of a condensed matter realization of lorentz-violating qed in weyl semi-metals. *Phys. Rev. D*, American Physical Society, [S.l.], v. 86, n. 4, Aug 2012. ISSN 1550-2368. Disponível em: http://dx.doi.org/10.1103/PhysRevD.86.045001. Acesso em: 04 abr. 2022.

GU, Y.; QI, X.-L. Axion field theory approach and the classification of interacting topological superconductors. *arXiv e-prints*, [S.l.], 12 2015. Disponível em: https://arxiv.org/abs/1512.04919. Acesso em: 04 abr. 2022.

HALL, E. On a new action of the magnet on electric currents. *American Journal of Mathematics*, [S.l.], v. 2, n. 3, p. 287–292, 1879. Disponível em: https://www.semanticscholar.org/paper/8cb4395a5e74e952aad74ce8a08d96f3941e3bb9. Acesso em: 04 abr. 2022.

HALTER, J. An Effective Lagrangian for photons. *Phys. Lett. B*, [S.l.], v. 316, p. 155–157, 1993.

HANSSON, T. H. et al. Effective field theory for a p-wave superconductor in the subgap regime. *Phys. Rev. B*, American Physical Society, [S.l.], v. 91, p. 075116, Feb 2015. Disponível em: https://link.aps.org/doi/10.1103/PhysRevB.91.075116. Acesso em: 04 abr. 2022.

HANSSON, T. H.; OGANESYAN, V.; SONDHI, S.L. Superconductors are topologically ordered. *Annals of Physics*, [S.l.], v. 313, n. 2, p. 497–538, 2004. ISSN 0003-4916. Disponível em: https://www.sciencedirect.com/science/article/pii/S0003491604001046. Acesso em: 04 abr. 2022.

HASAN, M.Z.; KANE, C.L. Topological Insulators. *Rev. Mod. Phys.*, [S.l.], v. 82, n. 4, p. 3045–3067, 2010. Disponível em: https://doi.org/10.1103%2Frevmodphys.82.3045. Acesso em: 04 abr. 2022.

HASAN, M. Z.; MOORE, Joel E. Three-dimensional topological insulators. *Annual Review of Condensed Matter Physics*, [S.l.], v. 2, n. 1, p. 55–78, 2011. Disponível em: https://doi.org/10.1146/annurev-conmatphys-062910-140432. Acesso em: 04 abr. 2022.

HEES, H. v. The renormalizability for massive abelian gauge field theories re-visited. *arXiv e-prints*, [S.l.], 2003. Disponível em: https://arxiv.org/abs/hep-th/0305076. Acesso em: 04 abr. 2022.

HOOFT, G. 't. Computation of the quantum effects due to a four-dimensional pseudoparticle. *Phys. Rev. D*, American Physical Society, [S.l.], v. 14, p. 3432–3450, Dec 1976. Disponível em: https://link.aps.org/doi/10.1103/PhysRevD.14.3432. Acesso em: 04 abr. 2022.

______. How Instantons Solve the U(1) Problem. *Phys. Rept.*, [S.l.], v. 142, n. 6, p. 357–387, 1986. ISSN 0370-1573. Disponível em: https://www.sciencedirect.com/science/article/pii/0370157386901171. Acesso em: 04 abr. 2022.

HOOFT, G. 't et al. (Ed.). *Recent Developments in Gauge Theories*. New York: Springer, 1980. v. 59. 1-438 p. Disponível em: https://link.springer.com/book/10.1007/978-1-4684-7571-5. Acesso em: 04 abr. 2022.

HOOFT, G. 't; VELTMAN, M. J. G. One loop divergencies in the theory of gravitation. *Ann. Inst. H. Poincare Phys. Theor. A*, [S.l.], v. 20, p. 69–94, 1974.

HOŘAVA, P. Membranes at quantum criticality. *Journal of High Energy Physics*, Springer Science and Business Media LLC, [S.l.], v. 2009, n. 03, p. 020–020, mar 2009.

Disponível em: https://doi.org/10.1088/1126-6708/2009/03/020. Acesso em: 04 abr. 2022.

JACKIW, R. When radiative corrections are finite, but undetermined. *International Journal of Modern Physics B*, World Scientific Pub Co Pte Lt, [S.l.], v. 14, n. 19n20, p. 2011–2021, Aug 2000. ISSN 1793-6578. Disponível em: http://dx.doi.org/10.1142/S021797920000114X. Acesso em: 04 abr. 2022.

JACKIW, R.; KOSTELECKÝ, V. A. Radiatively induced lorentz and CPT violation in electrodynamics. *Phys. Rev. Lett.*, American Physical Society, [S.l.], v. 82, p. 3572–3575, May 1999. Disponível em: https://link.aps.org/doi/10.1103/PhysRevLett.82.3572. Acesso em: 04 abr. 2022.

KANE, C.; MELE, E. Z_2 topological order and the quantum spin hall effect. *Phys. Rev. Lett.*, American Physical Society, [S.l.], v. 95, p. 146802, Sep 2005.

KIM, J. E. Weak Interaction Singlet and Strong CP Invariance. *Phys. Rev. Lett.*, [S.l.], v. 43, p. 103, 1979.

KITTEL, C. *Introduction to solid state physics*. 8. ed. [S.l.]: Wiley, 2004. 680 p. ISBN 9780471415268.

KLITZING, K. v. et al. 40 years of the quantum hall effect. *Nature Reviews Physics*, [S.l.], v. 2, p. 1–5, 2020. Disponível em: https://www.semanticscholar.org/paper/ebbe85a11607cb2652980b88f587233c76f03eb8. Acesso em: 04 abr. 2022.

KLITZING, K. v.; DORDA, G.; PEPPER, M. New method for high-accuracy determination of the fine-structure constant based on quantized hall resistance. *Phys. Rev. Lett.*, American Physical Society, [S.l.], v. 45, p. 494–497, Aug 1980. Disponível em: https://link.aps.org/doi/10.1103/PhysRevLett.45.494. Acesso em: 04 abr. 2022.

KNETTER, C. G. Effective lagrangians with higher derivatives and equations of motion. *Phys. Rev. D*, American Physical Society, [S.l.], v. 49, p. 6709–6719, Jun 1994. Disponível em: https://link.aps.org/doi/10.1103/PhysRevD.49.6709. Acesso em: 04 abr. 2022.

KONG, X.; RAVNDAL, F. Quantum corrections to the qed vacuum energy. *Nuclear Physics B*, Elsevier BV, [S.l.], v. 526, n. 1–3, p. 627–656, Aug 1998. ISSN 0550-3213. Disponível em: http://dx.doi.org/10.1016/S0550-3213(98)00364-2. Acesso em: 04 abr. 2022.

KOSTELECKÝ, V. A. Gravity, lorentz violation, and the standard model. *Phys. Rev. D*, American Physical Society, [S.l.], v. 69, p. 105009, May 2004. Disponível em: https://link.aps.org/doi/10.1103/PhysRevD.69.105009. Acesso em: 04 abr. 2022.

KOSTELECKÝ, V. A.; LEHNERT, R. Stability, causality, and lorentz and cpt violation. *Phys. Rev. D*, American Physical Society, [S.l.], v. 63, n. 6, Feb 2001. ISSN 1089-4918. Disponível em: http://dx.doi.org/10.1103/PhysRevD.63.065008. Acesso em: 04 abr. 2022.

KOSTELECKÝ, V. A.; RUSSELL, N. Data tables for lorentz and *cpt* violation. *Rev. Mod. Phys.*, American Physical Society, [S.l.], v. 83, p. 11–31, Mar 2011. Disponível em: https://link.aps.org/doi/10.1103/RevModPhys.83.11. Acesso em: 04 abr. 2022.

KOSTELECKÝ, V. A.; SAMUEL, S. Spontaneous breaking of lorentz symmetry in string theory. *Phys. Rev. D*, American Physical Society, [S.l.], v. 39, p. 683–685, Jan 1989. Disponível em: https://link.aps.org/doi/10.1103/PhysRevD.39.683. Acesso em: 04 abr. 2022.

LANDAU, L. D. On the theory of phase transitions. i. *Phys. Z. Sowjet.*, [S.l.], v. 11, p. 26, 1937. Disponível em: http://cds.cern.ch/record/480039.

LI, R. et al. Dynamical axion field in topological magnetic insulators. *Nature Physics*, [S.l.], v. 6, n. 4, p. 284–288, abr. 2010.

LI, Yi; HALDANE, F. D. M. Topological nodal cooper pairing in doped weyl metals. *Phys. Rev. Lett.*, American Physical Society, [S.l.], v. 120, p. 067003, Feb 2018. Disponível em: https://link.aps.org/doi/10.1103/PhysRevLett.120.067003. Acesso em: 04 abr. 2022.

LIBERATI, S.; MACCIONE, L. Lorentz violation: Motivation and new constraints. *Annual Review of Nuclear and Particle Science*, Annual Reviews, [S.l.], v. 59, n. 1, p. 245–267, Nov 2009. ISSN 1545-4134. Disponível em: http://dx.doi.org/10.1146/annurev.nucl.010909.083640. Acesso em: 04 abr. 2022.

MACIEJKO, J.; NANDKISHORE, R. Weyl semimetals with short-range interactions. *Phys. Rev. B*, [S.l.], v. 90, n. 3, p. 035126, jul. 2014. Disponível em: https://doi.org/10.1103%2Fphysrevb.90.035126. Acesso em: 04 abr. 2022.

MACIEJKO, J. et al. Topological quantization in units of the fine structure constant. *Phys. Rev. Lett.*, American Physical Society, [S.l.], v. 105, p. 166803, Oct 2010. Disponível em: https://link.aps.org/doi/10.1103/PhysRevLett.105.166803. Acesso em: 04 abr. 2022.

MILLONNI, P. W. *Fast Light, Slow Light and Left-Handed Light.* [S.l.]: CRC Press, 2004.

MOORE, J. E. The birth of topological insulators. *Nature*, Nature Publishing Group, [S.l.], v. 464, n. 7286, p. 194–198, mar. 2010.

NAKAHARA, M. *Geometry, topology and physics.* Bristol: Institute of Physics Publishing, 1990. 573 p. ISBN 9780750306065.

NIELSEN, H. B.; NINOMIYA, M. No Go Theorem for Regularizing Chiral Fermions. *Phys. Lett. B*, [S.l.], v. 105, p. 219–223, 1981.

NIEUWENHUIZEN, v. P. On ghost-free tensor lagrangians and linearized gravitation. *Nuclear Physics B*, [S.l.], v. 60, p. 478–492, 1973.

ORITI, D. (Ed.). *Approaches to Quantum Gravity: Toward a New Understanding of Space, Time and Matter.* Cambridge: Cambridge University Press, 2009.

PECCEI, R. D. The Strong CP problem and axions. *Lect. Notes Phys.*, [S.l.], v. 741, p. 3–17, 2008.

PECCEI, R. D.; QUINN, H. R. Constraints Imposed by CP Conservation in the Presence of Instantons. *Phys. Rev. D*, [S.l.], v. 16, p. 1791–1797, 1977.

PECCEI, R. D.; QUINN, H. R. CP conservation in the presence of pseudoparticles. *Phys. Rev. Lett.*, American Physical Society, [S.l.], v. 38, p. 1440–1443, Jun 1977. Disponível em: https://link.aps.org/doi/10.1103/PhysRevLett.38.1440. Acesso em: 04 abr. 2022.

PÉREZ-VICTORIA, M. Exact calculation of the radiatively induced lorentz and cpt violation in qed. *Phys. Rev. Lett.*, American Physical Society, [S.l.], v. 83, n. 13, p. 2518–2521, Sep 1999. ISSN 1079-7114. Disponível em: http://dx.doi.org/10.1103/PhysRevLett.83.2518. Acesso em: 04 abr. 2022.

PESKIN, M. E.; SCHROEDER, D. V. *An introduction to quantum field theory*. Boulder, CO: Westview, 1995.

POTTING, R. Lorentz and CPT violation. *Journal of Physics: Conference Series*, IOP Publishing, [S.l.], v. 447, p. 012009, jul 2013. Disponível em: https://doi.org/10.1088/1742-6596/447/1/012009. Acesso em: 04 abr. 2022.

QI, X.; HUGHES, T.; ZHANG, S. Topological Field Theory of Time-Reversal Invariant Insulators. *Phys. Rev. B*, [S.l.], v. 78, p. 195424, 2008.

QI, X.-L. et al. Inducing a magnetic monopole with topological surface states. *Science*, American Association for the Advancement of Science, [S.l.], v. 323, n. 5918, p. 1184–1187, Feb 2009. ISSN 1095-9203. Disponível em: http://dx.doi.org/10.1126/science.1167747. Acesso em: 04 abr. 2022.

_____. Seeing the magnetic monopole through the mirror of topological surface states. *Science*, American Association for the Advancement of Science, [S.l.], v. 1, n. 5918, p. 22009, feb 2009. Disponível em: https://doi.org/10.1126%2Fscience.1167747. Acesso em: 04 abr. 2022.

QI, X.-L.; WITTEN, E.; ZHANG, S.-C. Axion topological field theory of topological superconductors. *Phys. Rev. B*, American Physical Society, [S.l.], v. 87, p. 134519, Apr 2013. Disponível em: https://link.aps.org/doi/10.1103/PhysRevB.87.134519. Acesso em: 04 abr. 2022.

QI, X. L.; ZHANG, S. C. Topological insulators and superconductors. *Rev. Mod. Phys.*, [S.l.], v. 83, n. 4, p. 1057–1110, 2011.

ROVELLI, C. Loop quantum gravity. *Living Reviews in Relativity*, Springer Science and Business Media LLC, [S.l.], v. 1, n. 1, Jan 1998. ISSN 1433-8351. Disponível em: http://dx.doi.org/10.12942/lrr-1998-1. Acesso em: 04 abr. 2022.

_____. *Quantum Gravity*. Cambridge: Cambridge University Press, 2004. (Cambridge Monographs on Mathematical Physics).

RYLANDS, C. et al. Chiral anomaly in interacting condensed matter systems. *Phys. Rev. Lett.*, American Physical Society, [S.l.], v. 126, n. 18, may 2021. Disponível em: https://doi.org/10.1103%2Fphysrevlett.126.185303. Acesso em: 04 abr. 2022.

SAZDJIAN, H. The 1/N expansion method in quantum field theory. *arXiv e-prints*, [S.l.], dec 2015. Disponível em: https://arxiv.org/abs/1512.06784. Acesso em: 04 abr. 2022.

SCALAPINO, D. J. A common thread: The pairing interaction for unconventional superconductors. *Rev. Mod. Phys.*, American Physical Society, [S.l.], v. 84, p. 1383–1417, Oct 2012. Disponível em: https://link.aps.org/doi/10.1103/RevModPhys.84.1383. Acesso em: 04 abr. 2022.

SCHWARTZ, M. D. *Quantum Field Theory and the Standard Model.* Cambridge: Cambridge University Press, 2013.

SEKINE, A.; NOMURA, K. Axion electrodynamics in topological materials. *Journal of Applied Physics*, AIP Publishing, [S.l.], v. 129, n. 14, p. 141101, Apr 2021. ISSN 1089-7550. Disponível em: http://dx.doi.org/10.1063/5.0038804. Acesso em: 04 abr. 2022.

SEZGIN, E.; NIEUWENHUIZEN, v. P. New ghost-free gravity lagrangians with propagating torsion. *Phys. Rev. D*, American Physical Society, [S.l.], v. 21, p. 3269–3280, Jun 1980. Disponível em: https://link.aps.org/doi/10.1103/PhysRevD.21.3269. Acesso em: 04 abr. 2022.

SHIFMAN, M. A.; VAINSHTEIN, A.I.; ZAKHAROV, V. I. Can Confinement Ensure Natural CP Invariance of Strong Interactions? *Nuclear Physics B*, [S.l.], v. 166, p. 493–506, 1980.

STANESCU, T. D. *Introduction to topological quantum matter & quantum computation.* [S.l.]: CRC Press, 2016.

STELLE, K. S. Renormalization of higher-derivative quantum gravity. *Phys. Rev. D*, American Physical Society, [S.l.], v. 16, p. 953–969, Aug 1977. Disponível em: https://link.aps.org/doi/10.1103/PhysRevD.16.953. Acesso em: 04 abr. 2022.

STONE, M.; LOPES, P. L. S. Effective action and electromagnetic response of topological superconductors and majorana-mass weyl fermions. *Phys. Rev. B*, American Physical Society, [S.l.], v. 93, p. 174501, May 2016. Disponível em: https://link.aps.org/doi/10.1103/PhysRevB.93.174501. Acesso em: 04 abr. 2022.

STREATER, R. F.; WIGHTMAN, A. S. *PCT, Spin Statistics, And All That.* New York, Amsterdam: W. A. Benjamin Inc., 1964.

THIEMANN, T. *Modern Canonical Quantum General Relativity.* Cambridge: Cambridge University Press, 2007. (Cambridge Monographs on Mathematical Physics).

THOULESS, D. J. et al. Quantized hall conductance in a two-dimensional periodic potential. *Phys. Rev. Lett.*, American Physical Society, [S.l.], v. 49, p. 405–408, Aug 1982. Disponível em: https://link.aps.org/doi/10.1103/PhysRevLett.49.405. Acesso em: 04 abr. 2022.

TONG, D. Quantum hall effect. *Lecture notes, DAMTP Cambridge*, [S.l.], 2016. Disponível em: http://www.damtp.cam.ac.uk/user/tong/qhe/qhe.pdf. Acesso em: 04 abr. 2022.

______. Gauge theory. *Lecture notes, DAMTP Cambridge*, [S.l.], 2018. Disponível em: https://www.damtp.cam.ac.uk/user/tong/gaugetheory/gt.pdf. Acesso em: 04 abr. 2022.

TSE, W.-K.; MACDONALD, A. H. Giant magneto-optical kerr effect and universal faraday effect in thin-film topological insulators. *Phys. Rev. Lett.*, American Physical Society, [S.l.], v. 105, p. 057401, Jul 2010. Disponível em: https://link.aps.org/doi/10.1103/PhysRevLett.105.057401. Acesso em: 04 abr. 2022.

TSUI, D. C.; STORMER, H. L.; GOSSARD, A. C. Two-dimensional magnetotransport in the extreme quantum limit. *Phys. Rev. Lett.*, American Physical Society, [S.l.], v. 48, p. 1559–1562, May 1982. Disponível em: https://link.aps.org/doi/10.1103/PhysRevLett.48.1559. Acesso em: 04 abr. 2022.

VAZIFEH, M. M.; FRANZ, M. Quantization and 2π periodicity of the axion action in topological insulators. *Phys. Rev. B*, American Physical Society, [S.l.], v. 82, p. 233103, Dec 2010. Disponível em: https://link.aps.org/doi/10.1103/PhysRevB.82.233103. Acesso em: 04 abr. 2022.

______. Electromagnetic response of weyl semimetals. *Phys. Rev. Lett.*, American Physical Society, [S.l.], v. 111, n. 2, Jul 2013. ISSN 1079-7114. Disponível em: http://dx.doi.org/10.1103/PhysRevLett.111.027201. Acesso em: 04 abr. 2022.

VILLALBA-CHÁVEZ, S.; GOLUB, A.; MüLLER, C. Axion-modified photon propagator, Coulomb potential and Lamb-shift. *Phys. Rev. D*, [S.l.], v. 98, n. 11, p. 115008, 2018.

VOLOVIK, G. E. *The Universe in a Helium Droplet.* [S.l.]: OUP Oxford, 2009. (International Series of Monographs on Physics). ISBN 9780199564842.

WAN, X. et al. Topological semimetal and fermi-arc surface states in the electronic structure of pyrochlore iridates. *Phys. Rev. B*, American Physical Society, [S.l.], v. 83, p. 205101, May 2011. Disponível em: https://link.aps.org/doi/10.1103/PhysRevB.83.205101. Acesso em: 04 abr. 2022.

WANG, Z.; ZHANG, S. Chiral anomaly, charge density waves, and axion strings from weyl semimetals. *Phys. Rev. B*, [S.l.], v. 87, n. 16, p. 161107, 2013.

WEI, H.; CHAO, S.-P.; AJI, V. Odd-parity superconductivity in weyl semimetals. *Phys. Rev. B*, American Physical Society, [S.l.], v. 89, p. 014506, Jan 2014. Disponível em: https://link.aps.org/doi/10.1103/PhysRevB.89.014506. Acesso em: 04 abr. 2022.

WEINBERG, S. The U(1) Problem. *Phys. Rev. D*, [S.l.], v. 11, p. 3583–3593, 1975.

______. A New Light Boson? *Phys. Rev. Lett.*, [S.l.], v. 40, p. 223–226, 1978.

______. A new light boson? *Phys. Rev. Lett.*, American Physical Society, [S.l.], v. 40, p. 223–226, Jan 1978. Disponível em: https://link.aps.org/doi/10.1103/PhysRevLett.40.223. Acesso em: 04 abr. 2022.

______. Phenomenological lagrangians. *Physica A: Statistical Mechanics and its Applications*, [S.l.], v. 96, n. 1, p. 327–340, 1979. ISSN 0378-4371. Disponível em: https://www.sciencedirect.com/science/article/pii/0378437179902231. Acesso em: 04 abr. 2022.

WEYL, H. Elektron und gravitation. i. *Zeitschrift fur Physik*, [S.l.], v. 56, n. 5-6, p. 330–352, maio 1929.

WILCZEK, F. Problem of strong p and t invariance in the presence of instantons. *Phys. Rev. Lett.*, American Physical Society, [S.l.], v. 40, p. 279–282, Jan 1978. Disponível em: https://link.aps.org/doi/10.1103/PhysRevLett.40.279. Acesso em: 04 abr. 2022.

_____. Two applications of axion electrodynamics. *Phys. Rev. Lett.*, [S.l.], v. 58, n. 18, p. 1799–1802, 1987. ISSN 00319007.

WILSON, A. H. The theory of electronic semi-conductors. *Proceedings of The Royal Society A: Mathematical, Physical and Engineering Sciences*, [S.l.], v. 133, n. 822, p. 458–491, 1931a.

_____. The theory of electronic semi-conductors. ii. *Proceedings of The Royal Society A: Mathematical, Physical and Engineering Sciences*, [S.l.], v. 134, n. 823, p. 277–287, 1931b.

WITTEN, E. Dyons of charge $e\theta/2\pi$. *Phys. Lett. B*, Elsevier BV, [S.l.], v. 86, n. 3-4, p. 283–287, oct 1979. ISSN 0370-2693. Disponível em: https://www.sciencedirect.com/science/article/pii/0370269379908384. Acesso em: 04 abr. 2022.

_____. Three lectures on topological phases of matter. *La Rivista del Nuovo Cimento*, SIF, [S.l.], v. 39, n. 7, p. 313–370, Jun 2016. ISSN 0393697X, 0393697X. Disponível em: https://arxiv.org/abs/1510.07698. Acesso em: 04 abr. 2022.

YAN, B.; FELSER, C. Topological materials: Weyl semimetals. *Annual Review of Condensed Matter Physics*, [S.l.], v. 8, p. 337–354, mar. 2017.

YANG, B.-J.; NAGAOSA, N. Classification of stable three-dimensional dirac semimetals with nontrivial topology. *Nature Communications*, Springer Science and Business Media LLC, [S.l.], v. 5, n. 1, Sep 2014. ISSN 2041-1723. Disponível em: http://dx.doi.org/10.1038/ncomms5898. Acesso em: 04 abr. 2022.

YOU, Y.; CHO, G. Yo.; HUGHES, T. L. Response properties of axion insulators and weyl semimetals driven by screw dislocations and dynamical axion strings. *Phys. Rev. B*, [S.l.], v. 94, n. 8, p. 085102, 2016.

ZEE, A. *Quantum Field Theory in a Nutshell.* 2. ed. Princeton: Princeton University Press, 2010. 608 p. ISBN 9781400835324. Disponível em: https://books.google.com.br/books?id=n8Mmbjtco78C. Acesso em: 04 abr. 2022.

ZENG, Bei et al. Quantum information meets quantum matter – from quantum entanglement to topological phase in many-body systems. *arXiv e-prints*, [S.l.], ago. 2015. Disponível em: https://arxiv.org/abs/1508.02595. Acesso em: 04 abr. 2022.

ZHANG, R.-Y. et al. Time circular birefringence in time-dependent magnetoelectric media. *Sci. Rep.*, [S.l.], v. 5, p. 13673, 09 2015.

ZYUZIN, A. A.; BURKOV, A. A. Topological response in weyl semimetals and the chiral anomaly. *Phys. Rev. B*, [S.l.], v. 86, n. 11, p. 115133, set. 2012.

APPENDIX A – Review on Fujikawa's method

This part reviews some calculation steps of the so-called Fujiwaka method to compute the chiral anomaly from the integral measure. The initial point is transformation

$$\psi(x) \to \psi'(x) = e^{i\frac{1}{2}\beta(x)\gamma^5}\psi(x) \qquad \text{and} \qquad \overline{\psi}(x) \to \overline{\psi}'(x) = \overline{\psi}e^{i\frac{1}{2}\beta(x)\gamma^5} \ , \tag{357}$$

with $\beta(x) = 2b_\mu x^\mu$, resulting in the elimination of the action term $\overline{\psi}\not{b}\gamma^5\psi(x)$ from action

$$S_0 = \int \mathrm{d}^4x\, \overline{\psi}(x) \left(i\not{\partial} + \not{b}\gamma^5 + ie\not{A}(x)\right) \psi(x), \tag{358}$$

since it transforms to

$$S_0 \to S_0' = \int \mathrm{d}^4x\, \overline{\psi}(x) \left(i\not{\partial} + ie\not{A}(x)\right) \psi(x), \tag{359}$$

This transformation also introduces a non-trivial Jacobian in the fermionic integral measure

$$\mathcal{D}\Big(\psi^\dagger, \psi, A\Big) \to \mathcal{D}\Big(\psi'^\dagger, \psi', A\Big) = \mathcal{J}^{-2} \cdot \mathcal{D}\Big(\psi^\dagger, \psi, A\Big) \ , \tag{360}$$

where $\mathcal{J}$ is the determinant of the chiral shift. To compute $\mathcal{J}^{-2}$ we will follow the steps of (ZYUZIN; BURKOV, 2012) (which is based on (FUJIKAWA, 1979; FUJIKAWA; SUZUKI, 2004)). First, we decompose the local chiral rotation in a series of infinitesimal transformations ds with $\psi(x) \to \psi'(x) = e^{i\frac{1}{2}\mathrm{d}s\beta(x)\gamma^5}\psi(x)$ (and $s \in [0,1]$). On the intermediary step s the Dirac operator is

$$\not{D} = \gamma^\mu \Big[\partial_\mu + ieA_\mu + ib_\mu(1-s)\gamma^5\Big] \tag{361}$$

This is a hermitian operator such that it has eigenfunctions $\phi(x)$ that obey $\not{D}\phi_n = \varepsilon_n\phi_n$ (where ε_n are real eigenvalues and ϕ_n spinor eigenfunctions with suppressed spinor indexes). We can follow the usual steps in the Jacobian calculation and expand the fields ψ and $\overline{\psi}$ in terms of complete orthonormal eigenvectors $\phi_n(x)$ resulting in

$$\psi(x) = \sum_n \phi_n(x)c_n \qquad \text{and} \qquad \overline{\psi}(x) = \sum_n \phi_n^*(x)\overline{c}_n \ , \tag{362}$$

where the c_n and $\overline{c}_n$ are new Grassmann variables. The transformed field ψ' also follows a similar expansion but with the Grassmann variables c_n' and $\overline{c}_n'$ given by

$$\psi'(x) = \sum_n \phi_n(x)c_n' \qquad \text{and} \qquad \overline{\psi}'(x) = \sum_n \phi_n^*(x)\overline{c}_n' \ . \tag{363}$$

The relations between $(c_n, \overline{c}_n)$ and $(c'_n, \overline{c}'_n)$ are

$$c'_n = \sum_m U_{nm} c_m \qquad \text{and} \qquad \overline{c}'_n = \sum_m U_{nm} \overline{c}_m \tag{364}$$

where U matrix represents the infinitesimal chiral transformation operator (obtainable from transformations (357)) and can be written as

$$U_{nm} = \delta_{nm} - \mathrm{d}s \, \frac{i}{2} \int \mathrm{d}^4x \, \phi^*_n(x)\theta(x)\gamma^5\phi_n(x) \tag{365}$$

Now, the Jacobian of the chiral transformation can be written using the matrix U simply as

$$\mathcal{J} = \det\left(U^{-2}\right) = e^{\ln\det\left(U^{-2}\right)} = e^{-2\,\mathrm{Tr}\ln(U)} = e^{i\mathrm{d}s\int \mathrm{d}^4x \sum_n \phi^*_n(x)\theta(x)\gamma^5\phi_n(x)} \tag{366}$$

Now we can concentrate [32] on the quantity

$$I(x) \equiv \sum_n \phi^*_n(x)\gamma^5\phi_n(x) \tag{367}$$

This quantity is ill-defined (naively because it looks like $\mathrm{Tr}(\gamma^5)$), and we must regularize the sum in a gauge-invariant way. A natural choice is

$$\sum_n \phi^*_n(x)\gamma^5\phi_n(x) = \lim_{M\to\infty} \sum_n \phi^*_n(x)\gamma^5\phi_n(x) e^{\varepsilon_n^2/M^2} \tag{368}$$

so that

$$I(x) = \lim_{M\to\infty} \sum_n \phi^*_n(x)\gamma^5 e^{-\not{D}^2/M^2}\phi_n(x) \tag{369}$$

where is was used $\not{D}\phi_n = \varepsilon_n\phi_n$. We can write this expression in operator form

$$I(x) = \lim_{M\to\infty} \langle x| \,\mathrm{Tr}\,\gamma^5 e^{-\not{D}^2/M^2}\, |x\rangle \tag{370}$$

$$= \lim_{M\to\infty} \int \frac{\mathrm{d}^4k}{(2\pi)^4}\, \mathrm{Tr}\,\gamma^5 e^{-ikx} e^{-\not{D}^2/M^2} e^{ikx} \tag{371}$$

Now, in order to compute the integral we must use the square of the Dirac operator (at the stage s) which is

$$\not{D}^2 = -D_\mu D_\mu - (1-s)^2 b_\mu b_\mu + \frac{ie}{4}[\gamma^\mu, \gamma^\nu]F_{\mu\nu} + i(1-s)[\gamma^\mu, \gamma^\nu] b_\mu D_\nu \gamma^5 \tag{372}$$

[32] For a more general computation see (GÓMEZ; URRUTIA, 2021)

meaning that

$$I(x)=\lim_{M\to\infty}\int\frac{\mathrm{d}^4k}{(2\pi)^4}\,\mathrm{Tr}\,\gamma^5\exp\left[\frac{(ik_\mu+D_\mu)^2}{M^2}+\frac{(1-s)^2b_\mu b_\mu}{M^2}\right.$$
$$\left.-\frac{ie}{4M^2}\left[\gamma^\mu,\gamma^\nu\right]F_{\mu\nu}-\frac{i(1-s)}{M^2}\left[\gamma^\mu,\gamma^\nu\right]b_\mu\left(ik_\nu+D_\nu\right)\gamma^5\right] \tag{373}$$

Since the momentum k is being integrated we can rescale it by $k_\mu\to Mk_\mu$ so that

$$I(x)=\lim_{M\to\infty}\int\frac{\mathrm{d}^4k}{(2\pi)^4}M^4\,\mathrm{Tr}\,\gamma^5\exp\left[\frac{(iMk_\mu+D_\mu)^2}{M^2}+\frac{(1-s)^2b_\mu b_\mu}{M^2}\right.$$
$$\left.-\frac{ie}{4M^2}\left[\gamma^\mu,\gamma^\nu\right]F_{\mu\nu}-\frac{i(1-s)}{M^2}\left[\gamma^\mu,\gamma^\nu\right]b_\mu\left(iMk_\nu+D_\nu\right)\gamma^5\right] \tag{374}$$

Now the only non-zero term in the Taylor series of the exponential must be $\propto M^4$ (a condition from the limit) and contain four $\gamma-$matrices (a condition from the trace). The only surviving term is

$$I(x)=\frac{e^2}{16}\lim_{M\to\infty}\int\frac{\mathrm{d}^4k}{(2\pi)^4}e^{k^2}\,\mathrm{Tr}\,\gamma^5[\gamma^\mu,\gamma^\nu]\left[\gamma^\alpha,\gamma^\beta\right]F_{\mu\nu}F_{\alpha\beta} \tag{375}$$
$$=-\frac{e^2}{32}\,\mathrm{Tr}\,\gamma^5[\gamma^\mu,\gamma^\nu]\left[\gamma^\alpha,\gamma^\beta\right]F_{\mu\nu}F_{\alpha\beta} \tag{376}$$
$$=-\frac{e^2}{32\pi^2}\epsilon^{\mu\nu\alpha\beta}F_{\mu\nu}F_{\alpha\beta} \tag{377}$$

Going back to the Jacobian $\mathcal{J}$ in equation (366)

$$\mathcal{J}=\exp\left(-i\,\mathrm{d}s\,\frac{e^2}{32\pi^2}\int\mathrm{d}^4x\,\beta(x)\epsilon^{\mu\nu\alpha\beta}F_{\mu\nu}F_{\alpha\beta}\right) \tag{378}$$

and the full transformation is

$$\mathcal{J}=\exp\left(-i\frac{e^2}{32\pi^2}\int\mathrm{d}^4x\,\beta(x)\epsilon^{\mu\nu\alpha\beta}F_{\mu\nu}F_{\alpha\beta}\right) \tag{379}$$

The action term $\mathcal{J}^{-2}=e^{S_{\mathrm{Anomaly}}}$ is

$$S_{\mathrm{Anomaly}}=\frac{e^2}{32\pi^2}\int\mathrm{d}^4x\,\beta(x)F\tilde{F} \tag{380}$$

where $F\tilde{F}=F^{\mu\nu}\tilde{F}_{\mu\nu}=\frac{1}{2}\epsilon_{\mu\nu\alpha\beta}F^{\mu\nu}F^{\alpha\beta}$. Therefore the chiral rotation introduces a new term to the action. It is important to notice that the presence of fermionic interactions changes this only to nonlinear order (RYLANDS et al., 2021).

APPENDIX B – Feynman's rules for the interactions

In this appendix, I will revise Feynman's rules to fixate the notation and any possible misunderstanding. All terms are computed using the renormalized action described in eq. (230) which is

$$\mathcal{L}_R = \mathcal{L}_{\text{Proca}} + \mathcal{L}_{\text{axion}} + \mathcal{L}_{\text{interaction}} + \mathcal{L}_{\text{counterterms}} + \mathcal{L}_{4\gamma} + \mathcal{L}_{2\gamma,2\theta} \tag{381}$$

$$\mathcal{L}_{\text{Proca}} = -\frac{1}{4}Z_3 F_{\mu\nu}F^{\mu\nu} + \frac{1}{2}Z_M M^2 A_\mu A^\mu \tag{382}$$

$$\mathcal{L}_{\text{axion}} = \frac{1}{2}Z_\theta \partial_\mu\theta\partial^\mu\theta - \frac{1}{2}Z_m m^2\theta^2 \tag{383}$$

$$\mathcal{L}_{\text{interaction}} = \frac{1}{4}Z_g g\theta\tilde{F}_{\mu\nu}F^{\mu\nu} \tag{384}$$

$$\mathcal{L}_{\text{counterterms}} = \frac{\delta_s}{2m_s^2}(\partial_\mu\theta)\Box(\partial^\mu\theta) + \frac{\delta_{gh}}{2m_{gh}^2}(\partial F)^2 \tag{385}$$

$$\mathcal{L}_{4\gamma} = \frac{1}{4!}Z_4 C_4 A^4 - \frac{1}{4!}Z_5\frac{A^2}{M_2^2}F^2 \tag{386}$$

$$\mathcal{L}_{2\gamma,2\theta} = -\frac{1}{4}Z_{a\theta}C_{a\theta}\theta^2 A^2 + \frac{1}{4}Z_{\theta f}\frac{\theta^2}{m_{\theta f}^2}F^2 \tag{387}$$

The order is; free pseudo-scalar and vector fields, axionic interaction, and for the Next-to-leading interaction terms (four photon and two-photon-two-axion interations). The counterterms will be included in the renormalization factors as usual in renormazation perturbative process (see (SCHWARTZ, 2013) for more information).

B.1 Free field

The photon and axion propagators associated with the free action will be, respectively:

$$G_0^{\alpha\beta}(x,x') = \int \frac{\mathrm{d}^4p}{(2\pi)^4}\frac{-i}{p^2 - M^2 + i\varepsilon}\left(g^{\alpha\beta} - \frac{p^\alpha p^\beta}{M^2}\right)e^{ip(x-x')}\,, \tag{388}$$

$$\Delta_0(x,x') = \int \frac{\mathrm{d}^4p}{(2\pi)^4}\frac{i}{p^2 - m^2 + i\varepsilon}e^{ip(x-x')}\,, \tag{389}$$

From now on we will omit the $i\varepsilon$ for convenience. The massless photon is obtained from the limit of zero Procca mass, *i.e.* $M = 0$, one recovers the usual photon propagator found in textbooks (SCHWARTZ, 2013). It is convenient to write this in momentum space we get massive vector field

$$D_0^{\nu\lambda}(p) = \frac{-i}{p^2 - M^2} P^{\nu\lambda}(p) \tag{390}$$

with $P_{\mu\nu} = g_{\mu\nu} - p_\mu p_\nu / M^2$ and for the massive pseudo-scalar field

$$\Delta_0(p^2) = \frac{i}{p^2 - m^2} \tag{391}$$

The Feynman's rules associated with thee free sector are

μ ν $$= \frac{-i}{p^2 - M^2} P^{\mu\nu}(p) \tag{392}$$

 $$= \frac{i}{p^2 - m^2} \tag{393}$$

and the counter-terms are

μ  ν $$= -i\delta_3(p^2 g_{\mu\nu} - p_\mu p_\nu) + i(\delta_M + \delta_3) M^2 g_{\mu\nu} \tag{394}$$

 $$= -i(\delta_\theta p^2 + \delta_m m^2) \tag{395}$$

B.2 Axion Interactions

The Axionic interaction (defined in eq. (206) or eq. (384)) is not usually studied in courses of QFT. It is necessary to take extra precautions with the direction of the momentum in this interaction because it has an explicit momentum dependency that can be easily seen if we open the derivatives as in

$$\frac{1}{4} Z_g g \phi \tilde{F}_{\mu\nu} F^{\mu\nu} = Z_g g \phi \epsilon_{\mu\nu\alpha\beta} \partial^\alpha A^\beta \partial^\mu A^\nu \tag{396}$$

One example of a similar interaction term can be found in (SCHWARTZ, 2013). In our case, this Lagrangian term generates a vertex with two photons and a scalar field. For each photon line, we get a momenta factor, together with a $-i$ (i) factor for in going (outgoing) lines *times*, a Levi-Civitta tensor, and i times an axion coupling constant. The Levi-Civitta tensor is coupled with the momentum associated with the photon lines. We can do partial integration to change the photon momenta for the pseudo-scalar but it does not change the final result since the sum of the momenta that goes in and out the vertex must be the same i.e. momentum conservation (SCHWARTZ, 2013). The Feynman graph associated a vertex with all momenta going out

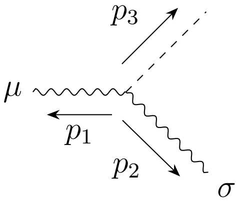

$$= (-igZ_g)\epsilon_{\mu\nu\alpha\beta}p_1^{\alpha}p_2^{\mu} \equiv V_{\mu\nu}(p_1, p_2) \tag{397}$$

It is also common to say that one gets a factor of ip when the particle is created (emerges from the vertex) and $-ip$ when the particle is destroyed (enters the vertex).

B.3 **Counter-terms**

The next-to-leading counter-terms (reminiscent of the problematic ghost states explored in section 5.2), described in equations (230) or (385), follow the same reasoning as the free field counter-terms in appendix B.1. The Feynman rules for those factors are described in (VILLALBA-CHÁVEZ; GOLUB; MüLLER, 2018; CHRISPIM; BRUNI; GUIMARAES, 2021) and are given by

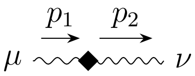

$$= i\frac{\delta_{gh}}{m_{gh}^2}p_1^2\Big(p_2^2 g^{\mu\nu} - p_2^{\mu}p_2^{\nu}\Big) \tag{398}$$

$$= -i\frac{\delta_s}{m_s^2}p^4 \tag{399}$$

B.4 **Four-massive vector interaction**

The 4γ contribution has two different contributions (as one can see in eq. (231) or in eq. (386)) describe a four-massive vector (or four massive photon) vertex. Both can be described by the graph represented in

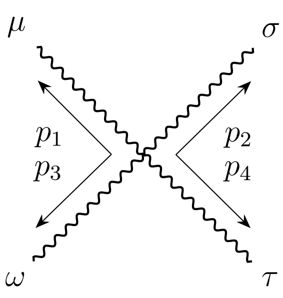

$$= \frac{1}{6}iZ_4C_4T^{(1)}_{\mu\nu\rho\sigma} + \frac{i}{12}\frac{Z_5}{M_2^2}T^{(2)}_{\mu\nu\rho\sigma}(p_1, p_2, p_3, p_4) \tag{400}$$

with

$$T^{(1)}_{\mu\nu\rho\sigma} = (g^{\mu\sigma}g^{\nu\rho} + g^{\mu\rho}g^{\nu\sigma} + g^{\mu\nu}g^{\rho\sigma}) \tag{401}$$

$$\begin{aligned} T^{(2)}_{\mu\nu\rho\sigma}(p_1, p_2, p_3, p_4) = &[g^{\rho\sigma}p_1^{\nu}p_2^{\mu} - g^{\mu\nu}g^{\rho\sigma}(p_1 \cdot p_2)] + (p_2 \to p_3, \nu \leftrightarrows \rho) \\ &+ (p_2 \to p_4, \nu \leftrightarrows \sigma) \\ &+ [g^{\mu\sigma}p_2^{\rho}p_3^{\nu} - g^{\mu\sigma}g^{\nu\rho}(p_2 \cdot p_3)] + (p_3 \to p_4, \rho \leftrightarrows \sigma) \\ &+ (p_2 \to p_4, \sigma \leftrightarrows \nu) \end{aligned} \tag{402}$$

Here the notation indicates that the rule $(p_i \to p_j, \kappa \leftrightarrows \alpha)$ is applied to the expression inside the preceding $[\cdots]$. The difference between the two contributions is the momentum dependency. This is the same case as in the axion interaction term, the presence of derivatives acting on the vector fields introduces the momentum variable but with the extra problem that here we must include all the possible combinations. This is the reason for the $T^{(2)}_{\mu\nu\rho\sigma}$ being so convoluted.

B.5 Two photon, two pseudo-axion interaction

The final interaction term (defined in eq. (232) or in eq. (387)) is a vertex composed of two pseudo-scalar field together with two massive vector. In a similar way to the 4γ interaction here both terms will contribute to the same graph with distinct factors (one with momentum dependency and one without it). The Feynman graph of this interaction is represented in

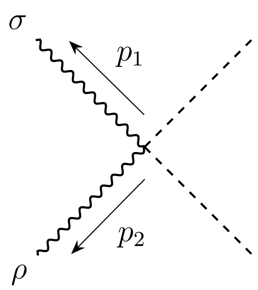

$$= -2iZ_{a\phi}C_{a\phi}g^{\rho\sigma} + (2i)\frac{Z_{\phi f}}{m^2_{\phi f}}(p_3^{\sigma}p_4^{\rho} - g^{\rho\sigma}(p_3 \cdot p_4)) \tag{403}$$

APPENDIX C – Dirac algebra

C.1 Definitions

The Dirac matrices γ_μ follows Clifford algebra, they obey the anti-commutation relations

$$\{\gamma_\mu, \gamma_\nu\} \equiv \gamma_\mu\gamma_\nu + \gamma_\nu\gamma_\mu = 2g_{\mu\nu} \tag{404}$$

with $\mu, \nu = 0, 1, 2, 3$ in $3+1$ space-time. These properties also means that

$$\gamma^\mu\gamma^\nu = -\gamma^\nu\gamma^\mu \text{ for } \mu \neq \nu \tag{405}$$

and

$$\left(\gamma^0\right)^2 = -\left(\gamma^i\right)^2 = \mathbb{1} \tag{406}$$

where $\mathbb{1}$ is the identity matrix. It is usual to define an “extra” matrix by $\gamma_5 = i\gamma^0\gamma^1\gamma^2\gamma^3$ that obeys

$$\left\{\gamma^5, \gamma_\nu\right\} = 0\ . \tag{407}$$

C.2 Spinors definitions in Weyl basis

In this thesis I will work basically using the Weyl basis, so it is convenient to review it briefly. In this notation, the gamma matrix are

$$\gamma^\mu = \begin{pmatrix} 0 & \sigma^\mu \\ \overline{\sigma}^\mu & 0 \end{pmatrix} \tag{408}$$

with $\sigma^\mu = (\mathbb{1}_2, \sigma^i)$ and $\overline{\sigma}^\mu = (\mathbb{1}_2, -\sigma^i)$, here $\mathbb{1}_2$ is the 2 for 2 identity matrix. The Pauli matrices are

$$\sigma_0 = \begin{pmatrix} 1 & 0 \\ 0 & 1 \end{pmatrix} = \mathbb{1}_2 \tag{409}$$

$$\sigma_1 = \begin{pmatrix} 0 & 1 \\ 1 & 0 \end{pmatrix} \tag{410}$$

$$\sigma_2 = \begin{pmatrix} 0 & -i \\ i & 0 \end{pmatrix} \tag{411}$$

$$\sigma_3 = \begin{pmatrix} 1 & 0 \\ 0 & -1 \end{pmatrix} \tag{412}$$

These matrix obey $[\sigma_i, \sigma_j] = 2i\epsilon_{ijk}\sigma_k$, $\{\sigma_i, \sigma_j\} = 2\delta_{ij}\mathbb{1}_2$ and $\sigma_j\sigma_k = \delta_{jk}\mathbb{1}_2 + i\epsilon_{jkl}\sigma_l$. Furthermore, we have in the Weyl basis $\gamma_2^* = -\gamma_2$ and $\gamma_2^T = \gamma_2$. With this definitions we can write γ^5 matrices as

$$\gamma^5 = i\gamma^0\gamma^1\gamma^2\gamma^3 = \begin{pmatrix} -\mathbb{1}_2 & 0 \\ 0 & \mathbb{1}_2 \end{pmatrix} . \tag{413}$$

Furthermore we have the dagger operator that is defined by

$$A^\dagger = (A^*)^T = (A^T)^* \tag{414}$$

or

$$(A^\dagger)_{ij} = A^*_{ji} . \tag{415}$$

The Pauli matrices obey

$$\sigma^\dagger_\mu = \sigma_\mu . \tag{416}$$

It is also convenient to write

$$\begin{aligned} e^{i\beta\gamma_5} &= \cos\beta \mathbb{1}_4 + i\sin\beta\gamma_5 && (417) \\ &= \begin{pmatrix} \cos\beta & 0 \\ 0 & \cos\beta \end{pmatrix} + \begin{pmatrix} -i\sin\beta & 0 \\ 0 & i\sin\beta \end{pmatrix} && (418) \\ &= \begin{pmatrix} e^{-i\beta} & 0 \\ 0 & e^{i\beta} \end{pmatrix} && (419) \end{aligned}$$

that means that

$$e^{i\beta\gamma_5}(AP_L + BP_R) = e^{-i\beta}AP_L + e^{i\beta}BP_R \tag{420}$$

This identity will be important for the transformations necessary for the chiral transformations.

C.3 Weyl spinor definition

Dirac spinor is defined in terms of two Weyl spinors ψ_L and ψ_R through

$$\psi = \begin{pmatrix} \psi_L \\ \psi_R \end{pmatrix} \tag{421}$$

$$\overline{\psi} = \psi^\dagger \gamma^0 = \begin{pmatrix} \psi_R^\dagger & \psi_L^\dagger \end{pmatrix} \tag{422}$$

with

$$P_R = \frac{1+\gamma^5}{2} = \begin{pmatrix} 0 & 0 \\ 0 & \mathbb{1}_2 \end{pmatrix} \tag{423}$$

$$P_L = \frac{1-\gamma^5}{2} = \begin{pmatrix} \mathbb{1}_2 & 0 \\ 0 & 0 \end{pmatrix} \tag{424}$$

so that

$$P_R\psi = \begin{pmatrix} 0 \\ \psi_R \end{pmatrix} \tag{425}$$

$$P_L\psi = \begin{pmatrix} \psi_L \\ 0 \end{pmatrix} \tag{426}$$

resulting in $\psi_{R/L} = P_{R/L}\psi$.

C.4 Charge conjugate Weyl spinor definition

Using the definition of the charge conjugate

$$\mathbb{C} : \psi_L \to \psi_{Lc} = -i\sigma^2 \psi_R^* \tag{427}$$
$$\mathbb{C} : \psi_R \to \psi_{Rc} = i\sigma^2 \psi_L^* \tag{428}$$

or

$$\mathbb{C} : \begin{pmatrix} \psi_L \\ \psi_R \end{pmatrix} \to \begin{pmatrix} -i\sigma^2 \psi_R^* \\ i\sigma^2 \psi_L^* \end{pmatrix} \tag{429}$$

so that

$$\psi_c = -i\gamma_2 \psi^* = \begin{pmatrix} -i\sigma^2 \psi_R^* \\ i\sigma^2 \psi_L^* \end{pmatrix} . \tag{430}$$

It follows from the definition that

$$\begin{aligned}
\overline{\psi}_c &= \psi_c^\dagger \gamma^0 && (431)\\
&= (-i\gamma_2 \psi^*)^\dagger \gamma_0 && (432)\\
&= i\psi^T \gamma_2^\dagger \gamma_0 && (433)\\
&= \psi^T (-i\gamma_2) \gamma_0 && (434)\\
&= \psi^T \begin{pmatrix} 0 & -i\sigma^2 \\ i\sigma^2 & 0 \end{pmatrix} \begin{pmatrix} 0 & \mathbb{1}_2 \\ \mathbb{1}_2 & 0 \end{pmatrix} && (435)\\
&= \begin{pmatrix} \psi_L^T & \psi_R^T \end{pmatrix} \begin{pmatrix} -i\sigma^2 & 0 \\ 0 & i\sigma^2 \end{pmatrix} && (436)\\
&= \begin{pmatrix} -\psi_L^T i\sigma^2 & \psi_R^T i\sigma^2 \end{pmatrix} . && (437)
\end{aligned}$$

APPENDIX D – Four interaction pairing with mixed chirality

The pairing introduced in eq. (129) is

$$\mathcal{L}_{\text{int.}} = -\lambda^2 \left(\overline{\psi}(x)P_L\psi(x)\right)\left(\overline{\psi}(x)P_R\psi(x)\right) \ . \tag{438}$$

In the main text of section 2.3 the following auxiliary field were introduced

$$\phi(x) = \lambda\overline{\psi}(x)P_L\psi(x) \ , \tag{439}$$

$$\phi^*(x) = \lambda\overline{\psi}(x)P_R\psi(x) \ . \tag{440}$$

The van der Waerden notation is implicit used. The dotted and undotted spinor indexes: $\psi_{L\alpha}$ and $\psi_R^{\dot{\alpha}}$ are the left and right spinors. Spinor index contractions are defined as $\psi_R^\dagger(x)\psi_L(x) = \psi_R^{\dagger\alpha}(x)\psi_{L\alpha}(x) = \psi_{R\alpha}^\dagger(x)\varepsilon^{\alpha\beta}\psi_{L\beta}(x)$. And similarly for other billinears we shall encounter, for instance, $\psi_R(x)\psi_R(x) = \psi_{R\dot{\alpha}}\psi_R^{\dot{\alpha}} = \psi_R^{\dot{\alpha}}\varepsilon_{\dot{\alpha}\dot{\beta}}\psi_R^{\dot{\beta}}$ and $\psi_L(x)\psi_L(x) = \psi_L^{\alpha}(x)\psi_{L\alpha}(x) = \psi_{L\alpha}(x)\varepsilon^{\alpha\beta}\psi_{L\beta}(x)$.

D.1 **Explicit form**

This interaction term is composed of

$$\overline{\psi}(x)P_L\psi(x) = \psi^\dagger(x)\gamma^0P_L^2\psi(x) \tag{441}$$

$$= \psi^\dagger(x)P_R\gamma^0P_L\psi(x) \tag{442}$$

$$= \psi_R^\dagger(x)\psi_L(x) \tag{443}$$

and

$$\overline{\psi}(x)P_R\psi(x) = \psi^\dagger(x)\gamma^0P_R^2\psi(x) \tag{444}$$

$$= \psi^\dagger(x)P_L\gamma^0P_R\psi(x) \tag{445}$$

$$= \psi_L^\dagger(x)\psi_R(x) \tag{446}$$

where it was used the properties $P_{R/L}^2 = P_{R/L}$ and $\{\gamma_5, \gamma^\mu\} = 0$. The full interaction term is

$$\mathcal{L}_{\text{int.}} = -\lambda^2\left(\psi_R^\dagger(x)\psi_L(x)\right)\left(\psi_L^\dagger(x)\psi_R(x)\right) \ . \tag{447}$$

D.2 **Parity**

Acting with Parity

$$\mathbb{P} : \overline{\psi}(x)P_L\psi(x) \to \psi_L^\dagger\psi_R(\mathbb{P}x) = \overline{\psi}(x)P_R\psi(x) \tag{448}$$

and

$$\mathbb{P} : \overline{\psi}(x)P_R\psi(x) \to \psi_R^\dagger\psi_L(\mathbb{P}x) = \overline{\psi}(x)P_L\psi(x) \ . \tag{449}$$

Even though each term changes the interaction is invariant since it is composed of both

$$\mathbb{P} : \mathcal{L}_{\text{int}}(x) \to -\lambda^2\Big(\psi_L^\dagger\psi_R\Big)\Big(\psi_R^\dagger\psi_L\Big)(\mathbb{P}x) \equiv \mathcal{L}_{\text{int}}(\mathbb{P}x) \tag{450}$$

in terms of the auxiliary field this acts as $\mathbb{P} : \phi \to \phi^*$. If the field is parameterized as $\phi = \lambda v^3 e^{i\delta}$ then the condition for it to respect $\mathbb{P}$ is $\delta = 0$.

D.3 **Time-reversal**

Now considering time-reversal which acts as

$$\mathbb{T} : \overline{\psi}(x)P_L\psi(x) \to (-1)^2\psi_L^\dagger\sigma^3\sigma^1\sigma^1\sigma^3\psi_R(\mathbb{T}x) = \psi_R^\dagger\psi_L(\mathbb{T}x) = \overline{\psi}(x)P_L\psi(x) \tag{451}$$

and

$$\mathbb{T} : \overline{\psi}(x)P_R\psi(x) \to (-1)^2\psi_R^\dagger\sigma^3\sigma^1\sigma^1\sigma^3\psi_L(\mathbb{T}x) = \psi_L^\dagger\psi_R(\mathbb{T}x) = \overline{\psi}(x)P_R\psi(x) \tag{452}$$

where one must use eq. (416) along with ${\sigma^1}^2 = {\sigma^2}^2 = {\sigma^3}^2 = \mathbb{1}$, leading to

$$\mathbb{T} : \mathcal{L}_{\text{int}}(x) \to \mathcal{L}_{\text{int}}(\mathbb{T}x) \ . \tag{453}$$

The auxiliary field complex field is invariant under time-reversal.

D.4 **Charge conjugation**

With charge conjugation the transformation is

$$\mathbb{C} : \overline{\psi}(x)P_L\psi(x) \to (-i)^2\psi_L^\dagger\sigma^2\sigma^2\psi_R = \psi_R^\dagger\psi_L(x) = \overline{\psi}(x)P_L\psi(x) \tag{454}$$

and

$$\mathbb{C} : \overline{\psi}(x)P_R\psi(x) \rightarrow (-i)^2\psi_R^\dagger\sigma^2\sigma^2\psi_L = \psi_L^\dagger\psi_R(x) = \overline{\psi}(x)P_R\psi(x) \tag{455}$$

where one must use eq. (416) along with ${\sigma^1}^2 = {\sigma^2}^2 = {\sigma^3}^2 = \mathbb{1}$, leading to

$$\mathbb{C} : \mathcal{L}_{\text{int}}(x) \rightarrow \mathcal{L}_{\text{int}}(x) \ . \tag{456}$$

As in the time-reversal case, the auxiliary field is invariant under charge conjugation.

D.5 $U(1)$ **gauge**

Transforming with $\psi \rightarrow e^{i\beta}\psi$ or in terms of the left and right components $\psi_{R/L} \rightarrow e^{i\beta}\psi_{R/L}$ leads to

$$U(1) \text{ gauge} : \overline{\psi}(x)P_L\psi(x) \rightarrow \psi_R^\dagger e^{-i\beta}\psi_L e^{i\beta} = \psi_R^\dagger\psi_L \tag{457}$$

and

$$U(1) \text{ gauge} : \overline{\psi}(x)P_R\psi(x) \rightarrow \psi_L^\dagger e^{-i\beta}\psi_R e^{i\beta} = \psi_L^\dagger\psi_R \tag{458}$$

thus

$$U(1) \text{ gauge} : \mathcal{L}_{\text{int}}(x) \rightarrow \mathcal{L}_{\text{int}}(x) \ . \tag{459}$$

As expected, the ϕ field is invariant under gauge transformation.

D.6 $U(1)$ **chiral**

Transforming with $\psi \rightarrow e^{i\alpha\gamma_5}\psi$ or in terms of the left and right components

$$\psi_R \rightarrow e^{i\alpha}\psi_R \tag{460}$$
$$\psi_L \rightarrow e^{-i\alpha}\psi_L \tag{461}$$

leads to

$$U(1) \text{ chiral} : \overline{\psi}(x)P_L\psi(x) \rightarrow \psi_R^\dagger e^{-i\alpha}\psi_L e^{-i\alpha} = e^{-2i\alpha}\psi_R^\dagger\psi_L = e^{-2i\alpha}\overline{\psi}(x)P_L\psi(x) \tag{462}$$

and

$$U(1)\ \text{chiral} : \overline{\psi}(x)P_R\psi(x) \to \psi_L^\dagger e^{i\alpha}\psi_R e^{i\alpha} = e^{2i\alpha}\psi_L^\dagger\psi_R = e^{2i\alpha}\overline{\psi}(x)P_R\psi(x)\ . \tag{463}$$

Each term transforms, but the full interaction is invariant because they cancels mutually

$$U(1)\ \text{chiral} : \mathcal{L}_{\text{int}}(x) \to \mathcal{L}_{\text{int}}(x)\ , \tag{464}$$

with this we can see that the auxiliary field transforms as

$$U(1)\ \text{chiral} : \phi(x) \to e^{2i\alpha}\phi(x)\ . \tag{465}$$

APPENDIX E – Extended spinor algebra

E.1 Extended spinor algebra definitions

The extended spinor is defined as

$$\Psi = \begin{pmatrix} \psi \\ \psi_c \end{pmatrix} \tag{466}$$

$$\overline{\Psi} = \begin{pmatrix} \overline{\psi} & \overline{\psi}_c \end{pmatrix} \tag{467}$$

with ψ_c defined in equation (430). To make this more clear we can open its components

$$\Psi = \begin{pmatrix} \psi_L \\ \psi_R \\ -i\sigma^2\psi_R^* \\ i\sigma^2\psi_L^* \end{pmatrix} = \begin{pmatrix} \psi_{L\uparrow} \\ \psi_{L\downarrow} \\ \psi_{R\uparrow} \\ \psi_{R\downarrow} \\ -i\sigma^2\psi_{R\uparrow}^* \\ -i\sigma^2\psi_{R\downarrow}^* \\ i\sigma^2\psi_{L\uparrow}^* \\ i\sigma^2\psi_{L\downarrow}^* \end{pmatrix}. \tag{468}$$

E.1.1 Transformation of the extended spinor

The system may be characterized by the following transformations:
$U(1)$ gauge symmetry

$$\Psi(x) \to e^{-i\alpha(x)\rho_3}\Psi(x) \tag{469}$$

$$A_\mu \to A_\mu - \frac{i}{e}\partial_\mu\alpha(x) \tag{470}$$

$U(1)$ (global) chiral symmetry (anomalous)

$$\Psi(x) \to e^{-i\beta\gamma^5}\Psi(x) \tag{471}$$

Charge conjugation ($\mathbb{C}$)

$$\Psi(x) \to \rho_1 \Psi(x) \tag{472}$$
$$A_\mu \to -A_\mu \tag{473}$$

Parity ($\mathbb{P}$): $\mathbb{P}x = (t, -x, -y, -z)$

$$\Psi(x) \to i\tau_1 \Psi(\mathbb{P}x) \tag{474}$$
$$A_\mu(x) \to (A_0(\mathbb{P}x), -A_i(\mathbb{P}x)) \tag{475}$$

Time reversal ($\mathbb{T}$): $\mathbb{T}x = (-t, x, y, z)$

$$\Psi(x) \to -\sigma_2 \Psi(\mathbb{T}x) \tag{476}$$
$$A_\mu(x) \to (A_0(\mathbb{T}x), -A_i(\mathbb{T}x)) \tag{477}$$

E.1.2 Dirac action in terms of the extended spinor

It is not difficult to use the definition of the extended spinor Ψ in the massless Dirac Lagrangian. The process start with

$$\mathcal{L}_1 = \overline{\psi}\tilde{\not{D}}\psi, \qquad \tilde{\not{D}} = i\not{\partial} + \not{b}\gamma^5 + ie\not{A}\ . \tag{478}$$

Now using the definition of the Charge conjugation $\mathbb{C}$ (section C.4) together $\mathbb{C}^2 = 1$

$$\begin{aligned}
\overline{\psi}\tilde{\not{D}}\psi &= \frac{1}{2}\Big(\overline{\psi}\tilde{\not{D}}\psi + \overline{\psi}\tilde{\not{D}}\psi\Big) && (479)\\
&= \frac{1}{2}\Big(\overline{\psi}\tilde{\not{D}}\psi + \overline{\psi}\mathbb{C}^2\tilde{\not{D}}\mathbb{C}^2\psi\Big) && (480)\\
&= \frac{1}{2}\Big(\overline{\psi}\tilde{\not{D}}\psi + \overline{\psi}_c\tilde{\not{D}}_c\psi_c\Big) && (481)
\end{aligned}$$

with $\tilde{\not{D}}_c = i\not{\partial} + \not{b}\gamma^5 - ie\not{A}$. Now using the extended spinor definition we can write this as a matrix so that

$$\begin{aligned}
\overline{\psi}\tilde{\not{D}}\psi &= \frac{1}{2}\overline{\Psi}\begin{pmatrix}\tilde{\not{D}} & 0\\ 0 & \tilde{\not{D}}_c\end{pmatrix}\Psi && (482)\\
&= \frac{1}{2}\overline{\Psi}\left(\begin{pmatrix}i\not{\partial} + \not{b}\gamma_5 & 0\\ 0 & i\not{\partial} + \not{b}\gamma_5\end{pmatrix} + \begin{pmatrix}ie\not{A} & 0\\ 0 & -ie\not{A}\end{pmatrix}\right)\Psi && (483)\\
&= \frac{1}{2}\overline{\Psi}\Big[\Big(i\not{\partial} + \not{b}\gamma_5\Big)\rho_0 + ie\not{A}\rho_3\Big]\Psi\ . && (484)
\end{aligned}$$

It is important to remember that the terms inside the brackets are 8×8 matrices because the Kronecker product is being suppressed. To make this more clear the last term matrix structure explicitly is

$$\Gamma = \sigma \otimes \tau \otimes \rho \tag{485}$$

where σ, τ and ρ are Pauli matrices acting on spin, handiness and charge, respectively.

E.1.3 Interaction of the extended spinor

With this we can construct the following bilinears

$$\overline{\psi}_c \psi = \psi_L^T(-i\sigma^2)\psi_L + \psi_R^T(i\sigma^2)\psi_R \tag{486}$$
$$\overline{\psi}\psi_c = \psi_L^\dagger(i\sigma^2)\psi_L^* + \psi_R^\dagger(-i\sigma^2)\psi_R^* \tag{487}$$

and

$$\overline{\psi}_c \gamma^5 \psi = \psi_L^T(i\sigma^2)\psi_L + \psi_R^T(i\sigma^2)\psi_R \tag{488}$$
$$\overline{\psi}\gamma^5 \psi_c = \psi_L^\dagger(i\sigma^2)\psi_L^* + \psi_R^\dagger(i\sigma^2)\psi_R^* \tag{489}$$

Using the definition of $P_{R/L}$ we can construct

$$\overline{\psi}_c P_R \psi = \psi_R^T(i\sigma^2)\psi_R \tag{490}$$
$$\overline{\psi} P_R \psi_c = \psi_L^\dagger(i\sigma^2)\psi_L^* \tag{491}$$

and

$$\overline{\psi}_c P_L \psi = \psi_L^T(-i\sigma^2)\psi_L \tag{492}$$
$$\overline{\psi} P_L \psi_c = \psi_R^\dagger(-i\sigma^2)\psi_R^* \tag{493}$$

Now using the notation used in the article this can be put in the form

$$\overline{\psi}_c P_R \psi = \psi_R \psi_R \tag{494}$$
$$\overline{\psi} P_R \psi_c = \psi_L^\dagger \psi_L^\dagger \tag{495}$$

and

$$\overline{\psi}_c P_L \psi = \psi_L \psi_L \tag{496}$$
$$\overline{\psi} P_L \psi_c = \psi_R^\dagger \psi_R^\dagger \tag{497}$$

and the four fermion interaction in eq. (134) is

$$\mathcal{L}_{\text{int.}}(x) = -\lambda_R^2 \psi_R \psi_R \psi_R^\dagger \psi_R^\dagger - \lambda_L^2 \psi_L \psi_L \psi_L^\dagger \psi_L^\dagger \tag{498}$$

$$= -\lambda_R^2 (\overline{\psi}_c P_R \psi)(\overline{\psi} P_L \psi_c) - \lambda_L^2 (\overline{\psi}_c P_L \psi)(\overline{\psi} P_R \psi_c) \ . \tag{499}$$

Now we can concentrate on rewrite this expression using Ψ. In order to do this we can construct an analog of the projectors $P_{L/R}$ by noticing that

$$\frac{1}{2}(\rho_1 - i\rho_2)\Psi = \begin{pmatrix} 0 & 0 \\ 1 & 0 \end{pmatrix} \begin{pmatrix} \psi \\ \psi_c \end{pmatrix} = \begin{pmatrix} 0 \\ \psi \end{pmatrix} , \tag{500}$$

$$\frac{1}{2}(\rho_1 + i\rho_2)\Psi = \begin{pmatrix} 0 & 1 \\ 0 & 0 \end{pmatrix} \begin{pmatrix} \psi \\ \psi_c \end{pmatrix} = \begin{pmatrix} \psi_c \\ 0 \end{pmatrix} , \tag{501}$$

with this we can construct

$$\overline{\Psi} P_L \frac{1}{2}(\rho_1 + i\rho_2)\Psi = \begin{pmatrix} \overline{\psi} & \overline{\psi}_c \end{pmatrix} \begin{pmatrix} P_L \psi_c \\ 0 \end{pmatrix} = \overline{\psi} P_L \psi_c \ , \tag{502}$$

$$\overline{\Psi} P_R \frac{1}{2}(\rho_1 - i\rho_2)\Psi = \begin{pmatrix} \overline{\psi} & \overline{\psi}_c \end{pmatrix} \begin{pmatrix} 0 \\ P_R \psi \end{pmatrix} = \overline{\psi}_c P_R \psi \ . \tag{503}$$

Now using this we can construct the other two terms

$$\overline{\Psi} P_R \frac{1}{2}(\rho_1 + i\rho_2)\Psi = \overline{\psi} P_R \psi_c \ , \tag{504}$$

$$\overline{\Psi} P_L \frac{1}{2}(\rho_1 - i\rho_2)\Psi = \overline{\psi}_c P_L \psi \ . \tag{505}$$

Defining the operators $P_\pm = \frac{1}{2}(\rho_1 \pm i\rho_2)$ the interaction term of eq. (134) is

$$\mathcal{L}_{\text{int.}}(x) = -\lambda_R^2 (\overline{\psi}_c P_R \psi)(\overline{\psi} P_L \psi_c) - \lambda_L^2 (\overline{\psi}_c P_L \psi)(\overline{\psi} P_R \psi_c) \ , \tag{506}$$

$$= -\lambda_R^2 \Big(\overline{\Psi} P_R P_- \Psi\Big)\Big(\overline{\Psi} P_L P_+ \Psi\Big) - \lambda_L^2 \Big(\overline{\Psi} P_L P_- \Psi\Big)\Big(\overline{\Psi} P_R P_+ \Psi\Big) \ . \tag{507}$$

With this definition it is convenient to know the properties

$$\begin{aligned} e^{i\kappa\rho_3}(AP_+ + BP_-) &= \begin{pmatrix} e^{i\kappa} & 0 \\ 0 & e^{-i\kappa} \end{pmatrix} \begin{pmatrix} 0 & A \\ B & 0 \end{pmatrix} \\ &= \begin{pmatrix} 0 & e^{i\kappa} A \\ e^{-i\kappa} B & 0 \end{pmatrix} \\ &= e^{i\kappa} A P_+ + e^{-i\kappa} B P_- \end{aligned} \tag{508}$$

E.1.4 Transformation of the four fermion spinor interaction and auxiliary field $\phi_{R/L}$

In this section I will study the transformation properties of the interaction term

$$\mathcal{L}_{\text{int.}}(x) = -\lambda_R^2\Big(\overline{\Psi}P_RP_-\Psi\Big)\Big(\overline{\Psi}P_LP_+\Psi\Big) - \lambda_L^2\Big(\overline{\Psi}P_LP_-\Psi\Big)\Big(\overline{\Psi}P_RP_+\Psi\Big) \tag{509}$$

and the introduced auxiliary field (two sets of Hubbard-Stratanovich $\phi_{R/L}$) that were defined as

$$\phi_R = \lambda_R\psi_R\psi_R = \lambda_R\overline{\psi}_cP_R\psi = \lambda_R\overline{\Psi}P_RP_-\Psi \tag{510}$$
$$\phi_R^\dagger = \lambda_R\psi_R^\dagger\psi_R^\dagger = \lambda_R\overline{\psi}P_L\psi_c = \lambda_R\overline{\Psi}P_LP_+\Psi \tag{511}$$

and

$$\phi_L = \lambda_L\psi_L\psi_L = \lambda_L\overline{\psi}_cP_L\psi = \lambda_L\overline{\Psi}P_LP_-\Psi \tag{512}$$
$$\phi_L^\dagger = \lambda_L\psi_L^\dagger\psi_L^\dagger = \lambda_L\overline{\psi}P_R\psi_c = \lambda_L\overline{\Psi}P_RP_+\Psi \tag{513}$$

in the main text.

E.1.4.1 Parity

Defining Parity ($\mathbb{P}$): $\mathbb{P}x = (t, -x, -y, -z)$, with

$$\mathbb{P} : \Psi(x) \to i\tau_1\Psi(\mathbb{P}x) \tag{514}$$

and the terms of the interaction transforms as

$$\mathbb{P} : \Big(\overline{\Psi}P_RP_-\Psi\Big)(x) \to -i^2\Big(\overline{\Psi}\tau_1P_RP_-\tau_1\Psi\Big)(\mathbb{P}x) = \Big(\overline{\Psi}P_LP_-\Psi\Big)(\mathbb{P}x) \tag{515}$$
$$\mathbb{P} : \Big(\overline{\Psi}P_LP_+\Psi\Big)(x) \to \Big(\overline{\Psi}P_RP_+\Psi\Big)(\mathbb{P}x) \tag{516}$$

and

$$\mathbb{P} : \Big(\overline{\Psi}P_LP_-\Psi\Big)(x) \to \Big(\overline{\Psi}P_RP_-\Psi\Big)(\mathbb{P}x) \tag{517}$$
$$\mathbb{P} : \Big(\overline{\Psi}P_RP_+\Psi\Big)(x) \to \Big(\overline{\Psi}P_LP_+\Psi\Big)(\mathbb{P}x) \tag{518}$$

where one must notice that $\{\tau_1, \gamma_5\} = 0$. This leads to

$$\mathbb{P} : \mathcal{L}_{\text{int.}}(x) \to -\lambda_R^2\Big(\overline{\Psi}P_LP_-\Psi\Big)\Big(\overline{\Psi}P_RP_+\Psi\Big)(\mathbb{P}x) - \lambda_L^2\Big(\overline{\Psi}P_RP_-\Psi\Big)\Big(\overline{\Psi}P_LP_+\Psi\Big)(\mathbb{P}x) \tag{519}$$

This means that if $\lambda_R \neq \lambda_L$ then $\mathcal{L}_{\text{int.}}(x)$ does not respect $\mathbb{P}$. It is easy to see that this transformation acts changing $P_{R/L}$ to $P_{L/R}$, the auxiliary field thus obey

$$\phi_{R/L}(x) \to \phi_{L/R}(\mathbb{P}x) \ , \tag{520}$$

in another words, the condensate respects $\mathbb{P}$ if $\phi_R(x) = \phi_L(x)$.

E.1.4.2 Time-reversal

Defining Time reversal ($\mathbb{T}$): $\mathbb{T}x = (-t, x, y, z)$ so that

$$\Psi(x) \to -\sigma_2 \Psi(\mathbb{T}x) \tag{521}$$

$$A_\mu(x) \to (A_0(\mathbb{T}x), -A_i(\mathbb{T}x)) \tag{522}$$

which acts as

$$\mathbb{T} : \left(\overline{\Psi} P_R P_- \Psi\right)(x) \to (-1)^2 \left(\overline{\Psi} \sigma_2 P_R P_- \sigma_2 \Psi\right)(\mathbb{T}x) = \left(\overline{\Psi} P_R P_- \Psi\right)(\mathbb{T}x) \tag{523}$$

$$\mathbb{T} : \left(\overline{\Psi} P_L P_+ \Psi\right)(x) \to \left(\overline{\Psi} P_L P_+ \Psi\right)(\mathbb{T}x) \tag{524}$$

and

$$\mathbb{T} : \left(\overline{\Psi} P_L P_- \Psi\right)(x) \to \left(\overline{\Psi} P_L P_- \Psi\right)(\mathbb{T}x) \tag{525}$$

$$\mathbb{T} : \left(\overline{\Psi} P_R P_+ \Psi\right)(x) \to \left(\overline{\Psi} P_R P_+ \Psi\right)(\mathbb{T}x) \tag{526}$$

Each part respects time-reversal and the interaction so we have

$$\mathbb{T} : \mathcal{L}_{\text{int.}}(x) \to \mathcal{L}_{\text{int.}}(\mathbb{T}x) \tag{527}$$

and the auxiliary field transforms as

$$\phi_{R/L}(x) \to -\phi_{R/L}(\mathbb{T}x) \tag{528}$$

E.1.4.3 Charge conjugation

Charge conjugation ($\mathbb{C} : \Psi(x) \to \rho_1 \Psi(x)$) the interaction changes to

$$\mathbb{C} : \left(\overline{\Psi} P_R P_- \Psi\right)(x) \to \left(\overline{\Psi} \rho_1 P_R P_- \rho_1 \Psi\right)(x) = \left(\overline{\Psi} P_R P_+ \Psi\right)(x) \tag{529}$$

$$\mathbb{C} : \left(\overline{\Psi} P_L P_+ \Psi\right)(x) \to \left(\overline{\Psi} P_L P_- \Psi\right)(x) \tag{530}$$

and

$$\mathbb{C}:\Big(\overline{\Psi}P_LP_-\Psi\Big)(x)\to\Big(\overline{\Psi}P_LP_+\Psi\Big)(x) \tag{531}$$
$$\mathbb{C}:\Big(\overline{\Psi}P_RP_+\Psi\Big)(x)\to\Big(\overline{\Psi}P_RP_-\Psi\Big)(x) \tag{532}$$

This leads to

$$\mathbb{C}:\mathcal{L}_{\text{int.}}(x)\to-\lambda_R^2\Big(\overline{\Psi}P_RP_+\Psi\Big)\Big(\overline{\Psi}P_LP_-\Psi\Big)-\lambda_L^2\Big(\overline{\Psi}P_LP_+\Psi\Big)\Big(\overline{\Psi}P_RP_-\Psi\Big) \tag{533}$$

Again, the interaction breaks charge conjugation if $\lambda_R\neq\lambda_L$. In terms of the fields $\phi_{R/L}(x)$ this transformation reads

$$\phi_{R/L}(x)\to\phi^*_{L/R}(x) \tag{534}$$

That is, the condensate respects $\mathbb{C}$ if $\phi_R(x)=\phi^*_L(x)$.

E.1.4.4 $U(1)$ gauge

Under the transformation $\Psi(x)\to e^{i\alpha(x)\rho_3}\Psi(x)$ we have

$$U(1)\text{ gauge: }\Big(\overline{\Psi}P_RP_-\Psi\Big)(x)\to\Big(\overline{\Psi}e^{-i\alpha(x)\rho_3}P_RP_-e^{i\alpha(x)\rho_3}\Psi\Big)(x) \tag{535}$$
$$=e^{-2i\alpha(x)\rho_3}\Big(\overline{\Psi}P_RP_-\Psi\Big)(x)\ . \tag{536}$$

This follows for all terms, the change in the sign is due to the anticommuting properties of the Pauli matrices. The interaction transformation is

$$\begin{aligned}U(1)\text{ gauge: }\mathcal{L}_{\text{int.}}(x)\to&-\lambda_R^2e^{-2i\alpha(x)\rho_3}\Big(\overline{\Psi}P_RP_-\Psi\Big)e^{-2i\alpha(x)\rho_3}\Big(\overline{\Psi}P_LP_+\Psi\Big)\\&-\lambda_L^2e^{-2i\alpha(x)\rho_3}\Big(\overline{\Psi}P_LP_-\Psi\Big)e^{-2i\alpha(x)\rho_3}\Big(\overline{\Psi}P_RP_+\Psi\Big)\end{aligned} \tag{537}$$
$$=\mathcal{L}_{\text{int.}}(x) \tag{538}$$

The interaction term is respects gauge symmetry as expected. Now for the auxiliary field, one has

$$\phi_{R/L}\to e^{-2i\beta}\phi_{R/L}\ . \tag{539}$$

It is interesting to see how this acts on the chosen parametrization for the condensate fields, in terms of $R(x)$ and $L(x)$ (defined in eq. (146)) we have

$$\frac{R/L}{f} \to \frac{R/L}{f} - 2\beta, \tag{540}$$

This last equations tell us that any combination proportional do the difference between $R(x)$ and $L(x)$ is gauge symmetric.

E.1.4.5 $U(1)$ chiral

Under the transformation $\Psi(x) \to e^{i\beta\gamma^5}\Psi(x)$ we have

$$\begin{aligned} U(1) \text{ (global) chiral: } \left(\overline{\Psi} P_R P_- \Psi\right)(x) &\to \left(\overline{\Psi} e^{i\beta\gamma^5}\Psi(x) P_R P_- e^{i\beta\gamma^5}\Psi(x)\Psi\right)(x) && (541)\\ &= e^{-2i\beta\gamma^5}\left(\overline{\Psi} P_R P_- \Psi\right)(x) && (542)\end{aligned}$$

Again this follows for all terms and the interaction transformation is

$$\begin{aligned} U(1) \text{ (global) chiral: } \mathcal{L}_{\text{int.}}(x) \to &-\lambda_R^2 e^{-2i\beta\gamma^5}\left(\overline{\Psi} P_R P_- \Psi\right) e^{-2i\beta\gamma^5}\left(\overline{\Psi} P_L P_+ \Psi\right)\\ &- \lambda_L^2 e^{-2i\beta\gamma^5}\left(\overline{\Psi} P_L P_- \Psi\right) e^{-2i\beta\gamma^5}\left(\overline{\Psi} P_R P_+ \Psi\right) && (543)\\ =\ & \mathcal{L}_{\text{int.}}(x) && (544)\end{aligned}$$

Applying the transformation to the condensate we have

$$\phi_R \to e^{-2i\alpha}\phi_R, \tag{545}$$
$$\phi_L \to e^{+2i\alpha}\phi_L. \tag{546}$$

or using the condensate (defined in eq. (146))

$$\frac{R}{f} \to \frac{R}{f} - 2\alpha, \tag{547}$$
$$\frac{L}{f} \to \frac{L}{f} + 2\alpha \tag{548}$$

This last equations tell us that any combination with $R(x) + L(x)$ chiral symmetric.